Centre Européen de Recherche et de Formation Avancée en Calcul Scientifique
European Center for Research and Advanced Training in Scientific Computing

CERFACS
Scientific Activity Report
Jan. 2021 – Dec. 2023

CERFACS
42, Avenue Gaspard Coriolis, 31057 Toulouse Cedex 1, FRANCE.
Tel. : 33 (0) 561 19 31 31 – Fax : 33 (0) 561 19 30 30
secretar@cerfacs.fr – http://www.cerfacs.fr

Contents

Foreword

Welcome to the 2021-2023 CERFACS Scientific Activity Report.

CERFACS is a mutualized center of research, development, transfer and training regarding simulation, modelling and High Performance Computing (HPC) :

- ✓ Cerfacs designs and develops innovative methods and software solutions to meet the needs of the aeronautics, space, climate, energy and environment sectors, mainly for the benefit of its seven shareholders (Airbus, Cnes, EDF, Météo-France, Onera, Safran, TotalEnergies).
- ✓ Cerfacs welcomes young scientists and offers high-level training in all its fields of expertise.

The mission of CERFACS was defined in the statutes of the company during the creation of the Civil Society in 1996. It should be noted that CERFACS' statutes have evolved into a "Société par Actions Simplifiées" (SAS) at the end of December 2020 but the purpose of CERFACS has not changed and it is as follows:

- to develop scientific and technical research aimed at improving advanced computing methods, including a better understanding of the physical processes involved, and the development of high-performance algorithms for new computer architectures;
- to provide access, either on our own or in shared mode, to new-architecture computers likely to deliver significant performance gains;
- to transfer scientific knowledge and technical methods for application in major industrial sectors and fields;
- to train highly qualified personnel and offer advanced training in these methods, for the sectors and fields of application selected.
- and, more generally, any and all transactions, whether financial, commercial, industrial, civil, real estate or movable property, which may be directly or indirectly related to the above corporate purpose or to any similar or related purposes, and which may directly or indirectly promote the achievement of this purpose by the Company, its expansion, its development and its corporate assets.

CERFACS must always adjust its strategy to meet four key factors of success:

- To master and develop differentiating skills;
- To develop differentiating niches of expertise and innovation;
- To respond in priority to the mutualized needs of the shareholders;
- To be a key player in national and European networks.

This report reflects CERFACS Research activity over the last three years. During this period, we developed the Strategic Research Plan 2018-2022 and started the new Strategic Research Plan 2023-2027, based on a core of generic activities ”Strategic Axes” fed by ”Application Axes”. The Strategic Axes provide both methods, tools and building blocks. A very fruitful interaction between science and application is encouraged through Application Axes, developed with strong relationships with our shareholders.

CERFACS handled the following 5 themes in its core as Strategic Axes in 2018-2022:

- Linear algebra
- Excascale
- Numerical methods for PDE
- Coupling
- Data Driven Modelling (Data Assimilation, Uncertainty Quantification, Data Science)

Since 2023, CERFACS is handling the following 3 Strategic Axes :

- Numerical Algorithms: Sparse Linear Algebra - Discretization and Finite Elements - optimization , Novel numerical approaches applied to CFD (LBM & HOM)
- Sustainable programming:
  - Sustaining, Improving, optimizing, and refactoring legacy codes and Quantum, advanced programming Methods (DSL, PU, New Langages) & Technology
  - Coupling
  - HPC Workflow (including Data Management) & User Interface
- Data Driven Modelling:
- Data Assimilation, Uncertainty Quantification, Physics-based AI

6 Application Axes perfuse and sustain the Strategic Axes:

- HPC Simulation of Propulsion Systems
- HPC Simulation of Hydrogen-based energy production and clean energy systems
- HPC Simulation of Aerodynamics and Aerocoustics of Fixed/Mobile Surface
- Climate Variability and Predictability: From Ocean to Continental Impacts
- HPC Modelling for Environment and Safety
- HPC for modelling climate-air transport links

CERFACS’S ORGANIZATION
The CERFACS research teams are multidisciplinary with physicists, numerical analysts, algorithm and data scientists, computer engineers, ...
There were 3 research teams in CERFACS during 2021-2023:

- Parallel Algorithms and sCientific sOftware Operational Performances (Algo-Coop): Applied mathematics, Development of advanced numerical algorithms to be used on massively parallel computing platforms as well as Uncertainty Quantifications, Data Assimilation, Mesh Adaptation, Artificial Intelligence, Software Engineering and Research code industrialization

- Computational Fluid Dynamics (CFD): Aerodynamics, Combustion and Turbomachines
- Climate Modelling and Global Change (GLOBC): Climate, Data Assimilation & Couplers.

In addition to the research teams, a transverse team (named CSG) is devoted to computer support for the research teams and an administrative team provides administrative, financial and human resources support. To maintain an excellent collaboration with the scientific community, team leaders are very high-level scientists: some of them share their activities between CERFACS and their laboratory (either national or European). A catchword for CERFACS is ”pooling” : Pooling of tools, methods and building blocks between the activities of the ”core” and those applications and sharing interests between shareholders.

Beyond activities directly managed and funded by the shareholders (”heart”), CERFACS must also find a certain level of own resources. CERFACS does this, in the majority of cases, competitively (calls for proposals, tenders...) through:

- Either research grants offered by regional organizations (Regional Council), national agencies (ANR, DGA, DGAC, PIA, FUI, FRANCE 2030), private research foundations and European Commission or international organizations;
- Or research contracts with other agencies and / or industries, ensuring that the themes of recent activities are in synergy with the activities developed in the ”heart” or supported by research grants and ensuring that resources made it possible to contribute to the overall operation.

CERFACS'S PARTNERSHIPS

CERFACS must maintain a strong link with the scientific community for the purpose of complementarity and coherence. This is achieved through partnerships and common laboratories.

- With CNRS: it has been considered more appropriate to seek certification through scientific recognition through the creation of an Associate Research Unit (URA) rather than to direct entry into CERFACS as a shareholder itself. SUC URA (for ”Sciences of the Universe” at CERFACS) was created in 1998, renewed in 2002, again in 2006 and 2010, each time for 4-year terms. This team was very well evaluated by the HCERES agency in 2014-2015 and since January 2016, this URA has been evolved in ”**Climate, Environment, Coupling, Uncertainties**” CECI **UMR 5318**. This partnership is very satisfactory for all partners. This research unit is built from an organizational point of view in GLOBC team, even if it has relationships with the other CERFACS teams. Its activities are ongoing to the satisfaction of the CNRS and the CERFACS on climate variability and change, Aviation and Environment, Coupling Tools, Data Assimilation, HPC, Big data & Uncertainty quantification. It should also be noted that this unit can accommodate some CNRS permanent researchers and engineers in CERFACS (5 so far).
- With CEA: Different departments and CEA laboratories are interested in the activities of CERFACS, particularly in the field of climate modelling, hydraulics and software; but when CERFACS turned into civil society, CEA did not wish to acquire stakes in the civil society. However, CEA has decided to continue since 1997 the collaboration with CERFACS: an agreement is regularly renewed (the latter one going to December 2024). In consideration for the license to use specific software developed by CERFACS, their maintenance and the provision of new releases and rights granted to CEA, CEA agrees to provide each year to CERFACS an access to Computing Center Research and Technology (CCRT) and gives to CERFACS a financial contribution.
- With Inria: Established in November 2009 for 4 years, the first action was a joint laboratory with the HiePACS project (Highly Scalable Parallel Algorithms for Numerical Simulations borders) whose objective was to develop multidisciplinary advanced skills in applied mathematics and computer HPC

to treat multiscale simulations borders on machines petaflops and exaflops. This allowed cooperation between Inria Bordeaux and the ALGO and CFD teams. One Inria researcher is welcomed in CERFACS. Since September 1, 2022, a joint Inria, AIRBUS & Cerfacs team has been created : CONCACE ≪ COmposabilité Numérique et parallèle pour le Calcul haute performanCE ≫.

- With IRIT: IRIT is a leading player in research in computer science and algorithmics for linear algebra, control and optimization and wishes to develop its activities in the field of high performance computing in connection with industrial applications. CERFACS develops advanced methods for scientific computing and numerical simulation high performance, both for research and for industrial applications. The ALGO team in CERFACS and APO team in IRIT have a significant history of collaboration. This agreement is under discussion to be renewed.
- CERFACS is member of IRT (Technological Research Institute) Saint-Exupery and member of ANITI, the Artificial and Natural Intelligence Toulouse Institute with the participation of 2 senior researchers in each of them.

This activity report is written in independent parts so that readers interested mainly in a particular field will easily find both a detailed description of the work that has been achieved, and a complete list of references, including papers in the reviewed literature and internal reports (which can be made available upon request). I sincerely hope that through the detailed reports of the teams you will find interest to continue our collaboration or to initiate new ones.

Enjoy your reading.

Dr Catherine LAMBERT - CERFACS President

CERFACS Structure

As a “Société par Actions Simplifiées” CERFACS is governed by two bodies.
Firstly, the “Comité stratégique”, composed of 7 experts nominated by the 7 shareholders (see table i), follows quite closely the CERFACS activities and the financial aspects. It meets four times per year.
Secondly, the Board of Governors is composed of the 7 representatives of CERFACS shareholders and of 2 invited personalities, including the Chairman of the Scientific Council. It meets twice a year.

CERFACS Scientific Council met 3 times during this period 2021-2023 under the chairmanship of Dr Jean-François Minster and then Jean-Yves Berthou.

CENTRE NATIONAL D’ETUDES SPATIALES (CNES)	21.31%
METEO-FRANCE	21.31%
AIRBUS	13.11%
ELECTRICITE DE FRANCE (EDF)	13.11%
SAFRAN	13.11%
OFFICE NATIONAL D’ETUDES ET DE RECHERCHES AEROSPATIALES (ONERA)	9.02%
TOTAL	9.02%

Table i: CERFACS Shareholders with the % of participation

The general organization of CERFACS is depicted in the following CERFACS chart.

CERFACS chart as of Dec. 31, 2023

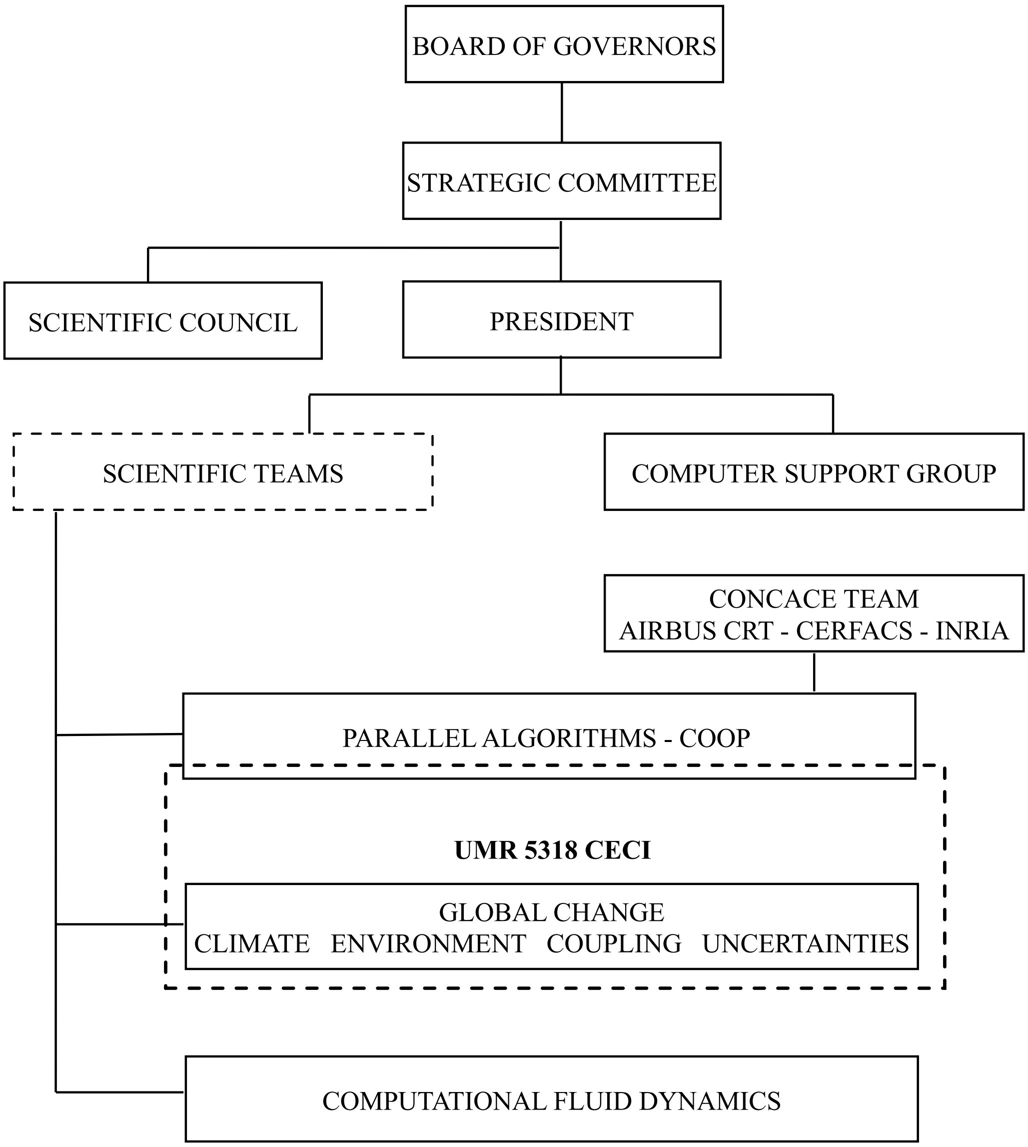

CERFACS Staff

The staff of the scientific teams and of the computing support group, consisting of, on December 31, 2023, a total of 152 scientists and technical staff is shown in Tables ii, iii, and iv.

POSITION	ALGO-COOP	CFD	CSG	GLOBC
Team Leader	0,2	0,3	1,0	0,2
Senior	6,4	8,3	0,0	6,9
Research Engineer	1,5	5,2	4,0	11,1
Post Doc	4,5	13,5	0,0	3,0
Ph.D Student	9,4	40,5	0,0	10,6
Studies Engineer	4,2	6,6	0,0	1,6
Trainee-Teacher	0,4	6,4	0,0	2,3
Consultant	0,4	0,4	0,0	1,0
Technician	0,7	0,0	1,0	0,0

Table ii: 2021 Full time equivalent teams distribution.

POSITION	ALGO-COOP	CFD	CSG	GLOBC
Team Leader	0,2	0,3	1,0	0,2
Senior	6,9	9,8	0,0	6,3
Research Engineer	3,1	4,6	4,0	14,8
Post Doc	1,8	15,5	0,0	1,0
Ph.D Student	9,6	41,5	0,0	12,3
Studies Engineer	3,9	5,9	0,0	2,3
Trainee-Teacher	1,8	6,2	0,2	1,2
Consultant	0,4	0,5	0,0	1,2
Technician	0,2	0,0	1,0	0,0

Table iii: 2022 Full time equivalent teams distribution.

POSITION	ALGO-COOP	CFD	CSG	GLOBC
Team Leader	0,2	1,0	1,0	0,2
Senior	6,8	10,0	0,0	5,0
Research Engineer	2,9	5,2	4,0	11,4
Post Doc	3,0	13,6	0,0	2,5
Ph.D Student	7,2	47,3	0,0	10,8
Studies Engineer	2,4	6,5	0,0	2,4
Trainee-Teacher	1,7	4,0	0,0	0,2
Consultant	0,4	1,0	0,0	0,9
Technician	1,0	0,0	0,0	0,0

Table iv: 2023 Full time equivalent teams distribution.

CERFACS Wide-Interest Seminars

François Rogier, Jérôme Morio, Sidonie Lefèvre, Eric Savin et Guillaume Puigt (ONERA) *Présentation du LMA2S (Laboratoire de Mathématiques Appliquées à l'Aéronautique et au Spatial), le laboratoire de Mathématiques Appliquées de l'ONERA.* (2021, March 5th)

Christine Mounaïm-Rousselle (Laboratoire PRISME, Université d'Orléans.) *Ammoniac comme combustible : où en sommes nous ?* (2021, March 18th)

Catherine TESSIER (ONERA, Toulouse) *Sensibilisation à l'intégrtité scientifique.* (2022, January 10th)

Travis Mitchel (University of Queensland.) *The phase field lattice Boltzmann method and its efficient implementation on multi-GPU architectures with TCLB.* (2022, June 24th)

Nicolas GOURDAIN, Jérôme FONTANE (ISAE-SUPAERO.) *Les améliorations technologiques peuvent-elles rendre l'aviation compatible avec l'accord de Paris ?* (2022, November 21st)

Pierre Kestener (CEA) *Refactoring code Abinit for GPU computing: an overview of difficulties and solutions* (2023, March 7th)

Laurent Joly, Director of the Institute for Sustainable Aviation Scott Delbecq, Associate Professor at ISAE-SUPAERO Thomas Planès, Associate Professor at ISAE-SUPAERO *Interdisciplinarity for a science with impact? The case of the Institute for Sustainable Aviation and the development of a sectoral IAM.* (2023, October 16th)

Mohsen Talei (University of Melbourne) *Integration of renewable gas with the energy network and its impact on end users for a science with impact?* (2023, December 21st)

1

Parallel Algorithms and COOP

Introduction

The Algo-COOP team conducts research on advanced numerical algorithms, high performance computing (HPC) and on scientific software to address the solution of problems in Computational Science and Engineering on massively parallel computing platforms. Thus Algo-COOP studies the design, the analysis, and the implementation of novel methods for current supercomputers. One critical point is the very high computational cost when high fidelity results and thus increasingly larger and more complex systems must be solved. Then highly efficient algorithms both in memory and computational cost are crucial. This refers both to the classical linear and nonlinear solvers for dense and sparse problems, as well as to topics such as parallel mesh generation, partitioning, and load balancing. Furthermore, new methods are required for complex nonlinear problems or when the stochastic nature must be considered.

Increasingly also the traditional software techniques have proven inadequate to deal with the quickly evolving complexity of applications and the heterogeneous nature of current HPC architectures. Especially the dominance of GPUs in high-end systems has triggered the need to rethink algorithms and software. As a consequence, we have also seen a renewed interest in using reduced floating point precision. With all these continuing changes, the sustainability of scientific software has become a major concern. This is the driving force behind the recent Algo-COOP research activities aimed to protect the investment in HPC software. This is crucial since software typically has a much longer lifetime than the HPC systems on which it runs. Partly this issue has been addressed by research on using code metrics on large scale scientific codes, but it has also been the driver behind our projects on automatic code generation and using domain specific languages.

Algo-COOP builds on more than three decades of successful work on parallel numerical methods at the forefront of computational mathematics and HPC, constantly expanding its scope into new areas. The field is characterized by the continued progress in computer technology to ever higher degree of parallelism so that constantly new algorithms with improved scalability are needed. The trend towards using an abundance of data from sensors and measurements (e.g., from satellites) creates further algorithmic challenges. Especially the advent of new computational paradigms, such as machine learning and artificial intelligence (AI) has created new challenges and opportunities for HPC applications. Especially AI has reached overarching importance potentially having a deep impact on scientific computing in general, and HPC, in particular. These latter activities are also linked to data driven approaches that have been central to Algo-COOP research in the form of data assimilation research. Further oriented at the future, research has also been started on special aspects of quantum computing for scientific applications.

In many applications, classical forward simulations are the building blocks for more complex and challenging computational goals. These include optimizaton problems, inverse problems, and novel data driven computing methods, such as the need to produce massive amounts of input for advanced deep learning methods. In the past years, Algo-COOP has successfully developed such new research directions. In this wide field, the specific Algo-COOP focus lies on physically and mathematically well-founded approaches. Therefore these activities do not only include mainstream AI techniques, but also the systematic quantification of uncertainties.

Naturally the listed research topics are broad, but they are also closely interconnected. In particular, the efficient solution of large linear systems remains a central building block for many scientific computing problems. Consequently, more than ever, many recent developments rely on the broad scientific expertise available in the Algo-COOP team. This includes mathematical topics such as numerical analysis, partial differential equation, data assimilation, stochastics on the one side, but also expertise in advanced

software engineering, computer architecture, performance analysis, meshing and load balancing, artificial intelligence and workflow management, on the other. For the past success at Algo-COOP, it has been essential to have this wide range of research expertise available in a productive and collaborative environment.
Beyond the internal interaction, Algo-COOP research is frequently performed in collaboration with the shareholders of CERFACS, with FAU, with INRIA, with IRIT, or with other external partners, often within large scale European projects. For example, linear algebra and solvers-related research activities have often been conducted jointly with colleagues at IRIT or with INRIA (in the new joint Concace lab), while data assimilation research is jointly done with ECWMF and the AI-related topics are often associated with the ANITI project. Research using Lattice Boltzmann methods and automated code generation, on the other hand, relies on the availability of the WALBERLA, a parallel open source Lattice-Boltzmann framework developed in collaboration with FAU in Erlangen. Two PhD students of the Algo-COOP team have graduated both at French universities and at FAU Nuremberg in cotutelle-agreements, one further such PhD is under way.
We emphasize that the role of Algo-COOP within CERFACS is to bridge from the fundamental results in mathematics and computer science to problems coming from real-life applications. Thus, researchers in the team do not only suggest and analyse novel parallel algorithms and methods (such as new approaches involving AI techniques), but they also work on realising them on advanced computer architectures (such as GPUs) for the benefit of collaborators within and outside of CERFACS.
Finally, Algo-COOP takes an active part in the training programme at CERFACS and it maintains a well-received blog on HPC-related issues. Algo-COOP members have also been regularly attending and organizing seminars, workshops and international conferences in numerical optimization, numerical linear algebra, high performance computing, computational science and engineering, and data assimilation. A special highlight was the organization of the workshop “Sparse Days” in Saint-Girons in 2022, with J. Dongarra, the year’s Turing-Award winner, as keynote speaker.

Ulrich Ruede

Numerical Linear Algebra

2.1 Multigrid methods

2.1.1 Geometric multigrid methods for plasma fusion applications

In the context of the Energy oriented Center of Excellence, we have developed a geometric multigrid algorithm for the solution of a 2D Poisson-like problem

$$-\nabla \cdot (\alpha \nabla u) = f \text{ in } \Omega \tag{2.1}$$

with Ω being some specified domain and $\alpha : \mathbb{R} \to \mathbb{R}$ being a varying coefficient, also refered to as *density profile* [ALGO-COOP68, ALGO-COOP69]. This gyrokinetic Poisson equation arises as a subproblem of Tokamak fusion reactor simulations. It is often posed on disk-like cross sections of the Tokamak that are represented in generalized polar coordinates. On the resulting curvilinear anisotropic meshes, we discretize the differential equation by finite differences or low order finite elements. In the case of finite differences, we use a direct discretization of the energy functional that induces a discretization of the differential operator. Following this approach, the discrete equations are naturally symmetric if the energy functional was self-adjoint, a property that may be lost when using standard difference formulas on nonuniform meshes or when the differential operator has varying coefficients. Low order finite difference systems can be derived by this approach in a systematic way and on logically structured meshes they become compact difference formulas. Furthermore, using an implicit extrapolation technique similar to multigrid τ-extrapolation, the approximation order can be increased. This technique can be naturally integrated in a matrix-free geometric multigrid algorithm. Special smoothers are developed to deal with the mesh anisotropy arising from the polar coordinate system and mesh grading. Representative numerical results for the order of convergence of the different methods are presented in Figure 2.1

One goal of the development of our solver, that we call GMGPolar, was its integration into GyselaX developed at CEA. In a follow-up reseach, we compared our solver to two existing solvers finely tuned to solve this problem, in terms of the accuracy of the solution, and their computational efficiency [ALGO-COOP42]. We also consider practical implementation aspects, including the parallel efficiency of the code, potentially enabling an integration of the solvers in a state-of-the-art first-principle gyrokinetic simulation framework. The first, the Spline FEM solver, uses C1 polar splines to construct a finite element method which solves the equation on curvilinear coordinates. The resulting linear system is solved using a conjugate gradient method. The second, the GMGPolar solver, uses a symmetric finite difference method to discretise the differential equation. The resulting linear system is solved using a tailored geometric multigrid scheme, with a combination of zebra circle and radial line smoothers, together with an implicit extrapolation scheme. The third, the Embedded Boundary solver, uses a finite volume method on Cartesian coordinates with an embedded boundary scheme. The resulting linear system is solved using a multigrid scheme. The Spline FEM solver is shown to be the most accurate. The GMGPolar solver is shown to use the least memory. The Embedded Boundary solver is shown to be the fastest in most cases. All three solvers are shown to be capable of solving the equation on a realistic non- analytical geometry.

2.1.2 Multigrid methods for the hybrid high order (HHO) discretization

The use of modern discretization technologies such as hybrid high-order (HHO) methods, coupled with appropriate linear solvers, allow for the robust and fast solution of partial differential equations (PDEs).

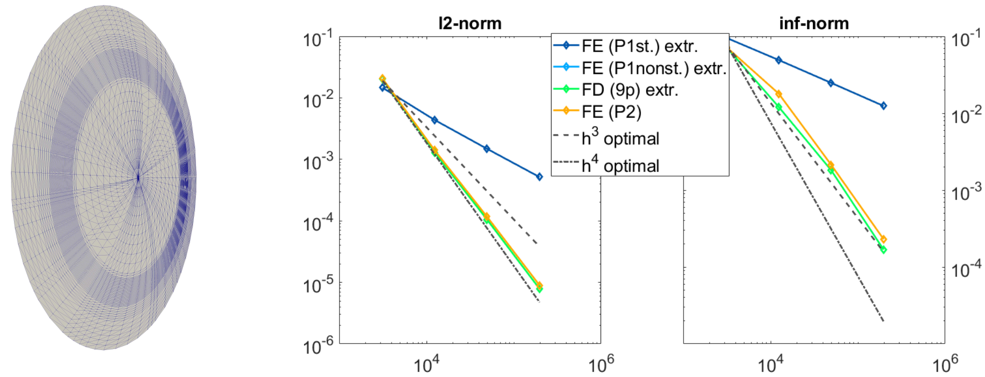

Figure 2.1: Left: Mesh for a disk-like domain, obtained as mapping F from cartesian to generalized polar coordinates [ALGO-COOP68]. Right: Error convergence in ℓ_2- and $\inf$-norm for direct solution of finite difference and finite element discretizations for $-\nabla \cdot (\alpha \nabla u) = f$ in $\Omega_L = (\mathbf{10^{-6}}, 1.3) \times [0, 2\pi)$, for an f, $\Omega = F(\Omega_L)$ and parameters given in [ALGO-COOP69], Dirichlet boundary conditions in r, periodic boundary conditions in θ.

Although efficient linear solvers have recently been made available for simpler cases, complex geometries remain a challenge for large-scale problems.

2.1.2.1 An h-Multigrid Method for HHO Discretizations

In [ALGO-COOP47], we consider a second-order elliptic PDE discretized by the hybrid high-order method, for which globally coupled unknowns are located at faces. To efficiently solve the resulting linear system, we propose a geometric multigrid algorithm that keeps the degrees of freedom on the faces at every grid level. The core of the algorithm lies in the design of the prolongation operator that passes information from coarse to fine faces through the reconstruction of an intermediary polynomial of higher degree on the cells. High orders are natively handled by the use of the same polynomial degree at every grid level. The proposed algorithm requires a hierarchy of nested meshes, such that the faces (and not only the elements) are successively coarsened. Numerical tests on homogeneous and heterogeneous diffusion problems show fast convergence, scalability in the mesh size and polynomial order, and robustness with respect to heterogeneity of the diffusion coefficient.

2.1.2.2 Towards robust, fast solutions of elliptic equations on complex domains through HHO discretizations and non-nested multigrid methods

In [ALGO-COOP48], we propose a geometric multigrid algorithm for unstructured non-nested meshes. The non-nestedness is handled in the prolongation operator through the use of the L^2-orthogonal projection from the coarse elements onto the fine ones. However, as the exact evaluation of this projection can be computationally expensive, we develop a cheaper approximate implementation that globally preserves the approximation properties of the L^2-orthogonal projection. Additionally, as the multigrid method requires not only the coarsening of the elements, but also that of the faces, we leverage the geometric flexibility of polytopal elements to define an abstract non-nested coarsening strategy based on element agglomeration and face collapsing. Finally, the multigrid method is tested on homogeneous and heterogeneous diffusion problems in two and three space dimensions. The solver exhibits near-perfect asymptotic optimality for moderate degrees of approximation.

2.1.2.3 High-order multigrid strategies for HHO discretizations of elliptic equations

In [ALGO-COOP51], we compare various multigrid strategies for the fast solution of elliptic equations discretized by the hybrid high-order method. Combinations of h-, p-, and hp-coarsening strategies are considered, combined with diverse intergrid transfer operators. Comparisons are made experimentally on 2D and 3D test cases, with structured and unstructured meshes, and with nested and non-nested hierarchies. Advantages and drawbacks of each strategy are discussed for each case to establish simplified guidelines for the optimization of the time to solution.

2.1.2.4 Algebraic Multigrid Preconditioner for Statically Condensed Systems Arising from Lowest-Order Hybrid Discretizations

In [ALGO-COOP49], we address the numerical solution of linear systems arising from the hybrid discretizations of second-order elliptic partial differential equations. Such discretizations hinge on a hybrid set of degrees of freedom (DoFs), respectively, defined in cells and faces, which naturally gives rise to a global hybrid system of linear equations. Assuming that the cell unknowns are only locally coupled, they can be efficiently eliminated from the system, leaving only face unknowns in the resulting Schur complement, which is also called the statically condensed matrix. We propose in this work an algebraic multigrid (AMG) preconditioner specifically targeting condensed systems corresponding to lowest-order discretizations (piecewise constant). Like traditional AMG methods, we retrieve geometric information on the coupling of the DoFs from algebraic data. However, as the condensed matrix only gives information on the faces, we use the uncondensed version to reconstruct the connectivity graph between elements and faces. An aggregation-based coarsening strategy mimicking a geometric coarsening or semicoarsening can then be set up to build coarse levels. Numerical experiments are performed on diffusion problems discretized by the hybrid high-order method at the lowest order. Our approach uses a K-cycle to precondition an outer flexible Krylov method. The results demonstrate similar performances, in most cases, compared to a standard AMG method and a notable improvement on anisotropic problems with Cartesian meshes.

2.1.2.5 Fast Linear Solvers for Incompressible CFD Simulations with Compatible Discrete Operator Schemes

Finding a robust and efficient solver for (non-)symmetric systems that arise in incompressible Computational Fluid Dynamics (CFD) is of great interest to both academia and industry. We consider the Compatible Discrete Operator (CDO) discretization that has recently been devised for CFD simulations in the context of incompressible Stokes and Navier-Stokes flows. The discrete problems resulting from CDO schemes yield large saddle-point systems that require relevant numerical methods suitable to deal with large indefinite and poorly conditioned linear systems. In [ALGO-COOP108], we focus on two segregated methods: the augmented Lagrangian Uzawa method and the generalized Golub-Kahan bidiagonalization, as well as a monolithic method based on an algebraic transformation by change of variables. We also employ algebraic multigrid (AMG) preconditioned Krylov solvers such as the Flexible Conjugate Gradient (FCG) method, and the Flexible Generalized Minimal Residual (FGMRES) method, to solve the linear systems. Using the CFD software code saturne, we compare the numerical performance with respect to the choice of linear solvers and numerical strategies for the saddle-point problem. In the numerical experiments, the AMG preconditioned Krylov methods show robustness in test cases of Stokes and Navier-Stokes problems.

2.2 Solution techniques for indefinite systems with block structure

2.2.1 Extensions of the Augmented Block Cimmino Method to the Solution of Full Rank Rectangular Systems

For the solution of large sparse unsymmetric systems, Duff et al. al. [SIAM J. Sci. Comput., 37 (2015), pp. A1248–A1269] proposed an approach based on the block Cimmino iterations in [Numer. Math., 35 (1980), pp. 1–12], in which the solution is computed in a single iteration, so we call it a pseudodirect solver. In this approach, matrices are augmented with additional variables and constraints so that a partitioning of the matrix in blocks of rows defines mutually orthogonal subspaces. The augmented system can then be solved efficiently with a sum of projections onto these orthogonal subspaces. In [ALGO-COOP54], we present an extension of this method to the minimum norm solution of underdetermined systems and to the solution of least-squares problems. In the latter case, a partitioning of the matrix in blocks of columns rather than rows is used, and the system must be suitably augmented to define mutually orthogonal subspaces again to recover the least-squares solution of the original problem. This article proves the equivalence between the solution of the original and the augmented system. In order to complete the extension to overdetermined systems, we also propose an iterative block conjugate gradient acceleration [SIAM J. Sci. Comput., 16 (1995), pp. 1478–1511] for the solution of least-squares problems. The efficiency of both the iterative and the augmented pseudodirect approaches, as implemented in the ABCD-Solver, is illustrated on large rectangular matrices from the SuiteSparse Matrix Collection. - While writing the cited article, we have learnt with great sadness that our co-author, long-term collaborator, advisor, and good friend Constantin Popa passed away. We would like to dedicate this work to his memory.

2.2.2 Fast iterative solvers for thermo-hydro-mechanic models for an underground nuclear waste disposal facility

The following research has been inspired by the Cigéo project which is about the construction of an underground nuclear waste disposal facility. The detailed modeling of underground phenomena is of major interest in several industrial fields ranging from oil and gas to nuclear waste storage and civil engineering. This is particularly the case for coupled phenomena where several physics come into play and can make it difficult to understand their respective influences. Nuclear waste storage is an illustrative example of a thermo-hydro-mechanics (THM) coupled problem. Nuclear wastes generate heat that increases the fluid and soil temperature, thus changing not only the volume of each phase due to thermal expansion but also the values of the material parameters which are functions of temperature. The numerical simulation of these problems results in the solution of a coupled system of nonlinear partial differential equations (PDE). Due to implicit time discretization, often preferred for its unconditional stability, the solution of large ill-conditioned linear systems turns out to be the heaviest task in terms of computational burden. The design of scalable parallel solvers is thus an essential topic to benefit from the massive computational power of computer architectures. This is the concern of this research work. We are interested in the development of fast iterative solvers for the solution of PDEs obtained in the modelling of saturated THM problems that describe the behavior of a soil in which a weakly compressible fluid evolves. It is used for the evaluation of the THM impact of high-level activity radioactive waste exothermicity within a deep geological disposal facility. We developed a block preconditioner for the fully coupled THM equations [ALGO-COOP74]. We investigated Block Jacobi and Block Gauss-Seidel variants for the preconditioner, where both share the same tailored sub-solvers (Krylov methods preconditioned by AMG preconditioners). Numerical results reflect the good performance of the proposed preconditioners in terms of strong and weak scalability. Weak scalability is achieved until more than 2000 cores (see Figure 2.2) and more than one billion degrees of freedom. The final solver has been implemented within PETSc. Through this interface, it has furthermore been made available for simulations in code_aster at EDF.

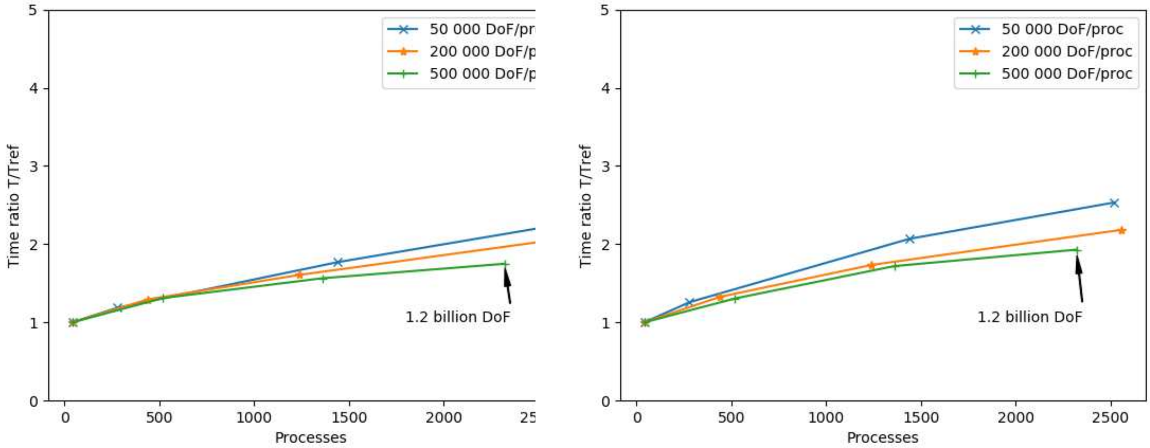

(a) Block Jacobi preconditioner (b) Block lower Gauss-Seidel preconditioner

Figure 2.2: Weak scalability

2.2.3 Inexact inner-outer Golub-Kahan bidiagonalization method: A relaxation strategy

In [ALGO-COOP45], we study an inexact inner-outer generalized Golub-Kahan algorithm for the solution of saddle-point problems with a two-times-two block structure. In each outer iteration, an inner system has to be solved which in theory has to be done exactly. Whenever the system is getting large, an inner exact solver is, however, no longer efficient or even feasible and iterative methods must be used. We focus in this work on a numerical study showing the influence of the accuracy of an inner iterative solution on the accuracy of the solution of the block system. Emphasis is further given on reducing the computational cost, which is defined as the total number of inner iterations. We develop relaxation techniques intended to dynamically change the inner tolerance for each outer iteration to further minimize the total number of inner iterations. We illustrate our findings on a Stokes problem and validate them on a mixed formulation of the Poisson problem.

2.2.4 Deflation for the off-diagonal block in symmetric saddle point systems

Deflation techniques are typically used to shift isolated clusters of small eigenvalues in order to obtain a tighter distribution and a smaller condition number. Such changes induce a positive effect in the convergence behavior of Krylov subspace methods, which are among the most popular iterative solvers for large sparse linear systems. In [ALGO-COOP105], we develop a deflation strategy for symmetric saddle point matrices by taking advantage of their underlying block structure. The vectors used for deflation come from an elliptic singular value decomposition relying on the generalized Golub-Kahan bidiagonalization process. The block targeted by deflation is the off-diagonal one since it features a problematic singular value distribution for certain applications. One example is the Stokes flow in elongated channels, where the off-diagonal block has several small, isolated singular values, depending on the length of the channel. Applying deflation to specific parts of the saddle point system is important when using solvers such as CRAIG, which operates on individual blocks rather than the whole system. The theory is developed by extending the existing framework for deflating square matrices before applying a Krylov subspace method like MINRES. Numerical experiments confirm the merits of our strategy and lead to interesting questions about using approximate vectors for deflation.

2.3 Linear solvers with artificial intelligence techniques

In this work, we investigate the training and use of an artificial neural network for the preconditioning of large linear systems. The aim is to solve a large linear system, which is a discretisation of a Helmholtz differential equation, as quickly as possible using a preconditioned Krylov-like iterative method such as Flexible GMRES. The implementations are written in Python and are divided into two main repositories: one for the Flexible GMRES algorithm, and another for learning neural networks. Currently, a preconditioning matrix is built column by column by solving a set of large sparse block structured least squares problems. This method is relatively easy to implement, but suffers from high computational cost and consequently high energy consumption. Furthermore, although we are considering a parametrized family of linear systems, we have to recalculate a preconditioner each time the parameters change. Since a neural network aims to approximate a complex functional dependence of any kind, it is a natural idea to use it to build a parameter invariant preconditioner to speed up convergence. We will present in detail a different approach to learning the neural network, along with several architectures that have been tested in this work. We will show with some examples that the naive approach of building a preconditioner in an unsupervised way suffers from the lack of knowledge of the data distribution of the Krylov basis vectors that appear during the FGMRES iterations. As a result, this paper demonstrates a particular iterative algorithm for learning a network. The main difficulty in implementing this type of algorithm stems from the fact that the differentiation of several iterative steps becomes numerically unstable and leads to the explosion of gradients. To overcome this difficulty, we use a replay buffer during training, which is a known approach from the reinforcement learning domain where it is used to collect experience for an agent parameters update. We will detail the different learning strategies where the replay buffer is used and explicitly show its advantages and any numerical challenges that arise. We will also present the implementation details of different learning strategies and neural network architectures.

2.4 Block low-rank single precision coarse grid solvers for extreme scale multigrid methods

Extreme scale simulation requires fast and scalable algorithms, such as multigrid methods. To achieve asymptotically optimal complexity, it is essential to employ a hierarchy of grids. The cost to solve the coarsest grid system can often be neglected in sequential computings, but cannot be ignored in massively parallel executions. In this case, the coarsest grid can be large and its efficient solution becomes a challenging task. In [ALGO-COOP43], we propose solving the coarse grid system using modern, approximate sparse direct methods and investigate the expected gains compared with traditional iterative methods. Since the coarse grid system only requires an approximate solution, we show that we can leverage block low-rank techniques, combined with the use of single precision arithmetic, to significantly reduce the computational requirements of the direct solver. In the case of extreme scale computing, the coarse grid system is too large for a sequential solution, but too small to permit massively parallel efficiency. We show that the agglomeration of the coarse grid system to a subset of processors is necessary for the sparse direct solver to achieve performance. We demonstrate the efficiency of the proposed method on a Stokes-type saddle point system solved with a monolithic Uzawa multigrid method. In particular, we show that the use of an approximate sparse direct solver for the coarse grid system can outperform that of a preconditioned minimal residual iterative method. This is demonstrated for the multigrid solution of systems of order up to 10^{11} degrees of freedom on a petascale supercomputer using 43,200 processes.

2.5 Randomized linear algebra

Advances in data collection and numerical simulation have changed the dynamics of scientific research and motivated the need for randomized algorithms to surmount challenges of complexity, robustness and scalability. Randomized algorithms are particularly powerful in tackling solutions of large-scale nonlinear inverse problems, and PDE constrained optimization that are not amenable to conventional deterministic approaches. Randomized algorithms, use random sampling and parallel computations to create a low-rank approximation a m-by-n matrix A which captures most of the essential information of the original matrix while being computationally efficient. Efficient low rank approximations play a key role in many geophysical applications and data analysis. Since these approaches are probabilistic approaches, especially in numerical linear algebra they weren't widely used when they are first introduced. The recognition of these approaches took some time and only in the early 2000s, practical randomized algorithms for low-rank matrix approximation and least-squares problems are introduced. Inspired by this research, Halko et al. [2011] [1] proposed an efficient algorithm now widely known as the Randomized SVD (RSVD) algorithm together with the stochastic analysis of the randomized low rank approximation error in the standard Gaussian case. A thorough understanding of error analysis has played a crucial role in making randomized approaches more practical and valuable across a diverse set of applications including data assimilation (see section 3.3).

The theoretical analysis of the randomized algorithms is critical for providing guarantees on their behavior, and in this regard, the stochastic analysis of the randomized low rank approximation error in the Gaussian case plays a central role. Indeed, several randomized methods for the approximation of dominant eigen or singular modes recently proposed can be rewritten as low rank approximation methods. However, despite the large variety of algorithms, the existing theoretical frameworks for their analysis rely on specific structure for the covariance matrix which are not adapted to all the algorithms. In this project, we propose a general framework for the stochastic analysis of the low rank approximation error in Frobenius norm for centered and non-standard Gaussian matrices. We propose bounds in expectation and in probability that hold under minimalist assumptions on the covariance matrix. Our bounds have clear interpretations that enable to derive properties and practical choices for the covariance matrix resulting in efficient low-rank approximation algorithms. We then illustrate the versatility of our general result by deriving analysis for two known cases. A comparison with the corresponding prior works shows that our bounds have comparable accuracy. Finally, we present numerical experiments on a data assimilation toy problem.

[1] N. Halko, P. G. Martinsson, and J. A. Tropp. Finding structure with randomness: Probabilistic algorithms for constructing approximate matrix decompositions. SIAM Review, 53, 2011.

Data assimilation

3.1 Multilevel and multifidelity methods for data assimilation

3.1.1 Multivariate extensions of the Multilevel Best Linear Unbiased Estimator for ensemble-variational data assimilation

Multilevel estimators aim at reducing the variance of Monte Carlo statistical estimators, by combining samples generated with simulators of different costs and accuracies. In particular, the recent work of [8] on the multilevel best linear unbiased estimator (MLBLUE) introduces a framework unifying several multilevel and multifidelity techniques. In [ALGO-COOP102], the MLBLUE is reintroduced using a variance minimization approach rather than the regression approach of [8]. We then discuss possible extensions of the scalar MLBLUE to a multidimensional setting, i.e., from the expectation of *scalar* random variables to the expectation of random *vectors*. Several estimators of increasing complexity are proposed: a) multilevel estimators with scalar weights, b) with element-wise weights, c) with spectral weights and d) with general matrix weights. The computational cost of each method is discussed. We finally extend the MLBLUE to the estimation of second-order moments in the multidimensional case, i.e., to the estimation of covariance matrices. The multilevel estimators proposed are d) a multilevel estimator with scalar weights and e) with element-wise weights. In large-dimension applications such as data assimilation (DA) for geosciences, the latter estimator is computationnally unaffordable. As a remedy, we also propose f) a multilevel covariance matrix estimator with optimal multilevel localization, inspired by the optimal localization theory of [6]. Some practical details on weighted MLMC estimators of covariance matrices are also provided.

3.1.2 Multilevel Monte Carlo estimation of background error covariances in ensemble-variational data assimilation

In ensemble variational (EnVar) DA systems, background-error covariances are sampled from an ensemble of forecasts evolving with time. One possible way of generating this ensemble is by running an Ensemble of Data Assimilations (EDA) that samples all possible error sources (initial condition errors, boundary condition errors, model errors). Large ensemble sizes are desirable to minimize sampling errors, but generating a single ensemble member is usually expensive due to the cost of integrating the physical model. In practice, ensembles with coarser spatial resolutions are sometimes used, allowing for cheaper generation of individual members, and thus larger ensemble sizes.

Multilevel Monte Carlo (MLMC) methods propose to go beyond this usual trade-off between grid resolution and ensemble size, by expressing a fine-grid estimator as an astute combination of estimators computed on a hierarchy of spatial grids. Starting from a Monte Carlo covariance estimator on a coarse grid but with a large ensemble size, correction terms are added to form a quasi-telescopic sum. The correction terms come from EDAs of increasing spatial resolutions and decreasing ensemble sizes, with a pairwise stochastic coupling between EDAs of two successive resolutions. The expectation of this MLMC estimator is equal to the expectation of the Monte Carlo estimator on the finest grid, so that no bias is introduced by the coarse resolution forecasts. Without increasing the computational cost, MLMC effectively reduces the variance of the covariance estimator, i.e., reduces the sampling noise on covariances. In [ALGO-COOP4], we presented the theoretical basis of MLMC and described how it could be applied to the multilevel estimation of covariance matrices. The proposed approach was illustrated on a quasi-geostrophic model by comparing the usual single-resolution ensemble estimate with the MLMC estimate, in terms of mean square error of the covariance estimators, and in terms of quality of the resulting analyses for one assimilation cycle.

3.2 Data assimilation and Machine Learning

This activity falls within the framework of the Data Assimilation and Machine Learning chair of the Artificial and Natural Intelligence Toulouse Institute (ANITI). The objective of the chair is to promote a synergy between data assimilation (DA) and machine learning (ML) to study new algorithms as well as their efficient implementation on modern computer architectures. Data-driven methods to forecast dynamics through time using ML has become very popular and lead to numerous studies. These research works have influenced two new ideas for merging DA with ML: ML assisted by DA and DA using ML techniques. On the one hand, DA methodologies help ML approaches especially when the available data are noisy and sparse. On the other hand, ML methodologies help DA to handle more complex models and error distributions. The main topic addressed in this activity is to explore how ML can improve the performance of well-established techniques in DA, both in terms of accuracy and in the use of computational resources. Two main activities within this chair are detailed in the following subsections.

3.2.1 Latent space data assimilation by using deep learning

We have exploited the latent structure provided by auto-encoders to design a latent-space filtering algorithm based on the ensemble transform Kalman filter with model-error correction (ETKF-Q). Model dynamics are also propagated within the latent space via a surrogate neural network. This novel ETKF-Q-Latent (ETKF-Q-L) algorithm has been tested on a tailored instructional version of the Lorenz 96 equations, named the augmented Lorenz 96 system, which possesses a latent structure that accurately represents the observed dynamics. Numerical experiments with this particular system show that the ETKF-Q-L approach both reduces the computational cost and provides better accuracy than state-of-the-art algorithms such as the ETKF-Q. These results are published in a journal paper [ALGO-COOP75]. We applied the proposed algorithm to a quasi-geostrophic (QG) model used within the Object Oriented Prediction System (OOPS). The numerical results show that QG model can be represented in a reduced dimension and performing DA within this reduced (latent) space may both improve the accuracy and reduce the computational cost.

3.2.2 Data Assimilation Networks: End-to-end learning

The Bayesian framework used in DA aims at estimating the posterior conditional probability density function based on the error statistics of noisy observations and the dynamical system. State-of-the-art DA methods used for ensemble DA are sub-optimal due to the common use of Gaussian error statistics and linearization of non-linear dynamics. To achieve a good performance, these methods based on the use of ensembles often require case-by-case fine-tuning by using explicit regularization techniques such as inflation and localization. We have proposed a fully data driven deep learning framework generalizing recurrent Elman networks and DA algorithms [ALGO-COOP41]. Our approach approximates a sequence of prior and posterior densities conditioned on noisy observations using a log-likelihood cost function. By construction, our approach can be used for general nonlinear dynamics and non-Gaussian densities. As a first step, we evaluated the performance of the proposed approach by using a fully and partially observed Lorenz-96 system in which the outputs of the recurrent network are fitted to Gaussian densities. Through numerical experiments, we showed that our approach, without using any explicit regularization technique, achieves comparable performance to the state-of-the-art methods, IEnKF-Q and LETKF, across various ensemble sizes.

3.3 Randomized algorithms for data assimilation

A thorough understanding of the error analysis of randomized algorithms (see section 2.5) has played a crucial role in making randomized approaches more practical and valuable across a diverse set of applications. These methods are now widely used in many applications including DA. For instance, [1] proposed to replace the traditional sequential Conjugate Gradients (CG) iterations with a fully parallel Randomized SVD (RSVD) approach within a variational DA algorithm. While the proposed method is parallelizable, it no longer guarantees a monotonic decrease of the quadratic subproblems like the CG method. This means that when the parallel RSVD method is truncated before convergence, there is no guarantee that the solution is better than the initial iterate. Instead, [2, 3] proposed using RSVD to estimate spectral information for a preconditioner for different formulations of a weak-constraint variational DA problem.

We have explored the use of RSVD with the standard strong-constraint formulation of variational DA. We first performed a detailed analysis of an approach where RSVD is used in combination with a deterministic spectral limited memory preconditioner (spectral-LMP). In the current operational setting at ECMWF and Météo-France, the spectral-LMP is derived from spectral information gathered during the preceding GN iteration. Consequently, the construction of the spectral-LMP only becomes possible at the start of the second GN iteration. Nevertheless, by employing RSVD, we can acquire spectral information as early as the first GN iteration, showcasing one of the principal advantages of integrating RSVD into this framework. We have already demonstrated the potential of RSVD in the PhD research conducted by [9], using the Lorenz-96 system. Furthermore, during the internship of [4], we have extended our numerical experiments to the QG model of OOPS. More recently, as part of the internship of [7], we have improved the convergence of CG by implementing a scaled RSVD-LMP. In this approach, we set the scaling parameter based on theoretical results that ensure better convergence. Further work aims at incorporating additional scaling parameters into the scaled LMP, conducting a thorough error analysis when spectral information is approximated, and performing numerical experiments within the OOPS framework.

3.4 Covariance modelling and estimation for data assimilation

3.4.1 Specifying background-error covariances from an Ensemble of Data Assimilations for global ocean initialization and reanalysis

As part of an EU-funded project for the Copernicus Climate Change Service (C3S), we have worked closely with ECMWF scientists to provide a step improvement in their ocean DA capabilities for operational forecasting and reanalysis [ALGO-COOP44]. One of the main objectives of the project was to develop an EDA to provide objective estimates of background error. For this purpose, we developed two different approaches for extracting information from ensembles to capture 'errors of the day' in the specification of the background-error covariances. In the first approach, an innovative estimation and filtering methodology has been developed to derive background-error variances and correlation length-scales from ensembles. This methodology was first applied to compute a seasonal climatology of background-error statistics which, after appropriate tuning, resulted in a significant improvement of the performance of the system even without errors of the day. A second approach was to use the ensemble perturbations to construct a localised sampled background-error covariance matrix to account for more complex covariance structures than can be achieved with existing methods. While the second approach still needs to mature, at some point it will be used to complement the modelled covariance matrix with climatological parameters in a hybrid representation of the background-error covariance matrix.

Many of new features in the background-error covariance matrix (developed largely by CERFACS) have been integrated into ECMWF's latest ocean DA system (OCEAN6), due to become operational in early

2024. In parallel, the UK Met Office, who are also partners in the development of the ocean DA software (NEMOVAR), applied the second approach above in an operational EDA configuration of the Met Office ocean forecasting system. Forecast performance from that system is also noticeably improved from the use of ensemble covariances [ALGO-COOP71]. As part of a new EU-funded C3S project, we are making further improvements to the ensemble-based background-error covariance matrix, notably to enable it to account for scale-dependent background errors.

3.4.2 Impact of correlated observation errors on the conditioning of variational data assimilation problems

An important class of nonlinear weighted least-squares problems arises from the assimilation of observations in atmospheric and ocean models. In variational DA, inverse error covariance matrices define the weighting matrices of the least-squares problem. For observation errors, a diagonal matrix (i.e., uncorrelated errors) is often assumed for simplicity even when observation errors are suspected to be correlated. While accounting for observation-error correlations should improve the quality of the solution, it also affects the convergence rate of the minimization algorithms used to iterate to the solution. If the minimization process is stopped before reaching full convergence, which is usually the case in operational applications, the solution may be degraded even if the observation-error correlations are correctly accounted for. In [ALGO-COOP58], we explore the influence of the observation-error correlation matrix ($\mathbf{R}$) on the convergence rate of a preconditioned conjugate gradient (PCG) algorithm applied to a one-dimensional variational DA (1D-Var) problem. We design the idealized 1D-Var system to include two key features used in more complex systems: we use the background error covariance matrix ($\mathbf{B}$) as a preconditioner (B-PCG); and we use a diffusion operator to model spatial correlations in $\mathbf{B}$ and $\mathbf{R}$ (e.g., as in [5]). Analytical and numerical results with the 1D-Var system show a strong sensitivity of the convergence rate of B-PCG to the parameters of the diffusion-based correlation models. Depending on the parameter choices, correlated observation errors can either speed up or slow down the convergence. In practice, a compromise may be required in the parameter specifications of $\mathbf{B}$ and $\mathbf{R}$ between staying close to the best available estimates on the one hand and ensuring an adequate convergence rate of the minimization algorithm on the other. An illustration is provided in Figure 3.1.

3.4.3 An evaluation of methods for normalizing diffusion-based covariance operators in variational data assimilation

Developing effective ways to model and cycle the background-error covariance matrix is an active area of research in DA. An important aspect of this problem when using a filter to model the background-error correlations is the computation of normalization factors to ensure that the diagonal elements of the modelled correlation matrix are all equal to one. Updating the parameters of a flow-dependent correlation model on each DA cycle requires updating the normalization factors, which is costly using traditional methods such as randomization.

In [ALGO-COOP94], we discuss the normalization problem within the context of a diffusion filter-based covariance model used for background-error modelling in a variational DA system for the global ocean. We evaluate various methods for estimating normalization factors when the diffusion tensor of the correlation model is derived from an ensemble of ocean states. Our results show that estimates produced using inexpensive methods derived from analytical considerations of the diffusion equation can have significant errors, especially near boundaries. Estimates obtained using randomization with a small sample size ($\sim$100) are more accurate in a globally averaged sense but are noisy and can have unacceptably large errors locally.

Next, we focussed on the specific problem of accounting for flow-dependent correlation parameters in the vertical component of the diffusion operator only, which is important for improving the assimilation

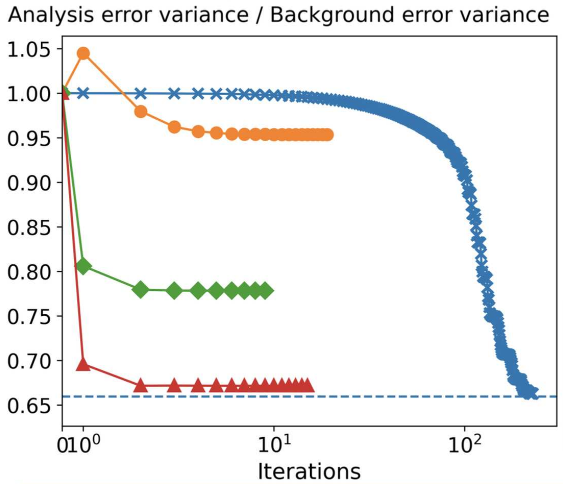

Figure 3.1: The effect of different parameter specifications in the observation-error covariance matrix ($\mathbf{R}$) on the convergence of the B-preconditioned conjugate gradient method, as measured by the ratio of the analysis error variance to the background error variance as a function of the B-PCG iteration counter. In this idealized experiment, the theoretical minimum is given by the horizontal dashed line. The blue curve corresponds to an experiment where the 'true' $\mathbf{R}$ parameters have been used. Convergence is very slow, but the theoretical minimum is eventually attained after an impractical number of iterations. The orange curve corresponds to an experiment where the correlations are neglected altogether. Convergence is much faster but the solution is far from the theoretical minimum. The green curve corresponds to an experiment where correlations are also neglected but the variance is optimally inflated. Convergence is faster and more accurate but the solution is still far from the theoretical minimum. Finally, the red curve corresponds to an experiment where correlations are retained but the spectral decay rate of the correlation function is adjusted to be 'less Gaussian'. Convergence is rapid and the solution is very close to the theoretical minimum ([ALGO-COOP47]).

of surface observations. Remarkably accurate estimates are obtained by approximating the normalization matrix as a separable product of two normalization matrices: one computed using randomization with the horizontal diffusion operator only and the other computed using randomization, or even an exact (brute-force) method, with the vertical diffusion operator only. If the parameters of the horizontal component of the diffusion operator are static then only the normalization factors of the flow-dependent vertical component need to be recomputed on each DA cycle. This result is of significant practical interest since the vertical diffusion operator employs an inexpensive direct solver and thus can be applied, on each DA cycle, with randomization or the exact method to obtain a good approximation of the normalization matrix.

3.4.4 Application of deep learning to the estimation of normalization coefficients in diffusion-based covariance models

The normalization problem described in the previous section has characteristics that make it an ideal candidate for an ML solution strategy. Given an 'ensemble' of diffusion tensors, a corresponding set of accurate normalization factors can be computed using an exact method or a randomization method with a large sample. Then, a Neural Network (NN) can be trained on this set using the diffusion tensor, grid information, boundary geometry, and possibly other factors as predictors. As a proof of concept, this problem was studied by F. Skrunes during his internship at CERFACS, using a two-dimensional (2D) diffusion operator applied in relatively low (1 degree horizontal) resolution global version of the

NEMOVAR DA system. Key features of the NN architecture included: 1) the use of a Convolutional NN (CNN), with appropriately scaled diffusion tensor to ensure equivariance to translation; 2) the use of a distance-to-the-coast predictor in the CNN to reduce errors near coastlines; and 3) the use of a relatively small training data-set (10). Figure 3.2 illustrates how accurately the CNN is capable of reproducing the exact normalization factors. Variations of this approach are currently being explored by ECMWF and the Met Office for possible application with their operational versions of NEMOVAR.

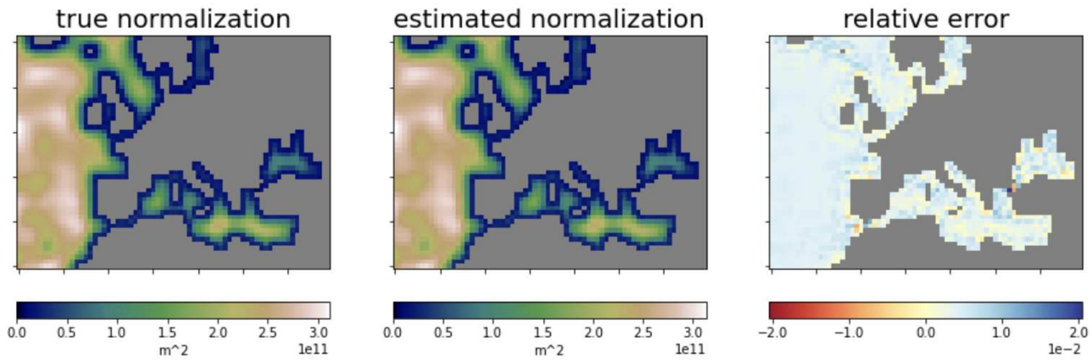

Figure 3.2: Left panel: the exact normalization factors associated with a 2D diffusion-based correlation model applied in a global ocean model (here showing a zoom over European seas). Middle panel: the normalization factors estimated using a CNN that was trained with a set of 10 normalization-factor fields where each member of the set is associated with a different, randomly-perturbed diffusion tensor. Right panel: the relative error between the estimated and exact normalization factors.

References

[1] N. Bousserez, J. J. Guerrette, and D. K. Henze, (2020), Enhanced parallelization of the incremental 4D-Var data assimilation algorithm using the Randomized Incremental Optimal Technique, *Quarterly Journal of the Royal Meteorological Society*, **146**.

[2] I. Daužickaitė, A. S. Lawless, J. A. Scott, and P. J. van Leeuwen, (2021), On time-parallel preconditioning for the state formulation of incremental weak constraint 4D-Var, *Quarterly Journal of the Royal Meteorological Society*, **147**, 3521–3529.

[3] I. Daužickaitė, A. S. Lawless, J. A. Scott, and P. J. van Leeuwen, (2021), Randomised preconditioning for the forcing formulation of weak-constraint 4D-Var, *Quarterly Journal of the Royal Meteorological Society*, **147**, 3719–3734.

[4] J.-G. de Damas, (2022), Randomized SVD preconditioners with an application to data assimilation. Internship supervised by S. Gürol and Y. Diouane.

[5] O. Guillet, A. T. Weaver, X. Vasseur, M. Michel, S. Gratton, and S. Gürol, (2019), Modelling spatially correlated observation errors in variational data assimilation using a diffusion operator on an unstructured mesh, *Quarterly Journal of the Royal Meteorological Society*, **145**, 1947–1967.

[6] B. Ménétrier and T. Auligné, (2015), Optimized Localization and Hybridization to Filter Ensemble-Based Covariances, *Monthly Weather Review*, **143**, 3931–3947.

[7] O. Mouhtal, (2023), Randomized scaled spectral preconditioners with an application to data assimilation. Internship supervised by S. Gürol, Y. Diouane and D. Orban.

[8] D. Schaden and E. Ullmann, (2020), On Multilevel Best Linear Unbiased Estimators, *SIAM/ASA Journal on Uncertainty Quantification*, **8**, 601–635.

[9] A. Scotto di Perrotolo, (2022), *Randomized numerical linear algebra methods with application to data assimilation*, PhD thesis, ISAE, Toulouse.

Methods and algorithms for uncertainty quantification

4.1 Stochastic preconditioning of domain decomposition methods for elliptic equations with random coefficients

In [ALGO-COOP76], we aim at developing an efficient preconditioned iterative domain decomposition (DD) method for the sampling of linear stochastic elliptic equations. To this end, we consider a non-overlapping DD method resulting in a Symmetric Positive Definite (SPD) Schur system for almost every sampled problem. To accelerate the iterative solution of the Schur system, we propose a new stochastic preconditioning strategy that produces a preconditioner adapted to each sampled problem and converges toward the ideal preconditioner (i.e., the Schur operator itself) when the numerical parameters increase. The construction of the stochastic preconditioner is trivially parallel and takes place in an off-line stage, while the evaluation of the sample's preconditioner during the sampling stage has a low and fixed cost. One key feature of the proposed construction is a factorized form combined with Polynomial Chaos expansions of local operators. The factorized form guarantees the SPD character of the sampled preconditioners while the local character of the PC expansions ensures a low computational complexity. The stochastic preconditioner is tested on a model problem in 2 space dimensions. In these tests, the preconditioner is very robust and significantly more efficient than the deterministic median-based preconditioner, requiring, on average, up to 7 times fewer iterations to converge. Complexity analysis suggests the scalability of the preconditioner with the number of subdomains.

4.2 Recycling Krylov subspace strategies for sequences of sampled stochastic elliptic equations

In [ALGO-COOP113], we are interested in the quantification of uncertainties in discretized elliptic partial differential equations with a random coefficient field. In sampling-based approaches, this relies on solving large numbers of symmetric positive definite (SPD) linear systems with different matrices. In particular, we consider the case in which these operators are sampled by Markov chain Monte Carlo, which leads to sequences of correlated matrices. We investigate recycling Krylov subspace strategies for the iterative solution of sequences of linear systems formed with such matrices. The linear systems are solved using initialized conjugate gradient (Init-CG) methods, where approximate eigenvectors of the previously sampled operator are used to set an initial guess, and deflated conjugate gradient (Def-CG) methods, where the Krylov subspace is augmented with these vectors. The following aspects of eigenvector approximation, and their effect on deflation and initialization, are investigated in this context: (i) projection technique, and (ii) refreshing strategy of the eigen-search space. Our numerical experiments show that, when not using a preconditioner, these aspects only impact convergence behaviors of Def-CG at the early stages of the sampling sequence. Second, unlike sequences with multiple right-hand sides and a constant operator, our experiments with multiple matrices show that, even for highly correlated matrices, Init-CG does not reproduce the convergence behavior of Def-CG. Finally, the limits of deflation used as a means to compensate for the inefficiency of block-Jacobi (bJ) preconditioners are investigated. For small systems, using a bJ preconditioner while deflating with at least as many approximate eigenvectors as the number of bJ blocks achieves similar convergence behaviors to PCG with a constant algebraic multigrid (AMG) preconditioner. For larger systems, although the effect of deflation is improved when using the right refreshing strategy of the eigen-search space, the combination of deflation with bJ preconditioners does not scale as well as using PCG with a constant AMG preconditioner based on the median realization of the coefficient field.

Data Science and Artificial Intelligence

Data Science has come a long way at CERFACS since it started in 2017. What started as highly exploratory work has now branched out into deep research activities, spanning all teams and a large array of applicative fields. In this section we'll look at a number of impactful research topics that have been explored at CERFACS over the last 3 years, namely for data assimilation techniques in geoscience and reservoir modeling (Sec. 5.1), to produce innovative subgrid-scale models (Sec. 5.2), to explore new data-driven numerical resolution methods (Sec. 5.3), and to expand the capacities of surrogate modeling (Sec. 5.4). Efforts to produce common tools for the physics community to lower the barriers of access to AI tools for physics solvers are also showcased (Sec. 5.1).

Looking ahead, generative AI is a rapidly expanding field, which has yet to make its mark in physics-driven AI. In 2023, Soufiane Mrini interned at CERFACS to investigate the potential for diffusion models to generate full 3D turbulent flow. This continued the work initiated in 2019 by Aakash Patil, but with a novel deep learning architecture. Target configurations included homogeneous isotropic turbulence and atmospheric flow configurations. More work is expected on this topic in years to come.

Data-driven methods have also become much better integrated into the everyday work of CERFACS, across all activities. These enable the exploitation of data that would otherwise stay under-used. CERFACS has even become a reference on the topic, leading to collaborations to help other labs analyze their data [CFD124, ALGO-COOP60].

5.1 Neural generative methods for control-space mapping

Camille Besombes successfully defended his PhD at CERFACS in 2021 [ALGO-COOP114]. Central to his research was the innovative use of Generative Adversarial Networks (GANs), a type of neural network, for the task of mapping high-dimensional physical fields onto a more manageable low-dimensional latent space.

This process is akin to dimensionality reduction, where the aim is to capture the essence of fields of interest that lie within a sprawling high-dimensional space, by representing them within a more compact, low-dimensional manifold. What sets Besombes' approach apart from many existing reduction techniques is its *non-linear* and *unsupervised* nature. Rather than relying on modeler-prescribed mappings, the function here is entirely data-driven.

Throughout his PhD and the associated publication [CE108], C. Besombes demonstrated the versatility of this method. He explored its applications in atmospheric sciences (Fig. 5.1 to identify plausible solution fields, as well as in determining acceptable rock facies distributions for initializing sub-surface flow simulations. This latter application caught the attention of CERFACS' shareholder, TotalEnergies, leading to its implementation in their toolchain.

5.2 CNNs for subgrid-scale modeling

Subgrid-scale (SGS) modeling lies at the heart of numerous computational fluid dynamics (CFD) methodologies. By their very nature, these models serve as approximations for phenomena that aren't resolved directly in simulations. Traditionally, their formulation leans heavily on data-centric methods that

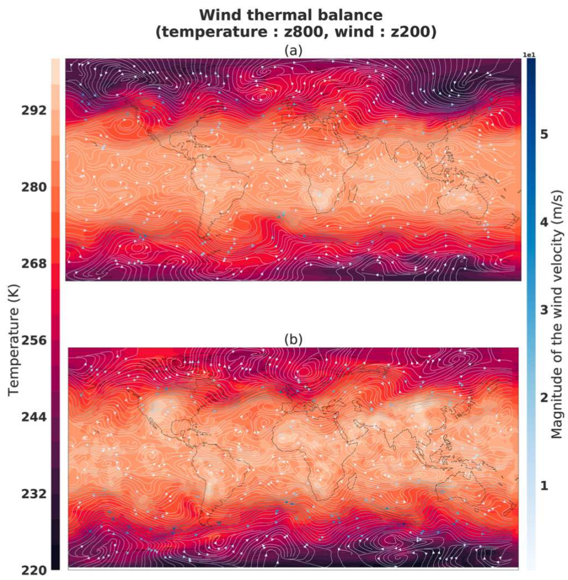

Figure 5.1: Thermal wind balance (a) from a simulated dataset, and (b) generated by a trained GAN [ALGO-COOP114]

often employ rudimentary, predominantly linear techniques. However, with the advent of deep learning, convolutional neural networks (CNNs) have emerged as a potent tool that can leverage contextual effects to improve on these simple models, with excellent potential to push SGS modeling forward.
CERFACS actively investigates several such promising uses of deep learning for SGS modeling, namely for flame-turbulence interactions (Sec. 5.2.1) and wall friction modeling (Sec. 5.2.2).

5.2.1 Data-driven models for flame-turbulence interactions

In 2021, a significant milestone was achieved by Victor Xing, who illustrated the feasibility of leveraging neural networks to predict combustion SGS quantities. In addition, he extrapolated these findings to broader, intricate configurations that mirror real-world flames [ALGO-COOP96] (Fig. 5.2). This innovation holds

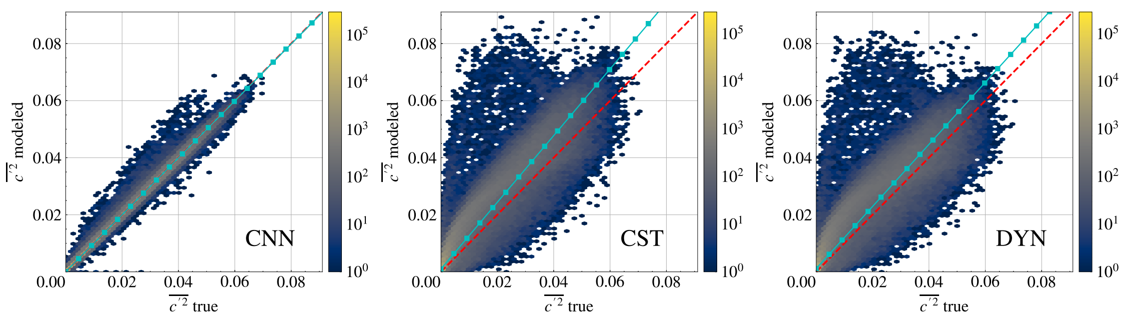

Figure 5.2: Subgrid-scale variance of the progress variable as predicted by the deep learning model (left, CNN), the constant β Charlette model (center, CST) and the dynamic Charlette model (right, DYN).

the promise of integrating neural network-based SGS models directly into codes. V. Xing's contributions culminated in a successful PhD defense in 2022 [ALGO-COOP123]. V. Xing also worked on the premise of what would become PhyDLL (Sec. 5.5). All his work led to him successfully defending his Ph.D. in 2022 [ALGO-COOP123], publishing a book chapter in 2022 [ALGO-COOP2], and another paper in 2023 in collaboration with the university of Münich [ALGO-COOP89]. Building on this momentum, the research is being furthered by Victor Coulon in his ongoing PhD.

5.2.2 Data-driven wall friction modeling

The large-eddy simulation of wall-bounded turbulent flows at high Reynolds numbers is made more efficient by the use of wall models that predict the wall shear stress, allowing coarser cell sizes at the wall. In a first paper [ALGO-COOP55], written by Dorian Dupuy during his postdoc, examined a data-driven approach for the modeling of the wall shear stress using filtered high-fidelity numerical data from two fully developed turbulent channel flows and two turbulent flows with separated regions: a three-dimensional diffuser and a backward-facing step. The model was a multilayer perceptron based on the flow information in the vicinity, given by the distance to the wall and the velocity components at a given number of grid points above the wall. It was Mach number equivariant at the quasi-incompressible limit, Galilean invariant, statistically rotational invariant and could extrapolate to flow conditions unseen in the training dataset. The relevance of the machine-learning procedure was verified *a priori* using the filtered numerical data and *a posteriori* by performing wall-modeled large-eddy simulations implementing the model. The results showed that the model was able to leverage the local spatial information to discriminate developed wall turbulence and separated regions in flow configurations not included in the training dataset.

A fundamental limitation of this initial work was the need to interpolate the local field onto a regular grid for input to the network. This incurred overheads, but more importantly left no guidelines as to how to treat complex geometries. Expanding on his previous work, D. Dupuy presented a machine-learning methodology to develop data-driven wall-shear-stress models that could directly operate, *a posteriori*, on the unstructured grid of the simulation. The model architecture was based on graph neural networks, and trained on a database which included fully developed boundary layers, adverse pressure gradients, separated boundary layers, and laminar–turbulent transition. The relevance of the trained model was verified *a posteriori* for the simulation of a channel flow, a backward-facing step and a linear blade cascade. These results led to a publication in 2023 [CFD143].

5.3 AI for innovative numerics

As the ever-evolving frontier of computational research progresses, the marriage between traditional numerical methods and artificial intelligence (AI) is becoming increasingly significant. At the crossroads of these disciplines, innovative strategies are emerging that merge the robustness of classical methods with the adaptive capabilities of machine learning. In particular, AI offers a dynamic approach to addressing the intricacies of numerical computations, providing tailored solutions that can dynamically respond to the complexities and nuances of the problem at hand. This section delves into two such groundbreaking methods. The first (Sec. 5.3.1) illuminates how data-driven techniques are redefining locally-adaptive numerical schemes, optimizing them for specific physical fields. The second (Sec. 5.3.2) reveals the transformative potential of Convolutional Neural Networks (CNNs) in re-envisioning preconditioning techniques for Poisson solvers. Through these developments, CERFACS has showcased the transformative power of AI in enhancing the efficiency, accuracy, and adaptability of numerical methods in contemporary research scenarios.

5.3.1 Data-driven locally-adaptive numerical schemes

Numerical schemes are at the heart of the accuracy and speed of many Partial Differential Equations (PDE) solvers, notably in CFD, with current ongoing work including at CERFACS on promising high-order methods. When designing such an algorithm, many tradeoffs are necessary, *e.g.* between the stability, the dissipation rate, and the dispersion rate of the scheme. The mathematical tools used to derive these schemes have long relied on frequency-based analysis, seeking a global tradeoff between these characteristics. Recently however, the machine learning community has demonstrated that data-driven techniques could learn to tune numerical schemes dynamically, both in space and in time, to optimize them further for the actual physical field solved for, with examples in CFD. Demonstrations however are mostly limited to matrix-like meshes, impossible to adapt directly to most production-ready software.
Luciano Drozda successfully defended his PhD in 2023 [ALGO-COOP115]. He showed as soon as 2021 how the philosophy of these approaches is compatible with high-accuracy, unstructured numerical schemes, coining an altered two-step Taylor-Galerkin scheme with locally and temporally adaptative behavior "ML-TTGC" [ALGO-COOP5]. This led to a collaboration with Braude University in Israel, funded by a dedicated France-Israel collaboration grant. Such a collaboration has shown that ML-TTGC performs near-perfectly on simple configurations with highly deformed meshes and strong gradients. It also led to a solid theoretical foundation to define the optimal values to train the neural network on, published in 2023 [CFD140].

5.3.2 Same for less: CNNs for efficient preconditioning in Poisson solvers

Another interesting approach to exploit CNNs arises in cases of elliptical PDEs, notably Poisson's equation in CFD. Indeed, solving for Poisson's equation on large meshes traditionally requires Krylov subspace iterative methods, which can take up a significant portion of compute time in *e.g.* incompressible predictor/corrector solvers (to compute the pressure correction), or in plasma solvers (for the electric field). Preconditioning techniques aim to reduce drastically the number of iterations needed to solve the problem. Ekhi Ajuria showed that a CNN can effectively produce excellent initial guesses for the iterative process, leading to a significant decrease of number of iterations, hence a lower cost of the computation [CFD107]. What's more, by construction this approach yields identical accuracy compared to the traditional incompressible solver, offering a guarantee that few deep-learning based techniques in CFD can claim to achieve today. These results were shown to scale to 2D and 3D Navier-Stokes simulations [ALGO-COOP3], suggesting that applicability of these methods on realistic cases is now within reach.

5.4 AI for surrogate modeling

Many engineering and scientific problems are characterized by:

1. large quantities of data previously gathered about their operation and behavior, whether through previous evaluation of costly models, or in-situ observations;

2. the need to explore variations of this behavior in a multitude of variations on the conditions, similar to those previously recorded.

The process of drawing laws of behavior from a number of observations, and generalizing it to nearby conditions is known as *surrogate modeling*. This can be done with a variety of techniques, the most basic of which is linear regression. Machine learning (ML) techniques expand the range of available functions to explore, and are leveraged to achieve better descriptions of the data, as well as better interpolation and extrapolation of the system behaviour outside the data points. Notably, ML tools offer new ways to approach high-dimensional problems, for which classical regression techniques are not well suited.

CERFACS has a long history of surrogate modeling for a variety of earth science and engineering problems. Recently, some efforts have focused on using machine learning techniques to this end. A few are highlighted in this section, namely for subsurface reservoir flows (Sec. 5.4.1), aircraft landing load estimation (Sec. 5.4.2), and flood near-term forecasting (Sec. 5.4.3).

5.4.1 Reservoir flow models

Subsurface reservoirs exploited by the Oil&Gas industry contain low Reynolds porous media flows over large space- and timescales, and are computationally challenging to simulate. The structure of the reservoir is always known only to a limited extent, through indirect measurements such as seismic studies. One technique central to the reconstruction of the reservoir topology, *i.e.* the distribution of rock facies underground, is known as *history matching*. This process relies on simulating the flow through various reservoir topologies a great number of times, creating ensembles and progressively assimilating the time-varying in-situ observations of the field, such as well pressures and flow rates. This can quickly lead to large numbers of simulations, and the technique becomes limited by their cost.

Data-driven surrogates for reservoir simulation can represent a cost-effective alternative to first-principle solvers. However, the very high dimensionality of the problem, as well as the need for stability of the resolution over large timescales, is challenging for purely data-driven approaches. A popular approached today is to include physical constraints into the learning process to help guide it. Abderrahmane Yewgat developed a new Physics-Constrained Deep Learning approach in his PhD in 2021 that combined neural networks with a reduced physics approach: Capacitance Resistive Model (CRM). CRMs are data-driven methods that are based on a simple material balance approximation in the reservoir. CRM can be used to analyze the underlying connections between producer wells and injector wells that can then be used to better allocate water injection. Such analysis can usually require very long tracer tests or very expensive 4D seismic acquisition and interpretation. CRMs can provide directly these wells connection information using only available production and pressure data. The problem with CRM approaches, based on classical optimizers, is that they often detect spurious correlations and can be not very robust and reliable. In a paper [ALGO-COOP97], A. Yewgat showcased a new physics-constrained deep learning approach called Deep-CRM, which performed production data regularization via the neural network approximation that helped to provide a better CRM parameter identification. He showed on a synthetic and in real reservoir case that Deep-CRM was able to identify most of the injector-producer connections with higher accuracy with respect to traditional CRM. Deep-CRM produced also better liquid production forecasts on the performed blind tests.

5.4.2 Landing loads

Surrogate modelling can be adversely affected by the high-dimensionality of some engineering systems, as weel as their complex non-linearities and temporal dependencies, leading to inaccurate or brittle surrogate models. In a 2022 paper [ALGO-COOP70], Michele Lazzara showed an innovative dual-phase Long-Short Term Memory (LSTM) Autoencoder-based surrogate model to predict an aircraft dynamic landing response over time, conditioned by an exogenous set of design parameters. The LSTM-Autoencoder was adopted as a dimensionality-reduction tool that extracted the temporal features and the nonlinearities of the high-dimensional dynamical system response, and learned a low-dimensional representation of it. Then, a Fully Connected Neural Network was trained to learn the simplified relationship between the input parameters and the reduced representation of the output. For this application, the results demonstrated that the LSTM-AE based model outperformed both Principal Component Analysis and Convolutional-Autoencoder based surrogate models, in predicting the parameters-dependent high-dimensional temporal system response.

M. Lazzara successfully defended his Ph.D. in 2023 [10].

5.4.3 Flood modeling

Emergency services seek more reliable and extended flood forecasting models in order to be more effective in their actions. Théo Defontaine started a PhD in 2020 on this topic, and showed how Machine Learning (ML) models could improve and extend discharge prediction results from empirical Lag and Route model used by a flood forecasting operational service. Specifically, a scarce dataset (40k points) was built, consisting of 36 observed flood events over the past 15 years on the Garonne River upstream from the city of Toulouse (France). At the problem input, hourly guage observations from upstream stations, as well as hyetometric products of spatialized rainfall observations were used. A number of ML models (Linear Regression, Gradient Boosting Regressor, Multilayer Perceptron) were then trained to forecast water height in Toulouse at 6-hour and 8-hour lead times during flooding events. Using an empirical splitting strategy adapted to the scarce database of the Garonne case, the robustness of the strategy to a lead time extension was showcased when using only homogeneous water-level data. The models were then re-trained by adding heterogeneous rainfall-runoff data at the input to improve results at both lead times. Overall, this work showed how ML models allowed to improve the accuracy of discharge prediction compared to operation state-of-the-art systems. Better yet, it discussed many insights into the pitfalls of applying data-driven techniques for this type of scarce, time-evolving dataset, with potential repercussions for many other rainfall basins. A conference paper has been presented on this topic [CE115], and a full journal paper is expected to be submitted soon. Théo Defontaine should defend his PhD in early 2024.

5.5 PhyDLL: coupling physical solvers and deep learning

PhyDLL[1] is an open-source library [ALGO-COOP29] developed by CERFACS and its partners in the RAISE European Center of Excellence[2], during the postdoc of Anass Serhani. It aims to facilitate coupling of massively parallel physical solvers with distributed deep learning. For now, it focuses on inference use-cases, but will be adapted to include on-the-fly training.
PhyDLL has been show to scale effectively on several supercomputing architectures (Fig. 5.3). It

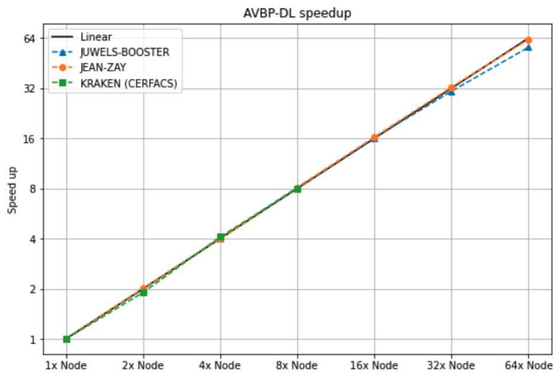

Figure 5.3: Scaling of PhyDLL (used in an AVBP-DL LES) up to 64 compute nodes (256 A100 GPUs, 3072 CPUs).

also enables effective distributed inference *via* domain decomposition (Fig. 5.4a), and avoids errors at the subdomain frontiers (Fig. 5.4b) by transmitting neighboring “halos” for each subdomain inference (Fig. 5.4c). PhyDLL is now used by several of CERFACS’ partners (implemented in Barcelona Super

[1] https://phydll.readthedocs.io/en/latest/
[2] https://www.coe-raise.eu/

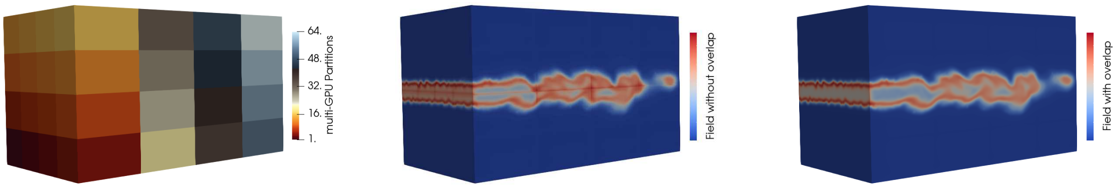

(a) GPU partitioning for inference (b) Simple distributed inference (c) Inference with halo

Figure 5.4: Domain decomposition inference according to the number of available GPUs (a) lead to discontinuous values at the boundaries of theses subdomains (b) when treated naively. PhyDLL facilitates the transfer of “halos” of arbitrary thickness to perform overlapping inference, and ultimately provide smooth inference fields (c).

Computing’s code Alya, in Météo-France’s ARPEGE solver, and investigated to be integrated in RWTH Aachen’s solver m-AIA). Developement of this library will continue in 2024 and beyond, since this tool appears to be a good aggregator for the physics community that has an interest for hybrid AI.

[10] M. Lazzara, (2023), *Apprentissage Profond pour la Modélisation de Systèmes Dynamiques Non-linéaires de Haute Dimension avec Traitement de Séries Temporelles Multivariées*, phd thesis, Ecole doctorale MITT: Mathématiques, informatique et télécommunication de Toulouse.

Sustainable programming

The sustainable programming activity is focused on maintaining, improving and communicating on CERFACS's technological advantage using high performance computing on our and our partners current codes but also study new solutions to prepare for the future. Theses activity are always linked with real life usages from CERFACS.

6.1 High performance computing activities

6.1.1 Portability optimization and technology watch

During the period covered by this report, two prominent hardware architectures gained widespread adoption: the AMD Zen CPU architecture and NVIDIA's GPU accelerated architectures, including V100, A30, and A100. Collaborative porting activities were conducted through bilateral agreements with IBM, the contrat de progres IDRIS/GENCI-HPE, the cellule de veille technologique GENCI, and the ICARUS and Excellerat CoE projects.

The focal point of these porting endeavors was the CFD code AVBP, with significant efforts directed towards its adaptation. The initiation of GPU porting on NVIDIA systems dates back to 2018, facilitated by the expertise of J. Legaux, who joined our team as a permanent engineer in late 2021. To enable GPU acceleration for legacy codes, we opted for the OpenACC framework from PGI/NVIDIA. This decision was driven by the robust support from NVIDIA, coupled with close collaboration between NVIDIA, IDRIS, and HPE in porting the code to the JEANZAY system from IDRIS.

Although the choice of OpenACC proved controversial due to its limited support for other accelerated architectures, it has proven to be a strategic one. AVBP stands out as one of the few fully ported codes in the market for NVIDIA GPUs. The integration of NVIDIA GPU support for research purposes occurred in 2020 (refer to Figure 6.1) and was subsequently expanded. In spring 2023, a preliminary release was provided to our industrial stakeholders on the CCRT system TOPAZE, broadening the coverage of our GPU-accelerated capabilities.

Additionally, within the framework of the COEC and EXCELLERAT European Centers of Excellence, our efforts extended to enhancing portability for AMD GPUs. An operational prototype was successfully developed and released in spring 2023, specifically tailored for windfarm simulations. This achievement followed a significant challenge posed on the CINES/GENCI Adastra system (refer to Figure 6.2), marking a significant milestone in our collaborative endeavors.

6.1.1.1 Automatic source transformation for ARPEGE

Building on our experience with OpenACC, a collaboration with METEO FRANCE started in the end of 2021 to help them study and apply porting strategies for ARPEGE on GPU systems, this activity being spearheaded by J. Legaux. ARPEGE is a very complex and large code that is constantly evolving, with a codebase optimized for the efficient usage of traditional CPUs. Therefore, the porting strategies relies on automatic source to source transformation of the code in order to keep a single reference codebase while providing the possibility to evaluate various porting strategies or target architectures.The first task on this activity was to evaluate the in-house source converter fxtran from METEO FRANCE and ECMWF's loki

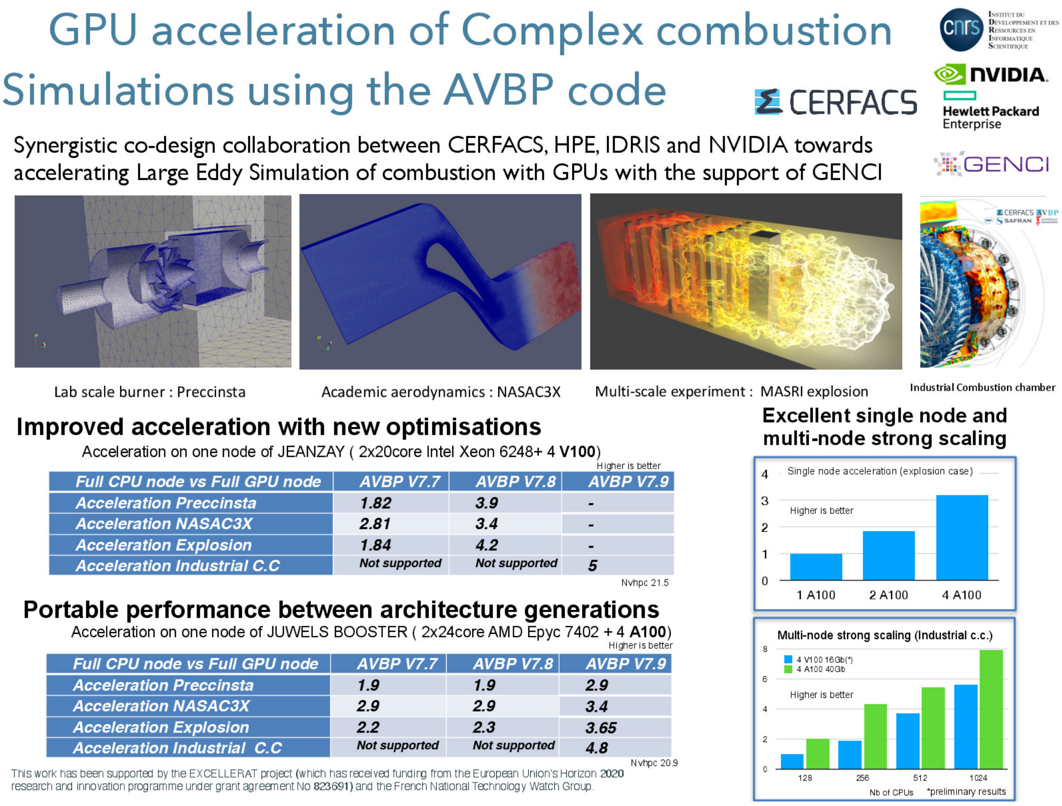

Figure 6.1: GPU port success story with NVIDIA and GENCI.

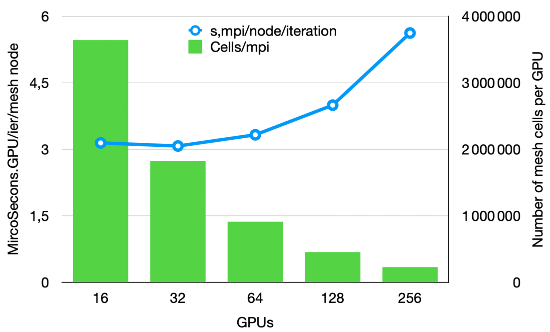

Figure 6.2: Performance of the GPU prototype of AVBP on MI250 AMD hardware on a windfarm simulation.

Kernel	1A100 vs 1 CPU core	1 A100 vs 76 CPU cores
ACDRME	x10.33	x2.96
ACDRAG	x19.66	x2.11
ACTKE	x45.14	x1.88
CUCALLN	x62.09	x2.1
ACVPPKF	x50.31	x1.79

Table 6.1: Obtained acceleration on ARPEGE Kernels using one gpu versus one core or full node cores.

framework to this regard. Report[ALGO-COOP110] concludes with the choice of the loki framework to conduct the porting process.
The next task was the actual porting of increasingly complex kernels extracted from ARPEGE. The data layout for the kernels is a grid covering the earth with an atmosphere column at each point. The original code is optimized for vectorization and caching on CPU by treating small packs of columns. Experiments on a simple kernel confirmed that this layout is really ineffective on a GPU and the retained strategy was to convert the code to the SCC (Single Column Coalesced) scheme where a single thread will compute the whole kernel at once but only for a single column, and neighbouring threads will compute neighbouring data in memory to ensure coalescence. Another issue with the original ARPEGE kernels is that they rely heavily on automatic arrays in subroutine, but GPUs threads do not have enough local memory to support this. Therefore the porting process also had to transform these local arrays allocation into pointer definitions that target a large buffer space in the global memory. Another benefit in this porting process development is that it allowed to pinpoint problematic patterns in the code that prevent automatic transformation, which helped to improve the coding guidelines for ARPEGE developers. Details on this work can be found in report[ALGO-COOP111], a summary of the performance gains on the 5 targeted kernels can be seen here in table 6.i.
A currently ongoing third task consists in integrating these transformations in larger parts of the code instead of individual kernels. The main difficulty of this task lies in the automatic identification of data needed for the GPU ported sections and the implementation of their transfers between main memory and GPU memory.

6.1.2 Code generation for lattice Boltzmann methods

In the scope of computational frameworks for high performance computing, the challenge of developing highly efficient and adaptable software solutions is a daunting task. This challenge stems from the need to express mathematical equations in code while ensuring that the software can be specialized for diverse processing units, including powerful accelerators like GPUs. Addressing this issue is crucial within the massively parallel multiphysics framework known as WALBERLA. Here, this challenged is addressed by exploring metaprogramming techniques. Thus combining the high level description of a numeric problem with low-level specialized compute kernels for the code hot spots.An overview of the approach is depicted in Figure 6.3.
At its core, the approach employed in WALBERLA centers around a symbolic representation of numerical problems that can be represented in a stencil notation on a regular cartesian grid. The most prominent method falling in this category is the Lattice Boltzmann Method (LBM). Its numerical equations are derived problem specific in the Python package *lbmpy*, which leverages the open-source library *SymPy*[1] and extends its capabilities. By adopting this strategy, the LBM can be systematically deconstructed into its fundamental components, thus allowing for modularization and optimization of each step of the process [15, 16, 12].
Modularization occurs at the mathematical level, culminating in the creation of an optimized update rule. The end result is a set of highly specialized, problem-specific LBM compute kernels that minimize Floating

[1] `https://www.sympy.org/en/index.html`

Point Operations (FLOPs) while preserving a commendable degree of modularity within the source code. This modularity serves as a foundation for the software's adaptability.
From the symbolic description, an Abstract Syntax Tree (AST) is constructed within the *pystencils* Intermediate Representation (IR) [11]. This tree-based representation not only accommodates architecture-specific AST nodes but also incorporates pointer access in subsequent kernels. Within this representation, spatial access specifics are encapsulated through the *pystencils* `Field` class. Moreover, constant expressions and fixed model parameters can be evaluated directly to reduce computational overhead.
A notable aspect of this approach is its ability to generated method specific additional kernels needed to solve numerical problems. These are compute kernels for boundary conditions, as well as kernels for the packing and unpacking of data to fill communication buffers for MPI operations. Thus contributing to the software's adaptability in distributed computing environments.
The intermediate representation of the compute-kernels is translated into a clearly defined interface by the backends of *pystencils*. This interface maintains a straightforward structure, accepting raw pointers for array accesses alongside their corresponding shape and stride information. Such a design ensures that the kernels can be seamlessly integrated into existing C/C++ software structures.
Additionally, by using the Python C-API, the low-level kernels can be mapped to Python functions, enabling interactive development through *lbmpy*/*pystencils* as standalone packages. This allows rapid development of new methods.
The Lattice Boltzmann Method (LBM) is renowned for its high memory demands. As research has shown, highly optimized compute kernels are often restricted by the memory bandwidth of compute nodes or accelerators. Therefore, it becomes pertinent to explore the possibility of energy consumption reduction by optimizing the frequency of compute kernels. This is a noteworthy consideration, especially given the high level of optimization achieved in *lbmpy*, resulting in notably low FLOP counts in the code's most critical areas.

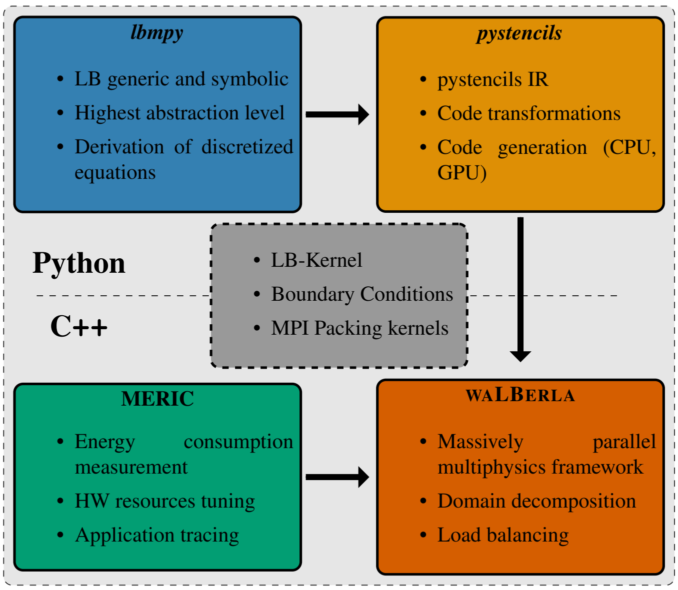

Figure 6.3: Overview of the software stack with *lbmpy*, *pystencils*, WALBERLA and the software tuning. With the high-level Python packages *lbmpy* and *pystencils* the numerical equations are derived, discretized and, finally, lower-level C-Code is generated from this symbolic representation. The generated code can be combined with the C++ framework WALBERLA and compiled. The executable has been optimized in terms of the energy consumption.

6.1.3 Energy optimization of lattice Boltzmann methods

The landscape of computing hardware procurement undergoes a transformative shift, marked by the emergence of energy costs as a critical consideration. Traditionally, the development and utilization of code placed a strong emphasis on raw performance. However, with the continuous escalation of energy expenses and advancements in runtime optimization and hardware fine-tuning, a new era has dawned. Contemporary strategies for deploying code on cutting-edge hardware now necessitate the mitigation of energy impact.

In a collaborative endeavor between the EuroHPC project SCALABLE and IT4Innovations, our focus was directed towards runtime energy tuning. We specifically investigated lattice Boltzmann codes, including WALBERLA and ProLB. Our primary goal was to assess the feasibility and advantages of utilizing readily available energy-efficient tools. A critical metric in this pursuit is energy efficiency, quantified as the performance achieved per unit of power consumption, denoted as Flop per second per Watt. In the context of the lattice Boltzmann Method (LBM) code, performance is more precisely characterized by the number of lattice updates executed per second (MLUPs/W).

Our optimization efforts encompassed two main directions: static and dynamic tuning. In the static tuning approach, hardware behavior remains constant throughout the code's runtime, optimized for average power consumption. In contrast, dynamic tuning allows real-time adjustments, adapting the hardware profile to the ongoing code operations. Drawing on the expertise gained from IT4I's participation in the Runtime Exploitation for Application Dynamism for Energy-efficient eXascale computing (READEX) project, we implemented the MERIC approach for both static and dynamic tuning, with a specific focus on ProLB and WALBERLA on CPUs as part of the SCALABLE project.

To gauge the energy savings achieved, we harnessed a range of on-board techniques tailored to diverse systems. For instance, we made use of the High Definition Energy Efficient Monitoring (HDEEM) system, which read power consumption data from system hardware sensors and stored this information in integrated memory on Atos—Bull—Eviden systems [14]. Alternatively, the Running Average Power Limit (RAPL) hardware power controller on Intel processors played a pivotal role [13].

In Figure 6.4, we provide a comprehensive summary of runtime changes across various scenarios, with a specific focus on the utilization of WALBERLA in a simulation of an airplane landing gear (LAGOON). The results are presented in three tables, shading light on the potential trade-offs between runtime efficiency and energy consumption.

In the context of the SCALABLE project, we showed substantial advancements in energy efficiency achieved through a nuanced understanding of application intricacies. Remarkable reductions, up to 20%, in energy consumption have been demonstrated, whether on CPU runtimes or using accelerated hardware such as NVIDIA GPUs within the EuroHPC systems. These gains were realized with minimal user intervention. However, a challenge lies in the current limitations associated with user permissions, restricting the ability to optimize processor/GPU behaviors in most HPC centers. However, the accelerated code exhibited exceptional energy efficiency, also in the default hardware configuration. This notable efficiency stems from the inherent energy efficiency of Nvidia's top HPC GPU. While our comparison faced slight discrepancies due to the usage of different power monitoring systems, we endeavored to compensate by incorporating estimated power consumption data from the remaining on-node components of the accelerated node. The presented measurements align closely with expected figures for such advanced hardware, indicating the highly effective utilization of GPUs in WALBERLA's accelerated implementation.

This research not only signifies a leap in energy-efficient computing but also underlines the potential for even greater strides in the future. As technologies continue to evolve and collaborative efforts drive innovation, the landscape of high-performance computing stands poised for a transformative era of unparalleled energy efficiency and computational power.

This work and the additional dynamic tuning are slated to be published by the end of 2023.

core [GHz] / uncore [GHz]	1.9	2.1	2.3	2.5	2.6	turbo
1.6	−38.57	−30.37	−24.25	−18.23	−16.17	−4.8
1.8	−35.92	−27.98	−22.16	−15.83	−12.65	−2.04
2	−33.47	−26.18	−19.97	−14.26	−11.33	−1.21
2.2	−32.79	−24.04	−17.78	−12.34	−9.53	−0.2
2.4	−30.96	−22.88	−16.5	−10.87	−8.16	−0.12

core [GHz] / uncore [GHz]	1.9	2.1	2.3	2.5	2.6	turbo
1.6	12.65	13.66	13.52	11.93	10.5	1.05
1.8	12.43	13.54	13.12	12.13	11.37	2.33
2	10.98	11.63	11.85	10.56	9.63	1.35
2.2	7.79	9.93	10.21	8.86	8.04	0.72
2.4	5.36	7.06	7.37	6.57	5.7	−0.52

core [GHz] / uncore [GHz]	1.9	2.1	2.3	2.5	2.6	turbo
1.6	21.98	22.52	20.04	17.46	14.87	2.24
1.8	21.13	21.66	19	16.53	15.03	3.08
2	18.75	19.12	16.7	14.78	13.26	1.97
2.2	15.4	15.48	14.66	12.9	11.28	1
2.4	11.74	11.83	11.5	9.48	8.65	−0.31

Figure 6.4: Static tuning energy performance measurements on the lagoon case. top: runtime impact middle:HDEEM energy impact bottom: RAPL energy impact.

6.1.4 Quantum computing

In parallel to the usual high performance platforms and expected innovations, this period saw an increase in interest towards quantum computing. Primarily driven by IBM, Google and Microsoft, since 2021 practical quantum computing has started to become a reality or at least hint of a reality on real applications with the addition of a constellation of small to medium enterprises and European financial initiatives. Our focus on this topic has been concentrated on the core business of CERFACS: solving partial differential equations.
The first foray into quantum programming allowed for the evaluation of the IBM Q programming model Qiskit with in mind the resolution of the 1D wave equation [ALGO-COOP91]. This algorithm capable of the same results as classical solvers is based on the hamiltonian approach and allowed for in depth algorithmic cost and precision analysis of the state of the art quantum solutions at the time. This work was continued in the Phd of Adrien Suau in collaboration with LIRMM and Total Energie Nouvelles this time beside hamiltonian solvers, variational algorithms such as VQLS were investigated for matrix inversions adding beside Qiskit the myQLM quantum framework from ATOS (now EVIDEN) as an implementation method. The Phd was defended in the end of 2022. Two additional highlights were singled out by publication: first, the development of a quantum profiler tool [ALGO-COOP92] and the analysis of the origin of error rates in quantum circuits in real hardware using qubit tomography [ALGO-COOP93].

This activity has been continued a Phd collaboration between PasQal BMW Erlangen and CERFACS . The goal of the PhD is to develop robust Quantum Computing approach for solving transient PDEs. Quantum Enhanced Physics-Informed Neural Networks (Q-PINNs) or Differentiable Quantum Circuits (DQCs) are near-term variational quantum circuits that are more expressive and can do multi-physics simulations and design optimization without needing exponentially more resources. Initially, classical approaches have been investigate to better understand their pros and cons as well as current quantum approaches. Focus then centered on solving PDE's using physics informed neural networks (PINNs) and then enhancing them using Differential Quantum Circuits. A first implementation using JAX and Pennylane has been performed. The first results were presented in QuApps 2022 conference `https://quapps-conference.com`.

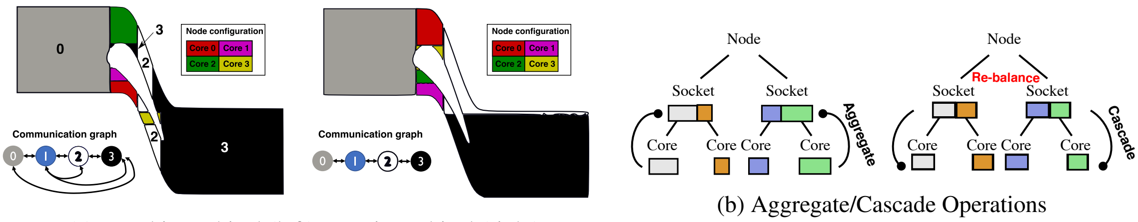

(a) Non-hierarchical (left) vs. Hierarchical (right)

(b) Aggregate/Cascade Operations

Figure 6.5: (a) Schematic of non-hierarchical vs. hierarchical partition (data) placement on 4 compute nodes each with 4 cores, the colored partitions are core partitions of node rank 1 (colored blue in the communication graph) and (b) aggregate/cascade hierarchical memory operations.

With this initial results, aerodynamics simulations use-cases on different 2D shapes have been tackled. An abstract has been accepted in QTML 2023.
Currently, work is advancing on the technical aspects of suitable test and validation benchmark problems (inviscid flow over a semi-infinite 2D wedge, transport equation in the flow field, etc.) which will lead to new aerodynamics simulations using the quantum-enhanced models and will be the base of a future upcoming scientific publications.

6.1.5 Topology-aware Unstructured Mesh Partitioning and Load-Balancing

There is a growing demand in HPC to exploit fully the hardware topology for optimal memory placement ranging from NUMA locality, off-/on-socket locality and network locality (minimum hop to memory) to achieve maximum compute throughput on new exascale and existing petascale infrastructure. Failing to place data in the right memory hierarchy can lead to abysmal degradation in performance especially when the increase in the problem and the partition sizes are substantial. Therefore data partitioning and load-balancing in distributed parallel programs must be topology-aware to fulfill this need. This motivated us in the COOP team to develop kalpaTARU, a Topology-AwaRe massive-scale Unstructured mesh partitioning/ load-balancing and adaptation infrastructure (erstwhile TreePart/Adapt). We implemented two fundamental building blocks of hierarchical memory access namely, cascade and aggregate (see fig. 6.5(b)) operating on an abstract rooted tree (graph) structure for the placement optimization problem starting from a root to the leaf partitions. Load-balancing/partitioning algorithms are implemented on top of this tree structure enabling both optimal placement of data in the right hierarchy and use the fastest memory access path available. Lastly we employed advanced MPI3 features like the one-sided Remote Memory Access (RMA) and Shared Memory primitives to improve memory access time via zero-copy communication and a novel blind send/receive algorithm. Additional fine-grain granularity in partitioning is achieved by cache block partitioning at the leaf with partial-distance-2 coloring to prevent data-race (fine-grain parallelism).
Two major achievements of this work are (i) the ability to perform online partitioning and load-balancing AVBP on more than $26k$ MPI ranks (see fig. 6.6) and (ii) improve the MPI communication and extract additional performance by better partition placement and zero-copy shared memory communication.

6.1.6 Parallel Unstructured Adaptive Mesh Refinement (AMR)

AMR module in kalpaTARU is presently the main backbone of all large-scale adaptive mesh workflow and tools in CERFACS. It consists of two main components, (i) a standalone command-line interface (CLI) and (ii) a library API for interfacing with an external solver. We have successfully demonstrated the library coupling with AVBP and presented the results at the HiFiLeD symposium 2021 [ALGO-COOP21]. The framework was also used in the PhD thesis of Sengupta [ALGO-COOP119] (LEFEX project) to

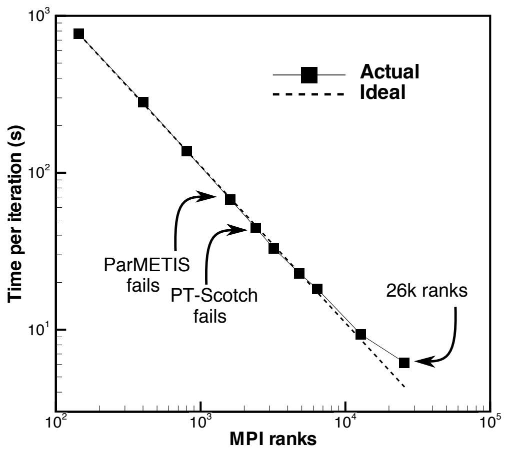

(a) Weak scaling of mesh partitioning in AVBP

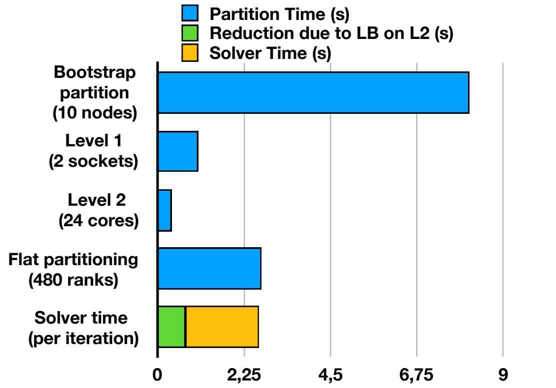

(b) Load-balancing improvement by exploiting topology

Figure 6.6: kalpaTARU (a) online hierarchical mesh partitioning and (b) topological load-balancing solver time improvement in AVBP.

successfully demonstrate the AMR/AVBP coupling to efficiently simulate explosion problems, accurately capturing the flame and vortex structures. We continued to refine the framework and leveraged it in other projects, namely, EXCELLEART 2, AIRBUS AMR, ...

6.1.7 Anamika Visual Domain Specific Language (DSL) : A Code-generation Approach to Deep Graph Nets

Data Flow (DFG) and Control Flow (CFG) Graphs are the two fundamental pillars of modern compilers. Typically a high-level computer program is parsed by a compiler and two specific graphs are generated, namely (i) DFG: where each edge in the graph is a relation between two operations in the program, such that data produced by one operation is consumed by the other and (ii) CFG: which represents the relation between two operations in a program expressing its execution order and actual implementation. DFG is a fundamental constraint of the program and provides a high-level blueprint of the program. CFG on the other hand merely provides the implementation details of this blueprint. The compiler utilizes these graphs to optimize the generated machine code such that it runs with the optimal performance using the hardware instructions on the given hardware. Typical use of CFG is determining if a given set of operations can be performed in parallel (e.g. loop structures).

This natural separation between DFG and CFG lead us in the COOP team to build Anamika, a visual data-flow DSL to draw DFG blueprints of Mesh Graph Net machine learning models. Each vertex in the graph describes a high level ML operation (CFG) on the data that flows through the edges of the graph. The machine learning program is thus described using this DFG represented as a Direct Acyclic Graph (DAG), starting from a data source and ending in a data sink (loss function). A code generator consumes the DAG blueprint to generate it's implementation given the hardware constraints (CPU/GPU) and memory layout (SoA/AoS). In Anamika, the DFG-DAG is constrained in an auto-differentiation (AD) friendly manner to easily accommodate both memory and compute optimizations of inference and training models. Presently, it uses Tapenade AD tool from INRIA to generate gradient of the ML model for training. Two code-generation back-ends to generate C and Fortran code are implemented and the inference successfully runs in parallel on the GPU/CPU using OpenACC. The framework was developed and presented at the Extreme

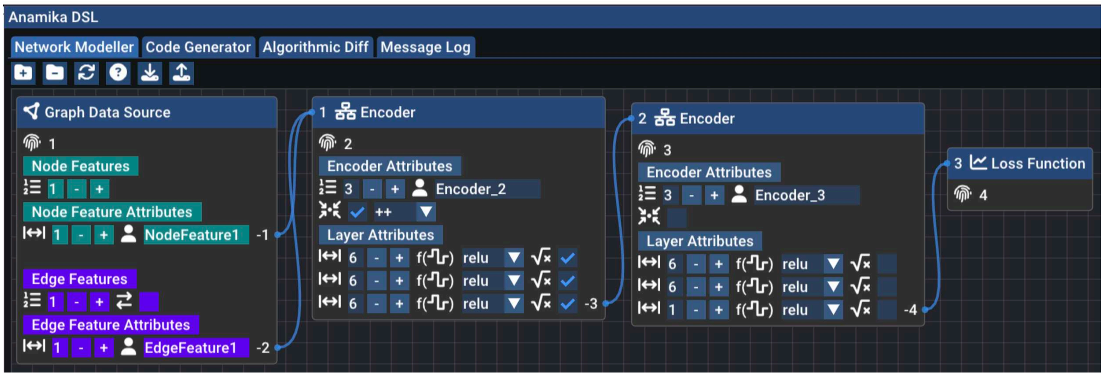

Figure 6.7: Data-flow graph modeling in Anamika visual DSL (data source to sink).

CFD workshop (ECFD6), 2023. An online demo is freely hosted based on the web assembly (WASM) version of Anamika at the URL `https://pavanakumar.gitlab.io/anamika/`.

6.2 HPC workflow and data management

6.2.1 Homogenization/Standardization of HPC Workflows

The automation of High-Performance Computing (HPC) workflows, which orchestrate a series of computational tasks, signifies a significant step towards maturity in HPC tooling. This transition from manual operations to standardized workflows streamlines processes and reduces the learning curve for users.

6.2.1.1 Workflow Solutions in Focus

Within the realm of HPC, various workflow solutions have been actively explored, particularly in the context of exascale computing.
Lemmings: `https://pypi.org/project/lemmings-hpc`, an open-source Python package initially developed by CERFACS, simplifies the submission of interdependent jobs on HPC cluster schedulers. While originally tailored for Computational Fluid Dynamics (CFD) applications, Lemmings proves versatile in automating recursive job scenarios.
Scales: `https://www.ssc-services.de/en/`, introduced in collaboration with the European project EXCELLERAT, addresses the needs of small and medium-sized enterprises (SMEs) lacking HPC expertise. This web-based solution resembles Gitlab Pipelines `https://docs.gitlab.com/ee/ci/pipelines/`, offering an intuitive learning curve for users.
The JUBE benchmarking environment, `https://www.fz-juelich.de/en/ias/jsc/services/user-support/jsc-software-tools/jube`, developed by the Jülich Supercomputing Centre in Germany, offers a script-based framework for benchmark set creation, execution, and result evaluation. While primarily focused on benchmarking, JUBE plays a pivotal role in assessing the long-term viability and performance consistency of HPC solutions.

6.2.1.2 Homogenization of Workflows

Efforts to simplify industrial access to HPC resources center on refining workflow creation, particularly for real-world simulations. Key insights include unified, chronological logging, unique workflow instance identifiers, avoiding file movement, versioning and documentation, sandbox schedulers, mockup solvers, and user-friendly end-user commands.

6.2.1.3 Automated Static Mesh Refinement for Exascale Simulations

In the context of advancing supercomputing towards exascale simulations (10^{18} operations per second), the challenge of mesh generation is addressed. Traditional trial-and-error meshing approaches become cost-prohibitive at exascale, leading to the proposal of an Automated Static Mesh Refinement (ASMR) method. ASMR iteratively enhances mesh fidelity based on simulation feedback, aiming to provide cost-effective high-quality meshes and solutions.

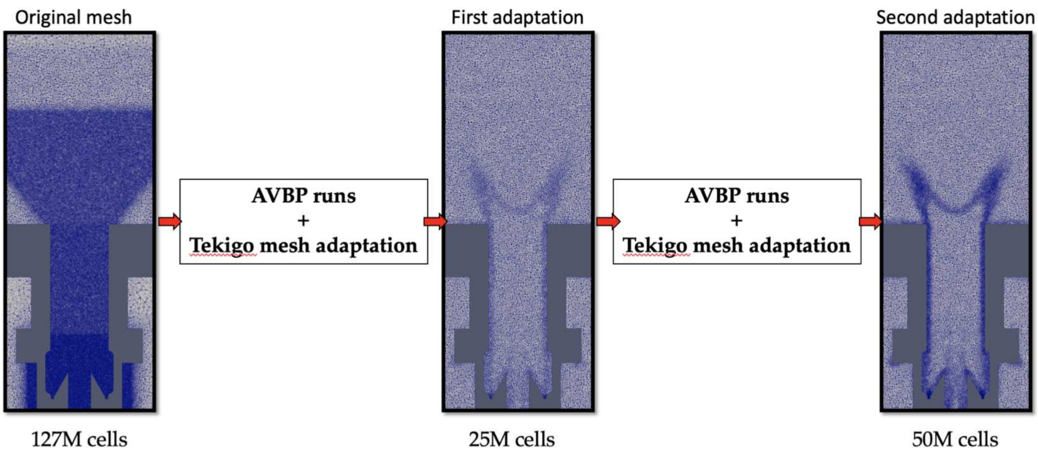

Figure 6.8: Sketch of the ASMR workflow. The run-and-refine loop is automated in a workflow to generate larges meshes (aim: 1 Billion point) with the help of increasingly fine computations

6.2.2 Computational Waste in Supercomputing

Supercomputers are powerful machines designed for high-speed calculations, enabling experts to answer complex questions. However, the cost of operating these facilities is substantial.
One growing concern in supercomputing is computational waste, which involves inefficient resource usage. This includes leaving supercomputers idle for extended periods and running jobs that yield no meaningful results. With the increasing computational power of supercomputers, wasted resources become a more significant issue.
For instance, the exascale supercomputer Aurora is estimated to consume 60MW of electricity, which translates to substantial costs. Even a mere 1% of its annual electricity consumption at a low price of 10 cents per KW.h amounts to $525,000. We'll provide an overview of running jobs on supercomputers, introduce new metrics to measure waste, and discuss two major sources of waste: understayer jobs and overstayer jobs. Finally, we'll explore strategies to engage users in optimizing their workloads.

6.2.2.1 Understanding Supercomputer Workloads

In the following, the term ”computational waste” is the under-performance of the machine workload due to bad job requests from the users.

6.2.2.2 Sources of Waste

Waste occurs when jobs don't align with the requested resources and durations:

- **No-Stayers (Yellow)**: Jobs that crash instantly, wasting the time used to keep resources idle.
- **Understayers (Bright Orange)**: Jobs shorter than requested, leading to less-efficient resource use : more idle times, less accurate schedule.
- **Overstayers (Dark Brown)**: Jobs running beyond the requested time, resulting in computations that cannot be save. Resources are used and occupied without use.

The accuracy of a job request is calculated by dividing the actual job duration by the requested duration. Accurate requests are close to 1, while very short or long jobs have lower accuracy. Most users tend to overestimate job durations, resulting in inefficiencies.

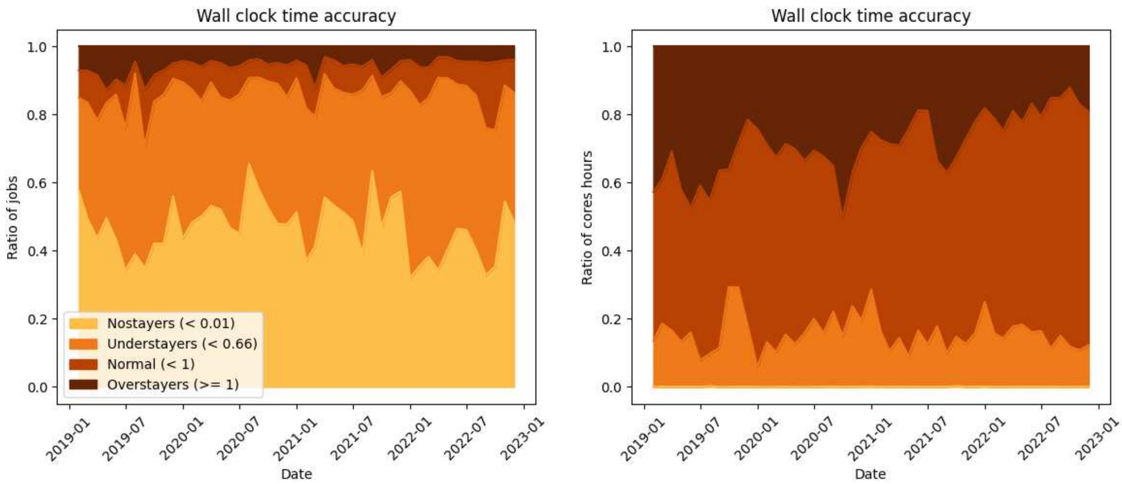

Figure 6.9: The share of users accuracy on Kraken in 2022, by job numbers (left) and by CPU hours. Half of submitted jobs are no-stayers (yellow,instant crash), 30% of CPU hours are done by over-stayers (brown, run until kicked out)

6.2.2.3 Engaging Users for Optimization

Users play a crucial role in workload optimization. Instead of traditional training materials, peer-to-peer communication and data visualization are more effective in promoting good practices. We've introduced a ranking system based on user accuracy and success to identify exemplary users. This encourages others to follow top users and reduce computational waste.
Computational waste is a significant concern in supercomputing, driven by inefficient resource usage. Engaging users and promoting better practices can lead to reduced waste, increased resource availability, and improved user experiences.

6.2.3 Mapping Softwares

Mapping software is necessary to mitigate the technical debt of legacy codes. Indeed, a new developer can either spend months sifting through code linearly to understand how various components connect, or they

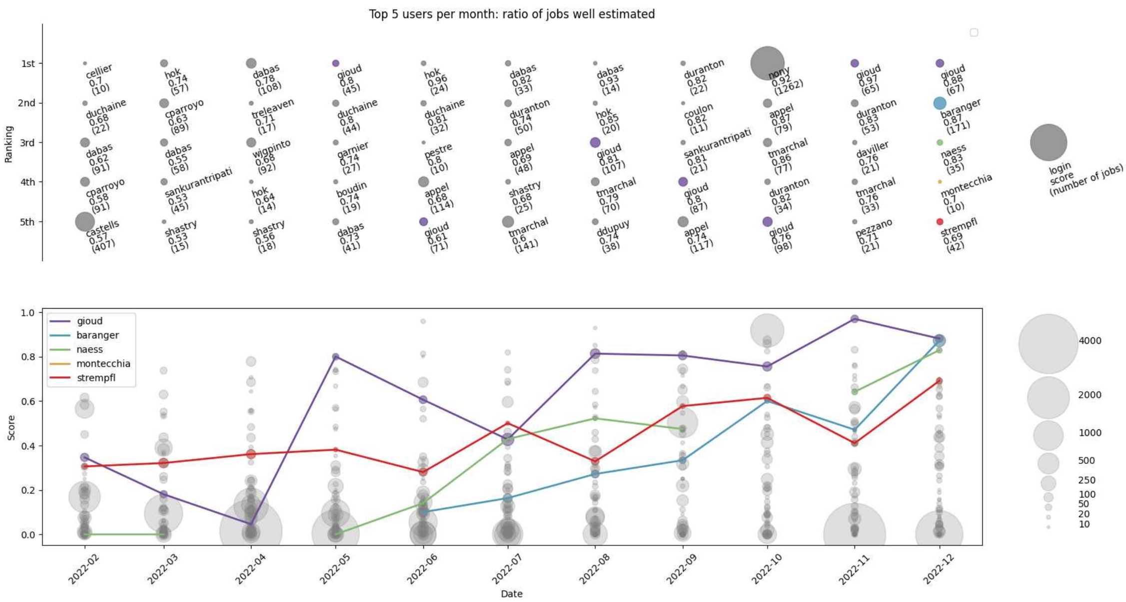

Figure 6.10: The monthly top 5, a ranking system based on user accuracy, applied to Cerfacs users on supercomputer Kraken in 2022

could be provided with a map. This is where a global callgraph of software comes into play. Much like a map that offers a visual representation of a city's layout and landmarks, a callgraph visually represents how different parts of software relate and interact.

Moreover, modern developers spend more time reading code than their counterparts a decade ago. With the ever-increasing complexity and size of codebases, expecting someone to read code linearly is impractical. Codebases that were complex a decade ago are now potentially indecipherable.

Access to a software's "geography" allows developers to view the code from a higher vantage point. It enables them to focus on specific areas while understanding the broader architectural context. This not only saves time but also provides valuable insights into code quality, including architecture, dependencies, size, and complexity.

6.2.3.1 The Role of Callgraphs as Software Maps

The idea of using callgraphs as software maps holds significant promise. Callgraphs make it easier to comprehend code interactions, navigate through the codebase, identify performance bottlenecks, locate potential error-prone areas, and simplify code maintenance. They also serve as a reference point for discussions, fostering better communication and teamwork among developers.

However, the transition from theory to practice is not without challenges:

1. Creating a comprehensive global callgraph can be time-consuming and resource-intensive, particularly for large and complex codebases.

2. Global callgraphs may be challenging to interpret, especially for developers unfamiliar with the codebase or software development processes.

3. Maintaining global callgraphs as code evolves can be cumbersome, requiring continuous updates.

4. Large and detailed global callgraphs can overwhelm users, making it difficult to find specific information.

To address these challenges, the Marauder's Map tool developed at CERFACS aims to utilize callgraphs as software maps while mitigating these drawbacks.

6.2.3.2 Practical Applications

In the context of the Center of Excellence Excellerat Phase II, CERFACS is developing the Marauder's Map tool to overcome these challenges.
Think of a world map—it provides an overview of countries, oceans, and poles. However, when driving or hiking, you rely on maps with smaller scales that show streets and buildings. Similarly, in software geography, global callgraphs offer an overarching view of the codebase, but their real utility shines when users can navigate smaller sections of the graph and select the information they need.
Two different visualizations are introduced: the tree graph and the global callgraph.

6.2.3.3 The Tree Graph - Understanding Code Architecture

The tree graph presents the desired code architecture. Functions are grouped and represented as circles whose size corresponds to the number of lines of code. Functions are organized by files, files by folders, and so on, following a tree graph structure. Circular packing is preferred to highlight these nestings.

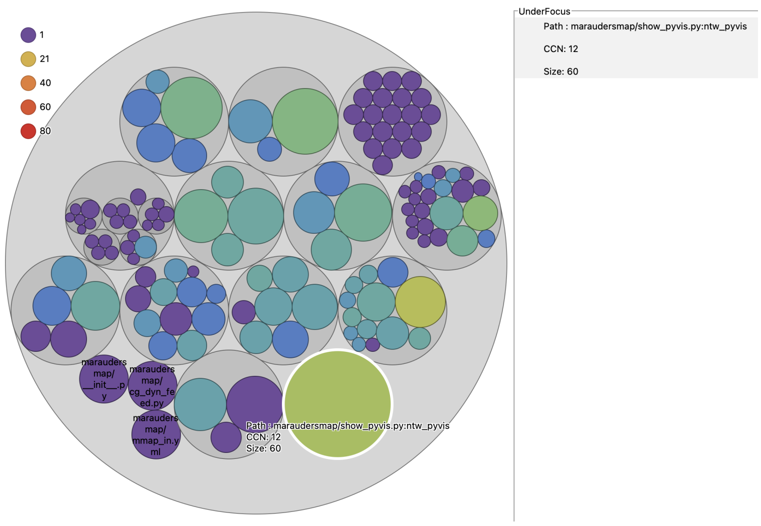

Figure 6.11: A tree graph revealing the mental map promoted by developers.

However, this mental map can be misleading as it doesn't reveal relationships between code stored in different files, making certain connections invisible.

6.2.3.4 The Global Callgraph - Revealing Actual Code Relations

A callgraph represents the calling relationships between subroutines, focusing on code blocks and their dependencies. Unlike the tree graph, it disregards names and storage strategies. It retains routines as circles proportional to their size and links them when one routine calls another. This forms a directed graph, and node placement can be calculated using n-body problem approximations like the Barnes-Hut simulation.

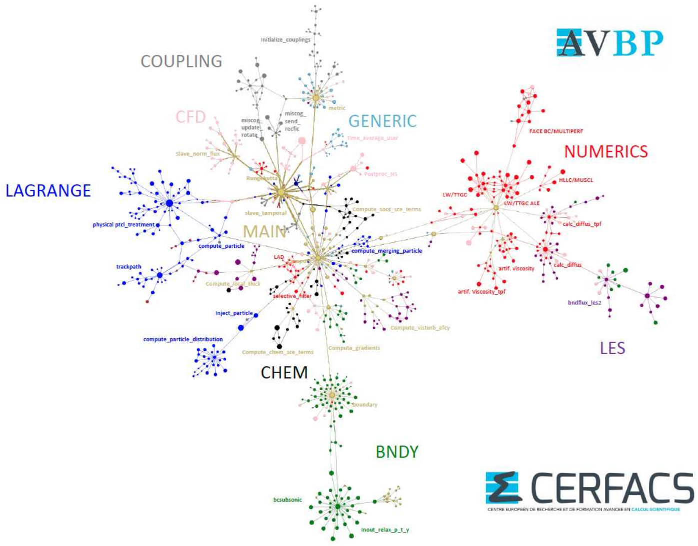

Figure 6.12: A global callgraph of the HPC large eddy simulation software AVBP, illustrating code block relationships. The structure emerges from the convergence of the Barnes-Hut algorithm.

Global callgraphs offer beginners a comprehensive view but also enable more specific and expert searches. The ability of the human eye to detect patterns becomes invaluable. Geometrical shapes within a callgraph reveal crucial insights, much like real maps disclose historical features.
In summary, while global callgraphs provide an essential starting point, their true power emerges when they allow users to navigate and focus on specific aspects of the code's geography.

References

[11] M. Bauer, J. Hötzer, D. Ernst, J. Hammer, M. Seiz, H. Hierl, J. Hönig, H. Köstler, G. Wellein, B. Nestler, and U. Rüde, (2019), Code Generation for Massively Parallel Phase-Field Simulations, In *SC '19: Proceedings of the International Conference for High Performance Computing, Networking, Storage and Analysis*, Association for Computing Machinery, 1–32.

[12] M. Bauer, H. Köstler, and U. Rüde, (2021), lbmpy: Automatic code generation for efficient parallel lattice Boltzmann methods, *Journal of Computational Science*, **49**.

[13] C. Gough, I. Steiner, and W. Saunders, (2015), *CPU Power Management*, Apress, Berkeley, CA, 21–70.

[14] D. Hackenberg, T. Ilsche, J. Schuchart, R. Schöne, W. Nagel, M. Simon, and Y. Georgiou, (2014), HDEEM: High Definition Energy Efficiency Monitoring, In *Energy Efficient Supercomputing Workshop (E2SC)*, 1–10.

[15] F. Hennig, M. Holzer, and U. Rüde, (2023), Advanced Automatic Code Generation for Multiple Relaxation-Time Lattice Boltzmann Methods, *SIAM Journal on Scientific Computing*, **45**, C233–C254.

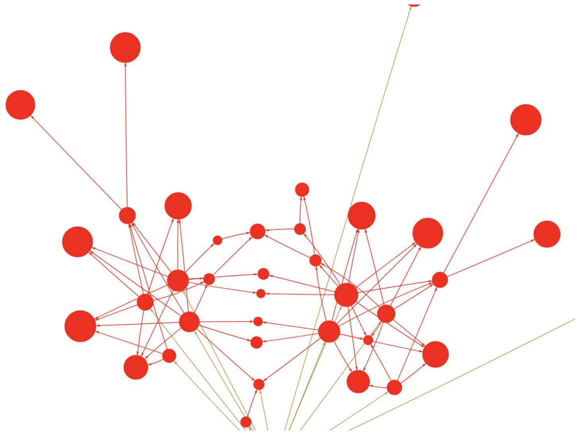

Figure 6.13: This close-up on the NUMERICS scheme of AVBP show the almost perfect duplication between the fixed-mesh numerical schemes and the moving-mesh ones. Each dot is a routine, each edge is a call to an other routine. The size reflect the number of Fortran statements. A change on one side should always be applied to the other side.

[16] M. Holzer, M. Bauer, H. Köstler, and U. Rüde, (2021), Highly efficient lattice Boltzmann multiphase simulations of immiscible fluids at high-density ratios on CPUs and GPUs through code generation, *The International Journal of High Performance Computing Applications*, **35**, 413–427.

[17] O. Vysocky, M. Beseda, L. Riha, J. Zapletal, M. Lysaght, and V. Kannan, (2018), MERIC and RADAR Generator: Tools for Energy Evaluation and Runtime Tuning of HPC Applications, In *High Performance Computing in Science and Engineering*, T. Kozubek, M. Cermak, P. Tichy, R. Blaheta, J. Sistek, D. Lukas, and J. Jaros, eds., Cham, Springer International Publishing, 144–159.

Publications

7.1 Books

[ALGO-COOP1] M. Mohr, U. Ruede, B. Wohlmuth, and H.-p. Bunge, (2023), *Impact of Scientific Computing on Science and Society*, vol. 58, Springer International Publishing.

[ALGO-COOP2] V. Xing and C. Lapeyre, (2023), *Machine Learning and its Application to Reacting Flows*, vol. 44 of LNEN, SPRINGER.

7.2 Conferences Proceedings

[ALGO-COOP3] E. Ajuria Illarramendi, M. Bauerheim, N. Ashton, C. Lapeyre, and B. Cuenot, (2023), Performance Study of Convolutional Neural Network Architectures for 3D Incompressible Flow Simulations, In *Proceedings of the Platform for Advanced Scientific Computing Conference*, 1–11.

[ALGO-COOP4] M. Destouches, P. Mycek, J. Briant, S. Gürol, A. Weaver, S. Gratton, and E. Simon, (2022), Multilevel Monte Carlo estimation of background error covariances in ensemble variational data assimilation, In *EGU General Assembly, Vienna, Austria and online, EGU22-336*.

[ALGO-COOP5] L. Drozda, P. Mohanamuraly, Y. Realpe, C. Lapeyre, A. Adler, G. Daviller, and T. Poinsot, (2021), Data-driven Taylor-Galerkin finite-element scheme for convection problems - The symbiosis of Deep Learning and differential equations, In *35th Conference on Neural Information Processing Systems (NeurIPS 2021), Sydney, Australia - Virtual conference*.

[ALGO-COOP6] I. Duff, (2021), Jack - Invited plenary talk, In *New directions in numerical linear algebra and high performance computing: celebrating the 70th birthday of Jack Dongarra, July 7-8*.

[ALGO-COOP7] D. Ernst, G. Hager, M. Holzer, M. Knorr, and G. Wellein, (2021), Opening the Black Box: Performance Estimation during Code Generation for GPUs, In *Proceedings of the IEEE 33rd International Symposium on Computer Architecture and High Performance Computing, Belo Horizonte – Brazil*.

[ALGO-COOP8] J.-N. Grad, A. Reinauer, and M. Holzer, (2023), ESPResSo and LbmPy: Re-usable and modular interface between particle-based and lattice-based simulation codes, In *RSE23 - Conference for Research Software Engineering in Germany, Paderborn*.

[ALGO-COOP9] J.-N. Grad, R. Weeber, M. Holzer, and C. Holm, (2022), Making use of established codes instead of re-inventing the wheel: Using lattice-based methods from waLBerla into ESPResSo, In *Software Engineering, Online*.

[ALGO-COOP10] S. Gürol, M. Peyron, A. Fillion, S. Gratton, P. Boudier, V. Marchais, and G. Goret, (2022), Latent Space Data Assimilation - Invited conference, In *Recent Advances in Numerical Linear Algebra for PDEs, Optimization, and Data Assimilation, ICMS, Bayes Centre, Edinburgh*.

[ALGO-COOP11] F. Hennig, M. Holzer, and U. Ruede, (2021), Automatic Code Generation for the Cumulant Lattice Boltzmann Method, In *Conference: ICMMES 2021, Online*.

[ALGO-COOP12] M. Holzer and U. Ruede, (2021), lbmpy: A Generic Tool for Interactive Development of Highly Efficient Lattice Boltzmann Methods, In *Proceedings of the International Conference for Mesoscopic Methods in Engineering and Science, Online*.

[ALGO-COOP13] M. Holzer, M. Bauer, and U. Ruede, (2021), lbmpy: Fast and Flexible Multi-Phase Lattice Boltzmann Simulations for High Density Ratios with Code Generation, In *Presented at The Platform for Advanced Scientific Computing (PASC) Conference, Online*.

[ALGO-COOP14] M. Holzer, G. Staffelbach, I. Rocchi, J. Badwaik, A. Herten, R. Vavrik, O. Vysocky, L. Riha, R. cuidard, and U. Ruede, (2023), Scalable Flow Simulations with the Lattice Boltzmann Method - Invited conference, In *CF ´23: Proceedings of the 20th ACM International Conference on Computing Frontiers*, 297–303.

[ALGO-COOP15] M. Holzer, (2021), Combining particle-based and continuum modelling in soft matter physics with ESPResSo, PyStencils, and LbmPy, In *ESPResSo Summer School, ICP Stuttgart University*.

[ALGO-COOP16] M. Holzer, (2022), Simulating the dynamics of soft matter with ESPResSo, PyStencils and LbmPy, In *ESPResSo Summer School, ICP Stuttgart University*.

[ALGO-COOP17] M. Holzer, (2023), Tackling Performance Challenges of Large Scale Lattice Boltzmann Applications using Metaprogramming Techniques within the Multiphysics Framework WaLBerla, In *Airbus Scientific Computing Conference 2023, Hamburg*.

[ALGO-COOP18] M. Lazzara, M. Chevalier, J. Garay Garcia, C. Lapeyre, and O. Teste, (2022), Improving Surrogate Model Prediction by Noise Injection into Autoencoder Latent Space, In *IEEE 34th International Conference on Tools with Artificial Intelligence (ICTAI), Macao, China*.

[ALGO-COOP19] M. Lazzara, M. Chevalier, C. Lapeyre, and O. Teste, (2023), NeuralODE-Based Latent Trajectories into AutoEncoder Architecture for Surrogate Modelling of Parametrized High-Dimensional Dynamical Systems, In *Artificial Neural Networks and Machine Learning – ICANN 2023, Crete, Greece, September 26-29*, 497–508.

[ALGO-COOP20] A. Ordonez Egas, N. Tardieu, C. Kruse, and D. Ruiz, (2022), Robustness and weak scalability assessment of a preconditioner for coupled Thermo-Hydro-Mechanics problems, In *CSMA 2022, 15ème Colloque National en Calcul des Structures, Presqu´île de Giens, France*, hal–03717698.

[ALGO-COOP21] S. S. P. Mohanamuraly and G. Staffelbach, (2021), KalpaTARU – Topology-AwaRe massively parallel Unstructured mesh infrastructure : loadbalancing, adaptation and more, In *2nd HiFiLeD symposium, September*.

[ALGO-COOP22] U. Ruede, C. Kruse, M. Kühn, and N. Kohl, (2022), Textbook multigrid efficiency and energy extrapolation - invited conference, In *Gatipor - Inria Paris*.

[ALGO-COOP23] U. Ruede, H. Schottenhamml, A. Anciaux-Sedrakian, and F. Blondel, (2021), Actuator-Line simulation of wind turbines using the Lattice Boltzmann Method, In *EoCoE-II Consortium Meeting, June 15th*.

[ALGO-COOP24] U. Ruede, (2021), Parallel Matrix-free Multigrid for Extreme Scale Computing, In *Webinar of the European Energy-Oriented Center of Excellence (EoCoE), January*.

[ALGO-COOP25] U. Ruede, (2021), Scalable Multiphysics Simulations - Invited conference, In *Online Workshop on Applied Mathematics, Nov 4-5, Ostrava*.

[ALGO-COOP26] U. Ruede, (2022), Parallel Multigrid for Exascale Simulations - invited conference, In *MATHĒMATICA SŌLIS ET TERRAE: AN AUSTRALIAN ACADEMY OF SCIENCE - ELIZABETH AND FREDERICK WHITE RESEARCH CONFERENCE*.

[ALGO-COOP27] U. Ruede, (2022), waLBerla - a scalable multi-physics framework - invited conference, In *HPC user forum - virtual*.

[ALGO-COOP28] H. Schottenhamml, A. Anciaux-Sedrakian, F. Blondel, A. Borras-Nadal, J. Joulin, and U. Ruede, (2022), Evaluation of a lattice Boltzmann-based wind-turbine actuator line model against a Navier-Stokes approach, In *Journal of Physics: Conference Series, Wind and Wind Farms, Measurement and Testing, Torque, Delft*, vol. 2262, 022027.

[ALGO-COOP29] A. Serhani, V. Xing, D. Dupuy, C. Lapeyre, and G. Staffelbach, (2022), High-performance hybrid coupling of a CFD solver to deep neural networks, In *33rd Parallel CFD International Conference, Alba, Italy*.

[ALGO-COOP30] G. Staffelbach, (2022), High Performance Computing for Combustion - invited conference, In *18 ème Ecole de Combustion du GFC, 31 mai - 2 juin*, IMFT, Toulouse.

[ALGO-COOP31] G. Staffelbach, (2022), The simulation of the energy transition and energy of simulation - invited conference, In *EuroHPC Summit Week, Paris, France*.

[ALGO-COOP32] G. Staffelbach, (2023), LES of combustion @CCRT ressources 20 years of progress and what lies beyond - invited conference, In *20 ans du CCRT - 5 Décembre*.

[ALGO-COOP33] D. Thönnes and U. Ruede, (2023), Model-Based Performance Analysis of the HyTeG Finite Element Framework, In *Platform for Advanced Scientific Computing Conference, PASC 2023, Davos, 26 - 28 June*.

7.3 Journal Publications

[ALGO-COOP34] E. Agullo, M. Altenbernd, H. Anzt, L. Bautista-Gomez, T. Benacchio, L. Bonaventura, H. Bungartz, S. Chatterjee, F. Ciorba, N. DeBardeleben, D. Drzisga, S. Eibl, C. Engelmann, W. Gansterer, L. Giraud, D. Göddeke, M. Heisig, F. Jézéquel, N. Kohl, X. Li, R. Lion, M. Mehl, P. Mycek, M. Obersteiner, E. Quintana-Orti, F. Rizzi, U. Ruede, M. Schulz, F. Fung, R. Speck, L. Stals, K. Teranishi, S. Thibault, D. Thönnes, A. Wagner, and B. Wohlmuth, (2022), Resiliency in numerical algorithm design for extreme scale simulations, *International Journal of High Performance Computing Applications*, **36**, 251–285.

[ALGO-COOP35] A. Ambekar, U. Ruede, and V. Buwa, (2022), Forces governing the dynamics of liquid spreading in a packed beds, *Journal of Fluid Mechanics*, **948**, article number A13.

[ALGO-COOP36] A. Ambekar, U. Ruede, and V. Buwa, (2022), Particle-resolved simulations of local liquid spreading in packed beds: Effect of wettability at varying particle size, *Physics of Fluids*, **34**, 062111.

[ALGO-COOP37] A. Ambekar, C. Schwarzmeier, U. Ruede, and V. Buwa, (2022), Particle-resolved turbulent flow in a packed bed: RANS, LES, and DNS simulations, *AICHE Journal*, **69**, e17615.

[ALGO-COOP38] E. Barrela, P. Berthet, O. Thual, and C. Lapeyre, (2023), Four-Dimensional History Matching Using ES-MDA and Flow-Based Distance-to-Front Measurement, *Energies*, **16**, Article number 7984.

[ALGO-COOP39] M. Bauer, S. Eibl, C. Godenschwager, N. Kohl, M. Kuron, C. Rettinger, F. Schornbaum, C. Schwarzmeier, D. Thönnes, H. Köstler, and U. Ruede, (2021), waLBerla: A block-structured high-performance framework for multiphysics simulations, *Computers and Mathematics with Applications*, **81**, 478–501.

[ALGO-COOP40] M. Bauer, H. Kostler, and U. Ruede, (2021), lbmpy: Automatic code generation for efficient parallel lattice Boltzmann methods, *Journal of Computational Science*, **49**, 101269.

[ALGO-COOP41] P. Boudier, A. Fillion, S. Gratton, S. Gürol, and S. Zhang, (2023), Data Assimilation Networks, *Journal of Advances in Modeling Earth Systems*, **15**, Article number e2022MS003353.

[ALGO-COOP42] E. Bourne, P. Leleux, K. Kormann, C. Kruse, V. Grandgirard, Y. Güçlü, M. Kühn, U. Ruede, E. Sonnendrücker, and E. Zoni, (2023), Solver comparison for Poisson-like equations on tokamak geometries, *Journal of Computational Physics*, **488**, Article number 112249.

[ALGO-COOP43] A. Buttari, M. Huber, P. Leleux, T. Mary, U. Ruede, and B. Wohlmuth, (2022), Block low-rank single precision coarse grid solvers for extreme scale multigrid methods, *Numerical Linear Algebra with Applications*, **29**, e2407.

[ALGO-COOP44] M. Chrust, M. Balmaseda, P. Browne, M. Martin, A. Storto, A. Vidard, A. Weaver, and H. Zuo, (2021), Ensemble of Data Assimilations in the ocean for better exploitation of surface observations, *ECMWF Newsletter*, **168**.

[ALGO-COOP45] V. Darrigrand, A. Dumistrac, C. Kruse, and U. Ruede, (2022), Inexact inner-outer Golub-Kahan bidiagonalization method: A relaxation strategy, *Numerical Linear Algebra with Applications*, e2484.

[ALGO-COOP46] D. Di Pietro, D. Antonio, F. Hülsemann, P. Matalon, P. Mycek, and U. Ruede, (2021), Algebraic multigrid preconditioner for statically condensed systems arising from lowest-order hybrid discretizations - Working paper or preprint, hal–03272468.

[ALGO-COOP47] D. Di Pietro, F. Hülsemann, P. Matalon, P. Mycek, U. Ruede, and D. Ruiz, (2021), An H-Multigrid Method for Hybrid High-Order Discretizations - Special Section Copper Mountain 2020, *SIAM Journal on Scientific Computing*, **43**, S839–S861.

[ALGO-COOP48] D. Di Pietro, F. Hülsemann, P. Matalon, P. Mycek, U. Ruede, and D. Ruiz, (2021), Towards robust, fast solutions of elliptic equations on complex domains through hybrid high-order discretizations and non-nested multigrid methods, *International Journal for Numerical Methods in Engineering*, **122**, 6576–6595.

[ALGO-COOP49] D. Di Pietro, F. Hülsemann, P. Matalon, P. Mycek, and U. Ruede, (2023), Algebraic Multigrid Preconditioner for Statically Condensed Systems Arising from Lowest-Order Hybrid Discretizations, *SIAM Journal on Scientific Computing*, **45**, S329–S350.

[ALGO-COOP50] D. Di Pietro, P. Matalon, P. Mycek, and U. Ruede, (2022), High-order multigrid strategies for HHO discretizations of elliptic equations, *HAL Preprint*, hal–03531293.

[ALGO-COOP51] D. Di Pietro, P. Matalon, P. Mycek, and U. Ruede, (2022), High-order multigrid strategies for Hybrid high-order discretizations of elliptic equations, *Numerical Linear Algebra with Applications*, **30**, e2456.

[ALGO-COOP52] L. Drozda and D. Matignon, (2023), Diffusive series representation for the Crandall model of acoustic impedance, *Meccanica*, **58**, 555–564.

[ALGO-COOP53] I. Duff, P. Leleux, D. Ruiz, and S. Torun, (2023), Row Replicated Block Cimmino, *SIAM Journal on Scientific Computing*, **45**, C207–C232.

[ALGO-COOP54] A. Dumitrasc, P. Leleux, C. Popa, U. Ruede, and D. Ruiz, (2021), Extensions of the Augmented Block Cimmino Method to the Solution of Full Rank Rectangular Systems, *SIAM Journal on Scientific Computing*, S516–S539.

[ALGO-COOP55] D. Dupuy, N. Odier, and C. Lapeyre, (2023), Data-driven wall modeling for turbulent separated flows, *Journal of Computational Physics*, **487**, Article number 112173.

[ALGO-COOP56] D. Ernst, M. Holzer, G. Hager, M. Knorr, and G. Wellein, (2023), Analytical performance estimation during code generation on modern GPUs, *Journal of Parallel and Distributed Computing*, **173**, 152–167.

[ALGO-COOP57] L. Giraud, Y.-F. Jing, and Y. Xiang, (2022), A Block Minimum Residual Norm Subspace Solver with Partial Convergence Management for Sequences of Linear Systems, *SIAM Journal on Matrix Analysis and Applications*, **43**, 710–739.

[ALGO-COOP58] O. Goux, S. Gürol, A. Weaver, Y. Diouane, and O. Guillet, (2023), Impact of correlated observation errors on the conditioning of variational data assimilation problems, *Numerical Linear Algebra with Applications*, **31**, e2529.

[ALGO-COOP59] O. Goux, J. Pfeffer, A. Blazquez, A. Weaver, and M. Ablain, (2023), A mass conserving filter based on diffusion for Gravity Recovery and Climate Experiment (GRACE) spherical harmonics solutions, *Geophysical Journal International*, **234**, 56–72.

[ALGO-COOP60] T. Guiberti, N. Shohdy, S. Cardona, X. Zhu, L. Selle, and C. Lapeyre, (2023), Chemiluminescence- and machine learning-based monitoring of premixed ammonia-methane-air flames, *Applications in Energy and Combustion Science*, **16**, Article number 100212.

[ALGO-COOP61] F. Hennig, M. Holzer, and U. Ruede, (2022), Advanced Automatic Code Generation for Multiple Relaxation-Time Lattice Boltzmann Methods, *arXiv preprint*, arXiv:2211.02435.

[ALGO-COOP62] F. Hennig, M. Holzer, and U. Ruede, (2023), Advanced Automatic Code Generation for Multiple Relaxation-Time Lattice Boltzmann Methods, *SIAM Journal on Scientific Computing*, **45**, C233–C254.

[ALGO-COOP63] M. Holzer, M. Bauer, J. Koster, and U. Ruede, (2021), Highly efficient lattice Boltzmann multiphase simulations of immiscible fluids at high-density ratios on CPUs and GPUs through code generation., *International Journal of High Performance Computing Applications*, **35**, 413–427.

[ALGO-COOP64] S. Iversen, A. Sperrevik, and O. Goux, (2023), Improving sea surface temperature in a regional ocean model through refined sea surface temperature assimilation, *Ocean Science*, **19**, 729–744.

[ALGO-COOP65] Y. Jang and S. Shaw, (2021), A priori error analysis for a finite element approximation of dynamic viscoelasticity problems involving a fractional order integro-differential constitutive law, *Advances in Computational Mathematics*, **47**, Article number 46.

[ALGO-COOP66] N. Kohl, D. Bauer, F. Böhm, and U. Ruede, (2023), Fundamental data structures for matrix-free finite elements on hybrid tetrahedral grids, *International Journal of Parallel Emergent and Distributed Systems*, **39**, 51–74.

[ALGO-COOP67] N. Kohl, M. Mohr, S. Eibl, and U. Ruede, (2022), A massively parallel eulerian-lagrangian method for advection-dominated transport in viscous fluids, *SIAM Journal on Scientific Computing*, **44**, C260–C285.

[ALGO-COOP68] M. Kühn, C. Kruse, and U. Ruede, (2021), Energy-Minimizing, Symmetric Discretizations for Anisotropic Meshes and Energy Functional Extrapolation, *SIAM Journal on Scientific Computing*, **43**, A2448–A2472.

[ALGO-COOP69] M. Kühn, C. Kruse, and U. Ruede, (2022), Implicitly Extrapolated Geometric Multigrid on Disk-Like Domains for the Gyrokinetic Poisson Equation from Fusion Plasma Applications, *Journal of Scientific Computing*, **91**, Article number 28.

[ALGO-COOP70] M. Lazzara, M. Chevalier, M. Colombo, J. Garay Garcia, C. Lapeyre, and O. Teste, (2022), Surrogate modelling for an aircraft dynamic landing loads simulation using an LSTM AutoEncoder-based dimensionality reduction approach, *Aerospace Science and Technology*, **126**, Article number 107629.

[ALGO-COOP71] D. Lea, J. While, M. Martin, A. Weaver, A. Storto, and M. Chrust, (2022), A new global ocean ensemble system at the Met Office: Assessing the impact of hybrid data assimilation and inflation settings, *Quarterly Journal of the Royal Meteorological Society*, **148**, 1996–2030.

[ALGO-COOP72] T. Mitchell, M. Holzer, C. Schwarzmeier, M. Bauer, U. Ruede, and C. Leonardi, (2021), Stability assessment of the phase-field lattice Boltzmann model and its application to Taylor bubbles in annular piping geometries, *Physics of Fluids*, **33**, 083325.

[ALGO-COOP73] P. Mohanamuraly and J. Müller, (2021), An Adjoint assisted Multilevel Multifidelity Method for Uncertainty Quantification And Its Application To Turbomachinery Manufacturing Variability, *International Journal for Numerical Methods in Engineering*, **122**, 2179–2204.

[ALGO-COOP74] A. Ordonez Egas, N. Tardieu, C. Kruse, D. Ruiz, and S. Granet, (2023), Scalable block preconditioners for saturated thermo-hydro-mechanics problems, *Advanced Modeling and Simulation in Engineering Sciences*, **10**, Article number 10.

[ALGO-COOP75] M. Peyron, A. Fillion, S. Gürol, V. Marchais, S. Gratton, P. Boudier, and G. Goret, (2021), Latent space data assimilation by using deep learning, *Quarterly Journal of the Royal Meteorological Society*, **147**, 3759–3777.

[ALGO-COOP76] J. Reis, O. Le Maître, P. Congedo, and P. Mycek, (2021), Stochastic preconditioning of domain decomposition methods for elliptic equations with random coefficients, *Computer Methods in Applied Mechanics and Engineering*, **381**, 113845.

[ALGO-COOP77] C. Rettinger and U. Ruede, (2022), An efficient four-way coupled lattice Boltzmann – discrete element method for fully resolved simulations of particle-laden flows, *Journal of Computational Physics*, **453**, 110942.

[ALGO-COOP78] C. Rettinger, S. Eibl, U. Ruede, and B. Wowinckel, (2022), Rheology of mobile sediment beds in laminar shear flow: Effects of creep and polydispersity, *Journal of Fluid Mechanics*, **932**, Article number A1.

[ALGO-COOP79] C. Rettinger, U. Ruede, S. Vollmer, and R. Frings, (2022), Effect of sediment form and form distribution on porosity: a simulation study based on the discrete element method, *Granular Matter*, **24**, Article number 118.

[ALGO-COOP80] C. Rettinger, M. Tabesh, U. Ruede, S. Vollmer, and R. Frings, (2023), On the use of packing models for the prediction of fluvial sediment porosity, *Earth Surface Dynamics*, **11**, Pages 1097 – 1115.

[ALGO-COOP81] U. Ruede and N. Kohl, (2022), Textbook Efficiency: Massively Parallel Matrix-Free Multigrid for the Stokes System, *SIAM Journal on Scientific Computing*, **44**, C124–C155.

[ALGO-COOP82] D. Schuster, E. Climent, and U. Ruede, (2023), Particle laden flows around a circular cylinder from the hydrodynamic to granular regime, *International Journal of Multiphase Flow*, **165**, Article number 104487.

[ALGO-COOP83] C. Schwarzmeier and U. Ruede, (2022), Analysis and comparison of boundary condition variants in the free-surface lattice Boltzmann method, *arXiv preprint*, arXiv:2207.13962.

[ALGO-COOP84] C. Schwarzmeier and U. Ruede, (2022), Comparison of refilling schemes in the free-surface lattice Boltzmann method, *AIP Advances*, **12**, 115324.

[ALGO-COOP85] C. Schwarzmeier and U. Ruede, (2023), Analysis and comparison of boundary condition variants in the free-surface lattice Boltzmann method, *International Journal for Numerical Methods in Fluids*, **95**, 820–850.

[ALGO-COOP86] C. Schwarzmeier, M. Holzer, T. Mitchell, M. Lehmann, F. Hausl, and U. Ruede, (2023), Comparison of free-surface and conservative Allen–Cahn phase-field lattice Boltzmann method, *Journal of Computational Physics*, **473**, 111753.

[ALGO-COOP87] C. Schwarzmeier, C. Rettinger, S. Kemmler, J. Plewinski, F. Nunez-Gonzalez, H. Kostler, U. Ruede, and B. Vowinckel, (2023), Particle-resolved simulation of antidunes in free-surface flows, *Journal of Fluid Mechanics*, **961**, Article number R1.

[ALGO-COOP88] T. Sengupta, V. Suman, S. Sengupta, and P. Sundaram, (2023), Quantifying parameter ranges for high fidelity simulations for prescribed accuracy by Lax–Wendroff method, *Computers and Fluids*, **254**, Article number 105794.

[ALGO-COOP89] J. Shin, V. Xing, M. Pfitzner, and C. Lapeyre, (2023), Probabilistic deep learning of turbulent premixed combustion, *AIP Advances*, **13**, Article number 085110.

[ALGO-COOP90] A. Suau, J. Nelson, M. Vuffray, A. Lokhov, L. Cincio, and C. Coffrin, (2021), Single-Qubit Cross Platform Comparison of Quantum Computing Hardware, *arXiv Quantum Physics*, e–Print arXiv: 2108.11334v1.

[ALGO-COOP91] A. Suau, G. Staffelbach, and H. Calandra, (2021), Practical Quantum Computing: solving the wave equation using a quantum approach, *ACM Transactions on Quantum Computing*, **2**, 1–35.

[ALGO-COOP92] A. Suau, G. Staffelbach, and A. Todri-Sanial, (2022), qprof: a gprof-inspired quantum profiler, *ACM Transactions on Quantum Computing*, **4**, 1–28.

[ALGO-COOP93] A. Suau, M. Vuffray, A. Lokhov, L. Cincio, and C. Coffrin, (2022), Vector Field Visualization of Single-Qubit State Tomography, *arXiv Quantum Physics*, e–Print arXiv: 2205.02483v1.

[ALGO-COOP94] A. Weaver, M. Chrust, B. Ménétrier, and A. Piacentini, (2021), An evaluation of methods for normalizing diffusion-based covariance operators in variational data assimilation, *Quarterly Journal of the Royal Meteorological Society*, **147**, 289–320.

[ALGO-COOP95] L. Werner, C. Rettinger, and U. Ruede, (2021), Coupling fully resolved light particles with the lattice Boltzmann method on adaptively refined grids, *International Journal for Numerical Methods in Fluids*, **93**, 3280–3303.

[ALGO-COOP96] V. Xing, C. Lapeyre, T. Jaravel, and T. Poinsot, (2021), Generalization Capability of Convolutional Neural Networks for Progress Variable Variance and Reaction Rate Subgrid-Scale Modeling, *Energies*, **14**, 5096.

[ALGO-COOP97] A. Yewgat, D. Busby, M. Chevalier, C. Lapeyre, and O. Teste, (2022), Physics-constrained deep learning forecasting: an application with capacitance resistive model, *Computational Geosciences*, **26**, 1065–1100.

7.4 Technical Reports

[ALGO-COOP98] Y. Achari Berrada, B. Jaderberg, V. Elfving, G. Staffelbach, U. Ruede, H. Vögel, and E. Shishenina, (2023), Application of Quantum Computing to solving transient Partial Differential Equations for Aerodynamics, technical report.

[ALGO-COOP99] E. Bourne, P. Leleux, K. Kormann, C. Kruse, V. Grandgirard, Y. Güçlü, M. Kühn, U. Ruede, E. Sonnendrücker, and E. Zoni, (2022), Solver comparison for Poisson-like equations on tokamak geometries, technical report, HAL Id: cea-03786723.

[ALGO-COOP100] G. Coulaud, (2022), Report on using convolutional neural networks to estimate normalization coefficients for diffusion-based correlation operators, working note, Cerfacs - Toulouse, France.

[ALGO-COOP101] J.-G. De Damas, (2022), Randomized SVD Preconditioners with an application to Data Assimilation, working note, ISAE SUPAERO - CERFACS.

[ALGO-COOP102] M. Destouches, P. Mycek, and S. Gürol, (2023), Multivariate extensions of the Multilevel Best Linear Unbiased Estimator for ensemble-variational data assimilation, technical report, Cerfacs.

[ALGO-COOP103] Y. Diouane, S. Gürol, A. Scotto di Perrotolo, and X. Vasseur, (2022), A general error analysis for randomized low-rank approximation methods, technical report, Cerfacs - Toulouse, France.

[ALGO-COOP104] I. Duff, P. Leleux, S. Torun, and D. Ruiz, (2022), Row Replicated Block Cimmino, technical report, Cerfacs - Toulouse, France.

[ALGO-COOP105] A. Dumitrasc, C. Kruse, and U. Ruede, (2023), Deflation for the off-diagonal block in symmetric saddle point systems - arXiv:2305.17693v1, technical report.

[ALGO-COOP106] A. Dumitrasc, C. Kruse, and U. Ruede, (2023), Generalized Golub-Kahan bidiagonalization for nonsymmetric saddle point systems - arXiv:2310.06952v1, technical report.

[ALGO-COOP107] S. Folke, (2022), Deep Learning methods for estimating normalisation coefficients of diffusion operators, working note, INSA - Cerfacs.

[ALGO-COOP108] Y. Jang, J. Bonelle, C. Kruse, F. Huelsemann, and U. Ruede, (2023), Fast Linear Solvers for Incompressible CFD Simulations with Compatible Discrete Operator Schemes - Preprint hal-04087358, technical report.

[ALGO-COOP109] P. Leleux, C. Schwarz, M. Kühn, C. Kruse, and U. Ruede, (2023), Complexity analysis and scalability of a matrix-free extrapolated geometric multigrid solver for curvilinear coordinates representations from fusion plasma applications, technical report, HAL Id: hal-04356523.

[ALGO-COOP110] J. Légaux and G. Staffelbach, (2022), ARPEGE GPU porting collaboration - Report on the fxtran and loki tools for automatic code transformation, technical report, Cerfacs - CNRM.

[ALGO-COOP111] J. Légaux and G. Staffelbach, (2023), Report on the GPU porting of ARPEGE kernels using loki for automatic code transformation, technical report.

[ALGO-COOP112] J. Toplis, (2023), Rapport de Stage M1 MAPI3 - Stage de recherche en quantification d'incertitude, working note, Université Toulouse III Paul Sabatier - Cerfacs.

[ALGO-COOP113] N. Venkovic, P. Mycek, L. Giraud, and O. Le Maître, (2021), Recycling Krylov subspace strategies for sequences of sampled stochastic elliptic equations - hal-03366966 , version 1, technical report.

7.5 Thesis

[ALGO-COOP114] C. Besombes, (2021), *Parameterization using generative adversarial networks for control space reduction in data assimilation*, phd thesis, INPT Toulouse - Sciences de l'univers de environnement et de l'espace - Cerfacs.

[ALGO-COOP115] L. Drozda, (2023), *On the development of data-driven numerical schemes in Computational Fluid Dynamics*, phd thesis.

[ALGO-COOP116] P. Leleux, (2021), *Hybrid direct and iterative solvers for sparse indefinite and overdetermined systems on future exascale architectures*, phd thesis.

[ALGO-COOP117] P. Matalon, (2021), *Fast solvers for robust discretizations in computational fluid dynamics*, phd thesis, Unité de recherche : Institut Montpelliérain Alexander Grothendieck (IMAG) En partenariat international avec Friedrich-Alexander Universität, Erlangen-Nürnberg, Allemagne.

[ALGO-COOP118] A. Ordonez Egas, (2022), *Scalable linear solver for thermo-hydro mechanics with a second gradient of dilation regularization problems*, phd thesis, Ecole doctorale MITT: Mathématiques, informatique et télécommunication de Toulouse.

[ALGO-COOP119] S. Sengupta, (2022), *Advanced methods for meshes in High Performance Computing of explosion simulation*, phd thesis, Ecole doctorale MEGEP - CERFACS.

[ALGO-COOP120] A. Suau, (2022), *Implémentation, analyse et améliorations bas-niveau d'algorithmes quantiques pour le calcul scientifique*, phd thesis, Ecole doctorale EDI2S.

[ALGO-COOP121] N. Venkovic, (2023), *Preconditioning strategies for stochastic elliptic partial differential equations*, phd thesis.

[ALGO-COOP122] Y. Xiang, (2022), *Résolution de systèmes linéaires de grande taille avec un nombre massif de second-membres et apprentissage*, phd thesis, Université de Bordeaux, Ecole doctorale de Mathématiques et d'informatique.

[ALGO-COOP123] V. Xing, (2022), *Deep learning for subgrid-scale modeling in large eddy simulations of turbulent premixed combustion*, phd thesis, Ecole doctorale MEGEP - CERFACS.

2

Climate and Environment

Introduction

This part covers diverse research activities conducted by CERFACS in three main areas: Climate Modeling, Environmental Systems, and Coupling & Data for Climate. In Climate Modeling, the focus is on improving the reliability and usability of climate information. Research encompasses addressing discrepancies between global and regional climate models, exploring the impact of climate change on polar regions, understanding climate variability, and predicting oxygen minimum zones in oceanic regions. The development and evaluation of the C3PS climate prediction platform are also highlighted.

Moving on to Environmental Systems, CERFACS has collaborated with Météo-France from 2003 to 2023, on atmospheric chemistry data assimilation. The focus from 2021-2023 involves refining the 4DEnVar data assimilation method for air quality forecasts and improving ozone forecasts using IASI satellite data. Micrometeorology research delves into urban air pollutant dispersion and wildland fire behavior, utilizing large-eddy simulations. The application of data assimilation and artificial intelligence for environmental monitoring is explored, aiming to enhance understanding and develop realistic coupled atmosphere-fire models. In hydrology, machine learning and Gaussian process regression strategies are employed to improve flood prediction and reliability analysis.

The final section discusses Coupling & Data for Climate. It emphasizes the importance of accurate regridding in Earth System Models and presents benchmarking results for regridding libraries. Efficient methods for ocean-atmosphere and hydrology coupling are described, including the Schwarz method and longitudinal coupling between 1D and 2D hydrodynamics models. The text underscores the significance of data management in climate modeling, detailing CERFACS's involvement in open-source initiatives, climate indices workflow development, and collaboration with the European Open Science Cloud.

In summary, the comprehensive research activities span climate modeling improvements, atmospheric chemistry data assimilation, micrometeorology, hydrology, and advancements in coupling software, regridding libraries, and data management. The organization's commitment to enhancing climate research and Earth System Model development is evident throughout the text.

Climate Modeling

2.1 Introduction

Research activities are presented through four axes: Climate change, The role of polar regions in climate variability and change, Variability and predictability, and Physical forcing and predictability of oxygen minimum zones in eastern boundary current systems, which is new in the team. They cover a wide range of spatial and temporal scales, from short extreme events to century long changes, and from small-scale interaction involving ocean eddies to planetary scales. They also focus on various geographical domains, from the tropics to polar regions and almost always involve coupling between different components of the Earth climate system.

2.2 Climate change

2.2.1 Towards better climate information

Adapting to climate change requires reliable climate information and a substantial part of our work is aimed at improving the reliability and usability of climate information.
In previous work ([2]), we have shown that current regional climate models (RCMs) tend to warm much less and dry less over Western Europe in summer than their forcing global climate models (GCMs). With colleagues from CNRM ([CE179]), using a suite of numerical experiments with a global and a regional atmospheric model, we have shown that atmospheric physics, and aerosols as hypothesized in Boé et al. (2020), could explain a large part of discrepancies between GCM and RCM projections, with only a small role of model resolution, suggesting that current regional projections could be less realistic than global projections. Observations, through the emergent constraint approach, can help to reduce structural uncertainties in climate projections. In [CE167], with a novel method, we have shown that constraining GCM projections with past global and local observed temperature trends leads to even higher warming over France compared to unconstrained global projections. This result reinforces the idea that many current RCMs may significantly underestimate future climate changes, with important consequences for the impact studies based on their results.
[CE149] have explored the discrepancies in projected regional projections in the South-East Asia (SEA) region. They find a robust future intensification of summer precipitation across the CORDEX-SEA models over the northern part of SEA, whereas the ‘worst’ and ‘best’ performing models show opposite projections over the southern part. This work illustrates how the thorough evaluation of models’ skill in the present-climate (here, the spatio-temporal distribution of precipitation) with an understanding of key physical processes [CE150] can lead to more credible regional projections thanks to model sub-selection.

Ensembles of climate projections such as those from the Coupled Model Intercomparison Project (CMIP) are used to estimate ad-hoc the structural uncertainties in climate projections. However, as each climate model is developed more or less independently to provide the best estimate of climate changes, nothing guarantees that they collectively span the full range of structural uncertainties. In the PhD thesis of S. Peatier [CE236], a methodology based on a perturbed parameters ensemble has been designed to explore the full range of climate sensitivities compatible with a realistic representation of the present climate (Figure 2.1). This range turns out to be very large [CE161].

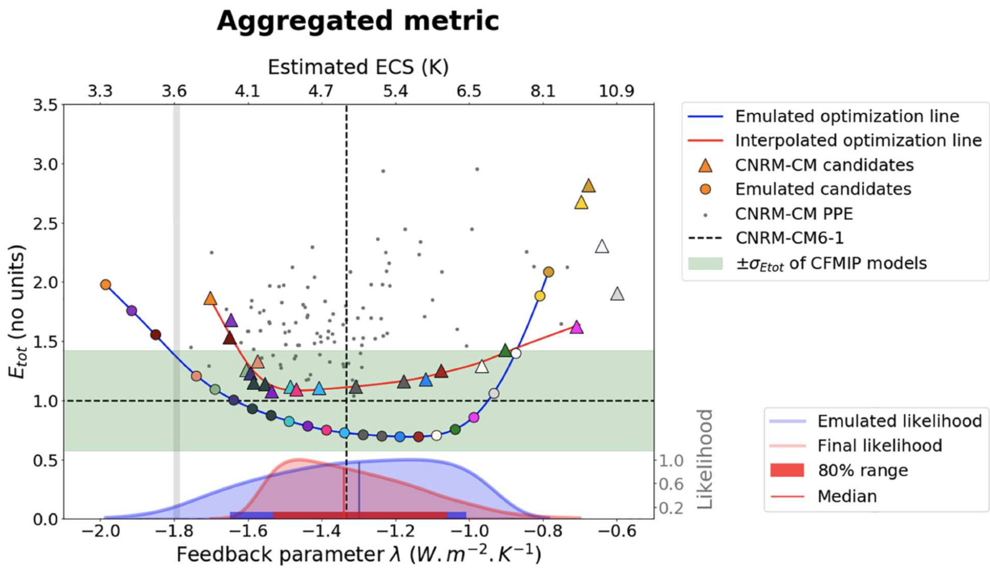

Figure 2.1: CNRM-CM simulations with optimized calibrations conditional on target values of feedback parameters λ. The plot shows the multivariate error Etot (y axis) as a function of the feedback parameter λ (bottom x axis) for the emulated optimal candidates (blue line). Twenty-three calibrations have been selected along the feedback range (colored disks) and used in ARPEGE-Climat to produce actual climate runs (colored triangles): 1 run crashed (gray thick line) and 15 others have associated errors within the standard deviation of the CFMIP models errors (green area). Disks and triangles of the same color correspond to the same calibration. The climate sensitivity is estimated from λ. The two relative likelihoods of the feedback parameter, estimated with Equation 3, are represented by the shaded distributions, with the 10th to 90th percentiles range (80% range) and the median in bright colors. The blue distribution is the initial likelihood function, estimated from the emulated optimal candidates (blue line). The red distribution is an adjusted likelihood function based on a smooth fit (using a cubic spline under tension interpolation) of CNRM-CM optimal candidates error metric along the feedback range (red line).

New paradigms in climate change impact studies emerge. It is now widely acknowledged that climate models should be specifically fit for the purpose of the impact study. Storylines based on a few carefully selected climate trajectories of specific interest or focused on singular extreme events are increasingly used, as limits to standard pseudo-probabilistic approaches have became clearer.

Complementary with extreme event attribution probabilistic approaches, we have pioneered a storyline conditional approach to extreme event attribution based on dynamical adjustment with constructed analogues of the atmospheric circulation [CE180]. We have applied this approach to the mega-heatwave that occurred in the Pacific Northwest during late June 2021. This extreme heatwave led to extreme temperatures with many records broken (including the all-time Canada record, 49.6°C on June 29th), and sparked extensive wildfires, including the one that destroyed the town of Lytton in British Columbia. We have shown that the main contribution to the heatwave amplitude and persistence is an atmospheric pattern termed Omega Block (a high-pressure dome surrounded by two lows). Intense surface solar radiation, subsidence through adiabatic warming and downward longwave radiation due to anomalous atmospheric

moisture are the main drivers of the extreme heatwave. The storyline approach also suggests that the event would have been severe even without the climate change signal [CE181].
The fit-for-purpose approaches require an impact study-specific selection of projections to downscale, which is very difficult to achieve with standard dynamical downscaling approach, given the cost of regional models. We have developed a new hybrid statistical-dynamical downscaling method based on the emulation of RCMs [CE109]. This method is as easy to use and as flexible as statistical downscaling, making it possible to select GCMs or members to downscale specifically for the impact study, but is also expected to provide results as robust as those of dynamical downscaling, capturing all potential mechanisms involved in climate changes as simulated by the emulated RCM.
We also have been exploring alternative approaches to standard probabilistic impact studies. They generally require long climate projections, in which deep convection cannot be explicitly resolved. This is likely to be particularly problematic when interested in the future evolution of extreme precipitation events. In this work, convection-permitting regional climate modeling at very high resolution with CNRM-AROME is used for the realistic simulation of observed extreme precipitation events, which are then transposed to a warmer future climate (i.e. 'futurization' of observed events) based on different possible storylines.

2.2.2 Impact of resolution

We have pursued our assessment of the impact of increased spatial resolution on several aspects. First, we provided insights into the mechanisms driving the weakening of the Atlantic Meridional Overturning Circulation (AMOC) in response to the projected increase in atmospheric carbon dioxide (CO2) concentration, by comparing the oceanic response in three configurations of a coupled climate model suite with varying ocean resolution (1º, 0.25º, 0.1º). Changes in the AMOC strength were found to be similar in the low and high resolution models, with however important differences in terms of the geostrophic and eddy contributions. A muted response was found in the medium resolution model (0.25º) highlighting the uncertainty that can arise when eddies are neither parameterized nor resolved in climate models [CE127].
In another study, based on eddy-permitting ensemble ocean simulations over multiple decades, we have shown that chaotic fluctuations can strongly influence regional decadal ocean heat content (OHC) and sea level trends [6]. As in-situ ocean measurements capture a combination of the atmospherically-forced response and this intrinsic ocean variability, it is key to assess and understand the imprint of the chaotic ocean variability recorded by the in-situ measurements. We have used a set of synthetic in-situ-like profiles extracted from the OCCIPUT ensemble [1] to compare the original ensemble outputs with the remapped, subsampled, in-situ-like profiles. Our results show that intrinsic variability may be large in eddy-active regions in the gridded model outputs, and remains substantial when using the in-situ sampling-based estimates [CE139]. The same result is also found on large spatial scales, for which atmospheric forcing is classically identified as the main driver.

2.2.3 Impact studies

Several of our studies have contributed to a better assessment and understanding of the impacts of climate change on Europe. [CE110] has shown the great role of the physiological impact of CO_2 on hydrological changes in Europe, which is generally not simulated by hydrological models used in impact studies. [CE128] have characterized the evolution of extreme temperatures over the main Euro-Mediterranean airports to better assess the impacts of climate change on air transport in the Ph.D thesis of V. Gallardo [CE232]. A focus on how uncertainty in atmospheric variables translate into aircraft weight restriction during the take off phase is investigated in S. Salles's PhD, under various emission scenario [CE97]. [CE166] have been interested in the evolution of Mediterranean cyclone characteristics. [CE174] found no evidence for an increased vulnerability of French crop production to climate hazards between since the 1960s. We have also investigated the impact of climate change on Clear Air turbulence (CAT) (M. Foudad

PhD thesis, Foudad et al. submitted). Our results show that over several regions in the Northern Hemisphere, in particular East Asia, positive CAT trends are found as a consequence of anthropogenic forcing, indicating that the response of CAT to global warming can be already detectable in the recent decades. Positive trends in CAT frequency are projected for different global warming levels over these regions at aircraft cruising altitudes. Nevertheless, over North Atlantic region, the different uncertainties are still large.

The impacts of climate change on variability and extremes may be as important as the impacts on means. It is therefore important to understand how changes in means and variability / extremes are linked. At the global scale, [CE104] have shown that future seasonal changes in extreme precipitation scale with changes in the mean. [CE143] have shown that ENSO teleconnections change with climate change over 50% of teleconnected regions in winter, generally, but not always towards an amplification of the historical teleconnections. [CE114] have shown a weakening of Atlantic Niño variability with climate change .

2.3 The role of polar regions in climate variability and change

The Arctic region is a hot spot of climate change, as it shows an amplified warming of near-surface air and ocean temperatures compared to the rest of the Earth and an associated rapid decline of sea ice in recent decades [5]. In previous work [4] and [CE111], we have shown that Arctic sea ice melt leads not only to a polar amplification of lower-troposphere warming but also to a weakening of midlatitude westerlies, a narrowing of the jet and a weak but signifiant reduction of the strength of the polar vortex. In the CNRM-CM6 model, interactions between the troposphere and the stratosphere were shown to contribute to the development of the dynamical response, by favoring vertical propagation of planetary waves. We showed that the atmospheric response to Arctic sea ice loss does not remain confined to high-latitudes, with a significant warming of North American and European lands and a cooling of central Asia as detailed in Chripko et al. (2021). As part of a collaboration with University of Louvain La Neuve, we further showed that sea ice decline is associated with more frequent and more persistent extreme warm temperatures over peripheral regions of the Arctic, with however limited changes in precipitation [CE116]. In line with previous studies, we showed that the atmospheric circulation response depends on the location of Arctic sea ice anomalies, with a dominant role for Barents-Karen sea melt anomalies which drive a robust negative North Atlantic Oscillation (NAO)-like pattern in winter in CMIP6 models [CE117].

A more realistic protocol with a multi-model approach has been used as part of the CMIP6 Polar Amplification Model Intercomparison Project (PAMIP). 16 atmospheric models have been forced by a prescribed sea-ice pattern that corresponds to the projected anomalies for a global-mean temperature increase of 2ºC with respect to preindustrial conditions. Each model includes 100 to 300 members which are run to 1 year. We contributed to this multi-model analysis which showed that the weakening of midlatitude westerlies in response to sea ice decline is robust but is underestimated by climate models, likely because of a too large atmospheric internal variability in the models, the so-called signal to noise paradox. These results were published in Nature Communications [CE176].

In addition to exploring atmospheric teleconnections, we have explored the large-scale oceanic response to Arctic sea ice decline for which dedicated multi-model coupled PAMIP experiments have been run. As part of the master 2 internships of Emma Bedossa and Emilie Gros, we showed that the projected decline of Arctic sea ice leads on decadal to multi-decadal time scales to a warming and freshening of the Central Arctic, reduced deep water formation in the North Atlantic subpolar gyre and hence a weakened Atlantic Meridional Overturning Circulation after about 50 years. This leads to a cooling and freshening of the eastern subpolar gyre because of a reduced northward transport of heat and salt by the North Atlantic current. While the oceanic response to Arctic sea ice loss shows common features among models, in particular when scaled by the amount of annual sea ice loss, there are marked differences in terms of patterns and time scale of the oceanic response in the Atlantic. This can partly be explained by the different experimental protocols that have been used to constrain sea ice, but also by the different model mean states, in particular the initial thickness anomalies in the Central Arctic, and by internal variability. These results will be presented at the WCRP Open Science Conference in Kigali in October 2023.

The polar regions experience fast transitions in terms of sea ice cover and thickness distribution with potentially large implications in terms of climate impacts locally and remotely. Yet, current generation climate models fail in accurately representing essential aspects of polar climate, such as Arctic sea ice loss, Antarctic sea ice variability, polar amplification, Arctic water mass changes and water mass transformation in Antarctic polynyas. As part of the Scale Aware Sea Ice Project (SASIP), we investigate whether a new sea ice model, neXtSIM, that includes a novel rheology that better represent mechanical processes within sea ice like fractures, leads and damage, yield a more realistic representation of sea ice regime changes in the Arctic and Antarctic. As an initial step for this work, we started gathering the sea ice developments to couple the neXtSIM model to the NEMO ocean model. We defined a novel two-grid model configuration that optimizes the MPI decomposition and scalability of the future GCM as described in [CE205] and [CE216]. Decadal-long simulations with an ocean-sea ice version forced by atmopsheric reanalysis will be run and analyzed in the coming winter and spring to assess the benefit of the new sea ice rheology.

2.4 Variability and predictability

2.4.1 Understanding the role of internal climate variability and associated mechanisms

The climate system responds to the interplay between human influence, natural drivers (solar and volcanic activity), and internal variability. Quantifying the relative influence of these factors is crucial for assessing and understanding past climate trends as well as the actual and future occurrence of extreme events. It is well established that internal variability arising from the chaotic nature of the climate system can amplify or obscure anthropogenically-forced signals, especially in the near-term and at regional scale. Accounting for the full range of possible future changes, including internal variability, is thus key in order to plan at best climate-related risks and local adaptation strategies. Communicating on the importance of internal variability and better accounting for its regional influence is thus central for the climate adaptation science, and application communities, especially for near-term planning. Promising methodologies to better account for the whole nature and range of uncertainties have recently emerged through so-called 'physical climate storyline' approaches, especially at regional scale. These consist in partitioning the full range of climate outcomes into a set of self-consistent and possible unfolding of physical trajectories of the climate system based on specified explanatory elements. In the PhD thesis of A. Line, we focus on Northern Europe winter climate changes over the 2020-2040 period and propose a set of internal variability storylines (IVS) to tackle related uncertainties. IVS are built from the combined evolution of the North Atlantic Oscillation (NAO) and the Atlantic Meridional Overturning Circulation (AMOC) diagnosed as drivers of variability for temperature over northern Europe. We show, based on a large ensemble of historical-scenario simulations performed with CNRM-CM6-1, that, depending on the [AMOC-NAO] doublet evolution, anthropogenically-forced changes can be either considerably amplified with much warmer-wetter mean conditions, almost doubled, or considerably masked with marginal warming and unchanged mean precipitation with respect to present day (Figure 2.2). Reframing the uncertain climate outcomes into the physical science space through IVS grapples the complexity of regional situations; it is also informative to more efficiently communicate towards the general public as well as for climate literacy in general.

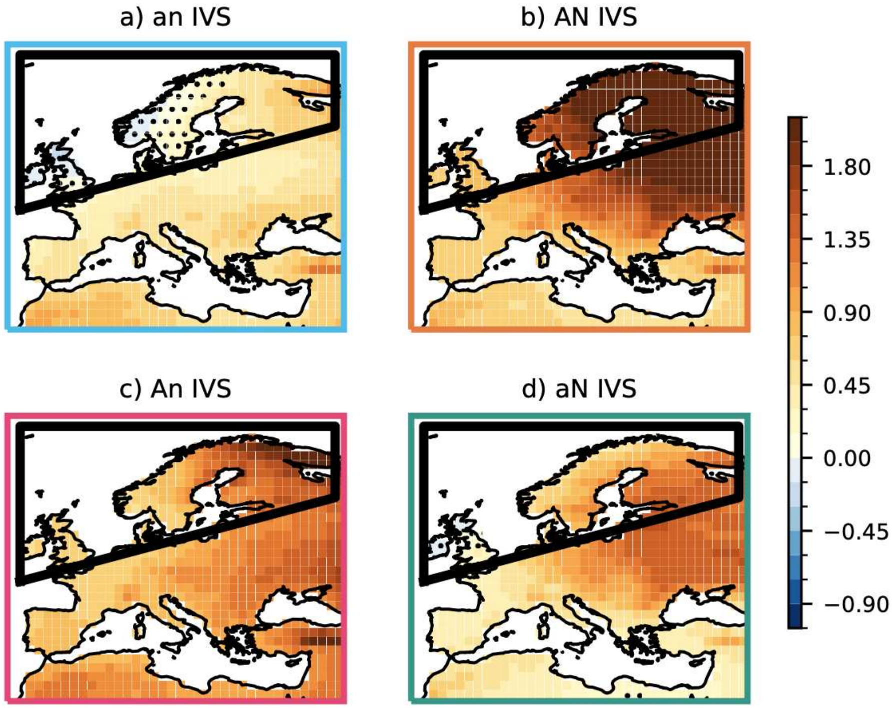

Figure 2.2: Regional temperature changes for the four internal variability storylines (an, AN, An, aN) based on the [AMOC-NAO] doublet evolution. Dots stand for non-significant values based on t-4statistics at the 95% level of confidence (pvalue > 0.05). The Northern Europe domain selected as the region of interest in this study is displayed. From Line et al. submitted

Understanding how the ocean internal variability actually impacts over climate over lands how these impacts are simulated by state-of-the-art climate models is a key challenge for the climate research community with important implications to obtain valuable climate predictions based on the ocean initialization. At decadal time scales, oceanic modes of variability such as the Atlantic multidecadal variability (AMV) seem to modulate the climate variations over the adjacent continental areas. The impacts of the AMV over the Euro-Mediterranean region have been documented in terms of mean climate, both in observations and models, but this is not the case for extreme events. Yet, the Mediterranean basin is considered as a climate change hotspot for which an assessment of the risks related to climate change is important since Heat Waves are expected to be more frequent in the next decades. To improve the understanding of the processes linking the AMV and climate decadal variability, the Decadal Climate Prediction Project (DCPP) endorsed by CMIP6, and the European H2020 PRIMAVERA project proposed a coordinated experimental protocol using partial coupling experiments. In these simulations, North Atlantic SSTs are restored toward anomalies representative of the observed AMV while the rest of the system evolves freely. Our goal is to assess the influence of the AMV and its amplitude on the European climate, particularly on Heat Waves duration, by using DCPP-compliant experiments from two climate models. We show that abnormally warm temperatures in the North Atlantic are associated with a higher occurrence of heatwave episodes over southern Europe and the Mediterranean, and this response is fairly robust in the two climate models analysed (Qasmi et al. 2021). For both models and a moderate amplitude of the AMV, the Heat Wave durations over the Mediterranean regions are from 3 days up to 6 days over the eastern Mediterranean longer relative to the AMV climatology. Other collaborations in the H2020-PRIMAVERA project enable us to study of the impact of AMV on the jet stream and extratropical cyclones ([CE169]) and on the Atlantic-Pacific teleconnections ([CE170], [CE132]).

2.4.2 Seasonal to decadal prediction of physics and biogeochemistry

In the context of the H2020-TRIATLAS project the CNRM-Cerfacs team has developed a new climate prediction plateform based on the CNRM-ESM2.1 model. This new system called C3PS is a new research tool for performing seasonal-to-decadal predictions for a wide array of climate and Earth system variables. C3PS operates through a seamless coupled full initialization for the atmosphere, land, ocean, sea ice and biogeochemistry components that allows a continuum of predictions across seasonal to decadal time-scales. For the decadal timescale, C3PS has also contributed to the Decadal Climate Prediction Project (DCPP-A) as part of the sixth Coupled Model Intercomparison Project (CMIP6). In Sanchez-Gomez et al. (to be submitted) we describe the main characteristics of this novel Earth system-based prediction platform, including the components of the model, the initialization scheme, the implementation of new forcings and the prediction framework. The initialisation procedure of C3PS consists of a full-field initialisation in which all the model components are initialised from an in-home reanalysis product obtained in two steps. The first step is a forced experiment in which ocean and biogeochemistry models are driven by JRA55do reanalysis following the GCP protocol. In the second step, the T and S of this forced experiment from step1 are used to constrain only the ocean physics of CNRM-ESM2.1 through sea surface restoring and a Newtonian damping in the ocean subsurface, as described in Sanchez-Gomez et al. 2016 ([9]).
We evaluate the C3PS initialisation procedure with recent observations and reanalysis and we discuss its overall performance in the light of the lesson learnt from the previous prediction platform as developed and used for CMIP5 and CMIP6. We believe that the study of the reconstructions created to initialize the climate prediction systems is relevant, and even more so in the context of the new applications offered in the prediction of marine biogeochemistry and carbon fluxes.
Regarding the forecast skill, the results show that at seasonal timescale, the predictive skill of C3PS is very similar to current forecasting systems as far as ENSO forecasting is concerned. At the decadal scale, the C3PS results show a significant predictive skill in surface temperature during the first two years after initialisation in several regions of the world. C3PS also exhibits potential predictive skill in net primary production (NPP). Most importantly, NPP skill is high in the areas of highest marine productivity, such as the equatorial and eastern boundary upwelling systems, in particular the Canary Upwelling System. C3PS also provides skillful predictions of ocean carbon uptake at multiannual scale over the areas of large carbon uptake variability such as North Atlantic and North Pacific oceans and Southern Ocean. All these results expand the possibility of applications of forecasting systems based on earth system models.
We have also contributed to the skill assessment in current sub-seasonal and seasonal prediction systems over different regions, such as the Sahel ([CE142]) and over Europe ([CE103]).

2.5 Physical forcing and predictability of oxygen minimum zones in eastern boundary current systems

An increasing number of climate models now include the marine biogeochemical component of the earth system in order to on the one hand simulate climate feedbacks associated with the carbon and nitrogen cycles and on the other hand address climate impacts on the marine ecosystems. A thorough evaluation of these systems is thus required to better understand feedbacks that modulate natural variability and to qualify their prediction capabilities in terms of the biogeochemical environment. This goes along with investigating the forcing mechanisms of ocean biogeochemistry particularly in eastern boundary upwelling systems that are very productive regions where climate pressures (warming, deoxygenation, acidification) have detrimental effect on marine life. CERFACS has been recently engaged in such studies in the framework of several international projects (H2020 TRIATLAS, H2020 project FutureMares, JPI Ocean&Climate project CE2COAST, ANID/IRD project CLAP). The focus has been on the Humboldt and Canary systems that hosts a so-called oxygen minimum zone (OMZ) consisting in poorly ventilated subsurface waters where oxygen concentration is sufficiently low to represent a respiratory barrier for most marine species. These OMZs are thought to be expanding under global warming but consensus amongst models remains low particularly in the tropical regions. Various investigations on this topic have been carried out relying on both regional and global modeling efforts at CECI, considering in particular that current-generation Earth System Models have still difficulties in simulating realistically the circulation in EBUS owing in part to their too low resolution. Regional model simulations have been carried out to investigate the interannual variability of the OMZ and its sensitivity to resolution. It was shown in particular that mesoscale dynamics is a major source of natural variability of the OMZ off Chile (Pizarro Koth et al., 2023). Based on the analysis of an ensemble of CMIP model simulations an emergent constraint on oxygenation along the coast of South America has been also established indicating that the OMZ in the South Eastern Pacific is more likely to shrink despite the on-going global ocean deoxygenation (Almendra et al., submitted). The unprecedented model resource produced by CECI/CNRM in the framework of the TRIATLAS project (Sanchez-Gomez et al. to be submitted) has been also the opportunity to evaluate the potential predictability of dissolved oxygen, with a focus on EBUS. Preliminary results indicate a good skill of the CECI/CNRM system up to 1 to 2 years leadtime in the tropical region in terms of oxygen (Figure xx). This opens up prospects for developing climate products and alert systems useful for coastal communities in EBUS. Such activity is planned to be developed in the next years in the framework of the collaboration with IRD.

References

[1] L. Bessières, S. Leroux, J.-M. Brankart, J. Molines, M.-P. Moine, P.-A. Bouttier, T. Penduff, L. Terray, B. Barnier, and G. Serazin, (2017), Development of a probabilistic ocean modelling system based on NEMO 3.5: application at eddying resolution, *Geoscientific Model Development*, 1091–1106.

[2] J. Boé, S. Somot, L. Corre, and P. Nabat, (2020), Large discrepancies in summer climate change over Europe as projected by global and regional climate models: causes and consequences, *Climate Dynamics*, **54**, 2981–3002.

[3] S. Chripko, R. Msadek, E. Sanchez-Gomez, L. Terray, L. Bessières, and M.-P. Moine, (2021), Impact of Reduced Arctic Sea Ice on Northern Hemisphere Climate and Weather in Autumn and Winter, *Journal of Climate*, **34**, 5847–5867.

[4] S. Chripko, (2020), *Rôle du déclin de la glace de mer en Arctique sur le climat des moyennes latitudes: téléconnexions atmosphériques*, phd thesis, Université Toulouse.

[5] B. Fox-Kemper and coauthors, (2021), Ocean, cryosphere and sea level change. IPCC Climate Change 2021: The Physical Science Basis, *eds Masson-Delmotte, V. et al., Cambridge Univ. Press,*.

[6] T. Penduff, G. Serazin, S. Leroux, S. Close, J. Molines, B. Barnier, L. Bessières, L. Terray, and G. Maze, (2018), Chaotic variability of ocean heat content: Climate-relevant features and observational implications., *Oceanography*, **31**, 63–71.

[7] P. Ruggieri, A. Bellucci, D. Nicoli, P. Athanasiadis, S. Gualdi, C. Cassou, F. Castruccio, G. Danabasoglu, P. Davini, N. Dunstone, R. Eade, G. Gastineau, B. Harvey, L. Hermanson, S. Qasmi, Y. Ruprich-Robert, E. Sanchez-Gomez, D. Smith, S. Wild, and M. zampieri, (2021), Atlantic Multidecadal Variability and North Atlantic Jet: a multi-model view from the Decadal Climate Prediction Project, *Journal of Climate*, **34**, 347–360.

[8] Y. Ruprich-Robert, E. Moreno-Chamarro, X. Levine, A. Bellucci, C. Cassou, F. Castruccio, P. Davini, R. Eade, G. Gastineau, L. Hermanson, D. Hodson, K. Lohmann, J. Lopez-Parages, P. Monerie, D. Nicoli, S. Qasmi, C. Roberts, E. Sanchez-Gomez, G. Danabasoglu, N. Dunstone, M. Martin-Rey, R. Msadek, J. Robson, and D. Smith, (2021), Impacts of Atlantic multidecadal variability on the tropical Pacific: a multi-model study, *npj Climate and Atmospheric Science*, **4**, Article number 33.

[9] E. Sanchez-Gomez, C. Cassou, Y. Ruprich-Robert, E. Fernandez, and L. Terray, (2016), Drift dynamics in a coupled model initialized for decadal forecasts, *Climate Dynamics*, **46**, 1819–1840.

Environmental Systems

3.1 Introduction

Research dedicated to Environmental Systems at CECI is shared over the three following topics: regional-to-global scale atmospheric chemistry, microscale meteorology such as air pollutant dispersion in urban environments and wildland fire, and inundation and flood forecasting, with a particular focus on data assimilation, metamodeling and high-fidelity numerical simulations. This research is multidisciplinary and addresses a wide variety of objectives (environment surveillance, early warning system, monitoring, reanalysis, scenarios, forecasting), spatio-temporal scales (from micro-/meso-scales to regional/global scales), simulation tools and algorithms (data assimilation, uncertainty quantification, machine learning, code coupling, high performance computing).

These research activities, mostly carried out with in the GLOBC team in synergy with the CECI research strategy, rely on collaborations with other research axis from the Climate and Environment topic (Climate Modeling and Coupling, HPC and Data for Climate) as well as on collaborations with ALGO, CFD and CSG teams at CERFACS.

Note that since the previous report on the 2019-2020 period, exploratory work has demonstrated the value of advanced methodological developments for environmental applications, with interesting prospects for operational applications. In atmospheric chemistry applications, hybrid ensemble-variational algorithms and direct radiance assimilation are proving to be very valuable to address chemistry-transport model errors and thereby improve air quality forecasts in CAMS. In micrometeorology, major modeling and methodological milestones related to ensemble predictions have been cleared thanks to dedicated PhD thesis works, making possible to move towards ensemble-based data assimilation embedding high-fidelity simulation data and opening new opportunities for future collaborations. In particular, the wildfire topic has attracted attention due to the occurrence of extreme events in Europe and France. For instance, CECI is now involved in the COST action CA22164 "European network on extreme fire behavior" for the 2023-2027 period. In the topic of inundation and flood forecasting, major application and methodological advancements have also been made through stronger collaboration with CNES (via the SCO program), allowing an enhanced use of remote sensing datasets and thereby further validation of the methodological components of the data assimilation system for inundation and flood forecasting.

3.2 Atmospheric chemistry data assimilation

CERFACS activities on atmospheric composition were carried out continuously over the period 2003-2023. During this period, they were supported by close collaboration with Météo-France and external funding from Europe (Copernicus and H2020 programs), CNES (Tosca program) and the Occitanie region. Research on atmospheric chemistry data assimilation at CECI was aimed to improve the accuracy of chemical forecasts and reanalyses using satellite and ground-based measurements.

Over the 2021-2023 period, the main efforts were devoted to methodological advancements of the data assimilation algorithm. One part was linked to building an advanced data assimilation scheme for CAMS operational air quality forecasts and reanalyses within the SEEDS project (Sentinel Earth Observation-based Emission and Deposition Service). Another part was devoted to finding ways to directly assimilate IASI (Infrared Atmospheric Sounding Interferometer) satellite radiances and improve model-based ozone forecasts, in order to overcome some of the issues encountered when using satellite retrievals.

3.2.1 Hybrid ensemble-variational data assimilation for air quality forecasts

Within the SEEDS project, the objective was to implement, test and validate an 4DEnVar data assimilation algorithm around the MOCAGE chemistry-transport model and based on the community data assimilation libraries JEDI [CE201]. This algorithm falls into the category of hybrid ensemble-variational data assimilation algorithms, which are known to improve the representation of uncertainties, in particular model errors. Within the atmospheric chemistry context, the 4DEnVar can account for model errors of various type (e.g. emissions and deposition) and propagate model corrections both in time and between linked chemical compounds, without requiring tangent linear and adjoint models. Moreover, it can be used to estimate hourly model biases, which are one of the main unresolved issues in air quality forecasts. The performance of the 4DEnVar was evaluated first using synthetic observation experiments, and then using real observations routinely assimilated in CAMS models at 10 km resolution, at hourly temporal resolution, for a data assimilation window of at least 24 hours, assimilating more than ten compounds simultaneously and using ensembles of forecasts of at least 30 members. This work represented the first attempt to use such type of hybrid ensemble-variational algorithm for operational air quality forecasts. To carry out these experiments, the MOCAGE model was specifically upgraded to run ensembles of air quality forecasts with perturbed parameters, and a large effort of numerical optimization was required to make the data assimilation algorithm compatible with operational usage.

We first validated the 4DEnVar data assimilation system with synthetic observation experiments (SOE) but using the real observation network used in CAMS services (O3, NO2, PM10 and PM2.5). The results confirmed the initial findings of Emili et al. (2016) [12] with an idealized model, i.e. a remarkable capacity of the 4DEnVar algorithm to address systematic forecast errors for both observed and some unobserved compounds (e.g. NO). However, some skills degradation appeared for other compounds included here in the control vector but not directly observed (NH3, HNO3, ISO). These results raised new scientific questions on the properties of the data assimilation algorithm that might be related to strong non-linearities of the chemical system and could not be addressed during the SEEDS project. Hence, we decided to use the analyses of the unobserved compounds only as diagnostic variables in the follow-up experiments.

First data assimilation experiments with real observations showed that the data assimilation system works well also in a real case scenario, but presented some additional challenges. In general, the 4DEnVar algorithm is quite good in correcting the temporal biases, but less efficient in improving the standard deviation at the same time. When the forecast error correction is employed, the forecast bias is significantly reduced, at the expenses of a small increase in standard deviation or even RMSE. Among the multiple parameters that configure the 4DEnVar algorithm, we found that a larger horizontal localization than our reference configuration provided systematically better results (also than the operational 3D-Var). Finally, the 4DEnVar algorithm has been run for 12 cycles (a total of 14 days) during two pollution episodes, in June and in April 2019. The MOCAGE 3D-Var has been run for the same periods using the CAMS operational configuration. A validation against a common set of independent ground measurements confirmed previous results and highlighted the significant benefits of the model error correction to improve the bias in air quality forecasts (Figure 3.1).

The 4DEnVar algorithm has a promising potential to address some limitations of most data assimilation schemes employed in CAMS. In particular, it provides a model error diagnostic that could be used as guidance to improve models or to reduce forecast biases. Its main weakness with respect to deterministic algorithms such as 3D-Var, is the increased cost of running an ensemble of air quality forecast. Also, some additional research is needed to implement a more comprehensive set of model perturbations in the ensemble. Within the SEEDS project, we limited the MOCAGE perturbations to emissions, deposition velocities and vertical diffusion, using very simple errors (multiplicative and global factors). They provided already reasonable outcome from our first data assimilation experiments. However, we also observed that using a meteorological ensemble as input for the air quality models could improve the realism of the background error covariances. Exploiting the variety of chemical mechanisms of the CAMS ensemble seems also a very interesting perspective for the application of the 4DEnVar scheme. In the end, a mixture of perturbed emissions, deposition, meteorology and chemical mechanisms would probably be the best way to tackle model uncertainties and maybe reduce some of the analysis errors encountered in this study. This would require an evolution of the current CAMS ensemble to take into account a larger number of uncertainties.

3.2.2 IASI radiance assimilation for ozone and desert dust monitoring

Ozone and desert dust play a crucial role in atmospheric processes and thereby require continuous monitoring, done at CERFACS through a 3D-VAR data assimilation system combining IASI observations and MOCAGE chemistry-transport model predictions. Direct assimilation of the satellite infrared radiances has been recently adopted for ozone analysis (Emili et al., 2019, [11]) to overcome some of the issues encountered when using Level 2 retrievals. However, the appearance of stratospheric biases was observed with both techniques (L1 and L2 assimilation). A possible culprit for analysis degradation is the mi-specification of the background or observation error covariances in the assimilation. The data assimilation system allows a diagnostic of the observation error covariance that has already proven effective in meteorological applications. This so called Desroziers diagnostics permit to infer information on the full error covariances (diagonal and off-diagonal terms) with a negligible numerical cost. The re-evaluation of the error covariance statistics for IASI ozone channels and their impact on the chemical forecasts was investigated within the framework of M. El Aabaribaoune's PhD thesis (2022, [CE230]). Results show that strong error correlations are present in the ozone window, due to redundant information content and radiative transfer errors. When these correlations are taken in account stratospheric biases are significantly reduced and the minimization algorithm converges faster [CE121, CE123].
M. El Aabaribaoune's PhD thesis [CE230] also investigated how to jointly correct ozone and desert dust concentration, in order to take advantage of the sensitivity of the spectrum measured by IASI to both species and to produce desert dust analyses. This required the inclusion of desert dust in the radiative transfer model and in the control variable. The optical thickness of the total aerosol AOD (Aerosols Optical Depth) and the total desert dust columns were evaluated. The optical thickness was compared with independent instruments (MODIS and AERONET), showing a significant and positive impact of the infrared assimilation on the aerosol fields.

3.3 Micrometeorology: large-eddy simulation, surrogate modeling and data assimilation

Research at CERFACS in the field of micrometeorology focuses on two main applications: the dispersion of air pollutants in urban environments, and the behavior of wildland fires. Both topics aim at deploying highly-resolved large-eddy simulations (LES) to accurately represent the main physical processes involved at the interface between the lowest part of the atmospheric boundary layer and a complex land surface (urban areas versus heterogeneous vegetation). These simulations are essential for improving our understanding of environmental systems, but we also see them as a key element in the monitoring of environmental emergencies, if combined with approaches based on artificial intelligence. Two main issues detailed below come into play in the construction of such "numerical laboratories".

(1) What is the best protocol for validating LES simulations, which despite their complexity and computational cost are subject to a variety of uncertainties?
Validation of a LES approach is not straightforward as there could be error compensation in the complex

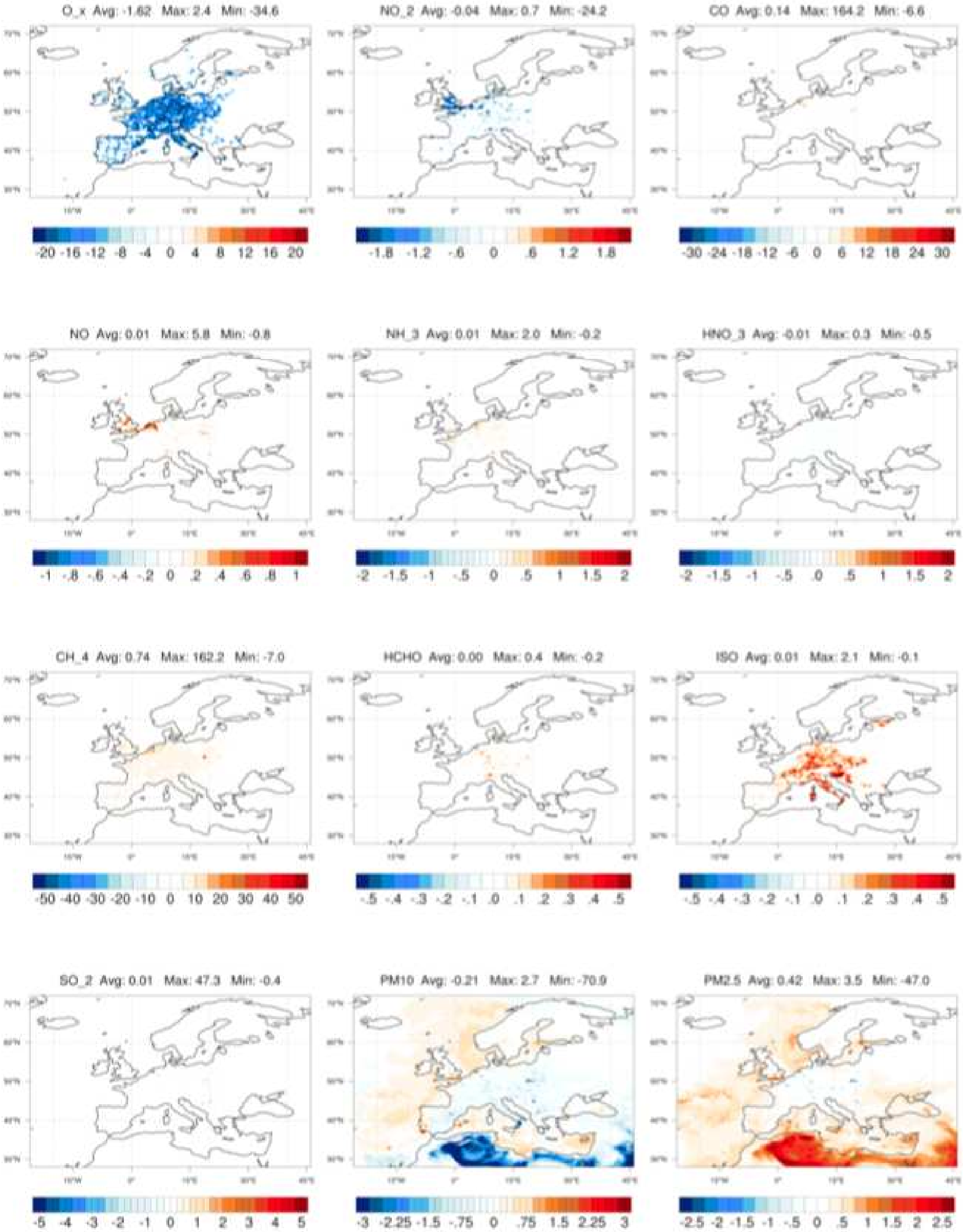

Figure 3.1: Surface maps of estimated model errors averaged for the 19th June 2019. Values are in ppbv for trace gases and $\mu g\, m^{-3}$ for aerosols compounds. Source : [CE201].

environmental modeling systems we are dealing with, and as the LES simulations for environmental applications are subject to uncertainties. These uncertainties can be aleatory due to the internal variability of the atmospheric boundary layer. Our research work on the 2021-2023 period highlights through the replicate of field-scale experiments, the significant impact of internal variability on microscale LES predictions, and proposes a statistical approach to quantify internal variability and its effect on validation scores. Note that internal variability is an issue we share with the climate modeling group at CERFACS.

(2) How to build a dedicated framework for uncertainty quantification and reduction in LES simulations?
In addition to internal variability, LES simulations also suffer from a lack of knowledge on the most influential input parameters, especially in the context of environmental emergency. It is therefore of primary importance to quantify the different sources of uncertainty in the LES simulations, i.e. to assess the weight of internal variability that is irreducible and to integrate available observational data to reduce uncertainties due to partially known parameters. To achieve this long-term objective, our research work on the 2021-2023 period focuses on designing and validating a multi-query LES framework, which is able at accurately and efficiently predicting quantities of interest.

The answer to these questions lies at the interface between computational fluid mechanics, micrometeorology, reduced-order modeling and data assimilation. The role of artificial intelligence based on machine learning and/or deep learning within this framework is currently being explored.

3.3.1 Air pollutant dispersion simulation and metamodeling

Accurately predicting the unsteady short-to-medium range plume dynamics and dispersion induced by point-source emissions remains a challenge for safety prevention and emergency risk assessment linked to air quality and health impact issues. LES have been identified at CERFACS as a promising tool to tackle this microscale challenge due to the complex, transient flow patterns induced by the presence of buildings of varying heights in a urban district or an industrial site. Over the 2021-2023 period, we addressed this problem through B. Nony's PhD thesis (2019-2023, in collaboration with LISN, funded by CERFACS) [CE235] and E. Lumet's PhD thesis (2020-2024, in collaboration with LAAS, funded by Université de Toulouse/Région Occitanie). This work was done around the AVBP legacy code developed by the CFD team at CERFACS and previously adapted to tackle environmental fluid flows of low Mach number. This work was partly supported by GENCI HPC computational resources and also benefited from CERFACS' access to Météo-France's computational resources.

3.3.1.1 Microscale internal variability assessment in LES simulations

We carried out a detailed validation of our microscale LES model using the AVBP legacy code within the framework of the Mock Urban Setting Test (MUST) field-scale experiment (Fig. 3.2). This model integrates a synthetic turbulence injection approach to have realistic inflow boundary conditions at the microscale domain boundaries that represent part of the atmospheric boundary-layer fluctuations. Moreover, to quantify microscale internal variability on the LES predictions, we designed a stationary bootstrap methodology inspired from the climate sciences literature.
For the quasi-neutral MUST trial we considered so far, we found that the LES predictions are in overall good agreement with the experimental measurements of wind velocity and tracer concentration, especially in terms of fluctuations and peaks of concentrations. We also found that both LES estimates and the experimental measurements are subject to significant internal variability, which induces substantial uncertainty in the standard air quality scores that are classically used for model validation. This highlighted that internal variability is essential to take into account in the LES model validation process. Still, internal variability cannot explained all the discrepancies between observations and LES estimates (Lumet et al., i press [13]). One direct perspective of this work is therefore to build a data assimilation framework to reduce

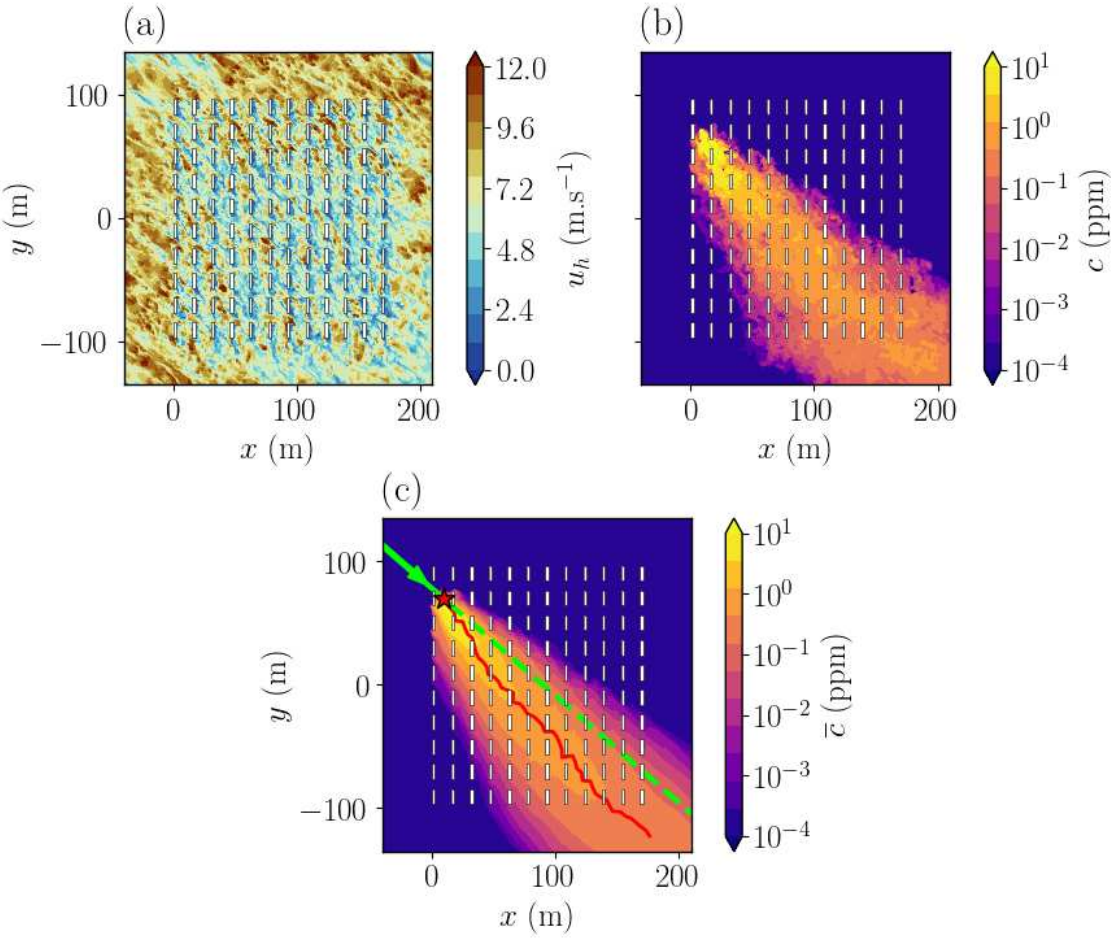

Figure 3.2: Horizontal cuts at $z = 1.6$ m of instantaneous (a) horizontal wind speed magnitude u_h (m s^{-1}) and (b) tracer concentration c (ppmv). (c) Horizontal cut of the time-averaged tracer concentration over the 200-s analysis period. White rectangles represent shipping containers from the MUST trial. The red star corresponds to tracer source location. The green line corresponds to the mean inlet wind direction, and the red line corresponds to the mean plume centerline, highlighting a plume shift due to the presence of containers. Source : Lumet et al. (accepted for publication in Boundary-Layer Meteorology journal [13].

LES model uncertainties by correcting inflow boundary conditions [14]. In a longer term, it would be of interest simulate more field-scale configurations and assess mesoscale and microscale internal variability under different atmospheric stability conditions.

3.3.1.2 Reduced-order modeling for LES simulations of air pollutant dispersion

LES simulations are particularly attractive to accurately represent near-field pollutant concentration spatial variability. However, due to their large computational cost, running such simulation in multi-query uncertainty quantification contexts is a challenge. To overcome this issue, we proposed a purely data-driven, non-intrusive reduced-order model (ROM) combining proper orthogonal decomposition (POD) and probabilistic Gaussian process regression (GPR) to efficiently predict tracer concentration field statistics of interest.

i) Idealized case
To properly design the POD-GPR model, we first investigated a two-dimensional case study corresponding to a turbulent atmospheric flow over a surface-mounted obstacle. This idealized configuration was helpful to build a solid LES database (made of 750 LES snapshots) based on perturbed inflow boundary conditions and emission source location, and to efficiently tune the GPR based on the available reduced-basis information and properties. The POD-GPR model was able to capture the wide range of spatial scales across the POD modes. However, one drawback of POD is that a large number of modes (hundred modes for the full training database) is required to accurately emulate near-source fine plume structures caused by the uncertainty in the emission source location (Nony et al., 2023 [CE154]). The robustness of the POD-GPR approach was also addressed under small data constraint. By reducing the number of training snapshots, a loss of consistency with physics principles was observed. For instance, non-physical noisy structures could appear in tracer-free regions. Still, the POD-GPR model prediction performance remained acceptable when considering at least one hundred LES snapshots in the training database, providing a first budget estimate for field-scale applications such as the MUST experiment. In terms of methodological perspectives, it would be interesting to further explore deep-learning-inspired techniques such as convolutional autoencoders as they provide a way to significantly improve compression performance and ROM prediction accuracy, even under the constraint of reduced training database [CE235]. It would be also interesting to move beyond a purely data-driven approach and continue our work on introducing physical constraints in the learning process to reduce prediction artifacts in case of small training data, for instance by mixing LES and lower-fidelity RANS (Reynolds-Averaged Navier-Stokes) data, i.e. by providing better turbulence closure terms in the RANS model using LES data [CE61].

ii) MUST field-scale trial
In a second step, we successfully extended the POD-GPR approach to the MUST field-scale experiment with the objective of emulating the three-dimensional LES concentration statistical predictions with respect to varying wind conditions [14]. We found that the LES field preprocessing step is a key model design choice when considering tracer concentration field statistics as the ROM output variables. For instance, for the mean concentration, using a log-transformation instead of linear centering as in [CE235] greatly improves POD accuracy. We also found that ROM validation metrics are strongly affected by the LES model internal variability. This internal variability provides the limit of precision that can be achieved when training a ROM from microscale LES data [14]. The resulting ROM can then be integrated in a data assimilation framework to generate ensemble predictions [14].
In terms of methodological perspectives, it would be interesting to further explore mixture-of-expert approaches to better represent the wide range of concentration values [CE122, 14] and to include more uncertain parameters in the ROM approach such as source location and atmospheric stability conditions.

3.3.2 Ensemble coupled atmosphere-fire simulations

Simulating landscape-scale wildland fire behavior remains a scientific challenge due to the complexity of the physical processes and to the cascade of uncertainties, from biomass fuel (type, properties, moisture content of dead and living fuels) to microscale meteorology. Coupled atmosphere-fire models such as Meso-NH/BLAZE [CE112] provide an efficient way to represent the behavior of a large-scale wildland fire simultaneously solving for the fire spread, the plume updraft and their mutual interactions. In this framework, the main physical quantities of interest are the rate of fire spread and the surface heat fluxes. Both quantities are subject to significant uncertainties due to the simplified parameterizations but also due to the limited knowledge in the input parameters (in particular, biomass fuel parameters).
To improve wildland fire models and quantify related uncertainties, the long-term objective of this research is to develop a realistic coupled atmosphere/vegetation/fire modeling system able to simulate wildland fire events at geographical-to-meteorological scales, including a data assimilation approach aggregating all sources of available information from observations and from model predictions to control uncertainties. This is only possible thanks to a close collaboration with CNRM, which has been strengthened over the 2021-2023 period (in particular with the GMME – “Groupe de Météorologie de Moyenne Echelle” – group). The BLAZE model component has for instance been integrated in the version 5.6.0 of Meso-NH released in March 2023.
In the 2021-2023 period, our research efforts were focused on the modeling component to design and validate the Meso-NH/BLAZE coupled model through PhD work by A. Costes (2017-2021, in collaboration with CNRM, funded by ANR FIRECASTER piloted by University of Corsica) [CE229] and now W. Antolin (2021-2024, in collaboration with CNRM, funded by CERFACS). The main objective was to obtain more realistic near-surface wind conditions from the coupled atmosphere-fire model since they are known to be a key driver of wildland fire behavior.
Note that the wildfire topic enhances CERFACS’ visibility as (i) CECI has contributed to “Missions Interministérielles Incendie de Forêt” in 2022-2023 and to a conference-debate at the “Académie des Sciences” in December 2023 in collaboration with INRAe, University of Corsica and IRD, and (ii) CECI is also regularly involved in outreach communications about extreme wildfires (e.g. France Culture/France Inter radio shows, museum exhibitions).

3.3.2.1 Representation of the near-surface wind variability

As a first validation case study, the Meso-NH/BLAZE coupled model was evaluated against the FireFlux I field-scale experimental grass fire. We found good agreement between simulations (running at decametric resolution for the atmospheric component and at metric resolution for the fire component) and measurements [CE112]. In particular, we found that the fire-induced atmospheric flow near the land surface is correctly captured in two-way coupled mode, leading to a realistic spread rate. We also found that heat fluxes near the fire front significantly affect the near-surface wind and in turn the simulated fire spread. This highlights the importance of modeling accurate heat fluxes at the flaming front but also behind the flaming front in the already burnt area. And this motivates collaborations with experimentalists (e.g. with UPC through the 2022-2022 3DFIRELAB MSCA project, [CE78]) to obtain accurate heat flux observations for further model validation.
The correct representation of the intensity and variability of the near-surface wind under complex terrain and/or heterogeneous vegetation remains an open problem in the fire science community but is essential to make a coupled atmosphere-fire model applicable to actual wildfire events. Hence, to go further in the physical representation of the near-surface wind, ongoing efforts in the frame of W. Antolin’s PhD thesis aim at analyzing forest canopy drag effects on the near-surface flow and on the wildand fire spread [CE6]. Drag effects can be explicitly accounted for in Meso-NH using metric LES simulations [10]. Preliminary results tend to show the importance of accounting for the vegetation-flow interactions to have a realistic representation of fire spread.

Figure 3.3: Example of a coupled atmosphere/fire simulation of the FireFlux I experimental grass fire using Meso-NH/BLAZE. The fire front is represented as red colors, and the fire plume is represented using grey scale color. Source : [CE112].

3.3.2.2 Microscale internal variability assessment in coupled simulations

In the context of wildfire behavior that is a highly unsteady phenomenon, internal variability can be studied by generating an ensemble of independent Meso-NH/BLAZE coupled simulations that represents the plausible variability in the inflow turbulence. As a first step to assess internal variability in coupled atmosphere/fire simulations, such Meso-NH/BLAZE model ensemble was generated for the FireFlux I experimental grass fire (Costes et al. 2021, 2022 [CE112, CE113]). We found that the variability due to the incident turbulent structure remains very large, with stronger effects in altitude and at finer atmospheric resolution, and therefore impacts validation scores as in the air pollutant dispersion context. It is thus of primary importance of accounting for the variability of the near-surface wind flow at the scale of an experimental fire. This question will need to be studied in greater depth on the basis of real cases.

3.3.2.3 Sensitivity analysis for parameterized coupled atmosphere/fire simulations

As all coupled atmosphere-fire models, Meso-NH/BLAZE relies on a rate-of-spread parameterization to represent the fire front propagation speed as a parametric function of environmental factors characterizing biomass fuel properties and moisture content, near-surface wind conditions and terrain slope. In actual wildland fires, these input parameters are only partially known and induce significant uncertainties in the coupled model predictions. To estimate the envelope of plausible wildland fire behavior, we aim at designing a perturbed-physics ensemble prediction capability based on Meso-NH/BLAZE. To make the approach feasible, it is essential to identify the relevant subset of parameters to perturb to generate an ensemble of fire front positions and shapes. As a preliminary step, we designed a global sensitivity analysis framework based on Sobol' indices to rank the biomass fuel parameters by order of influence and applied it to typical grass fire conditions. We found that sensitivity indices are not constant with respect to the near-surface wind velocity and along the fireline [CE95]. This highlights the importance of exploring the spatial and temporal dependencies of coupled model sensitivities in future work.
This question will be studied in greater depth as part of the ANR JCJC FIREFLY project piloted by CECI

(2023-2027), with the aim of designing an airborne thermal infrared data assimilation system that includes an ensemble modeling approach to represent parametric uncertainties. Sensitivity analysis would be an helpful and efficient approach to choose which parameters to perturb according to their level of uncertainties and to their respective influence on the fire and atmospheric quantities of interest.

3.4 Surrogate modeling in hydrology

Two different strategies for surrogate modeling have been investigated over the last three years in the context of two PhD theses, with different objective. The first one is based on machine learning and aims at building a surrogate for a hydrology model. The second one is based on Gaussian process regression, with active learning and multi-fidelity, and aims at estimating a probability of failure.

Emergency services seek more reliable and extended flood forecasting models in order to be more effective in their actions. Theo Defontaine's PhD thesis (CERFACS-SCHAPI-SPC Toulouse, advisors : S. Ricci, C. Lapeyre - CERFACS) shows how machine learning models can improve and extend discharge prediction results with respect to results from an empirical Lag and Route model based on hourly measured water level at gauge stations on the Garonne River. With 36 flood events over the past 15 years, a scarce dataset (40k discharge data) is used to train and optimize a linear regression, a gradient boosting regressor and multi-layer perceptron model in order to forecast flood in Toulouse at 6-hour and 8-hour lead times from upstream stations providing gauge observations. The merits of adding heterogeneous data to this data base, with rainfall data, are demonstrated. It was shown that the strategy for data base splitting into learning and validating sets must be adapted to the scarcity of the database. The preliminary findings of this work were published in a conference proceeding [CE23] and the PhD results are reported in an article that is uncer review at HESS.

Reliability analysis in case of complex systems is often a challenging task. Such a study requires repeated calls to computationally intensive numerical solvers. These simulation codes aim at modeling the system's behavior. However, assessing the reliability of a system with respect to uncertainties is an essential step in the design process. Many methods have been investigated in the literature, allowing to estimate failure probabilities in the case of expensive high-fidelity solvers. Among them, the use of surrogate models built by active learning is a popular technique. As these methods are based on a potentially large number of evaluations of the high-fidelity codes, their associated computational cost can still be unaffordable. Thus, the use of lower fidelity solvers in the construction of surrogate models can be a relevant way to further reduce this computational cost. In the context of R. Espoeys's PhD thesis (ONERA-CERFACS, advisors S. Ricci, P. Mycek at CERFACS, M. Balesdent, L. Brévaut at ONERA) it is proposed to study different reliability analysis methods based on multi-fidelity surrogate models built using active learning. The performance of the considered approaches is evaluated with respect to two axes: the construction of the multi-fidelity surrogate models and the enrichment criterion. Different combinations between surrogate models and criteria are evaluated on four test cases. First, two analytical problems presenting different types of relationship between the fidelity solvers (linear, non-linear) are investigated. Then, two simplified-physics problems relative to hydraulic and aerospace engineering are studied. This work was reported in a book chapter under review and presented at the ASMO conference in 2022 [CE27]. A first illustration in hydrodynamics was proposed for the Manning equation applied to a rectangular channel with constant slope, considering as uncertainties the slope, the upstream contribution and the friction. Failure occurs when the free surface elevation exceeds the height of the dike. The previously-mentioned methods have been evaluated for two levels of fidelity, the low fidelity coming from the introduction of a model error in the calculation of the height water. For this test configuration, the NARGP method which takes into account the non-linearities between the different fidelity levels gives better results than AR1 or LMC, whatever the enrichment criterion. Perspectives for this work will focus on a more realistic hydrodynamic test case with

Telemac2D, where the fidelities relate to the mesh refinement. Surrogate modeling strategy will build on previous studies on Polynomial chaos expansion and Gaussian process strategies for Telemac2D over the Garonne model area at CERFACS [CE122].

3.5 Assimilation of heterogeneous data for flood forecasting

A strong theme at CECI is the quantification and reduction of uncertainties in geosciences for the assessment of environmental risks, using data assimilation algorithms, with a particular emphasis on the hydrodynamics of rivers and flooding. On this theme, CECI collaborates with its shareholder partners CNES, EDF and Météo-France as well as other academic or private institutes for the development of algorithmic strategies allowing the estimation and forecasting of flow rates and water levels at short to medium term deadlines with hydraulics and hydrology software. CECI is part of the Telemac consortium (www.opentelemac.org), Open Source software dedicated to resolving free surface flow equations and operated operationally by design offices and the flood forecasting services of the Vigicrue network. CECI is working on the development of data assimilation methods for Mascaret (1D) and Telemac (2D) as well as on the development of methods for coupling these solvers with each other, and/or with solvers dedicated to small and large scale hydrology (e.g. MORDOR, GRP, RAPID, CTRIP). CECI is involved, alongside CNES, in projects to exploit Earth observation space data for the description of continental water surfaces. Spatial data from altimetry, radar or optical measurement as well as topographical data are used to provide data for these 1D and 2D calculation models of fluvial and estuarine hydrodynamics, in addition to in-situ measurements. They are further assimilated via ensemble filtering methods based on the estimation of error covariances. CECI has been involved, alongside INRAE, in the SWOT mission preparation program via CNES's TOSCA for ten years, as well as in the SCO program, via the FloodDAM and FloodDAM-DT projects.
The perspectives for these topics lie in the recently funded ANR project SWIFT (Shallow Water modelling and satellite Imagery combination for improving Flood predicTion), various projects with CNES (TOSCA SWOT-HYDROS, SCO, R&T) as well as on going and up coming PhDs.

3.5.1 Hydrology-hydrodynamic modeling with data assimilation

Having a global hydrological-hydraulic model with a routing model such as a complete Saint-Venant model at a step of space (e.g.: 200 m) and time (e.g.: 15 min) is not not feasible numerically at the moment, for a forward model, and even less for an inverse model including data assimilation schemes. For this reason, hydrological and hydraulic modeling can be used separately, on restricted areas, potentially by forcing the local hydraulic model with a larger scale hydrological model upstream. For free-surface hydrodynamic modeling, the "only" parameters required are river bathymetry and frictional characteristics of river beds and floodplains. In this case, it seems possible to try to estimate them all using data assimilation from satellite observations only, which makes the approach possible in completely ungauged rivers. This work is currently being developed as part of projects linked to the SWOT mission.
We are interested in coupling hydrological models in the form of a time-varying boundary condition for a local hydrodynamic model. This a priori can then be corrected via data assimilation. This hydrology-hydraulic chain solution was investigated as part of A.-L. Tiberi's PhD thesis (CEREMA/CERFACS) with an hydrological rainfall-runoff model forced by a rainfall forecast to calculate inputs for the 1D hydraulic model [CE100, CE184]. An ensemble version was implemented to use the hydrological flow rates as input to the 1D Mascaret Model, making it possible to extend the hydraulic forecast deadline beyond the transfer time of the hydraulic network. The hydrological flow, resulting from an ensemble hydrological forecast, is inherently imperfect and must be corrected. Two solutions were proposed either via statistical calibration with a QRF method, or an overall Kalman filter from in-situ data assimilated into the 1D hydraulic model. It was shown in the works of Tiberi et al., 2021 [CE183] that both methods are subject to data availability to limit the many sources of uncertainty and that densification of the observation network would greatly

help, thus paving the way for a demonstration of relevance of data from SWOT type. More recently, as part of the SCO FloodDAM-DT project, CERFACS teams collaborated with JPL teams to chain the large-scale hydrological model RAPID with the Telemac2D hydrodynamic model. It has been shown that the assimilation of in-situ data in the river bed as well as the assimilation of flooded surface data from Sentinel-1 radar observation [CE151, CE152] make it possible to correct the hydrological inputs and simulate realistic hydrodynamics. This exercise was also carried out with the CNRM CTRIP [CE172] hydrology model.
A chained hydrologic-hydraulic model was implemented, using large-scale hydrologic model (namely ISBA-CTRIP) discharge forecasts as input to local and high fidelity hydrodynamic models. In the present study, uncertainties in the hydrology forcing from ISBA-CTRIP and as well as in hydraulic parameters are reduced with an EnKF implemented on the TELEMAC-2D solver. The data assimilation algorithm jointly assimilates in-situ water level measurements and water masks obtained from remote sensing Earth Observations. The SAR-derived binary wet/dry maps are expressed in terms of wet surface ratios over selected subdomains of the floodplain. The non-gaussianity of the errors in the WSR observations are dealt with a Gaussian anamorphosis function. The chained data assimilation strategy leads to a significant improvement of the 1D and 2D metrics with reduced RMSE and increased Critical Success Index. This work demonstrates that while imperfect, forcing provided by an hydrology model can be efficiently used as input to a local hydraulic model. This work also demonstrates that DA allows for an efficient reduction of the uncertainty in the hydrology products. These conclusions advocate for a multi-source strategy for the data assimilation algorithm implemented on top of a chained hydrology-hydraulic model favorable to extended lead time forecasts and modeling in ungauged catchments.

3.5.2 Merits of heterogeneous data for hydrodynamic models

The Garonne, on its downstream river part – after the confluence with the Lot and up to the commune of La Réole – experienced a major flood in February 2021, with a red alert on Marmande area issued by Vigicrue services. With a maximum height greater than 10.20 m reached at the Marmande and more than 6000 m^3/s, this makes it the highest flood since that of December 1981. This part of the Garonne, approximately 50 kilometers long, is characterized, during the strongest floods, by a significant mobilization of the entire extent of the flood plain - more than 5 kilometers wide in certain places. The prediction of the hydraulic state relies on the used of 1D and 2D hydrodynamics models that are uncertain as they use ancient bathymetric and topographic data in a Telemac2D model built by EDF in 1995. Both SPC Toulouse and CERFACS, in collaboration with CNES and EDF are putting efforts in updating Telemac2D model making the most of recently acquired in-situ measurement, high resolution IGN LIDAR and Pléiades data acquired in 2023. The work of M. Sadki at CERFACS was recently presented at the Telemac User Conference [CE96] and it shows that new in-situ and remote sensing data can benefit to a more accurate description of the river bed and floodplain (including the infrastructures). This effort will be pursued in close collaboration with CNES to work on the construction of an hydrocompatible digital elevation model from the recently acquired Pleiade images in the context of a CNES R&T study.

3.5.3 Remote sensing heterogeneous data assimilation

At CERFACS, work in modeling and assimilation for river hydrodynamics is based on three main building blocks: the Telemac hydrodynamic solver (www.opentelemac.org), the EnKF ensemble assimilation algorithm and an heterogeneous and large volume of data from in-situ and satellite observations. The 1D Mascaret and 2D Telemac solvers are used, they both belong to the Telemac software chain. They are mobilized via their API accessors, which allow functional control in Python allowing them to be instantiated, initialized, integrated, stopped and restarted. As part of the data assimilation project for hydrodynamics, we propose to demonstrate how data collection (bathymetry, topography and friction, water surface elevation, water extent, discharge) improve simulation and forecast with both Mascaret and Telemac. In the past years, most studies have focused on 1D modeling [CE144]. Over 2021-2023 period, we have strongly intensified our efforts on working with Telemac 2D and implementing an ensemble-based filter to assimilate the heterogeneous and ever expending in size and type catalogue of observations. This effort has greatly been supported by CNES with the TOSCA and SCO programs.

Data assimilation of remote sensing data
The inclusion of Earth observations from space into flood risk management presents a great opportunity to improve the ability to anticipate flooding, mitigate its impacts, and protect assets worldwide. The properties of inland water bodies are monitored by altimetry missions that provide along-track water surface elevation (WSE) from nadir (e.g., TOPEX/Poseidon, Jason, SARAL/AltiKa, Sentinel-3, Sentinel-6) or large-swath altimeters (SWOT), as well as from radar/optical missions (Sentinel-1/Sentinel-2) that provide high-resolution water extent maps. Data Assimilation combines in-situ measurements with numerical model outputs to reduce uncertainties in the model inputs such as roughness, inflow discharge, channel/floodplain geometry and/or hydraulic state. Thus, it allows to improve initial, boundary conditions and model parameters and state to issue improved forecasts. Leveraging multi-source observations, including remote sensing (RS) data allows densifying the observing network, both spatially and temporally, as well as diversifying their characteristics. Research studies at CERFACS during 2021-2023 period have shown that this allows for a better performance of the EnKF – that relies on the stochastic computation of forecast error covariance matrix amongst a limited number of perturbed simulations – to represent the dynamics of the flow in the river bed and floodplain. [CE151] and [CE152] focus on the assimilation of two-dimensional flood observations derived from remote-sensing Sentinel-1 images acquired during overflowing events. The binary wet/dry maps derived from backscatter images with a machine learning random forest algorithm are further expressed in terms of wet surface ratios (WSR) over a number of floodplain subdomains. This ratio is assimilated jointly with in-situ water-level gauge observations to improve the flow dynamics within the floodplain. An Ensemble Kalman Filter (EnKF) with a dual state-parameter analysis approach is implemented on top of a TELEMAC-2D hydrodynamic model. The EnKF control vector is composed of spatially-distributed friction coefficients and a corrective parameter of the inflow discharge. It is extended with the hydraulic states within the floodplain subdomains. This data assimilation strategy was validated and evaluated over a reach of the Garonne Marmandaise river. The observation operator associated with the WSR observations, as well as the dual state-parameter sequential correction, was first validated in the context of observing system simulation experiments. It was then applied to two real flood events that occurred in 2019 and 2021. The merits of assimilating synthetic aperture radar-derived WSR observations, in complement to the in-situ water-level observations, are shown in the parameter and observation spaces with assessment metrics computed over the entire flood events. It is also shown that the hydraulic state correction within the dual state-parameter analysis approach significantly improves the flood dynamics, especially during the flood recess. This work was more recently extended to the assimilation of water surface elevation from altimetry satellite, namely Sentinel-6-Michael Freilich (S6). These data were processed with fully-focused SAR allowing, for every S6 overpass, a profile of water surface elevation every 10 m along the river centreline. S6 data assimilation allows to substantially improve the water levels (both at observing stations and along the observed river segment) whenever there are observations available for assimilation (such as in-situ), with a fine spatial resolution of the WSE in the river, even though processing of S6 data for overflooding rivers still requires additional investigation. This study validated the assertion that a densification, in time and space, of the observing network, especially in the floodplain with remote sensing data and advanced data assimilation strategy, allows to improve the representation of the flow dynamics in the floodplains. It also advocates for the use of large-swath altimetry satellite such as SWOT that provides WSEs along the river and in the floodplain.

Treatment of non-Gaussian errors with Gaussian anamorphosis
Methodological efforts were investigated in the EnKF algorithm with regards to the classical hypothesis of linearity and gaussianity for observation errors. Some recent work ([CE153]) focuses on dealing with the non-gaussianity of WSR observations derived from S1 water mask. Indeed, the non-gaussianity of the observation errors associated with SAR-derived measurements break a major hypothesis for the

application of the EnKF, thus jeopardizing the optimality of the filter analysis. The novelty of this work lies in the treatment of the non-Gaussianity of the SAR-derived WSR observations with a Gaussian anamorphosis process. This data assimilation strategy was validated and applied over the Garonne-Marmande catchment (South-west of France) represented with the TELEMAC-2D hydrodynamic model, first in a twin experiment, and then for a major flood event that occurred in January-February 2021. It was shown that assimilating SAR-derived WSR observations, in complement to the in-situ water-level observations significantly improves the representation of the flood dynamics. Also, the Gaussian anamorphosis transformation brings further improvement to the analysis, while not being a critical component in the data assimilation strategy. This study heralds a reliable solution for flood forecasting over poorly gauged catchments thanks to available remote-sensing datasets.

Multi-mission data assimilation

With the objective of assimilating multmission-multisensor observations, research work has been carried out towards the assimilation of SWOT river products. Before the launch of the SWOT satellite, and also before the real data are made available (November 2023), CERFACS, in collaboration with CS-Group and INRAE has been working of the development of the Tools4SWOTsims tool box [CE200]. With the aim of investigating the use of SWOT products, before launch and before making the acquired data available, but also to explore various possible observation configurations (satellite constellation, re-visit periods, nature and amplitude of observation errors), the Tools4SWOTsims synthetic data generation chain is set up. It is based on the exploitation of scenes simulated by 1D or 2D hydrodynamic models and the launch of high-resolution or large-scale SWOT simulators. Tools4SWOTsims is deployed on the CNES cluster, made available on the CNES gitlab. The functionality of the tool box is extended to process 1D HECRAS hydrodynamic model outputs, and to process basins for which the topography is not known. The implementation of SWOT-like river products with the Telemac2D-EnKF was achieved in 2023 and observing system simulation experiments based on a reference simulation with a predefined set of friction parameters and input forcing discharge were carried out. This has led to the development of the dedicated observation operators to replicate the in-situ water level, Sentinel-1-derived flood extent and SWOT WSE observations at SWOT RP nodes and reaches. This stands in the extraction of the true WSE values at all observation times and locations, in order to generate synthetic in-situ data at stream-gauge stations, or to derive water masks and compute so-called wet surface ratio in several floodplain subdomains. The SWOT observations are synthesized with the SWOT-HR simulator applied on said WSE maps, providing pixel cloud data further processed by the RiverObs package. This chain aggregates WSEs over a selection of pixels and provides WSEs with high certainty at nodes every 200 m along the river centerline, and at river reach every 10 km, approximately. The observation operator associated with SWOT data computes the model equivalent of the pixel data aggregated over the selected TELEMAC-2D nodes. It relies on the selection of eligible pixels with appropriate water classes to issue WSEs with an error below 10 cm as prescribed in the SWOT requirements. A number of different EnKF data assimilation experiments are carried out considering different combinations of in-situ, S1 and SWOT observations. RS and in-situ data complement well as they present opposite characteristics in terms of frequency and spatial coverage, especially as RS provide data in the floodplain. Quantitative assessments based on 1D/2D metrics show promising results. This work heralds toward a reliable methodology for flood forecasting and flood risk assessment, for poorly-gauged or ungauged catchments, making the most of innovative Earth observation data and paving the way for upcoming Earth observation missions.

Assimilation of front-type water extent observations

Complementary to the previously-described studies on the assimilation of water surface ratio derived for flooding satellite images, we propose a framework for the direct assimilation of flood extent location and shape, aiming at treating them as innovative interface (front-type) information type that would overcome the limitations of classical amplitude error correction, such that those on WSE values, therefore allowing for the correction of flood edge position and/or deformation errors. In multiple research fields, data assimilation algorithms were developed to take into account 2D observations represented as images and treated as front-like information. An object-oriented approach based on the Chan-Vese contour fitting function used in image processing is used to compare the observed and the simulated wet/dry pixels interfaces. This front shape similarity measure was implemented and evaluated for data assimilation of SAR-derived flood extents in the context of flood modeling in the context of Q. Bonassies's PhD thesis [CE194] (CNES-CLS at CERFACS, advisors S. Ricci at CERFACS, C. Fatras at CLS and S. Peña Luque at CNES). Preliminary results were presented in the proceedings of the TUC2023 conference [CE14] focusing on the implementation of a parameter estimation EnKF algorithm for an idealized test case with Telemac. A more realistic test case is planned using front-like data extracted from the Sentinel-1 derived flood extents over the Garonne-Marmande area.

3.5.4 Digital twins and data platform for hydrology

For several years, in particular with the advent of the European Copernicus program or other ambitious bi-national projects in preparation such as SWOT, there has been a considerable increase in the quantity of space observations made available to the scientific and application communities. However, this wealth of data remains underexploited because access to the different databases can still be complex, with problems of management and manipulation of large volumes of data, as well as a lack of user expertise in the face of the diversity of products. Aware of this situation, space agencies are working to make this Earth observation data more accessible. This is particularly the case for CNES, and more specifically in the general field of hydrology. Indeed, CNES wishes to enrich and strengthen its hydrological platform Hysope II/hydroweb.next, designed as a development serving the scientific and application community and which contributes to the preparation of operational hydrology by facilitating the development and demonstration of new products. In 2018, CNES initiated a collaborative work with NASA/JPL by developing prototype to automate alert and mapping of flood extents in order to provide an environment for real-time flood monitoring and analysis, as well as reducing response time. This collaboration was the result of the FloodML project that demonstrated the capability of processing multi-temporal data from Sentinel/Landsat satellites to extract river extent anomalies using a machine learning method. As a continuity of this joint effort, in 2020, the Space Climate Observatory (SCO) launched the Flood Detection Alert and rapid Mapping project SCO-FloodDAM. This project provided a pre-operational processing chain that generates a flood risk indicator map based on past time-series, detected events, local digital surface models, land cover maps, hydrodynamics numerical model with data assimilation on which CERFACS has actively worked over the 2021-2023 period. These outputs allow to better prevent and assess flood events and provide quick response to decisions makers in several areas of interest, improving resolution, reactivity and adding a predictive capability. Within this framework, in 2022, the SCO-FloodDAM proceeds to SCO-FloodDAM-DT (Digital Twin) project (https://www.spaceclimateobservatory.org/fr/flooddam-dt) with a joint collaboration effort between CNES, NASA's partners (AIST and IDEAS) and JPL to develop a federated Earth System Digital Twin (ESDT) for water-cycle applications focused on flood events. This work entails a multi-agency effort to define and develop ESDT architectures focused on water resources and flood analyses where test case studies serve as demonstrators. These digital twin architectures aim at dynamically connecting existing hydrology/hydrodynamic models and continental water data (in-situ, airborne, remote-sensing (RS) data sources e.g. radar and optical) from both agencies (NASA & CNES) to produce large and local scale understanding and prediction. SCO-FloodDAM-DT project aims to develop a Federated Digital Twins solution with NASA IDEAS for alert systems and flood risk maps on local and global scales using space technologies. SCO-FloodDAM-DT products and the exploitation of its pre-operational chain aims to be at global scale depending on the availability of local physical models and in-situ and satellite data. The main processing blocks are (i) flood detection and alert, (ii) rapid flood extent mapping, and monitoring of ongoing flood events, (iii) short-term forecasting using computational fluid dynamics models (here Telemac 2D with data assimilation) to simulate water surface elevations at a local scale, and (iv) real-time measurement of financial risk of flooding at a site level based on assets over selected zones. CERFACS has been very active in the FloodDAM-DT project and the results of numerical modeling with assimilation of in-situ and remote sensing data over the demonstrative catchments are currently being hosted to the HydroWeb.next platform along with other data and results from FloodDAM-DT. This exercice paves the way for the implementation of Digital Twin Elements dedicated to hydrology.

References

[10] P. Aumond, V. Masson, C. Lac, B. Gauvreau, S. Dupont, and M. Berengier, (2013), Including the drag effects of canopies: Real case large-eddy simulation studies, *Boundary-Layer Meteorology*, **146**, 65–80.

[11] E. Emili, B. Barret, E. Le Flochmoën, and D. Cariolle, (2019), Comparison between the assimilation of IASI Level 2 ozone retrievals and Level 1 radiances in a chemical transport model, *Atmospheric Measurement Techniques*, **12**, 3963–3984.

[12] E. Emili, S. Gürol, and D. Cariolle, (2016), Accounting for model error in air quality forecasts: an application of 4DEnVar to the assimilation of atmospheric composition using QG-Chem 1.0, *Geoscientific Model Development*, **9**, 3933–3959.

[13] E. Lumet, T. Jaravel, M. Rochoux, O. Vermorel, and S. Lacroix, (2023), Assessing the internal variability of large-eddy simulations for microscale pollutant dispersion prediction in an idealized urban environment, *in press for publication in Boundary-Layer Meteorology*.

[14] E. Lumet, (2024), *Modélisation orientée données de la dispersion atmosphérique de polluants à micro-échelle : de la simulation haute-fidélité à l'assimilation de données*, ongoing phd thesis, Université de Toulouse 3 -Sciences de l'Univers, de l'Environnement et de l'Espace.

Coupling and Data for Climate

4.1 Introduction

The OASIS3-MCT coupler, a key element in Earth System Modelling, was released in version 5.0 in December 2021, with developments including Python bindings and a new environment to calculate the regridding weights with another library than the SCRIP. Used internationally, it received external funding and active user support. CERFACS co-organized the 6th Workshop on Coupling Technologies for Earth System Models. OpenPALM coupler development ceased, shifting focus to CWIPI library. Benchmarking of regridding libraries (SCRIP, ESMF, XIOS, YAC) highlighted strengths of ESMF and XIOS. Coupling methods for ocean-atmosphere and hydrology were explored, emphasizing the Schwarz method's efficiency in correcting asynchronous coupling issues. Data management efforts included climate indices workflow optimization and contributions to climate services standardization. CERFACS continued involvement in European projects, fostering data infrastructure development and engagement in the European Open Science Cloud.

4.2 Coupler development

4.2.1 The OASIS3-MCT coupler

The OASIS3-MCT coupler is an open source software developed at CERFACS to couple numerical codes modelling the different components of the Earth System. The last official version of the coupler, OASIS3-MCT_5.0, was released in December 2021 [CE224]. As previous versions, OASIS3-MCT_5.0 uses the Model Coupling Toolkit (MCT) developed by the Argonne National Laboratory (USA) to provides fully parallel coupling.
OASIS3-MCT is developed in an international perspective being one of the key elements of the sustained Research Infrastructure for the European Network for Earth System Modelling (ENES-RI) being currently set-up as an AISBL ("Association Internationale Sans But Lucratif") following the 3 IS-ENES (InfraStructure for ENES) European projects (https://is.enes.org). At the national level, OASIS3-MCT is one cornerstone of CLIMERI-France infrastructure for climate modelling and it is used in many French research laboratories in addition to CERFACS (CNRM, LOCEAN, LMD, LSCE, LA, LATMOS, LEGOS, LGGE, IFREMER, ENSTA, SHOM).
Besides the permanent manpower ensured by CERFACS (0.5 FTE) and CNRS (0.20 FTE), external funding for the 2021-2023 period came from IS-ENES3 (35 pms) and from the Centre of Excellence in Simulation of Weather and Climate in Europe (ESiWACE2, 16 pms). The list of OASIS3-MCT developments was established by the developers and reviewed and approved by the OASIS Advisory Board, see the 2023 OASIS3-MCT Evolution plan [CE223] for the most recent updates .
The most important developments for OASIS3-MCT during the 2021-2023 period were:

- The finalization of python and C bindings (included in OASIS3-MCT_5.0) ;
- The provision of a unified scripting environment to test the quality of SCRIP, ESMF and XIOS regridding libraries (included in OASIS3-MCT_5.0) ;

- The support of grid cell fractions evolving during the simulation (under finalization);
- The replacement of the SCRIP library with the YAC interpolation stack (under finalization).

OASIS3-MCT is used by at least 67 modelling groups over the 5 continents to assemble applications including global or regional configurations of ocean and atmosphere models but also sea ice, sea level, wave, ocean biogeochemistry, land, vegetation, river routing, hydrological and atmospheric chemistry models. OASIS3-MCT was used in 5 of the 7 European Earth System Models participating to CMIP6, and in particular in the climate model developed by the CNRM-CERFACS group. OASIS3-MCT 5.0 sources were downloaded about 230 times since its release in December 2021. It is interesting to note that the python interface is already used at SMHI (Sweden) and BSC (Spain) in a standalone regridding weight computation tools and at INRIA (France) for coupling an ocean model and a trained IA model for downscaling atmospheric fluxes.
Active user support was continuously delivered by CERFACS to the OASIS3-MCT user community during these past 3 years through mail exchanges and via the forum, by maintaining the web site (migrated to Cerfacs, see https://oasis.cerfacs.fr/), and by organizing training sessions. Due to the sanitary context, on-line training was preferred, in the form of a SPOC (Small Private Online Course, see https://cerfacs.fr/en/online-traning-sessions/). The SPOC on “Code Coupling with OASIS3-MCT” mixes theory, videos, quizzes and hands-on, and requires about 20 hours of work from each participant over 2 weeks. Collective sessions gathering in total 22 persons were organised in 2020, 2021 and 2022.
A total of 9 PMs of dedicated user support, including the visit of an OASIS developer to a chosen institute to help setting up or optimising a coupled system, was provided in the IS-ENES3 and ESiWACE2 context (see details in [CE211]):

- GEOMAR Kiel (Germany), for an upgrade of the OpenIFS-NEMO-AGRIF coupling (FOCI); and to introduce a new runoff interpolation algorithm in the existing OpenIFS-NEMO coupled model;
- DWD (Germany), to port the NEMO-ICON coupled model, including ICON internal and XIOS external I/O servers, on the new DWD vector machine NEC SX-Aurora TSUBASA;
- Météo-France PREVIMER R&D team (France), to ensure the efficient exchange of coupling fields between the NEMO ocean and MFWAM wave models.
- SMHI (Sweden), to help set up and check the rdy2cpl tool allowing generation of interpolation weights with SCRIP; this was the occasion to test the new pyOASIS interface and establish the efficacy of Python based coupled toys.

Finally, CERFACS co-organized of the 6th Workshop on Coupling Technologies for Earth System Models (CW2023) with the Argonne National Laboratory (USA) that took place in a hybrid format on January 18-20 2023, in Toulouse, France. This workshop gathered 32 researchers and engineers on site and about 80 additional people registered to follow it online. All details, including the programme and the recording of the presentations, are available at https://portal.enes.org/cw2023-toulouse/ . The responses to the satisfaction survey indicated that 90% of the respondents were overall very satisfied with the workshop, 70% found the presentations very interesting, 75% will participate in a next edition, and 90% found the organization very efficient.

4.2.2 The OpenPALM coupler

After many year of development of the OpenPALM code coupler and user support, CERFACS has stopped its development. The efforts now concentrate on the development, support and training of the CWIPI library developed by ONERA and used in many CFD applications at CERFACS (conjugate heat transfer, fluid/structure interaction, turbomachinery and coupling between fluid dynamics and Artificial intelligence for combustion and wall modeling). CERFACS researchers and engineers have participated during the period 2021-2023 in the development and validation of the new CWIPI interface which provides new functionalities and better parallel performances. A major on-going contribution performed in the context of the Phd thesis of Robin Cazalbou (co-direction between CERFACS and ONERA) concerns the optimization of CWIPI for massively parallel hydrid CPU-GPU environments. To do so, new geometrical algorithms for vertex localisation in a mesh adapted for GPU have been implemented in ParaDiGM (Parallel Distributed Generalized Mesh), the ONERA library on which CWIPI is based. Performance tests are currently performed offering interesting perspective for massively parallel hybrid CPU-GPU coupled simulations.

4.3 Benchmarking of coupling libraries

Components of Earth system models (ESMs) usually use different numerical grids because of the different environments they represent. Therefore, a coupling field sent by a source model has to be regridded to be used by a target model. The regridding has to be accurate and, in some cases, conservative, in order to ensure the consistency of the coupled model.
The benchmarking of the quality of four regridding libraries, SCRIP[1], ESMF[2], XIOS[3] and YAC[4] was realised [CE186] [CE225]. We evaluated five regridding algorithms with four different analytical functions for different combinations of six grids used in real ocean or atmosphere models. Four analytical functions were used to define the coupling fields to be regridded and calculated the metrics proposed by the CANGA project[5], including the mean, maximum, RMS misfit, and global conservation.
Figure 4.1 gives an example of the analysis done in this benchmark showing the relative misfit (%) of the remapping of a vortex function from a low-resolution icosahedral grid to a high-resolution icosahedral grid for 1st (top) and 2nd (bottom) order conservative remapping; this figure is for the YAC coupler but the other libraries show a similar improvement for the 2nd order compared to the 1st order.
The results show that, besides a few very specific cases that present anomalous values, the regridding functionality in YAC, ESMF and XIOS can be considered of high quality and do not present the specific problems observed for the conservative SCRIP remapping. A first performance analysis also demonstrated that ESMF and XIOS are much faster than the SCRIP and current work shows that this is also the case for YAC. This exercise also led us to conclude that benchmarking can be a great opportunity to favour interactions between users and developers of regridding libraries.

4.4 Coupling Methods

4.4.1 Methods for ocean-atmosphere coupling

Many Earth System Models (ESMs) use asynchronous coupling at the ocean-atmosphere interface and this algorithm suffers from temporal inconsistency. The Schwarz method [CE141] allows for correcting this time inconsistency, leading to a coherent ocean-atmosphere interface. The principle of the Schwarz method is to repeat each integration period many times with the same initial condition but, instead of using the surface variables calculated by the ocean during the previous coupling period (as in the asynchronous scheme), the atmosphere uses the coupling fields calculated by the ocean for that same coupling period during the previous iteration, and vice-versa for the ocean. This is repeated until convergence of the surface variables and fluxes.

[1]SCRIP: Spherical Coordinate Remapping and Interpolation Package, https://github.com/SCRIP-Project/SCRIP
[2]ESMF: Earth System Modelling framework, https://earthsystemmodeling.org
[3]XIOS:XML IO Serve http://forge.ipsl.jussieu.fr/ioserver
[4]YAC: Yet Another Coupler, https://dkrz-sw.gitlab-pages.dkrz.de/yac/
[5]https://github.com/CANGA/Remapping-Intercomparison

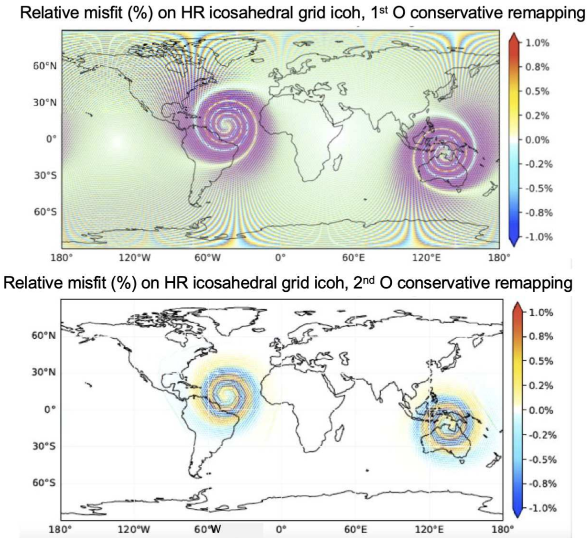

Figure 4.1: Relative misfit (%) of the remapping of a vortex function from a low-resolution icosahedral grid to a high- resolution icosahedral grid for a) 1st order, and b) 2nd order conservative remapping with the YAC coupler

In the framework of the COCOA ANR project, different simulations implementing Schwarz iterations were performed with CNRM-CM6-1D, a single-column version of CNRM-CM6-1 ([16]), for one point in the Indian ocean for one-day (November 13th 2011) and two-day (November 13th-14th 2011) periods. Different experiments were realized with different coupling periods i.e. 300s, 600s, 900s,1200s, 3600s, 3hrs, 6hrs, 12hrs, 24hrs. As already described in the 2019-2020 Scientific Activity Report, the Schwarz method is very efficient to reposition the diurnal cycle, which can be significantly lagged with asynchronous coupling. [CE226] presents the details of the simulations for the different coupling periods for the one-day and two-day experiments. It is concluded that the Schwarz iterative method represents an efficient way to correct the inconsistencies introduced by the asynchronous coupling and obtaining a coherent ocean-atmosphere interface. However, the cost involved would be clearly very high for 3D models as applying even only two iterations would double the cost of the simulation. Therefore, Schwarz iterations can be considered as a method to provide a clean reference coupled solution that can be used to evaluate the biases of other coupling methods.

4.4.2 Methods for coupling in hydrology

Previous works at CERFACS established the necessity and merits of multi-dimensional coupling strategies between 1D and 2D hydrodynamics models, EDF-LNHE, LHSV, ARTELIA, SCHAPI and INRIA. [15] presented the 1-D/2-D longitudinal coupling between MASCARET and TELEMAC on the Adour river. where 1D and 2D models are coupled at their longitudinal boundaries with an iterative Schwarz algorithm applied at each interface. The longitudinal coupling strategy was implemented making use of TELEMAC-

MASCARET APIs (Application Programming Interface) as well as complementary classes dedicated to data driven integration of the solvers, to be as non-intrusive as possible in the numerical solvers. Python language was used with Mpi4Py for easier portability within any workflow platform. These developments were integrated in the git source code repository for Telemac (opentelemac.org). Lateral coupling is ongoing work where the dynamics of the floodplains is represented with local 2D models that communicate with a 1D model in the river bed. The flux at the interface is computed with a Riemann solver.
The prototype that was developed and submitted for publication by Minh Le (LHSV), in Advances in Water Resources describes the methodology and implementation of the lateral coupling strategy which was carried out and tested on an academic case as well as on the case of Garonne Marmandaise. It was demonstrated that this coupled 1D-2D solution is more efficient in terms of calculation time than the complete 2D solution and that the results of the coupled 1D-2D model are qualitatively and quantitatively close to the complete 2D solution. Yet, this work should now be carried out on the updated version of the Telemac-Mascaret hydrodynamic simulation chain hosted on the EDF Git server, taking advantage of the Python APIs developed as the code versions evolve. It is also a matter of replacing the coupling functionalities of OpenPALM with functionalities scripted in Python.
On going work over 2021-2023 was organized with the following schedule, yet, due to limited resources and time, only the first two first tasks were taken care of. This work is led by Minh Le (LHSV), with support from Andrea Piacentini at CERFACS for technical aspects. Sébastien Bourban (LNHE, LSHV) and Sophie Ricci (CERFACS) also participate in the project, for supervision and monitoring. This work will continue in 2024:

- Identification of quantities and variables exchanged
- Identification of the APIs allowing these exchanges via Telemac's Python layers
- Development of additional classes in Python allowing exchanges, in order to complete the existing APIs within the updated version of Telemac.
- Replacement of coupling via OpenPALM with these scripts and classes in Python dedicated to coupling
- Development of classes allowing efficient parallel computing of solvers with task parallelism and domain decomposition.
- Validation of the coupling capabilities on the test case described in the submitted article.

This work will be led by Minh Le (LHSV), with support from Andrea Piacentini at CERFACS for technical aspects. Sébastien Bourban (LNHE, LSHV) and Sophie Ricci (CERFACS) will also participate in the project, for supervision and monitoring.

4.5 Climate data production, management and services

4.5.1 Data production and management for climate modelling

Data production and management activities for climate modelling did not slow down during the 2021-2023 period. They were marked by the production of new CMIP6 data as part of the EU-H2020 TRIATLAS project and the dissemination of data from the EU-H2020-APPLICATE project, the production of which had just been completed in the year preceding the current evaluation period.
APPLICATE served the CMIP6 polar amplification model comparison project (PAMIP). At Cerfacs, the production achieved in 2019-2020 represents 1,600 simulated years mainly carried out with the atmosphere-only version (AMIP) of the CNRM-CM6-1 model but also with its coupled version running on Météo-France HPC resources, using 5.3 million CPU hours, generating 300,000 data sets for a total volume of

38 TB. Between the end of 2020 and August 2021, the main physical variables were made available to the ESGF research community. This represents 50% of the total number of datasets produced.
TRIATLAS provided input for the CMIP6 Decadal Climate Prediction Project (DCPP), and in particular for the part devoted to initialized retrospective simulations (DCPP-A), on both decadal and seasonal scales. Decadal-scale simulations (CNRM-ESM2-1 version of the CNRM-CERFACS coupled model developed for CMIP6) were produced by Cerfacs on the Météo-France HPC system (4,650 years simulated, 25 million CPU hours used) over 2021-2022, generating 110 TB of data and 448,000 data sets. Simulations were run twice to assess sensitivity to the atmosphere initialization method (with slightly lower data production: 620 simulations instead of 930). Publication of TRIALTAS ESGF data began at the end of 2022 and is ongoing; to date, 13,000 datasets (30% of the volume) have been distributed.
The technical aspects of climate modelling are dealt with in close coordination with Météo-France/CNRM through various joint working groups. The data life cycle is handled by the Climat-Tech group, among others. Data-oriented software included in the modelling workflow (XIOS, dr2xml) is also a subject for the group extended to include IPSL climate modelling engineers (CLIMERI-Tech). The XIOS and dr2xml tools have undergone major improvements during the current evaluation period (for more details, see IS-ENES3 deliverable 8.3[6]). These developments will be capitalized on for the next CMIP7 exercise, enabling efficient output data flow, file format and metadata in line with FAIR principles and future CMIP standards.
Regarding the data production for CMIP, since July 2023 Cerfacs is member, jointly with CNRM, in one of the CMIP-IPO working group responsible for preparing and coordinating the next CMIP phase 7 on an international scale: the Data Request Task Team responsible for defining the variables required for each MIP theme (oceanography, cryosphere, land surface, atmosphere, clouds and aerosols) or downstream research communities (climate impacts, climate services, regional modeling).
In addition, the French climate modelling community (CLIMERI-France) is involved in the national Equipex+/PIA3 GAIA-DATA project (an 8-year project starting in December 2021), which aims to open up the boundaries between data from different earth science sectors (space observation, biodiversity, climate modelling,...) to facilitate multidisciplinary approaches. The project aims to make data hosted in regional thematic clusters accessible via a single portal. These data and service centers will be connected to a high-performance network, and will also offer adapted analysis tools (VRE, Virtual Research Environments). Cerfacs is involved in this project, together with CNRM, mainly as an expert in climate model data and metadata.

4.5.2 European and International Data Infrastructures

The development of the scientific data infrastructure for researchers at the European and international levels is very important to support our activities and the dissemination of our results. It includes developing data processing software, web interfaces, working on the standards for interoperability and automation, and on novel methods to process large amount of data. In continuation with previous years, we have continued to be involved in several major related European projects and initiatives, with always a very good reputation and visibility. Thanks to this reputation, we have the privilege of having to choose in which H2020 and Horizon Europe projects we want to get involved, according to our workforce and team objectives. During the last years, European funded projects that sustained those activities were H2020 IS-ENES3, Horizon Europe Climateurope2 and interTwin as well as the new large IRISCC project. The IS-ENES3 project has ended in March 2023, but it continues through the participation of CERFACS in the ENES Research Infrastructure (RI) and also into the HE IRISCC project. The contribution of CERFACS into the EUDAT CDI enables us to be informed on new consortiums as well as being able to contribute to the European Open Science Cloud (EOSC) that is largely pushed by the European Commission. There is also a good synergy between European and national funding with the new ANR funded projects under TRACCS, especially

[6] IS-ENES3 Deliverable 8.3: XIOS and Dr2xml new developments, https://raw.githubusercontent.com/IS-ENES3/IS-ENES-Website/main/pdf_documents/IS-ENES3_D8.3-VF.pdf

with PC-INVEST on the climate services that will provide co-funding for the processing back-ends, like the climate indices software icclim, and benefiting of standards, technologies and methodologies developed by the IS-ENES3 project for the platform climate4impact.eu. Major results are:

- Developments and significant optimization of the python-based open-source climate indices workflow back-end created and developed by CERFACS: icclim (https://icclim.readthedocs.io). Significant achievements: used for CMIP6 official products/indices and considered to be a backend of the Météo-France DRIAS national climate service platform.
- Contributing to the development of standard and guidance of climate services (HE Climateurope2 project).
- Development of a novel method to analyze climate simulations to identify and characterize the changes of climate extremes using Artificial Intelligence (Deep Learning), in the context of Digital Twins (HE interTwin project). In interTwin there is also coordination with the DestinE initiative lead by ECMWF.

References

[15] S. Barthélémy, S. Ricci, T. Morel, N. Goutal, E. Le Pape, and F. Zaoui, (2018), On operational flood forecasting system involving 1D/2D coupled hydraulic model and data assimilation, *Journal of Hydrology*, **562**, 623–634.

[16] A. Voldoire, R. Roehrig, H. Giordani, R. Waldman, Y. Zhang, S. Xie, and M.-N. Bouin, (2022), Assessment of the sea surface temperature diurnal cycle in CNRM-CM6-1 based on its 1D coupled configuration, *Geoscientific Model Development*, 3347–3370.

Publications

5.1 Books

[CE1] C. Cassou and V. Masson-Delmotte, (2023), *Parlons climat en 30 questions - Troisième édition*, ., la documentation française ed.

[CE2] J. Lavigne, C. Cassou, F. D'Amico, Plop, and Kankr, (2023), *Regards croisés sur un précipice immense... dans les émotions de la Terre : Climat, Biodiversité, une question sociale*, ., montagnes insolites association ed.

[CE3] C. Mechoso, S.-I. An, and S. Valcke, (2021), *Atmosphere-Ocean Modelling - Coupling and Couplers*, World Scientific.

[CE4] M. Rochoux, A. Costes, R. Paugam, and A. Trouvé, (2023), *Inversion et assimilation de données de télédétection - Estimation des paramètres géophysiques*, ISTE Editions.

5.2 Conferences Proceedings

[CE5] F. Adloff, B. Lawrence, S. Joussaume, M. Lautenschlager, J. Bessembinder, J. Biercamp, A. Cofino, A. D´Anca, U. Fladrich, A. Hines, M. Juckes, R. Kazeroni, P. Kershaw, S. Kindermann, P. Nassisi, C. Pagé, K. Serradell, and S. Valcke, (2021), From climate models to informing policy decisions: the end-to-end importance of an effective research infrastructure, In *vEGU21: Gather Online — 19–30 April*.

[CE6] W. Antolin, A. Costes, M. Rochoux, and P. Le Moigne, (2022), Accounting for the canopy drag effect on wildland fire spread in coupled atmosphere/fire simulations, In *IX International Conference on Forest Fire Research, Coimbra, 11-18 November, Portugal*.

[CE7] W. Antolin, M. Rochoux, and P. Le Moigne, (2023), Study of canopy drag effects during an experimental fire using Meso-NH, In *12th Meso-NH User´s Meeting, Toulouse, France, 18-20 Octobre*.

[CE8] M. Bador and L. Alexander, (2023), Future Seasonal Changes in Extreme Precipitation Scale With Changes in the Mean, In *Open Science Conference, World Climate Research Programme, Kigali, Rwanda, October 23-27*.

[CE9] M. Bador, R. Roca, J. Trules, S. Cloché, and L. Alexander, (2023), FROGS: a daily $1° \times 1°$ gridded precipitation database of rain gauge, satellite and reanalysis products, In *Open Science Conference, World Climate Research Programme, Kigali, Rwanda, October 23-27*.

[CE10] S. Baur, B. Sanderson, R. Séférian, and L. Terray, (2022), Solar Renewable Energy Resources under Solar Geoengineering, In *Climate Engineering Gordon Research Conference, Newry, ME, United States, 26 june - 01 july*, vol. GRC22.

[CE11] S. Baur, B. Sanderson, R. Séférian, and L. Terray, (2022), Thermal response timescales and associated spatial patterns in ESMs to pulse injections of climate forcers, In *EGU General Assembly, Vienna, Austria, 23 - 27 may*, vol. EGU22-5538.

[CE12] S. Baur, L. Terray, R. Séférian, and B. Sanderson, (2023), Change in wind energy potential under Solar Radiation Modification, In *28th General Assembly of the International Union of Geodesy and Geophysics, Berlin, Germany, July 11-20*.

[CE13] G. Blanchet, P. Kettig, T.-H. Nguyen, S. Ricci, A. Piacentini, C. Fatras, J. Poisson, and G. Valadeau, (2022), The FloodDAM project in SCO, In *Space4Insurance, Toulouse, France*.

[CE14] Q. Bonassies, S. Ricci, T.-H. Nguyen, A. Piacentini, M. Sadki, C. Fatras, A. Andral, S. Pena Luque, and R. Rodriguez Suquet, (2023), Front type implementation for flood extent and flood modelling image assimilation, In *Telemac User Conference, Karlsruhe, Germany, October 11-13*.

[CE15] Q. Bonassies, S. Ricci, S. Pena Luque, C. Fatras, T.-H. Nguyen, A. Piacentini, R. Rodriguez Suquet, and A. Andral, (2023), SAR data assimilation as front-like data for flood prediction, In *SHF2023, Toulouse, France, 28-30 Novembre*.

[CE16] F. Collet, M. Bador, J. Boé, L. Dubus, and B. Jourdier, (2023), Climate conditions associated with low wind power production and high electricity demand events in France, In *International Conference of Energy Meteorology (ICEM), Padoue, Italie, 27-29 Juin*.

[CE17] F. Collet, J. Boé, M. Bador, L. Dubus, and B. Jourdier, (2023), Characterization of climate conditions leading to compound low wind power production and high electricity consumption in France, In *Open Science Conference, World Climate Research Programme, Kigali, Rwanda, October 23-27*.

[CE18] A. Costes, C. Lac, M. Rochoux, and V. Masson, (2021), Analysis of the MesoNH-Fire model response to modeling assumptions and parametric uncertainties, In *Workshop ANR FireCaster, Cargèse (France), 15-19 November*.

[CE19] A. Costes, C. Lac, M. Rochoux, and V. Masson, (2021), Wildland fire behavior simulations using the coupled model Meso-NH/BLAZE and evaluation of the Meso-NH compressible version, In *Journées Utilisateurs Meso-NH, 2-3 December*.

[CE20] A. Costes, M. Rochoux, C. Lac, and V. Masson, (2021), Exploring the sensitivity of the atmospheric response to surface fire heat fluxes, In *AMS (American Meteorological Society) 20th Annual Student Conference, New Orleans (USA), 10-14 January*.

[CE21] T. Defontaine, S. Ricci, C. Lapeyre, E. Le Pape, and A. Marchandise, (2022), Flood Forecasting with Machine Learning in a scarce data layout, In *HydroInformatics Conference, Bucarest, Roumanie*.

[CE22] T. Defontaine, S. Ricci, C. Lapeyre, A. Marchandise, and E. Le Pape, (2022), Discharge forecasting with Machine Learning in a scarce data layout, In *HydroInformatics Conference, Bucarest, Roumanie*.

[CE23] T. Defontaine, S. Ricci, C. Lapeyre, E. Le Pape, R. Lamblin, A. Marchandise, and L. Routhe, (2023), Prévision de crues en Temps réel avec des algorithmes d'apprentissage par la donnée, en donnée pluie-débit restreinte, In *SHF2023, Toulouse, France, 28-30 Novembre*.

[CE24] S. El Garroussi, S. Ricci, M. De Lozzo, N. Goutal, and D. Lucor, (2021), Tackling uncertainty in flood forecasting model via a machine-learning based- surrogate model, In *UNCECOMP2021, 28-30 June*.

[CE25] S. El Garroussi, S. Ricci, M. De Lozzo, N. Goutal, and D. Lucor, (2021), Towards the reduction of uncertainty in hydraulic modles for better flood forecasting, In *Simhydro, 16-18 June*.

[CE26] C. Emery, S. Ricci, and A. Piacentini, (2022), Tools4SWOTsims and SMURF - Python libraries supporting the generation of the synthetical SWOT-like data in anticipation of the assimilation of real products for river hydrodynamic studies, In *AGU Fall Meeting, Chicago, USA*.

[CE27] R. Espoeys, M. Balesdent, S. Ricci, L. Brevault, and P. Mycek, (2022), Overview and comparison of reliability analysis techniques based on different multi-fidelity Gaussian Processes, In *ASMO-UK 12 / ASMO-Europe 1 / ISSMO Conference on Engineering Design Optimization, Leeds, UK*.

[CE28] R. Espoeys, L. Brevault, M. Balesdent, S. Ricci, and P. Mycek, (2023), Multifidelity Sequential Bayesian Optimization and Reliability Assessment Method for the Design of Complex Systems, In *5th ECCOMAS Thematic Conference on Uncertainty Quantification in Computational Sciences and Engineering (UNCECOMP), Athens, Greece, 12-14 June*.

[CE29] S. Fiore, C. Pagé, S. Joussaume, and F. Antonio, (2021), The IS-ENES use case, In *EGI Conference, 18-22 October*.

[CE30] M. Foudad, E. Sanchez-Gomez, T. Jaravel, M. Rochoux, and L. Terray, (2023), Impact du changement climatique sur les turbulences en ciel clair, liens avec l´EASA et Airbus - Invited conference, In *Commission Aviation de transport du CSM, Météo France, Saint-Mandé, 21 septembre*.

[CE31] M. Foudad, E. Sanchez-Gomez, T. Jaravel, M. Rochoux, and L. Terray, (2023), Past and Future Trends in Clear-Air Turbulence over the Northern Hemisphere - Invited conference, In *Séminaire University of Reading, UK, June 13*.

[CE32] M. Foudad, E. Sanchez-Gomez, M. Rochoux, T. Jaravel, and L. Terray, (2022), Analysis of recent trends of clear-air turbulence in wintertime over the northern hemisphere, In *AOGS 19th annual meeting*.

[CE33] M. Foudad, E. Sanchez-Gomez, M. Rochoux, T. Jaravel, and L. Terray, (2022), Present climate characterization and future changes in Clear-Air Turbulence (CAT) over the northern hemisphere, In *EGU General Assembly, Vienna, Austria and online, 23–27 May - EGU22-2796*.

[CE34] M. Foudad, E. Sanchez-Gomez, M. Rochoux, T. Jaravel, and L. Terray, (2023), Present climate characterization and future changes in Clear-Air Turbulence (CAT) over the northern hemisphere, In *EASA (European Union Aviation Safety Agency) Conference, Cologne, Germany, 23-24 march*.

[CE35] A. Gossard, S. Salles, B. Roiron, S. Ricci, N. Gourdain, E. Sanchez-Gomez, and V. Gallardo-Fernandez, (2022), Impact of Global Warming on Aircraft Aerodynamics and Engine Thrust at Take-Off Conditions, In *56th 3AF International Conference on Applied Aerodynamics, Toulouse, France*.

[CE36] T. Huang, C. David, G. Doran, J. Kang, G. Llewellyn, K. Marlis, S. Perez, W. Phyo, J. Roberts, C. Taglialatela, S. Kumar, N. Biswas, P. Stackhouse, D. Borges, M. Broddle, B. Macpherson, R. Rodriguez Suquet, S. Baillarin, F. Bretar, G. Blanchet, P. Kettig, S. Ricci, A. Piacentini, T.-H. Nguyen, G. Valladeau, J. Poisson, A. Froidevaux, A. Guiot, R. Raynal, T.-L. Huynh, C. Fatras, S. Brunato, and E. Guzzonato, (2023), OPEN-SOURCE FRAMEWORK FOR EARTH SYSTEM DIGITAL TWINS, In *AGU 2023, USA, 11-15 December 2023*.

[CE37] T. Huang, C. David, K. Marlis, S. Perez, C. Oaida, M. Wronkiewicz, N. Biswas, D. Borges, B. Macpherson, G. Blanchet, P. Kettig, S. Ricci, T.-H. Nguyen, J. Poisson, R. Raynal, J. Kang, M. Milosevich, W. Phyo, J. Roberts, S. Kumar, P. Stackhouse, M. Broddle, S. Baillarin, F. Bretar, R. Rodriguez, A. Piacentini, G. Valladeau, A. Froidevaux, and T.-L. Huynh, (2022), Federated Digital Twins for Flood Prediction and Analysis - Invited conference, In *AGU Fall Meeting, Chicago, USA, December 12-16*.

[CE38] R. Isphording, L. Alexander, M. Bador, D. Green, and J. Evans, (2023), A standardized benchmarking framework to assess downscaled rainfall simulations, In *Open Science Conference, World Climate Research Programme, Kigali, Rwanda, October 23-27*.

[CE39] P. Kettig, G. Baillarin, G. Blanchet, C. Taillan, S. Ricci, T.-H. Nguyen, T. Huang, A. Altinok, N.-T. Chung, G. Valladeai, C. Goeury, and A. Roumagnac, (2021), The SCO FloodDAM project: New observing strategies for flood detection, alert and rapid mapping, In *IGARSS 11-16 July*.

[CE40] V. Laborie, N. Goutal, and S. Ricci, (2021), Improving Water levels forecast in the Gironde estuary using Telemac2D and data assimilation by infering time-dependent boundary conditions, In *Simhydro, 16-18 June*.

[CE41] A. Liné, C. Cassou, and R. Msadek, (2021), Assessing the role of internal variability in Northern Europe winter temperatures at near-term (2020-2040) using a storyline approach, In *Workshop: Multi-annual to Decadal Climate Predictability in the North Atlantic-Arctic Sector, 21 sept.*

[CE42] A. Liné, C. Cassou, and R. Msadek, (2021), Assessing the role of internal variability on projections of Northern Europe surface air-temperature at near-term (2020-2039) using a storyline approach, In *EGU General Assembly 2021, vEGU21: Gather Online — 19–30 April*.

[CE43] E. Lumet, M. Rochoux, T. Jaravel, and S. Lacroix, (2021), Assimilation de données de capteurs mobiles pour la simulation de panache atmosphérique à micro-échelle, Atelier “Mesure de la qualité de l’air”, Instrumentation pour le suivi environnemental, In *Cycle d’ateliers nationaux 2021, online event, 29-30 September*.

[CE44] E. Lumet, M. Rochoux, S. Lacroix, T. Jaravel, and O. Vermorel, (2022), Sensitivity analysis of microscale pollutant dispersion large-eddy simulations towards observation network design, In *21st International Conference on Harmonisation within Atmospheric Dispersion Modelling for Regulatory Purposes, Aveiro, 27-30 September, Portugal*.

[CE45] E. Maisonnave, S. Berthet, J. Chanut, C. Bricaud, and R. Séférian, (2023), A multi-executable solution for the coarsening of the biogeochemistry in NEMO 4.2, In *DRAKKAR Ocean Modelling Workshop, 30 jan - 01 feb, Grenoble, France*.

[CE46] A. Marchandise, A. Escudier, J.-N. Audouy, L. Routhe, B. Combedouzon, Y. Lacaze, E. Le Pape, and S. Ricci, (2023), Capitalisation des données de la crue majeure de février 2021 sur la Garonne aval, exploitation actuelle et perspectives d’amélioration de la prévision des crues et des inondations, In *SHF2023, Toulouse, France, 28-30 Novembre*.

[CE47] A. Marchandise, A. Escudier, J.-N. Audouy, L. Routhe, B. Combedouzon, Y. Lacaze, E. Le Pape, and S. Ricci, (2023), Capitalisation des données de la crue majeure de février 2021 sur la Garonne aval, exploitation actuelle et perspectives d’amélioration de la prévision des crues et des inondations, In *SHF2023, Toulouse, 28-30 Novembre*.

[CE48] P. Nguyen, M. Bador, L. Alexander, and T. Lane, (2023), Selecting regional climate models based on their skill could give more credible precipitation projections over the complex Southeast Asia region, In *Open Science Conference, World Climate Research Programme, Kigali, Rwanda, October 23-27*.

[CE49] T.-H. Nguyen, A. Delmotte, C. Fatras, P. Kettig, A. Piacentini, and S. Ricci, (2021), Validation and Improvement of Data Assimilation for Flood Hydrodynamic Modelling Using SAR Imagery Data, In *Telemac User Meeting, 13-15 Oct. 2021*.

[CE50] T.-H. Nguyen, A. Piacentini, S. Munier, S. Ricci, R. Rodriguez Suquet, S. Le Gac, F. Boy, C. Fatras, Q. Bonassies, M. Sadki, and S. Pena Luque, (2023), Flood Forecast with Chained Hydrologic-Hydraulic Modelling and Data Assimilation, In *Telemac User Conference 2023, Karlsruhe, Germany, October 11-13*.

[CE51] T.-H. Nguyen, S. Ricci, A. Piacentini, P. Kettig, G. Blanchet, C. Fatras, E. Lavergne, and G. Baillarin, (2021), Adding EO-based Virtual Observations to Improve Data Assimilation for Flood Fluvial Forecasting, In *HydroSpace-GEOGloWS, 7-11 June*.

[CE52] T.-H. Nguyen, S. Ricci, A. Piacentini, P. Kettig, C. Fatras, and S. Baillarin, (2021), Assessing and Improving Fluvial Flood Forecast Performance Using Sentinel-1 Derived Flood Extent Maps, In *AGU Fall Meeting, New Orleans, LA and Online, USA*.

[CE53] T.-H. Nguyen, S. Ricci, A. Piacentini, P. Kettig, C. Fatras, and S. Baillarin, (2022), Assimilation of SAR-Derived Flood Extent Maps for Improving Fluvial Flood Forecast, In *ESA LivingPlanet, Bonn, Germany*.

[CE54] T.-H. Nguyen, S. Ricci, A. Piacentini, P. Kettig, C. Fatras, and S. Baillarin, (2022), Assimilation of SAR-derived flood observations for improving fluvial flood forecast, In *14 th International HydroInformatics Conference, Bucarest, Roumanie, July 04 - 08*, vol. 1136.

[CE55] T.-H. Nguyen, S. Ricci, A. Piacentini, R. Rodriguez, G. Blanchet, C. David, P. Kettig, and S. Baillarin, (2022), Uncertainty Reduction in Fluvial Flood Re-analysis by Assimilating SAR-derived Flood Extent Maps, In *AGU Fall Meeting, Chicago, USA, December 12-16*.

[CE56] T.-H. Nguyen, S. Ricci, A. Piacentini, R. Rodriguez Suquet, G. Blanchet, and S. Baillarin, (2022), Enhancing Flood Forecasting with Dual State- Parameter Estimation and Ensemble-based SAR Data Assimilation, In *Telemac User Conference, Paris, France*.

[CE57] T.-H. Nguyen, S. Ricci, A. Piacentini, R. Rodriguez Suquet, G. Blanchet, C. David, P. Kettig, and S. Baillarin, (2022), Uncertainty Reduction in Fluvial Flood Re-analysis by Assimilating SAR-derived Flood Extent Maps, In *AGU, 12-16 December 2022, Chicago, USA*.

[CE58] T.-H. Nguyen, S. Ricci, A. Piacentini, Q. Bonassies, R. Rodriquez-Suquet, S. Pena Luque, C. David, and K. Marlis, (2023), Reducing Uncertainties Of A Chained Hydrologic-Hydraulic Models To Improve Flood Extent Representation Using Multi-Source Earth Observation Data, In *IGARSS, Pasadena, USA, July 16-21*.

[CE59] T.-H. Nguyen, S. Ricci, A. Piacentini, C. Emery, R. Rodriguez Suquet, and S. Pena Luque, (2023), Merits of Assimilating SWOT Altimetry and Sentinel-1-derived flood extent Observations for Flood Forecasting - A Proof-of-Concept, In *HYDROSPACE 2023, Lisbonne, Portugal, November 27-December 1*.

[CE60] T.-H. Nguyen, S. Ricci, A. Piacentini, E. Simon, R. Rodriguez Suquet, and S. Pena Luque, (2023), Dealing with Non-Gaussianity of SAR-Derived Wet Surface Ratio for Flood Extent Representation Improvement, In *IGARSS, Pasadena, USA, July 16-21*, 1595–1598.

[CE61] B. Nony, M. Rochoux, T. Jaravel, and D. Lucor, (2023), Reduced-order model for microscale atmospheric dispersion combining multi-fidelity LES and RANS data, In *5th ECCOMAS Thematic Conference on Uncertainty Quantification in Computational Sciences and Engineering (UNCECOMP), Athens, Greece, 12-14 june*.

[CE62] B. Nony, M. Rochoux, D. Lucor, and T. Jaravel, (2021), Compound parametric metamodeling of large-eddy simulations for micro-scale atmospheric dispersion, In *20th International Conference on Harmonisation within Atmospheric Dispersion Modelling for Regulatory Purposes (HARMO), Tartu (Estonia), 14-18 June*.

[CE63] B. Nony, M. Rochoux, D. Lucor, and T. Jaravel, (2021), Metamodelling for micro-scale atmospheric pollutant dispersion large-eddy simulation, In *MascotNum Annual Conference, Aussois (France), 27-30 April*.

[CE64] B. Nony, M. Rochoux, D. Lucor, and T. Jaravel, (2022), Adaptive Gaussian process surrogate modelling of large-eddy simulations for microscale atmospheric dispersion, In *8th European Congress on Computational Methods in Applied Sciences and Engineering, Oslo, 05-09 June, Norway*.

[CE65] H. Oubanas, S. Ricci, P.-O. Malaterre, I. Gejadze, D. Quittard, T.-H. Nguyen, C. Emery, and A. Piacentini, (2023), Global River Discharges Estimation from SWOT Observations using Data Assimilation and Hydraulic Models, In *SWOT Meeting, Toulouse, France, 19-22 Septembre*.

[CE66] C. Pagé and A. Aoun, (2022), Building actionable climate products for end users using EGI-ACE resources - invited conference, In *EOSC Future-INFRAEOSC-07 use case webinar, online, 5-6 December*.

[CE67] C. Pagé and A. Aoun, (2022), Processing large datasets using EGI-ACE EOSC resources for the climate community, In *EGI Conference, Prague, Czech Republic, 19-23 Septembre*.

[CE68] C. Pagé, A. Aoun, and A. Spinuso, (2022), ICCLIM: Calculating Climate Indices and Indicators Made Easy, In *AMS 2022: 12th Symposium on Advances in Modeling and Analysis Using Python, 23 - 27 January, online*.

[CE69] C. Pagé, A. Aoun, A. Spinuso, L. Barring, and K. Zimmermann, (2022), Better Tailoring of Climate Information for End Users using Targeted Interfaces and Tools, In *EGU General Assembly, Vienna, Austria and online, May 23-27*.

[CE70] C. Pagé, A. Aoun, A. Spinuso, I. van der Neut, M. Veldhuizen, K. Zimmermann, and L. Barring, (2022), Making Climate Data Actionable: Pre-Computed Climate Indices Provided in an Interactive Platform, In *Scientific Gateways, San Diego, USA, 18-20 October*.

[CE71] C. Pagé, A. Aoun, A. Spinuso, M. Veldhuizen, I. van der Neut, K. Zimmermann, L. Barring, and P. Kershaw, (2022), Interactive and Flexible Environment for on-demand Climate Data Analysis, In *IWSG 2022 Workshop, 14th International Workshop on Science Gateways, Trento, Italy, 15-17 June*.

[CE72] C. Pagé, A. Aoun, A. Spinuso, K. Zimmermann, and L. Barring, (2022), Challenges in the road toward better FAIR support in downstream climate products, In *SciDataCon/RDA (International Data Week), Corée du Sud, online, 20-26 June*.

[CE73] C. Pagé, A. Aoun, A. Spinuso, K. Zimmermann, and L. Barring, (2022), Climate Data Analysis Tools Along With Pre-Computed Climate Indices Datasets to Support Climate Action, In *AGU Fall Meeting, Chicago, Illinois, USA, 12-16 December*.

[CE74] C. Pagé, A. Aoun, A. Spinuso, K. Zimmermann, and L. Barring, (2023), Climate Data Analysis Tools and Datasets to Support Climate Action, In *AMS 103rd Annual Meeting, Denver, Colorado, USA, 08-12 January*.

[CE75] C. Pagé, M. Plieger, W. Som de Cerff, A. Spinuso, R. Filgueira, M. Atkinson, C. Themeli, I. Klampanos, and V. Karkaletsis, (2021), Making Cyclone Tracking accessible to end users for Climate Research and Applications, In *vEGU21: Gather Online — 19–30 April*.

[CE76] C. Pagé, A. Spinuso, K. Zimmermann, L. Barring, and A. Aoun, (2021), Access to Analysis and Climate Indices Tools for Climate Researchers and End Users, In *AGU Fall Meeting, 13-17 december, New Orleans, LA, USA*.

[CE77] C. Pagé, (2022), Building a Climate indices dataset for climate change impacts assessment, In *EOSC Symposium, Prague, Czech Republic, 14-11 November*.

[CE78] R. Paugam, W. Mell, J.-B. Filippi, M. Rochoux, and M. Wooster, (2022), High-resolution fire behavior monitoring and plume simulation in the context of experimental fire, In *IX International Conference on Forest Fire Research, Coimbra, 11-18 November, Portugal*.

[CE79] S. Peatier, B. Sanderson, and L. Terray, (2023), Climate model tuning and parametric dependence of climate feedbacks, In *Open Science Conference, World Climate Research Programme, Kigali, Rwanda, October 23-27*.

[CE80] S. Peatier, B. Sanderson, and L. Terray, (2023), Exploring parametric dependance of climate feedbacks using a Perturbed Parameter Ensemble (PPE) - Invited conference, In *Séminaire NCAR, Bouder, USA, March 16*.

[CE81] S. Peatier, B. Sanderson, and L. Terray, (2023), Impact of ARPEGE-Climat tuning on climate feedbacks, In *Ateliers de Modélisation de l´Atmosphère, Centre International de Conférences - Météopole de Toulouse, 09/05-11/05*.

[CE82] S. Peatier, B. Sanderson, and L. Terray, (2023), On the Parametric Dependance of Climate Model Errors and Feedbacks - Invited conference, In *SIAM Conference on Mathematical and Computational Issues in the Geosciences (GS23), Bergen, Norway, 19/06 - 23/06*.

[CE83] S. Ricci, C. Emery, and A. Piacentini, (2022), Estimation of water surface elevation and discharge for rivers with SWOT. Tools4SWOThr: a python tool dedicated to the generation of inputs for SWOT simulators from river hydrodynamics model outputs., In *EGU General Assembly, Vienna, Austria and online*.

[CE84] S. Ricci, T.-H. Nguyen, S. Le Gac, F. Boy, A. Piacentini, R. Rodriguez Suquet, S. Pena Luque, Q. Bonassies, and C. Emery, (2023), Comparisons and Water Level Analyses using Sentinel-6MF Satellite Altimetry Data with 1D Mascaret and 2D Telemac Models, In *EGU General Assembly, Vienna, Austria, April 24-28*.

[CE85] M. Rochoux and M. Jappiot, (2021), Designing the future of wildfire modeling guided by high-resolution remote sensing data, In *Atelier TERATEC "Données satellitaires et Environnement", 23 June*.

[CE86] M. Rochoux and T. Nagel, (2022), Simulating microscale meteorology in urban environment - invited conference, In *Journée thématique SFT, Données climatiques pour le bâtiment, Paris, France, 8 Décembre*.

[CE87] M. Rochoux, A. Collin, A. Costes, C. Zhang, A. Trouvé, D. Lucor, and P. Moireau, (2021), Shape-oriented sensitivity analysis and data assimilation for wildland fire applications, In *International EnKF workshop 2021, online event, 7-9 June*.

[CE88] M. Rochoux, A. Costes, R. Paugam, and A. Trouvé, (2021), Data assimilation for landscape-scale wildland fire behavior, In *WCRP-WWRP Symposium on Data Assimilation and Reanalysis, online event, 13-18 September*.

[CE89] M. Rochoux, B. Nony, C. Zhang, D. Lucor, T. Jaravel, A. Collin, P. Moireau, and A. Trouvé, (2022), Assimilating fire front position and emulating boundary-layer flow simulations for wildland fire behavior ensemble prediction and reanalysis - invited conference, In *Séminaire UQSay, online 19 mai*.

[CE90] M. Rochoux, (2023), Combiner modélisation et mesures pour mieux comprendre et anticiper le comportement des incendies de forêt aux échelles géographiques - invited conference, In *Atelier, Drones et Sciences de l'Atmosphère, ENAC, Toulouse, 8 décembre*.

[CE91] M. Rochoux, (2023), Comprendre et anticiper le comportement des feux par l´assimilation de données et une modélisation couplée à l´atmosphère - invited conference, In *Conférence-débat à l'Académie des Sciences sur le thème de la ≪ Modélisation et monitoring des feux de forêts ≫, Institut de France, Paris, 5 décembre*.

[CE92] R. Rodriguez Suquet, S. Ricci, and T.-H. Nguyen, (2023), SCO-FloodDAM-DT. Towards a Digital Twin for flood detection, prediction and risk assessment - Invited conference, In *Forum, TERATEC, Paris, France, 30-31 Mai 2023*.

[CE93] R. Rodriguez Suquet, S. Ricci, T.-H. Nguyen, A. Piacentini, Q. Bonassies, C. Fatras, E. Lavergne, A. Andral, S. Brunato, V. Gaudissart, E. Guzzonato, G. Valladeau, J. Poisson, A. Froidevaux, A. Guiot, H. Thanh-Long, T. Huang, P. Kettig, G. Blanchet, and F. Bretar, (2023), The SCO-FLOODDAM project: towards a digital twin for flood detection, prediction and flood risk assessments, In *SHF2023, Toulouse, France, 28-30 Novembre*.

[CE94] R. Rodriquez-Suquet, T.-H. Nguyen, S. Ricci, A. Piacentini, Q. Bonassies, C. Fatras, E. Lavergne, S. Brunato, V. Gaudissart, E. Guzzonato, A. Froidevaux, A. Guiot, G. Valladeau, J. Poisson, T. Huang, F. Bretar, P. Kettig, and G. Blanchet, (2023), The SCO-FLOODDAM project: towards a digital twin for flood detection, prediction and flood risk assessments, In *IGARSS, Pasadena, USA, July 16-21*.

[CE95] F. Roubelat, A. Costes, W. Antolin, and M. Rochoux, (2022), Identifying the most influential parameters in experimental grass fire spread modeling using global sensitivity analysis, In *IX International Conference on Forest Fire Research, Coimbra, 11-18 November, Portugal*.

[CE96] M. Sadki, S. Ricci, A. Piacentini, T.-H. Nguyen, Q. Bonassies, R. Rodriguez Suquet, S. Pena Luque, N. Gasnier, A. Marchandise, E. Le Pape, G. Valladeau, and J. Poisson, (2023), Integrating new in situ, airborne and spaceborne elevation data to improve river floods hydraulic modeling, In *Telemac User Conference, Karlsruhe, Germany, October 11-13*.

[CE97] S. Salles, S. Ricci, and N. Gourdain, (2023), Modeling the impact of atmospheric variables on the performance of an aircraft during take-off: Towards the adaptation of air traffic operations to global warming, In *Meeting OpenTURNS, Saclay, France, 23 March*.

[CE98] L. Terray, (2022), Assessing the influence of low-frequency internal variability on extreme events - invited conference, In *Clivar Dynamics Panel annual workshop on External versus internal variability on decadal and longer time scales - Remote Attendance*.

[CE99] L. Terray, (2023), Dynamical adjustment in a nutshell - invited conference, In *ForceSMIP Hackathon, ETH, Zurich, Switzerland, August 29-31*.

[CE100] A.-L. Tiberi, N. Goutal, and S. Ricci, (2022), Prévisions d'ensemble hydrauliques pour la vigilance crues, In *MAR, Toulouse, France*.

[CE101] A.-L. Tiberi-Wadier, A. Belleudy, E. Le Pape, M.-H. Ramos, S. Ricci, and N. Goutal, (2023), Prévisions D'ensemble Hydrologiques Au Sein Du Réseau National De Prévision Des Crues En France "Vigicrues" : Expérimentations Avec Le PostTraitement Des Prévisions Dans Le Bassin De L'odet, In *SHF2023, Toulouse, 28-30 Novembre*, 950.

5.3 HDR

[CE102] M. Rochoux, (2022), *Modéliser le comportement des incendies de végétation : Comment composer entre modélisation physique et données en présence d'incertitudes ? Quelles prises de vue adopter pour comprendre les processus micrométéorologiques en jeu ?*, hdr, SDU2E: Océan, Atmosphère, Climat.

5.4 Journal Publications

[CE103] C. Ardillouze, D. Specq, L. Batté, and C. Cassou, (2021), Flow dependence of wintertime subseasonal prediction skill over Europe, *Weather and Climate Dynamics*, **2**, 1033–1049.

[CE104] M. Bador and L. Alexander, (2022), Future Seasonal Changes in Extreme Precipitation Scale With Changes in the Mean, *Earths Future*, **10**, e2022EF002979.

[CE105] A. Baker, M. Roberts, P. Vidale, K. Hodges, J. Seddon, B. Vannière, R. Haarsma, R. Schiemann, M. Kageyama, D. Kapetanakis, E. Tourigny, K. Lohmann, C. Roberts, and L. Terray, (2022), Extratropical Transition of Tropical Cyclones in a Multiresolution Ensemble of Atmosphere-Only and Fully Coupled Global Climate Models, *Journal of Climate*, **35**, 5283–5306.

[CE106] S. Baur, A. Nauels, Z. Nicholls, B. Sanderson, and C. Schleussner, (2023), The deployment length of solar radiation modification: an interplay of mitigation, net-negative emissions and climate uncertainty, *Earth System Dynamics*, **14**, 367–381.

[CE107] A. Bellucci, P. Athanasiadis, E. Scoccimarro, P. Ruggieri, S. Gualdi, G. Fedele, R. Haarsma, J. Garcia-Serrano, M. Castrillo, D. Putrahasan, E. Sanchez-Gomez, M.-P. Moine, C. Roberts, M. Roberts, J. Seddon, and P. Vidale, (2021), Air-Sea interaction over the Gulf Stream in an ensemble of HighResMIP present climate simulations, *Climate Dynamics*, **56**, 2093–2111.

[CE108] C. Besombes, O. Pannekoucke, C. Lapeyre, B. Sanderson, and O. Thual, (2021), Producing realistic climate data with generative adversarial networks, *Nonlinear Processes in Geophysics*, **28**, 347–370.

[CE109] J. Boé, A. Mass, and J. Deman, (2023), A simple hybrid statistical–dynamical downscaling method for emulating regional climate models over Western Europe. Evaluation, application, and role of added value?, *Climate Dynamics*, **61**, 271–294.

[CE110] J. Boé, (2021), The physiological effect of CO2 on the hydrological cycle in summer over Europe and land-atmosphere interactions, *Climatic Change*, **167**, Article number 21.

[CE111] S. Chripko, R. Msadek, E. Sanchez-Gomez, L. Terray, L. Bessières, and M.-P. Moine, (2021), Impact of Reduced Arctic Sea Ice on Northern Hemisphere Climate and Weather in Autumn and Winter, *Journal of Climate*, **34**, 5847–5867.

[CE112] A. Costes, M. Rochoux, C. Lac, and V. Masson, (2021), Subgrid-scale fire front reconstruction for ensemble coupled atmosphere-fire simulations of the FireFlux I experiment, *Fire Safety Journal*, **126**, 103475.

[CE113] A. Costes, Q. Rodier, C. Lac, M. Rochoux, and V. Masson, (2022), Effects of high-density gradients on wildland fire behavior in coupled atmosphere-fire simulations, *Journal of Advances in Modeling Earth Systems*, **14**, e2021MS002955.

[CE114] L. Crespo, A. Prigent, N. Keenlyside, S. Koseki, L. Svendsen, I. Richter, and E. Sanchez-Gomez, (2022), Weakening of the Atlantic Niño variability under global warming, *Nature Climate Change*, **12**, 822–827.

[CE115] T. Defontaine, S. Ricci, C. Lapeyre, A. Marchandise, and E. Le Pape, (2023), Flood forecasting with Machine Learning in a scarce data layout, *IOP Conference Series: Earth and Environmental Science*, **1136**.

[CE116] S. Delhaye, T. Fichefet, F. Massonnet, D. Docquier, R. Msadek, S. Chripko, C. Roberts, S. Keeley, and R. Senan, (2022), Summertime changes in climate extremes over the peripheral Arctic regions after a sudden sea ice retreat, *Weather and Climate Dynamics*, **3**, 555–573.

[CE117] S. Delhaye, F. Massonnet, T. Fichefet, R. Msadek, L. Terray, and J. Screen, (2023), Dominant role of early winter Barents–Kara sea ice extent anomalies in subsequent atmospheric circulation changes in CMIP6 models, *Climate Dynamics*.

[CE118] B. Dewitte, E. Concha, D. Saavedra, O. Pizarro, C. Martinez-Villalobos, D. Gushchina, M. Ramos, and A. Montecinos, (2023), The ENSO-induced South Pacific Meridional Mode, *Frontiers in Climate*, **4**, Article number 1080978.

[CE119] E. Diaz-Cabrera, C. Vega-Retter, N. Rojas-Hernandez, E. Meerhoff, B. Dewitte, and D. Veliz, (2023), Integrating genetic and biophysical approaches to estimate connectivity in an isolated, insular system: case of the culturally important marine gastropod Monetaria caputdraconis, *Journal of the Marine Biological Association of the United Kingdom*, **103**, e53.

[CE120] M. Duvallet, P. Dumas, D. Makowski, J. Boé, P. Mendez del Villar, and T. Ben-Ari, (2021), Rice yield stability compared to major food crops in West Africa, *Environmental Research Letters*, **16**, 124005.

[CE121] M. El Aabaribaoune, E. Emili, and V. Guidard, (2021), Estimation of the error covariance matrix for IASI radiances and its impact on the assimilation of ozone in a chemistry transport model, *Atmospheric Measurement Techniques*, **14**, 2841–2856.

[CE122] S. El Garroussi, S. Ricci, M. De Lozzo, N. Goutal, and D. Lucor, (2021), Tackling random fields non-linearities with unsupervised clustering of polynomial chaos expansion in latent space: application to global sensitivity analysis of river flooding, *Stochastic Environmental Research and Risk Assessment*, **35**, 1–26.

[CE123] E. Emili and M. El Aabaribaoune, (2021), Impact of Infrared Atmospheric Sounding Interferometer (IASI) thermal infrared measurements on global ozone reanalyses, *Geoscientific Model Development*, **14**, 6291–6308.

[CE124] G. Escobar-Franco, J. Boucharel, and B. Dewitte, (2022), On the Relationship Between Tropical Instability Waves and Intraseasonal Equatorial Kelvin Waves in the Pacific From Satellite Observations (1993–2018), *Frontiers in Marine Science*, **9**, 788908.

[CE125] R. Fablet, B. Chapron, L. Drumetz, E. Mémin, O. Pannekoucke, and F. Rousseau, (2021), Learning variational data assimilation models and solvers, *Journal of Advances in Modeling Earth Systems*, **13**, e2021MS002572.

[CE126] B. Ferster, L. Borchert, J. Mignot, M. Menary, C. Cassou, and A. Fedorov, (2023), Pantropical Indo-Atlantic temperature gradient modulates multi-decadal AMOC variability in models and observations, *npj Climate and Atmospheric Science*, **6**, Article number 165.

[CE127] A.-S. Fortin, C. Dufour, T. Merlis, and R. Msadek, (2023), Geostrophic and Mesoscale Eddy Contributions to the Atlantic Meridional Overturning Circulation Decline Under CO2 Increase in the GFDL CM2-O Model Suite, *Journal of Climate*, **36**, 6481–6498.

[CE128] V. Gallardo-Fernandez, E. Sanchez-Gomez, E. Riber, J. Boé, and L. Terray, (2023), Evolution of high-temperature extremes over the main Euro-Mediterranean airports, *Climate Dynamics*, **61**, 1717–1740.

[CE129] M. Grégoire, V. Garcon, H. Garcia, D. Breitburg, K. Isensee, A. Oschlies, M. Telszewski, A. Barth, H. Bittig, J. Carstensen, T. Carval, F. Chei, F. Chavez, D. Conley, L. Coppola, S. Crowe, K. Currie, M. Dai, B. Deflandre, B. Dewitte, R. Diaz, E. Garcia-Robledo, D. Gilbert, A. Giorgetti, R. Glud, D. Gutierrez, S. Hosoda, M. Ishii, G. Jacinto, C. Langdon, S. Lauvset, L. Levin, K. Limburg, H. Mehrtens, I. Montes, W. Naqvi, A. Paulmier, B. Pfeil, G. Pitcher, S. Pouliquen, N. Rabalais, C. Rabouille, V. Recape, M. Roman, K. Rose, D. Rudnick, J. Rummer, C. Schmechtig, S. Schmidtko, B. Seibel, C. Slomp, U. Rashid Sumalia, T. Tanhua, V. Thierry, H. Uchida, R. Wanninkhof, and M. Yasuhara, (2021), A Global Ocean Oxygen Database and Atlas for Assessing and Predicting Deoxygenation and Ocean Health in the Open and Coastal Ocean, *Frontiers in Marine Science*, **8**, 724913.

[CE130] M. Hariadi, G. van der Schrier, G.-J. Steeneveld, A. Sopaheluwakan, A. Tank, M. Roberts, M.-P. Moine, A. Bellucci, R. Senan, E. Tourigny, and D. Putrasahan, (2022), Evaluation of onset, cessation and seasonal precipitation of the Southeast Asia rainy season in CMIP5 regional climate models and HighResMIP global climate models, *International Journal of Climatology*, **42**, 3007–3024.

[CE131] M. Hariadi, G. van der Schrier, G.-J. Steeneveld, D. Nur Ratri, A. Sopaheluwakan, A. Tank, E. Aldrian, D. Gunawan, M.-P. Moine, A. Bellucci, R. Senan, E. Tourigny, D. Putrasahan, and U. Linarka, (2023), Evaluation of extreme precipitation over Southeast Asia in the Coupled Model Intercomparison Project Phase 5 regional climate model results and HighResMIP global climate models, *International Journal of Climatology*, **43**, 1639–1659.

[CE132] D. Hodson, P. Bretonnière, C. Cassou, P. Davini, N. Klingaman, K. Lohmann, J. Lopez-Parages, M. Martin-Rey, M.-P. Moine, P. Monerie, D. Putrasahan, C. Roberts, J. Robson, Y. Ruprich-Robert, E. Sanchez-Gomez, J. Seddon, and R. Senan, (2022), Coupled climate response to Atlantic Multidecadal Variability in a multi-model multi-resolution ensemble, *Climate Dynamics*, **59**, 805–836.

[CE133] D. Hodson, P. Bretonnière, C. Cassou, P. Davini, N. Klingaman, K. Lohmann, J. Lopez-Parages, M. Martin-Rey, M.-P. Moine, P. Monerie, D. Putrasahan, C. Roberts, J. Robson, Y. Ruprich-Robert, E. Sanchez-Gomez, J. Seddon, and R. Senan, (2023), Correction to: Coupled climate response to Atlantic Multidecadal Variability in a multi-model multi-resolution ensemble (Climate Dynamics, (2022), 59, 3-4, (805-836), 10.1007/s00382-022-06157-9), *Climate Dynamics*, **60**, Pages 4185.

[CE134] G. Irrmann, S. Masson, E. Maisonnave, D. Guibert, and E. Raffin, (2022), Improving ocean modeling software NEMO 4.0 benchmarking and communication efficiency, *Geoscientific Model Development*, **15**, 1567–1582.

[CE135] R. Isphording, L. Alexander, M. Bador, D. Green, and J. Evans, (2023), A Standardized Benchmarking Framework to Assess Downscaled Precipitation Simulations, *Journal of Climate*.

[CE136] C. Jones, J. Hickman, S. Rumbold, J. Walton, R. Lamboll, R. Skeie, S. Fiedler, P. Forster, J. Rogelj, M. Abe, M. Botzet, K. Calvin, C. Cassou, J. Cole, P. Davini, M. Deushi, M. Dix, J. Fyfe, N. Gillett, T. Ilyina, M. Kawamiya, M. Kelley, S. Kharin, T. Koshiro, H. Li, C. Mackallah, W. Muller, P. Nabat, T. Van Noije, P. Nolan, R. Ohgaito, D. Olivie, N. Oshima, J. Parodi, T. Reerink, L. Ren, A. Romanou, R. Séférian, Y. Tang, C. Timmreck, J. Tjiputra, E. Tourigny, K. Tsigaridis, H. Wang, M. Wu, K. Wyser, S. Yang, Y. Yang, and T. Ziehn, (2021), The Climate Response to Emissions Reductions Due to COVID-19: Initial Results From CovidMIP, *Geophysical Research Letters*, **48**, e2020GL091883.

[CE137] P. Kreussler, L. Caron, S. Wild, S. Loosveldt Tomas, F. Chauvin, M.-P. Moine, M. Roberts, Y. Ruprich-Robert, J. Seddon, S. Valcke, B. Vannière, and P. Vidale, (2021), Tropical Cyclone Integrated Kinetic Energy in an Ensemble of HighResMIP Simulations, *Geophysical Research Letters*, **48**, e2020GL090963.

[CE138] P. Linford, I. Pérez-Santos, I. Montes, B. Dewitte, S. Buchan, D. Narvaez, G. Saldias, E. Pinilla, R. Garreaud, P. Diaz, C. Schwerter, P. Montero, C. Rodriguez-Villegas, M. Caceres-Soto, G. Mancilla-Gutierrez, and R. Altamirano, (2023), Recent Deoxygenation of Patagonian Fjord Subsurface Waters Connected to the Peru–Chile Undercurrent and Equatorial Subsurface Water Variability, *Global Biogeochemical Cycles*, **37**, e2022GB007688.

[CE139] W. Llovel, N. Kolodziejczyk, S. Close, T. Penduff, J. Molines, and L. Terray, (2022), Imprint of intrinsic ocean variability in decadal regional sea level and ocean heat content trends using synthetic profiles, *Environmental Research Letters*, **17**, 044063.

[CE140] J. Lopez-Parages and L. Terray, (2022), Tropical North Atlantic Response to ENSO: Sensitivity to Model Spatial Resolution, *Journal of Climate*, **35**, 3–16.

[CE141] O. Marti, S. Nguyen, P. Braconnot, S. Valcke, F. Lemarié, and E. Blayo, (2021), A Schwarz iterative method to evaluate ocean–atmosphere coupling schemes: implementation and diagnostics in IPSL-CM6-SW-VLR, *Geoscientific Model Development*, **14**, 2959–2975.

[CE142] V. Martin-Gomez, E. Mohino, B. Rodrìguez-Fonseca, and E. Sanchez-Gomez, (2022), Understanding rainfall prediction skill over the Sahel in NMME seasonal forecast, *Climate Dynamics*, **59**, 3113–3133.

[CE143] S. McGregor, C. Cassou, Y. Kosaka, and A. Phillips, (2022), Projected ENSO Teleconnection Changes in CMIP6, *Geophysical Research Letters*, **49**, e2021GL097511.

[CE144] I. Mirouze and S. Ricci, (2021), Smurf: System for Modelling with Uncertainty Reduction, and Forecasting, *Journal of Open Research Software*, **9**, 2.

[CE145] E. Moreno-Chamarro, L. Caron, S. Loosveldt Tomas, J. Vegas-Regidor, O. Gutjahr, M.-P. Moine, D. Putrasahan, C. Roberts, M. Roberts, R. Senan, L. Terray, E. Tourigny, and P. Vidale, (2022), Impact of increased resolution on long-standing biases in HighResMIP-PRIMAVERA climate models, *Geoscientific Model Development*, **15**, 269–289.

[CE146] R.-S. Mouradi, C. Goeury, O. Thual, F. Zaoui, and P. Tassi, (2021), Physically interpretable machine learning algorithm on multidimensional non-linear fields, *Journal of Computational Physics*, **428**, 1–34.

[CE147] P. Munoz, A. Castillo, J. Valdes, and B. Dewitte, (2023), Oxidative conditions along the continental shelf of the Southeast Pacific during the last two millennia: a multiproxy interpretation of the oxygen minimum zone variability from sedimentary records, *Frontiers in Marine Science*, **10**.

[CE148] R. Ménard, S. Skachko, and O. Pannekoucke, (2021), Numerical discretization causing error variance loss and the need for inflation, *Quarterly Journal of the Royal Meteorological Society*, **147**, 3498–3520.

[CE149] P. Nguyen, M. Bador, L. Alexander, and T. Lane, (2023), Selecting regional climate models based on their skill could give more credible precipitation projections over the complex Southeast Asia region, *Climate Dynamics*, **61**, 3431–3452.

[CE150] P. Nguyen, M. Bador, L. Alexander, P. Todd, and T. Ngo-Duc, (2022), More intense daily precipitation in CORDEX-SEA regional climate models than their forcing global climate models over Southeast Asia, *International Journal of Climatology*, 6537–6561.

[CE151] T.-H. Nguyen, S. Ricci, C. Fatras, A. Piacentini, A. Delmotte, E. Lavergne, and P. Kettig, (2022), Improvement of Flood Extent Representation with Remote Sensing Data and Data Assimilation, *IEEE Transactions on Geoscience and Remote Sensing*, **60**, 1–22.

[CE152] T.-H. Nguyen, S. Ricci, A. Piacentini, C. Fatras, P. Kettig, G. Blanchet, S. Peña-Luque, and S. Baillarin, (2022), Dual State-Parameter Assimilation of SAR-Derived Wet Surface Ratio for Improving Fluvial Flood Reanalysis, *Water Resources Research*, **58**, e2022WR033155.

[CE153] T.-H. Nguyen, S. Ricci, A. Piacentini, E. Simon, R. Rodriguez Suquet, and S. Pena Luque, (2023), Gaussian Anamorphosis for Ensemble Kalman Filter Analysis of SAR-Derived Wet Surface Ratio Observations, *IEEE Transactions on Geoscience and Remote Sensing*, **62**.

[CE154] B. Nony, M. Rochoux, T. Jaravel, and D. Lucor, (2023), Reduced-order modeling for parameterized large-eddy simulations of atmospheric pollutant dispersion, *Stochastic Environmental Research and Risk Assessment*, **37**, 2117–2144.

[CE155] O. Pannekoucke and P. Arbogast, (2021), SymPKF (v1.0): a symbolic and computational toolbox for the design of parametric Kalman filter dynamics, *Geoscientific Model Development*, **14**, 5957–5976.

[CE156] O. Pannekoucke, R. Ménard, M. El Aabaribaoune, and M. Plu, (2021), A methodology to obtain model-error covariances due to the discretization scheme from the parametric Kalman filter perspective, *Nonlinear Processes in Geophysics*, **28**, 1–22.

[CE157] O. Pannekoucke, (2021), An anisotropic formulation of the parametric Kalman filter assimilation, *Tellus Series A-Dynamic Meteorology and Oceanography*, **73**, 1–27.

[CE158] A. Parouffe, V. Garcon, B. Dewitte, A. Paulmier, I. Montes, C. Parada, A. Mecho, and D. Veliz, (2023), Evaluating future climate change exposure of marine habitat in the South East Pacific based on metabolic constraints, *Frontiers in Marine Science*, **9**, Article number 1055875.

[CE159] R. Paugam, M. Wooster, W. Mell, M. Rochoux, J.-B. Filippi, G. Rücker, O. Frauenberger, E. Lorenz, W. Schroeder, B. Main, and N. Govender, (2021), Orthorectification of helicopter-borne high resolution experimental burn observation from infra red handheld imagers, *Remote Sensing*, **13**, Article number 4913.

[CE160] A. Paulmier, G. Eldin, J. Ochoa, B. Dewitte, J. Sudre, V. Garcon, J. Grelet, K. Mosquera-Vasquez, O. Vergara, and H. Maske, (2021), High-Sustained Concentrations of Organisms at Very low Oxygen Concentration Indicated by Acoustic Profiles in the Oxygen Deficit Region Off Peru, *Frontiers in Marine Science*, **8**, 723056.

[CE161] S. Peatier, B. Sanderson, L. Terray, and R. Roehrig, (2022), Investigating Parametric Dependence of Climate Feedbacks in the Atmospheric Component of CNRM-CM6-1, *Geophysical Research Letters*, **49**, e2021GL095084.

[CE162] A. Perrot, O. Pannekoucke, and V. Guidard, (2023), Toward a multivariate formulation of the parametric Kalman filter assimilation: application to a simplified chemical transport model, *Nonlinear Processes in Geophysics*, **30**, 139–166.

[CE163] M. Pizarro-Koch, O. Pizarro, B. Dewitte, I. Montes, A. Paulmier, V. Garcon, H. Sepulveda, A. Corredor-Acosta, C. Aguirre, and M. Ramos, (2023), On the interpretation of changes in the subtropical oxygen minimum zone volume off Chile during two La Niña events (2001 and 2007), *Frontiers in Marine Science*, **10**.

[CE164] M. Plu, G. Bigeard, B. Sic, E. Emili, L. Bugliaro, L. El Amraoui, J. Guth, B. Josse, L. Mona, and D. Piontek, (2021), Modelling the volcanic ash plume from Eyjafjallajökull eruption (May 2010) over Europe: evaluation of the benefit of source term improvements and of the assimilation of aerosol measurements, *Natural Hazards and Earth System Sciences*, **21**, 3731–3747.

[CE165] S. Qasmi, E. Sanchez-Gomez, Y. Ruprich-Robert, J. Boé, and C. Cassou, (2021), Modulation of the Occurrence of Heatwaves over the Euro-Mediterranean Region by the Intensity of the Atlantic Multidecadal Variability, *Journal of Climate*, **34**, 1099–1114.

[CE166] M. Reale, W. Cabos Narvaez, L. Cavicchia, D. Conte, E. Coppola, E. Flaounas, F. Giorgi, S. Gualdi, A. Hochman, L. Li, P. Lionello, Z. Podrascanin, S. Salon, E. Sanchez-Gomez, E. Scoccimarro, D. Sein, and S. Somot, (2021), Future projections of Mediterranean cyclone characteristics using the Med-CORDEX ensemble of coupled regional climate system models, *Climate Dynamics*, **58**, 2501–2524.

[CE167] A. Ribes, J. Boé, S. Qasmi, B. Dubuisson, H. Douville, and L. Terray, (2022), An updated assessment of past and future warming over France based on a regional observational constraint, *Earth System Dynamics*, **13**, 1397–1415.

[CE168] V. Rousseau, E. Sanchez-Gomez, R. Msadek, and M.-P. Moine, (2021), Mechanisms shaping wind convergence under extreme synoptic situations over the gulf stream region, *Journal of Climate*, 1–53.

[CE169] P. Ruggieri, A. Bellucci, D. Nicoli, P. Athanasiadis, S. Gualdi, C. Cassou, F. Castruccio, G. Danabasoglu, P. Davini, N. Dunstone, R. Eade, G. Gastineau, B. Harvey, L. Hermanson, S. Qasmi, Y. Ruprich-Robert, E. Sanchez-Gomez, D. Smith, S. Wild, and M. zampieri, (2021), Atlantic Multidecadal Variability and North Atlantic Jet: a multi-model view from the Decadal Climate Prediction Project, *Journal of Climate*, **34**, 347–360.

[CE170] Y. Ruprich-Robert, E. Moreno-Chamarro, X. Levine, A. Bellucci, C. Cassou, F. Castruccio, P. Davini, R. Eade, G. Gastineau, L. Hermanson, D. Hodson, K. Lohmann, J. Lopez-Parages, P. Monerie, D. Nicoli, S. Qasmi, C. Roberts, E. Sanchez-Gomez, G. Danabasoglu, N. Dunstone, M. Martin-Rey, R. Msadek, J. Robson, and D. Smith, (2021), Impacts of Atlantic multidecadal variability on the tropical Pacific: a multi-model study, *npj Climate and Atmospheric Science*, **4**, Article number 33.

[CE171] M. Sabathier, O. Pannekoucke, V. Maget, and N. Dahmen, (2023), Boundary Conditions for the Parametric Kalman Filter Forecast, *Journal of Advances in Modeling Earth Systems*, **15**, e2022MS003462.

[CE172] M. Sadki, S. Munier, A. Boone, and S. Ricci, (2023), Implementation and sensitivity analysis of the Dam-Reservoir OPeration model (DROP v1.0) over Spain, *Geoscientific Model Development*, **16**, 427–448.

[CE173] D. Saint-Martin, O. Geoffroy, A. Voldoire, J. Cattiaux, F. Brient, F. Chauvin, M. Chevalier, J. Colin, B. Decharme, C. Delire, H. Douville, F. Guérémy, E. Joetzjer, A. Ribes, R. Roehrig, L. Terray, and S. Valcke, (2021), Tracking Changes in Climate Sensitivity in CNRM Climate Models, *Journal of Advances in Modeling Earth Systems*, **13**, e2020MS002190.

[CE174] B. Schauberger, D. Makowski, T. Ben-Ari, J. Boé, and P. Ciais, (2021), No historical evidence for increased vulnerability of French crop production to climatic hazards, *Agricultural and Forest Meteorology*, **306**, 108453.

[CE175] R. Small, V. Rousseau, R. Parfitt, L. Laurindo, L. O´Neill, R. Masunaga, N. Schneider, and P. Chang, (2023), Near-Surface Wind Convergence over the Gulf Stream—The Role of SST Revisited, *Journal of Climate*, **36**, 5527–5548.

[CE176] D. Smith, R. Eade, M. Andrews, H. Ayres, A. Clark, S. Chripko, C. Deser, N. Dunstone, J. Garcia-Serrano, G. Gastineau, L. Graff, S. Hardiman, B. He, L. Hermanson, T. Jung, P. Knight, J. Knight, X. Levine, G. Magnusdottir, E. Manzini, D. Matei, M. Mori, R. Msadek, P. Ortega, Y. Peings, A. Scaife, J. Screen, M. Seabrook, T. Semmler, M. Sigmond, J. Streffing, L. Sun, and A. Walsh, (2022), Robust but weak winter atmospheric circulation response to future Arctic sea ice loss, *Nature Communications*, **13**, article number 727.

[CE177] F. Sudre, B. Dewitte, C. Mazoyer, V. Garcon, J. Sudre, and P. Penven, (2023), Spatial and seasonal variability of horizontal temperature fronts in the Mozambique Channel for both epipelagic and mesopelagic realms, *Frontiers in Marine Science*, **9**.

[CE178] A. Sylla, E. Sanchez-Gomez, J. Mignot, and J. Lopez-Parages, (2022), Impact of increased resolution on the representation of the Canary upwelling system in climate models, *Geoscientific Model Development*, **15**, 8245–8267.

[CE179] I. Taranu, S. Somot, A. Alias, J. Boé, and C. Delire, (2023), Mechanisms behind large-scale inconsistencies between regional and global climate model-based projections over Europe, *Climate Dynamics*, **60**, 3813–3838.

[CE180] L. Terray, (2021), A dynamical adjustment perspective on extreme event attribution, *Weather and Climate Dynamics*, **2**, 971–989.

[CE181] L. Terray, (2023), A Storyline Approach to the June 2021 Northwestern North American Heatwave, *Geophysical Research Letters*, **50**, e2022GL101640.

[CE182] S. Thual and B. Dewitte, (2023), ENSO complexity controlled by zonal shifts in the walker circulation, *Nature Geoscience*, **16**, 328–332.

[CE183] A.-L. Tiberi, N. Goutal, S. Ricci, P. Sergent, M. Taillardat, F. Bouttier, and C. Monteil, (2021), Strategies for hydrologic ensemble generation and calibration: On the merits of using model-based predictors, *Journal of Hydrology*, **599**.

[CE184] A.-L. Tiberi, N. Goutal, S. Ricci, P. Sergent, J. Viatgé, C. Monteil, and F. Bouttier, (2022), Etude de sensibilité globale comparée des modèles hydrologiques GRP et MORDOR-TS Comparative global sensitivity analysis on the hydrologic models GRP and MORDOR-TS, *La Houille Blanche*, **107**, 1–11.

[CE185] E. Tsartsali, R. Haarsma, P. Athanasiadis, A. Bellucci, H. de Vries, S. Drijfhout, I. de Vries, D. Putrahasan, M. Roberts, E. Sanchez-Gomez, and C. Roberts, (2022), Impact of resolution on the atmosphere–ocean coupling along the Gulf Stream in global high resolution models, *Climate Dynamics*, **58**, 3317–3333.

[CE186] S. Valcke, A. Piacentini, and G. Jonville, (2022), Benchmarking Regridding Libraries Used in Earth System Modelling, *Mathematical and Computational Applications*, **27**, article number 31.

[CE187] S. Valcke, (2021), Highlights from a workshop on the latest updates on coupling technologies and coupled applications in Earth System modelling, *Bulletin of the American Meteorological Society*, 1–15.

[CE188] R. Vautard, J. Cattiaux, T. Happé, J. Singh, R. Bonnet, C. Cassou, D. Coumou, F. D´ Andréa, D. Faranda, E. Fischer, A. Ribes, S. Sippel, and P. Yiou, (2023), Heat extremes in Western Europe increasing faster than simulated due to atmospheric circulation trends, *Nature Communications*, **14**, Article number 6803.

[CE189] D. Veliz, N. Rojas-Hernandez, P. Fibla, S. Cornejo-Guzman, C. Parada, and B. Dewitte, (2021), High levels of connectivity over large distances in the diadematid sea urchin Centrostephanus sylviae, *PLoS One*, **16**, e0259595.

[CE190] M. Wade, B. Rodriguez de Fonseca, M. Martin-Rey, A. Lazar, J. Lopez-Parages, and A. Gaye, (2023), Interdecadal changes in SST variability drivers in the Senegalese-upwelling: the impact of ENSO, *Climate Dynamics*, **60**, 667–685.

[CE191] R. Waldman, J. Hirschi, A. Voldoire, C. Cassou, and R. Msadek, (2021), Clarifying the relation between AMOC and thermal wind: application to the centennial variability in a coupled climate model, *Journal of Physical Oceanography*, **51**, 343–364.

[CE192] A. Walker, A. Johnson, A. Rogers, J. Anderson, R. Bridges, R. Fisher, D. Lu, D. Ricciuto, S. Serbin, and M. Ye, (2021), Multi hypothesis comparison of Farquhar and Collatz photosynthesis models reveals the unexpected influence of empirical assumptions at leaf and global scales, *Global Change Biology*, **27**, 804–822.

5.5 Technical Reports

[CE193] B. Andela, J. Bedia, R. Kazeroni, A. Cofino, C. Pagé, D. San Martin, S. Sénési, J. Servonnat, A. Spinuso, M. Veldhuizen, and K. Zimmermann, (2021), IS-ENES3 White Paper on provenance handling in the model evaluation process (Version 1), technical report, CECI, Université de Toulouse, CNRS, CERFACS, Toulouse, France - TR-CMGC-21-234.

[CE194] Q. Bonassies, S. Ricci, S. Pena Luque, C. Fatras, A. Andral, R. Rodriguez Suquet, T.-H. Nguyen, and A. Piacentini, (2023), Compte rendu d'avancement 2023 - Contrat de recherche doctoral CNES, technical report, Cerfacs - CNES.

[CE195] L. Coquart, G. Dejean, F. Blain, and S. Valcke, (2022), Migration du site web d'OASIS3-MCT sous WordPress au CECI-Cerfacs, technical report, CECI, Université de Toulouse, CNRS, CERFACS, Toulouse, France - TR-CMGC-22-91.

[CE196] L. Coquart, S. Valcke, and A. Craig, (2023), New modular compiling and testing environment for OASIS3-MCT, technical report, CECI, Université de Toulouse, CNRS, CERFACS, Toulouse, France - TR-CMGC-23-175.

[CE197] L. Coquart, S. Valcke, A. Craig, and E. Maisonnave, (2021), New Buildbot test suite for the OASIS3-MCT coupler Fortran source code, technical report, CECI, Université de Toulouse, CNRS, CERFACS, Toulouse, France, TR-CMGC-21-36.

[CE198] G. Dejean and F. Blain, (2022), Site Web OASIS3-MCT / Fonctionnement des modules Download, Forum et Sondages, technical report, Cerfacs.

[CE199] A. Delmotte, S. Ricci, T.-H. Nguyen, A. Piacentini, and P. Kettig, (2021), Rapport de Stage ENM: Apport de la donnée spatiale pour la prévision des crues et des inondations, technical report, CECI, Université de Toulouse, CNRS, CERFACS, Toulouse, France, TR-CMGC-21-106.

[CE200] C. Emery, S. Ricci, and A. Piacentini, (2021), ToolBox SWOT User's Guide, technical report, CECI, Université de Toulouse, CNRS, CERFACS, Toulouse, France - TR-CMGC-21-153.

[CE201] E. Emili, (2023), Tests and evaluation of 4DEnVar assimilation with synthetic and real observations and comparison with 3D-Var - Work Package 4 - D4.3/4.4: Report, technical report, CECI, Université de Toulouse, CNRS, CERFACS, Toulouse, France - TR-CMGC-23-73.

[CE202] C. Février, (2022), Etude de l'évolution du risque d'occurence de givrage dans la période observée, technical report, CECI, Université de Toulouse, CNRS, CERFACS, Toulouse, France - TR-CMGC-22-183.

[CE203] P. Gambron, R. Ford, A. Piacentini, and S. Valcke, (2021), pyOASIS - a python and C interface for OASIS3-MCT, technical report, CECI, Université de Toulouse, CNRS, CERFACS, Toulouse, France, TR-CMGC-21-56.

[CE204] E. Maisonnave and S. Berthet, (2022), Biogeochemistry coarsening in NEMO 4.2, technical report, CECI, Université de Toulouse, CNRS, CERFACS, Toulouse, France - TR-CMGC-22-86.

[CE205] E. Maisonnave and R. Bourdallé-Badie, (2022), Coupling NEMO global ocean with hemispheric Arctic and Antarctic ice models, technical report, CECI, Université de Toulouse, CNRS, CERFACS, Toulouse, France - Mercator-Océan International - TR-CMGC-22-18.

[CE206] E. Maisonnave and I. d'Ast, (2021), Energy consumption of the NEMO ocean model measured with the Energy Scope tool, working note, CECI, Université de Toulouse, CNRS, CERFACS, Toulouse, France - WN-CMGC-21-88.

[CE207] E. Maisonnave and J. Kjellsson, (2021), OASIS Dedicated Support 5th annual summary, technical report, CECI, Université de Toulouse, CNRS, CERFACS, Toulouse, France - TR-CMGC-21-150.

[CE208] E. Maisonnave, S. Berthet, and R. Séférian, (2021), OASIS based grid coarsening of TOP-PISCES biogeochemistry in the NEMO ocean model: performance, technical report, CECI, Université de Toulouse, CNRS, CERFACS, Toulouse, France - TR-CMGC-21-201.

[CE209] E. Maisonnave, (2021), Comment interpoler des flux atmosphériques vers un zoom AGRIF ? Le cas des grilles ECHAM et OpenIFS, technical report, CECI, Université de Toulouse, CNRS, CERFACS, Toulouse, France - TR-CMGC-21-200.

[CE210] E. Maisonnave, (2021), NEMO performance optimisation on NEC SX-Aurora TSUBASA, working note, CECI, Université de Toulouse, CNRS, CERFACS, Toulouse, France - WN-CMGC-21-37.

[CE211] E. Maisonnave, (2022), A climate community coupler: OASIS, working note, CECI, Université de Toulouse, CNRS, CERFACS, Toulouse, France - WN-CMGC-22-168.

[CE212] E. Maisonnave, (2022), NEMO performance on pre-Exascale processors : NEC SX-Aurora TSUBASA and Fujitsu PRIMEHPC FX700, working note, CECI, Université de Toulouse, CNRS, CERFACS, Toulouse, France - WN-CMGC-22-22.

[CE213] E. Maisonnave, (2022), OASIS Dedicated Support, 6th annual summary, technical report, CECI, Université de Toulouse, CNRS, CERFACS, Toulouse, France - TR-CMGC-22-139.

[CE214] E. Maisonnave, (2023), Frugal computations with NEMO latest versions on a NEC vector platform, working note, CECI, Université de Toulouse, CNRS, CERFACS, Toulouse, France - WN-CMGC-23-17.

[CE215] E. Maisonnave, (2023), Is the YAXT communication library as portable as the OASIS community coupler ?, working note, CECI, Université de Toulouse, CNRS, CERFACS, Toulouse, France - WN-CMGC-23-177.

[CE216] E. Maisonnave, (2023), NEMO/neXtSIM-DG preliminary coupling interface, working note, CECI, Université de Toulouse, CNRS, CERFACS, Toulouse, France - WN-CMGC-23-58.

[CE217] C. Pagé, K. Zimmermann, A. Aoun, M. Veldhuizen, A. Spinuso, I. van der Neut, and F. Striewski, (2021), An Interactive Platform for Climate Analysis using a Climate Indices Tool, technical report, CECI, Université de Toulouse, CNRS, CERFACS, Toulouse, France, TR-CMGC-21-235.

[CE218] M. Rochoux, E. Lumet, L. Thouron, G. Rea, F. Auguste, T. Jaravel, and O. Vermorel, (2021), Large-eddy simulation multi-model comparison of the MUST trial 2681829, technical report, CECI, Université de Toulouse, CNRS, CERFACS, Toulouse, France, TR-CMGC-21-72.

[CE219] B. Roiron, S. Ricci, V. Gallardo-Fernandez, E. Sanchez-Gomez, and N. Gourdain, (2021), L'impact du réchauffement climatique sur le décollage d'un avion - Stage 2020, technical report, CECI, Université de Toulouse, CNRS, CERFACS, Toulouse, France, TR-CMGC-21-34.

[CE220] A. Spinuso, W. Som de Cerff, P. Nassisi, and C. Pagé, (2021), First release of the ENES CDI software stack (D10.2), technical report, CECI, Université de Toulouse, CNRS, CERFACS, Toulouse, France, TR-CMGC-21-233.

[CE221] S. Valcke and G. Jonville, (2023), OASIS3-MCT regrid_environment, technical report, CECI, Université de Toulouse, CNRS, CERFACS, Toulouse, France - TR-CMGC-23-93.

[CE222] S. Valcke and A. Piacentini, (2022), Analysis and refactoring of the coupling grids generation procedure in NEMO 3.6, technical report, CECI, Université de Toulouse, CNRS, CERFACS, Toulouse, France - TR-CMGC-22-159.

[CE223] S. Valcke, L. Coquart, A. Craig, G. Jonville, and A. Piacentini, (2023), 2023 OASIS3-MCT Evolution Plan, technical report, CECI, Université de Toulouse, CNRS, CERFACS, Toulouse, France - TR-CMGC-23-95.

[CE224] S. Valcke, A. Craig, E. Maisonnave, and L. Coquart, (2021), OASIS3-MCT User Guide, OASIS3-MCT 5.0, technical report, CECI, Université de Toulouse, CNRS, CERFACS, Toulouse, France - TR-CMGC-21-161.

[CE225] S. Valcke, A. Piacentini, and G. Jonville, (2021), Benchmarking of regridding libraries used in Earth System Modelling SCRIP, YAC, ESMF and XIOS, technical report, CECI, Université de Toulouse, CNRS, CERFACS, Toulouse, France - TR-CMGC-21-145.

[CE226] S. Valcke, (2021), Schwarz iterations for ocean-atmosphere interface coherency in CNRM-CM6-1D, technical report, CECI, Université de Toulouse, CNRS, CERFACS, Toulouse, France - TR-CMGC-21-81.

[CE227] S. Valcke, (2022), Mise à jour de CNRM-CM6-1-LR avec OASIS3-MCT_5.0, technical report, CECI, Université de Toulouse, CNRS, CERFACS, Toulouse, France - TR-CMGC-22-88.

5.6 Thesis

[CE228] E. Barrela, (2023), *Calibration des hétérogénéités géologiques basée sur les données de production des fluides issus de réservoirs souterrains*, phd thesis, INPT- Cerfacs.

[CE229] A. Costes, (2021), *Couplage bidirectionnel feu-atmosphère pour la propagation des incendies de forêt : modélisation, incertitudes et sensibilités*, phd thesis, Université Toulouse 3 Paul Sabatier -SDU2E: Océan, Atmosphère, Climat.

[CE230] M. El Aabaribaoune, (2022), *Assimilation des luminances IASI dans un modèle de chimie transport pour la surveillance de l'ozone et des poussières désertiques*, phd thesis, Université de Toulouse 3 -Sciences de l´Univers, de l´Environnement et de l´Espace.

[CE231] G. Escobar-Franco, (2023), *Interactions between Kelvin and tropical instability waves in the equatorial pacific ocean*, phd thesis, Université de Toulouse 3 - SDU2E: Océan, Atmosphère, Climat.

[CE232] V. Gallardo-Fernandez, (2023), *Impacts of increasing high-temperature extremes on aircraft takeoff performance over the Euro-Mediterranean region*, phd thesis, Université de Toulouse 3 - SDU2E: Océan, Atmosphère, Climat.

[CE233] A. Liné, (2023), *Modulation du changement climatique européen à court terme par la variabilité interne multi-décennale*, phd thesis, INPT- Cerfacs.

[CE234] R.-S. Mouradi, (2021), *Non-linear data-driven modelling on multidimensional fields: an application to hydro-morphodynamic coastal flows*, phd thesis, I.N.P. Toulouse.

[CE235] B. Nony, (2023), *Modèles réduits en présence d´incertitudes pour la dispersion atmosphérique micro-échelle de polluant en milieu urbain : exploration de méthodes d´apprentissage pour l´émulation de modèles haute-fidélité*, phd thesis, Université de Toulouse 3 -Sciences de l´Univers, de l´Environnement et de l´Espace.

[CE236] S. Peatier, (2022), *Explorer l'incertitude des rétroactions climatiques à partir d'un ensemble de simulations atmosphériques avec perturbation des paramètres*, phd thesis, Université de Toulouse 3 -Sciences de l´Univers, de l´Environnement et de l´Espace.

[CE237] A.-L. Tiberi, (2021), *Prévisions d´ensemble hydrologiques et hydrauliques pour la vigilance crues*, phd thesis, Université Paris-EST.

3

Computational Fluid Dynamics

Introduction

The CFD team is the largest team at CERFACS. It is composed of around 80 members at the end of 2023 with 14 permanents, 45 PhD's and the remaining of Post-Docs and engineers. The team's activity can be split into three main parts as it is presented in this document:

- *Numerical methods* to solve partial differential equations, particularly those associated with Navier-Stokes or Boltzmann equations. Different approaches are used ranging from finite volume, discontinuous high-order method, and Lattice Boltzmann Method. These methods find applications in a variety of flow problems, whether they involve reacting or non-reacting systems.
- *Physical Models* to represent the physical processes. The team is particularly involved in the modelisation of turbulence, heat transfer, chemical reactions, and multiphase flows.
- *Applications* which feed new research topics to the team. Within this scope, applications encompass areas such as turbomachinery flows (aerodynamics, thermal flows, and aeroacoustics), combustion chambers, plasma-assisted propulsion, and explosions.

The following sections provide a summary of the most remarkable activities conducted since 2021. A few important points are mentioned here:

Academic excellence
The CFD team continues to publish in the best journals at a high rate. The number of papers published each year weighted by the number of permanent people is around 2 which is a typical ratio of CNRS laboratories in similar fields.

Year	Papers in A journals	PhD defended
2021	42	12
2022	30	14
2023	38	10

Table 1.1: Number of papers in rank A journals and PhD defended in the CFD team during the period

ERC and Synergy Grant
After the ERC (European Research Council) advanced grant INTECOCIS (2013-2018) in the field of thermoacoustics (https://intecocis.inp-toulouse.fr), the ERC advanced grant SIROCCO (2019-2024) in the field of hydrogen combustion (https://cerfacs.fr/scirocco/), CERFACS and IMFT have won a third ERC advanced grant: SELECT-H (Safe and Reliable Combustion Technologies powered by hydrogen) started in October 2023 for five years. It addresses challenges in hydrogen's high reactivity, focusing on fundamental combustion science, simulation tool development, and promoting the shift to hydrogen-powered systems. The initiative explores efficient hydrogen combustion in various applications and examines scenarios where combustion must be avoided, such as leaks. Through experiments and simulations, SELECT-H seeks to design safe and reliable hydrogen-powered units, contributing to a sustainable energy transition.
Moreover, the AVBP code of CERFACS will be used in the Synergy grant HYROPE (IMF Toulouse, ETH

Zurich, NTNU Trondheim, TU Darmstadt), accepted by the EU in October 2023 on new high-pressure sequential burners for low carbon power production.

Safety
Over the past three years, there has been substantial growth in the field of Computational Fluid Dynamics (CFD) for safety, prompting the establishment of a dedicated research unit within the CFD team. Safety computations within the team encompass a variety of scenarios, not only limited to combustion but extending into other domains as well. While numerous scenarios investigated at CERFACS involve the release of combustible gases into the air, the team also explores many other safety scenarios. One notable example is the dispersion of viruses, where AVBP can be directly applied. Another challenging area is the safety of batteries, where the occurrence of thermal runaway can trigger a sequence of events that require simulation.

New Fuels
One significant focus of the CFD group involves the exploration of novel fuels, specifically hydrogen (H2) and Sustainable Aviation Fuels (SAF). The advancement and integration of these fuels require the modification and enhancement of the AVBP solver. This thematic area holds great importance in the context of decarbonization efforts.
Considerable efforts have already been invested in enabling the utilization of AVBP within this framework. Specifically, the work has centered around accommodating turbulent combustion models and developing blends of fuel components. The goal is to refine and optimize the AVBP solver to accurately simulate the combustion characteristics associated with these alternative fuels.

New Numerical approaches for CFD
Multiple research groups are actively exploring novel numerical methods to solve the Navier-Stokes equations, and CERFACS is no exception. Within this context, CERFACS is engaged in the development and validation of Lattice Boltzmann Method and also high-order discontinuous techniques such as the Spectral Difference Method (SDM). This work is done in close collaboration with M2P2 in Marseille for the LBM part and ONERA for the SDM part. The ultimate goal is to compare all available methods (both standard and recent) to determine, for our shareholders, the most effective approaches (accuracy versus computational time) for a given application. It is unlikely that a single method will be the best for all applications.

Training
Currently, CERFACS provides two forms of training: (1) in-person sessions held in Toulouse and (2) SPOC sessions with online assistance. Among the SPOC sessions, three are specifically focused on Computational Fluid Dynamics (CFD), covering topics such as Lattice Boltzmann Method (LBM), thermoacoustics, and combustion. The SPOC approach enables us to expand our audience; for example, the recent ”combustion” session was highly appreciated with around 60 participants joining from various locations worldwide.

Numerics

2.1 Introduction

Numerics is at the root of CFD predictions as it dictates the way governing equations are resolved. It also impacts the code architecture as well as its efficiency and multiple strategies exist today. To ensure up-to-date capacities while taking advantage of the ever changing HPC environment, CERFACS continues to investigate, develop and test new numerical methods and algorithms. In the following, details around specific trends in the cell/vertex framework linked to AVBP, Spectral Difference (SD) methods linked to Jaguar or the Lattice Boltzman Method (LBM) are detailed.

2.2 AVBP Numerical Methods

This section highlights the work related to the AVBP solver. Developed over several years, this solver has proven its effectiveness across a wide spectrum of applications involving both reactive and non-reactive flows. It is based on the resolution of the Navier-Stokes equations, using Large Eddy Simulation (LES) for turbulence modeling, which leads to substantial computational demands.
There has been a continuous effort since the inception of AVBP to ensure its efficiency on massively parallel machines, and more recently, on GPUs. Concurrently, recent work has been focused on optimizing the numerical aspects. These efforts include the derivation and exploration of high-order schemes, the use of machine learning-based numerical methods, and the implementation of mesh adaptation techniques, as described in the subsequent sub-sections.

2.2.1 Towards High order and ML-based schemes for AVBP

Increased accuracy and/or robustness of legacy codes can be obtained through multiple strategies while benefiting from increased computing power. In the following, two approaches are detailed each resulting from a specific framework of research: *i.e.* the development of new numerical schemes in agreement with the high-order method framework and the use of Machine-Learning for numerics to investigate new and more robust methods.

First, the investment in high-order schemes is justified by the fact that such schemes provide higher robustness as demonstrated by the CN2020 project with SAFRAN. Indeed, these schemes although more computationally demanding provided solutions where standard methods could not converge due to mesh quality and irregularity. Based on this conclusion, CERFACS' CFD team investigated the capacity of extending AVBP's cell/vertex Taylor Galerkin schemes to build new sets of high-order schemes to preserve at least a third-order (or higher) accuracy in space irrespectively of mesh quality/regularity. As a result and in collaboration with Mike Rudgyard (original author of AVBP's TTGC scheme and code), Benjamin Martin's PhD work [CFD267] identified and derived a new set of schemes which were shown to meet the purpose, Fig. 2.1(a). For these schemes as well as for any high-order scheme, to make a difference in the long run, the added computing effort and efficiency of implementation need to be under control so additional costs can be justified. This is needed to guarantee their use and deployment in existing frameworks linked to legacy codes so end-users do use them. This last subject has been the purpose of

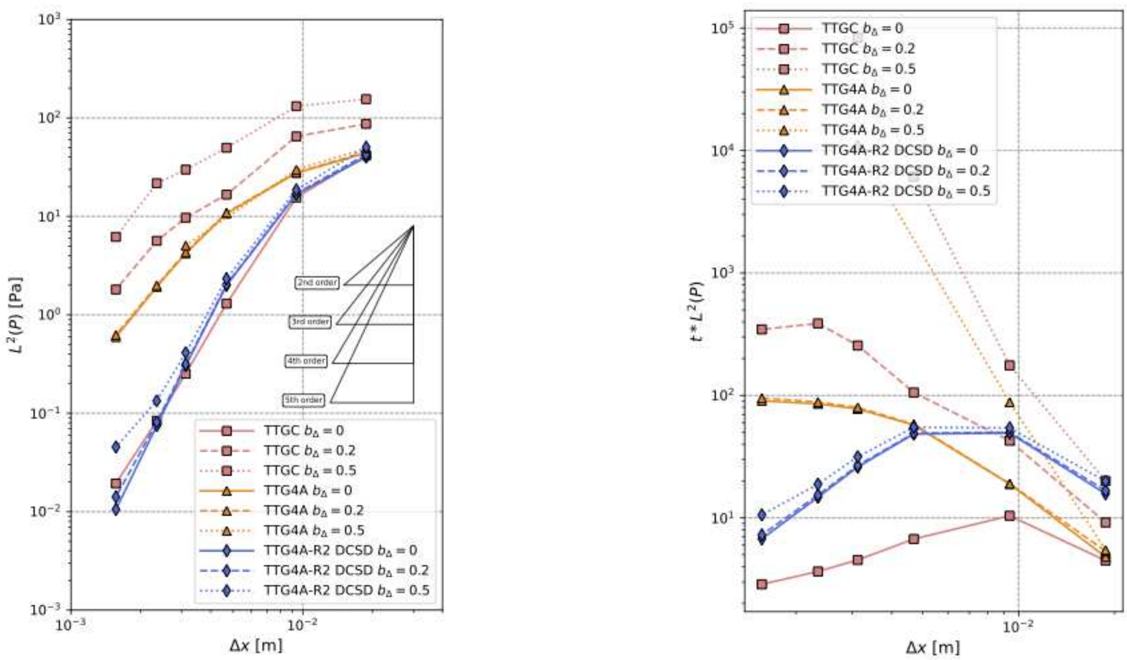

Figure 2.1: Comparisons of the newly developed high-order schemes for AVBP: (a) Order of convergence of existing and newly proposed high-order schemes for AVBP as a function of grid distortion. Here $b_\triangle$ stands for the mean edge cell relative variation: *i.e.* $b_\triangle = 0.2$ results in edge variation of 20% of the mean cell size present in the mesh; (b) Normalized computational effort/accuracy of the different schemes available within AVBP as a function of the cell mean grid size.

funding actions by CERFACS (CIR funding of a Post-doctorate fellow) as well as SAFRAN (though the funding of A. Boudin's PhD) and the support of CERFACS' industrial partners. As a result, different implementations of the previously identified high-order schemes have been proposed for testing in AVBP of non-reacting flows. This in-depth analysis allowed to considerably leverage initially identified costs of the new method as illustrated by Fig.2.1(b) where the error times the CPU effort associated for the investigated problem is provided as a function of the mean grid resolution is illustrated for various level of mesh perturbations/regularities.

Second, robustness can be guaranteed while going back to the fundamentals of numerical schemes: *i.e.* stability analysis. Typically, fundamental investigations of the numerical stability of Lax-Wendoroff scheme, used extensively in AVBP, were carried out in single as well as multi-dimensions, by including the effect of diffusion and reaction in the PhD thesis of Sengupta [CFD274] (funded by the LEFEX project). A summary of the findings was published in a journal article [CFD198]. The key insights from this work were then leveraged to build a novel local spectral error analysis called the Local Transfer Function Analysis (LTA). LTA reveals for the first time that local instabilities exist in TTGC scheme when the solution travels from a finer to the coarser region in irregular meshes and at a Burgers' shock. A fundamentally new path to designing numerical schemes using an impedance matching principle has hence emerged from the LTA. Results were obtained in the collaborative project with Braude University in Israel, funded by a dedicated France-Israel collaboration grant to work on constructing Machine Learned (ML) based TTGC schemes which guarantee both local and global stability. Such schemes have been successfully demonstrated to solve linear convection, Burgers' and compressible Euler equations on $1-/2-D$ regular and irregular

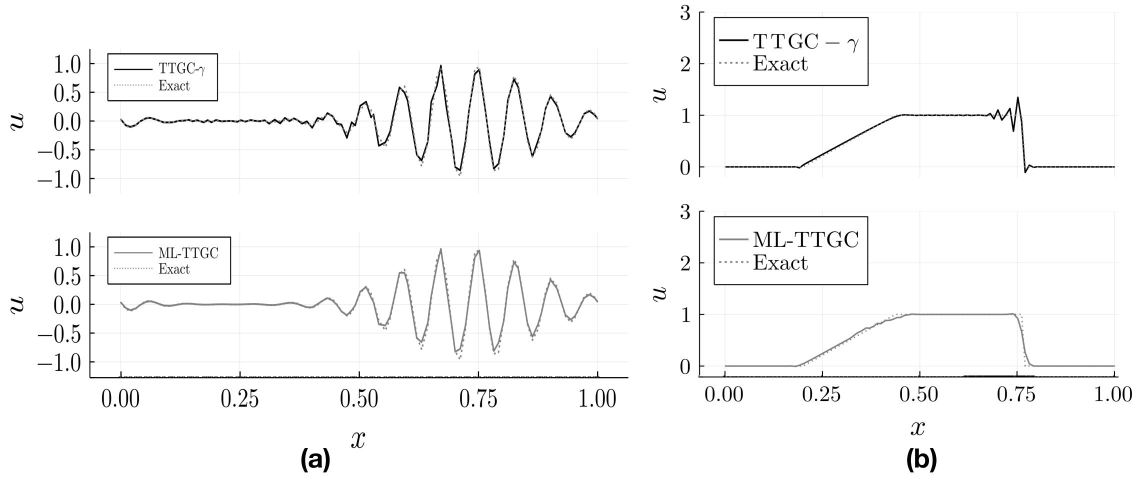

Figure 2.2: Comparison of numerical solution of ML-TTGC (machine-learned) and original TTGC scheme on an irregular mesh (randomly perturbed) for (a) linear convection of a wave packet with Nyquist wavenumber $kh = 0.8$ and (b) Burgers' solution to a square wave initial condition (with a Burgers' shock and an expansion wave).

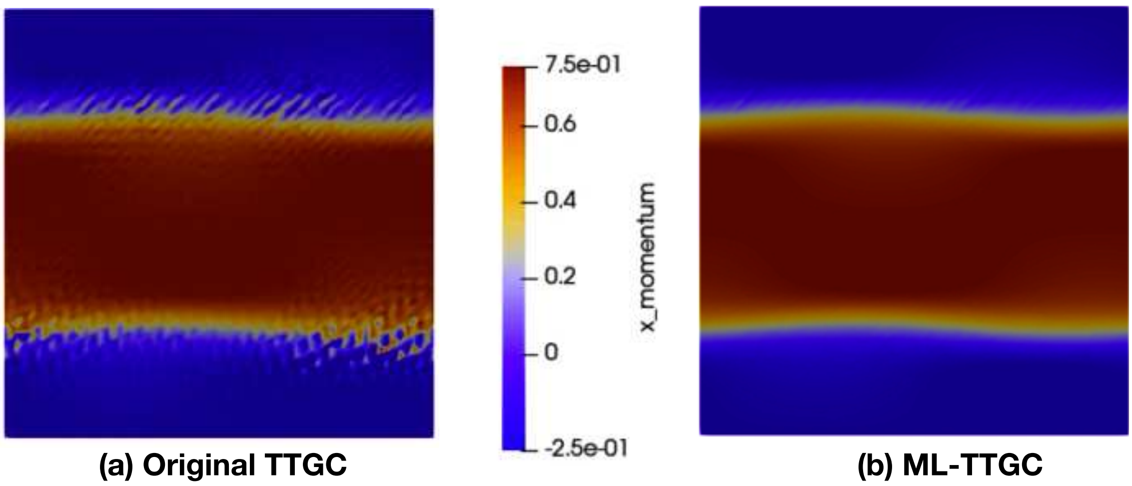

Figure 2.3: Comparison of numerical solution using compressible Euler's equation of (a) ML-TTGC (machine-learned) and (b) original TTGC scheme on an irregular 2D mesh (randomly perturbed) for a free shear flow problem; development of numerical instability is visible in (a) for the original TTGC scheme whereas ML-TTGC provides stable evolution in (b).

meshes. The newly developed schemes are indeed able to automatically adjust scheme parameters to ensure stable and accurate solution evolution in time and mitigate numerical oscillations even on highly irregular meshes. In Fig. 2.2(a-b) we show the improvement achieved in the numerical solution using the ML-TTGC scheme viz-a-viz the original TTGC scheme (in $1D$) for linear convection of a wave packet and for Burgers' solution to a square wave initial condition. In Fig. 2.3 the mitigation of numerical instability in the free shear problem by ML-TTGC is shown. Note that the new scheme mitigates numerical oscillations and enables stable solution evolution. The complete theoretical foundation of learning stable and accurate numerical schemes was published in 2023 [CFD140].

2.2.2 Boundary conditions

As discussed in the previous section, issues pertaining to scheme robustness on perturbed meshes are fundamental for legacy codes, especially in the context of industrial applications. These are indeed potential paths for improvement of future applications to benefit from the increased computing power made available compared to the transition to a new code. Such strategies are however only viable if the full extent of sources of uncertainties is indeed covered. Among all these contributions, boundary condition setting is probably of foremost importance although often overlooked from a purely mathematical point of view. Physical modeling is also to consider for high Reynolds turbulent flows but it is covered later on in this document.

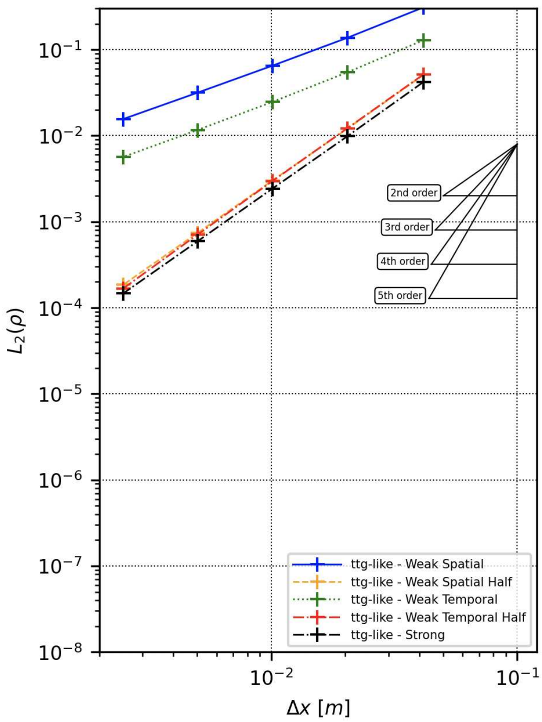

Figure 2.4: Evaluation of multiple boundary condition implementations and their effect on the observed accuracy and convergence of the solution as a function of the mesh resolution.

In terms of accuracy, boundary condition prescription has been a strength of CERFACS' CFD team especially when it comes to compressible solvers. Recent progress on the matter are still being pursued as detailed for example in the recent contribution of G. Daviller et al [83] or [CFD174, CFD173, 88]. In parallel to the effort of having higher-order numerical schemes, the development, and implementation of numerical boundary condition treatments are being pursued in the work of R. Costes funded by SAFRAN. In this work, conservation rules and numerical consistency of the boundary condition treatment are specifically addressed. Typical approaches encountered today in most CFD codes: *i.e.* predictor / corrector type of BC applications are being reworked. Indeed in the former, schemes are usually advanced in time throughout the computational domain irrespectively of the domain border thereby providing a first guess of the values of interest at the boundaries: *i.e.* predictor step at the boundaries. Then, boundaries are tested and corrections are applied depending on the strategy and type of boundary to be enforced: *i.e.* correction step. Although such methods have shown ease of implementation and maintenance of the code, they have inherent limitations due in principle to the fact that information needs to be reconstructed and approximated, a step that can be inconsistent with the scheme employed in the domain. The present research intends to alleviate such limitations by including the application of BC's within the scheme to remain consistent thereby removing the corrective step. Recent developments illustrated in Fig. 2.4 confirm for a simple convection problem that such methods and their adequate implementation can have a major impact on the accuracy of the solution as a function of the cell size.

2.2.3 Mesh adaptation

Mesh adaptation has been a subject of dedicated developments in AVBP for some years now. Two contexts are being specifically developed in conjunction with the COOP team.

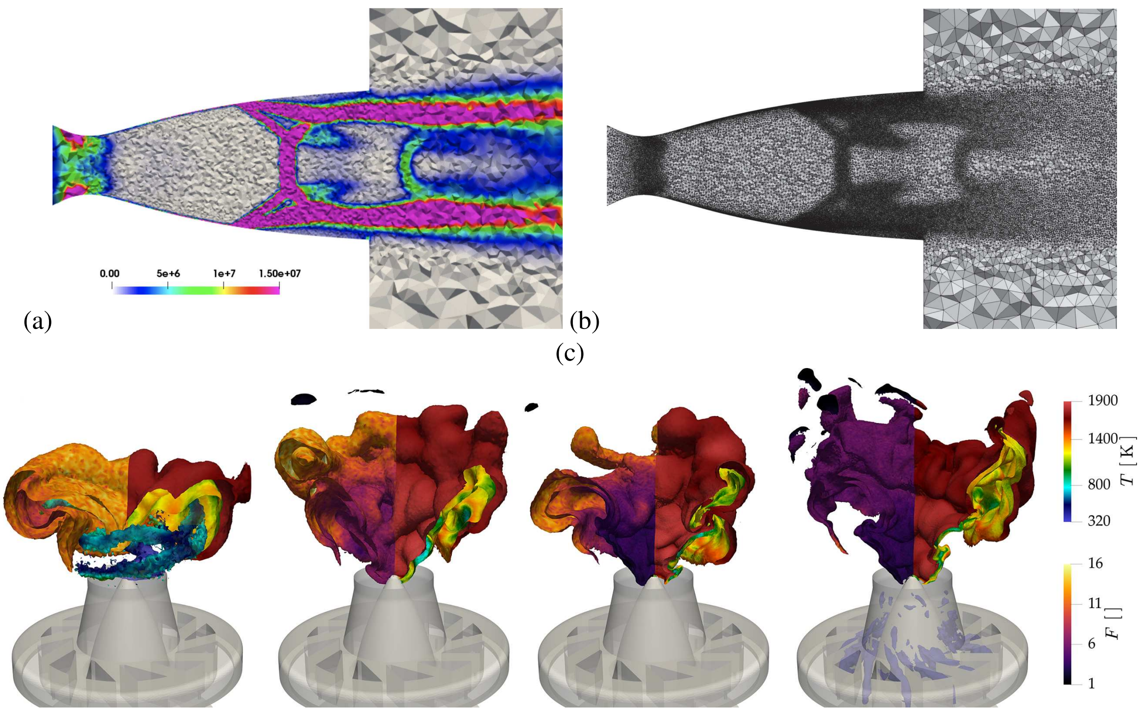

Figure 2.5: Static feature-based mesh adaptation: (a) view if the LIKE field obtained on an initial mesh along with (b) the adapted mesh; (c) use of a multi-criteria feature-based adaptation (*i.e.* near wall resolution, LIKE and flame measures) applied to the PRECCINSTA burner.

The first one is the so-called feature-based static approach. Here, the objective is to build physics-based metrics that aim at acquiring statistics based on flow modeling or grid quality and to adapt a given mesh once a first simulation has been obtained on a first guess mesh. Once obtained, the new mesh is used to produce a new prediction making use of the previous flow prediction as an initial condition and so on. This process can be iterated to yield more efficient and better quality predictions while controlling the mesh size. Progress and efforts in this context resulted in many contributions over the past years with the introduction of the LIKE criterion [81] as well as extensions targeting wall-modeled LES [CFD184] and reacting flows [CFD105, CFD247]. A typical example is the use of such a static adaptation strategy by W. Agostinelli [CFD105] on multiple flow problems as illustrated in Fig. 2.5. One important observation is that such an iterative process converges quite fast and only two to three simulations are usually sufficient indicating a valuable use for industrial applications.

In the second approach, called dynamic mesh adaptation, remeshing is triggered by the solver as the simulation proceeds. This is indeed very often required due to the specific flow physics that is totally transient, evolving in space as well as in time. The typical examples are security scenarios where fronts are present and travel in a domain with time. Much more intensive in terms of algorithmic developments and although such tools rely on the same libraries as the one used in the previous context, this approach requires highly efficient coupling methods to ensure that the added computing cost of this 'on-the-fly' remeshing does not over-shadow the computation. Dedicated developments in AVBP confirm the suitability of the developments either based on MMG or Kalpatura.

2.2.4 Numerical methods for two-phase flows

Efforts have been pursued to improve numerical methods when dealing with two-phase liquid-gas interfaces. This context is very challenging mainly because of the sharp density gradients encountered in such a physics. To ease the treatment of these problems, the MUSCL reconstruction technique for the HLLC Riemann numerical scheme has been reworked with the objective to improve its accuracy for irregular meshes, and to ease parallelization in the cell-vertex context of AVBP. Likewise, with dedicated and new thermodynamics being used for such problems, the corresponding characteristic boundary conditions have been extended to be in line with the dedicated Noble-Abel Stiffened Gas (NASG) equation of state. Such developments typically required the derivation of a fluxes Jacobian matrix, which also allows the use of TTGC scheme for the problem of liquid-gas interfaces (Fig. 2.6). Results have been published in [CFD189].

2.3 Spectral Difference Method

The next generation of CFD solvers will have to perform high-fidelity simulations (Large Eddy Simulation in most cases) in complex geometries. This requires accurate and fast simulations on unstructured grids. One promising way to acquire this feature is to use spectral discontinuous methods. CERFACS is working on one of them called Spectral Difference (SD) in a solver named JAGUAR. This solver is being developed in close collaboration with ONERA.

2.3.1 Turbulence injection

The injection of turbulence is a topic of interest in CFD [33, 39, 9]. Based on experience acquired with AVBP, the synthetic random Fourier method [1, 2, 17] has been implemented in JAGUAR since it represents a good compromise between accuracy and computational time. In this method, turbulent velocities fluctuations $\mathbf{u}'_{in}(\mathbf{x}, t)$ are injected at an inlet boundary using a sum of random Fourier modes

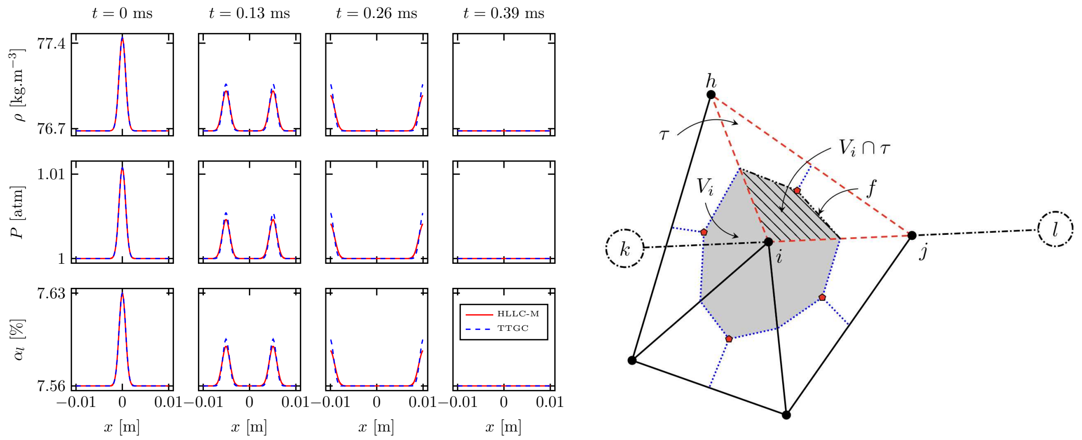

Figure 2.6: Left: Backward and forward acoustic waves with fully non-reflecting boundary conditions for liquid-gas thermodynamics (HLLC-MUSCL RK3 and TTGC schemes). Right: Virtual nodes (k and l) for MUSCL reconstruction on unstructured meshes.

computed from a given homogeneous isotropic turbulent (HIT) energy spectrum:

$$\mathbf{u}'_{in}\left(\mathbf{x},t\right) = 2\sum_{n=1}^{N} u_{tn}\cos\left(\boldsymbol{\kappa}_n.\left(\mathbf{x}-t\mathbf{u}_c\right)+\psi_n\right)\boldsymbol{\sigma}_n \tag{2.1}$$

where u_{tn}, ψ_n and $\boldsymbol{\sigma}_n$ are respectively the amplitude, the phase, and the direction of the n-th Fourier mode associated with the wavenumber vector $\boldsymbol{\kappa}_n$. $\mathbf{u}_c$ is the convected velocity vector. The injection of HIT is performed through a Navier Stokes Characteristic Boundary Condition subsonic inflow [25] and was validated on a spatial bi-periodic channel flow, illustrated by contours of Q-criterion colored by vorticity magnitude in Fig. 2.7a. Turbulent kinetic energy (TKE) evolution and root mean square (RMS) decays along the channel axis are represented in Fig. 2.7b and 2.7c, respectively. The injected HIT spectrum of Passot-Pouquet [24] is used in this case with $u_{rms} = 10$ m.s^{-1} and $L_e = 0.2$ mm. In Fig. 2.7b it can be seen that JAGUAR and AVBP give almost the same result of course for the same discretization. The turbulence injection was also tested successfully in wall-bounded channel and pipe flows. Finally, this method was extended to inject non-homogeneous and anisotropic turbulence [31, 29].

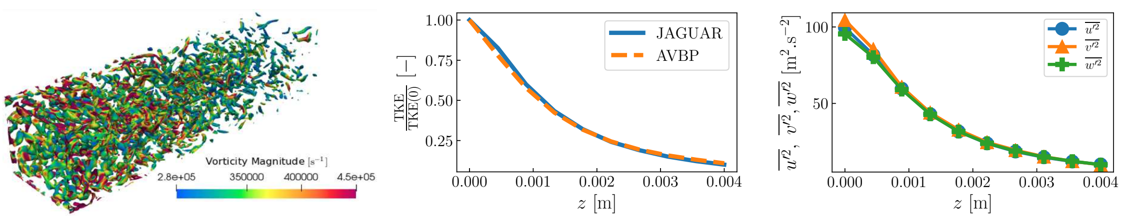

(a) Q-criterion

(b) TKE

(c) RMS velocities

Figure 2.7: Turbulence injection in a spatial bi-periodic channel. The flow is going from the left to the right

2.3.2 Turbulence Tripping

To induce the transition to turbulence in wall-bounded flows, employing a roughness element at the channel or pipe wall is a convenient approach. This method, known as the tripping method, can be implemented in two ways:

1. Introducing sets of actual steps in the channel or pipe geometry.
2. Simulating a step artificially by incorporating a source term.

The last approach is the one that has been chosen.
The artificially tripping approach was proposed by Boudet *et al.* [3] for a Cartesian geometry like flat plate or channel flows as shown in Figure 2.8a for a step of lengths L_x, L_y and L_z respectively in x, y and z directions. The source term is added in the axial momentum equation (z-axis in that case) on the region defined by the step with the following formula:

$$\mathbf{S}_{trip} = \frac{-1}{2L_z}\rho C_D w|w|\mathbf{e}_z \tag{2.2}$$

where C_D is a user-specified drag coefficient and w is the local velocity along z-axis. It will induce a drag force in the axial direction of the form:

$$\mathbf{F}_{trip} = \frac{1}{2}\rho L_x L_y C_D w|w|\mathbf{e}_z \tag{2.3}$$

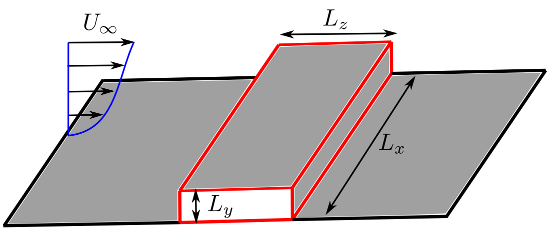

(a) Cartesian artificial tripping.

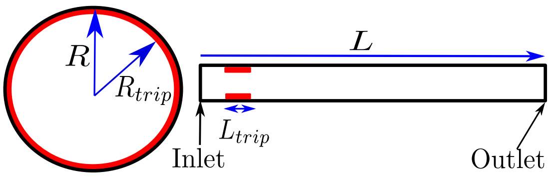

(b) Cylindrical artificial tripping.

Figure 2.8: Artificial tripping using a source term added to momentum equations.

The method can be also adapted to cylindrical geometries as shown in Figure 2.8b for an artificial annular step of length L_{trip} and radius R_{trip}. Both artificial tripping methods were implemented in JAGUAR and validated on wall-bounded channels as well as pipe flow test cases.

2.3.3 Combustion

During the period 2021-2023, simulations of turbulent reactive flows have been performed using the SD algorithm on hexahedral elements previously used to simulate laminar combustion. To go from laminar to turbulent reactive test cases, several additional features have been developed and implemented:

- The use of a positivity-preserving limiter [40, 18] maintains acceptable physical values for mass fractions, pressure and temperature.
- A new stable methodology, for computing the diffusive fluxes at an interface (SDLIFT formulation)
- The adaptation of the thickened flame model flame for LES (TFLES) [7] to the SD framework

Two turbulent reactive test cases have been successfully simulated with JAGUAR: the Cambridge burner [32] (see Figure 2.9) and the VOLVO configuration [30] (see Figure 2.10). All results can be found in [20, 19].

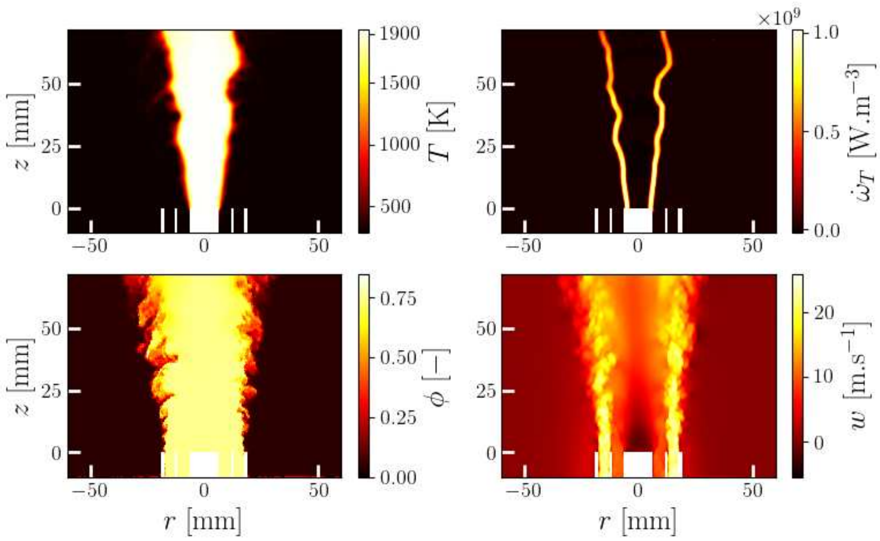

Figure 2.9: Contour plots in the burner mid-section of instantaneous temperature T (top-left), heat release rate $\dot{\omega}_T$ (top-right), equivalence ratio ϕ (bottom-left) and axial velocity (bottom-right) obtained with JAGUAR for the $p = 3$ case.

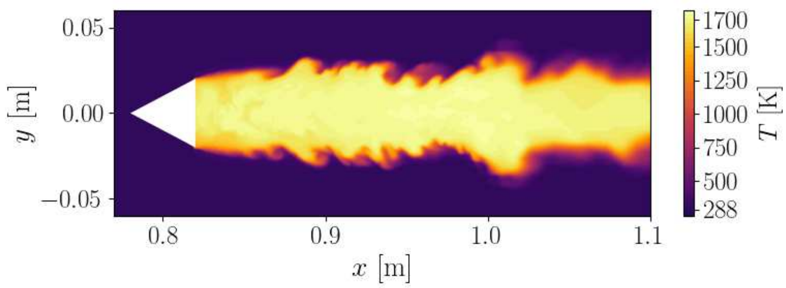

Figure 2.10: Instantaneous temperature field in the bluff-body region of the VOLVO test case.

2.3.4 Immersed Boundary Method

In the classical CFD framework, meshing a complex geometry can often be time-consuming. Some geometries may lead to the formation of distorted cells, lowering simulation quality. In order to bypass this problem, one can make use of Immersed Boundary Methods (IBM). In this framework, the mesh is not constrained by the geometry, and the boundary conditions are enforced via reconstruction methods. While IBMs are not new, their application in high-order methods is quite recent. Following the work of Kou *et al.*[15, 14, 36], an IBM based on the Volume Penalization Method (VPM) has been created in JAGUAR. To our knowledge, this is the first IBM to be made in the SD framework. The VPM considers the solid to be a porous media with very low porosity η. The solution $U = (\rho, \rho u, \rho e)^T$ is penalized in the solid with a local volumetric source term $S(U)$:

$$S(U) = \frac{\chi}{\eta} \begin{pmatrix} 0 \\ -\rho u \\ -\rho \frac{u^2}{2} \end{pmatrix} \tag{2.4}$$

where $\chi(x) = 1$ in the solid, and 0 in the fluid.
The VPM has been validated in the SD framework by simulating the 2D flow over a cylinder at $R_e = 40$ and comparing the pressure coefficient C_p around the cylinder with results from the body-fitted method, and the reference, as shown in Figure 2.11. Work is currently underway on a more extensive validation case centered around a complete channel flow configuration.

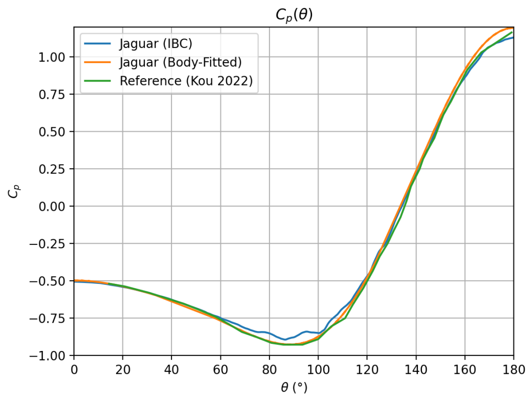

Figure 2.11: Pressure Coefficient C_p around a cylinder at $R_e = 40$

The VPM is a continuous IBM. Those methods are easy to implement, and do not depend on the spatial discretization scheme, but can blur the results near the interface and produce spurious oscillations. In Figure 2.11, a post-treatment step based on an inverse-distance weighted (IDW) interpolation was developed to help reduce the oscillations.

2.3.5 Entropy Preserving Scheme

Spectral discontinuous methods such as Discontinuous Galerkin, Spectral Difference, or Flux Reconstruction (FR) methods are by nature not able to cope with any discontinuity without producing spurious oscillations due to Gibbs effect. Recently, a strong interest appeared in entropy-stable schemes in the framework of the Discontinuous Galerkin approach following the pioneering works of Chen *et al.* [5], Carpenter *et al.* [4], and Gassner *et al.* [11]. Such a procedure requires two sets of Riemann solvers for the hyperbolic part of the equations. A method based on the blend of an entropy-conservative and an entropy-stable scheme was developed in the framework of the SD and FR methods. The proposed entropy-stable schemes are demonstrated to be conservative and high-order accurate. Several one-dimensional and two-dimensional test cases of increasing complexity have been simulated showing very good results. A view of the results for the Mach 3 wind tunnel with a step [38] test case simulated with JAGUAR is presented in Figure 2.12. Shock regions are well captured and Kelvin-Helmholtz instabilities, arising along the shear layer after the primary triple point, can be observed highlighting the low-dissipation property of the proposed scheme in smooth regions of the flow.

2.3.6 Shock treatment

An artificial viscosity-based shock capturing scheme is extended in the context of the high-order triangular Spectral Difference method for solving gas dynamics problems featuring discontinuities and shock waves. The equations are regularized thanks to an artificial diffusivity method combined with a shock sensor based on dilatation and vorticity fields valid for any polynomial order of approximation. The principle of the

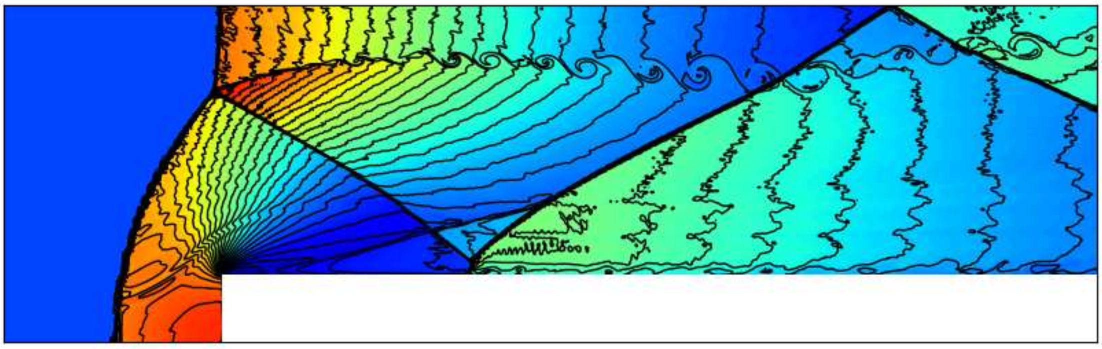

Figure 2.12: Density contours for the Mach 3 wind tunnel with a step test case at $t_f = 4$ s obtained with the Entropy-Stable Spectral Difference Lifted (ESSD-L) scheme implemented in JAGUAR. $180 \times 60 - 144 \times 12$ elements at $p = 5$, with an additional refinement zone near the corner of the step, are employed in all cases. 30 equidistant contour levels between 0.1 and 6.5 are set.

method is to add an artificial bulk viscosity β_a and conductivity κ_a directly into the stress tensor such as

$$\begin{cases} \tau_{ij} &= \mu\left(\left(\frac{\partial u_i}{\partial x_j} + \frac{\partial u_j}{\partial x_i}\right) - \frac{2}{3}\frac{\partial u_k}{\partial x_k}\delta_{ij}\right) + \beta_a \frac{\partial u_k}{\partial x_k}\delta_{ij} \\ q_j &= -(\kappa + \kappa_a)\frac{\partial T}{\partial x_j}. \end{cases} \tag{2.5}$$

The methodological novelty is an L^2 projection-based iterative Restriction Prolongation filtering operation introduced for high-order triangular elements. This filtering operation applied to the artificial bulk viscosity and thermal conductivity stabilizes the simulations and improves the quality of the shock-capturing approach. The methodology is validated on various canonical relevant compressible test cases. Numerical results demonstrate the performance and flexibility of the triangular high-order Spectral Difference method for solving simultaneously compressible flows and shock waves. The benefit of the proposed filtered artificial viscosity is highlighted in the figure 2.13 that simulates the classical double Mach reflection test case.

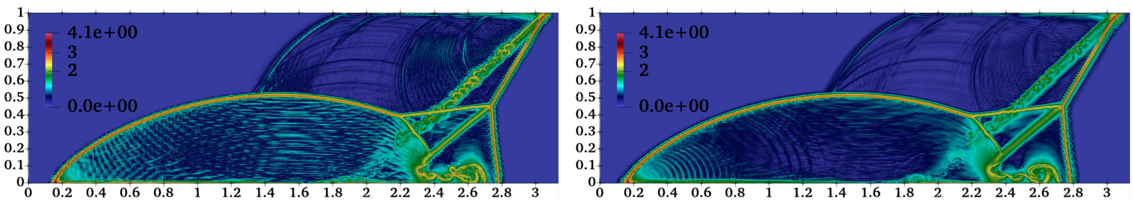

(a) Standard filtering scheme

(b) Improved filtering scheme

Figure 2.13: Double Mach reflection at $M = 10$. Schlieren $log_{10}(||\nabla\rho|| + 1)$ at $t = 0.2$ sec for two levels of iterative RP filter, $\mathcal{R}_{proj,2}$ (up) and $(\mathcal{R}_{proj,2})^3$ (bottom).

2.3.7 Multi-element

The work of A. Veilleux during her PhD thesis, defended in 2021, has enabled to extend the SD method in JAGUAR to triangle up to 6^{th} order [34] and tetrahedra up to 3^{th} order [35]. Since 2022, work has been underway to evaluate the SD method for jet aeroacoustics using unstructured tetrahedral meshes. In particular, Large Eddy Simulations of an isolated jet at Mach number $M = 0.9$ from Pprime Institute have been compared for both aerodynamic and far-field acoustics results.

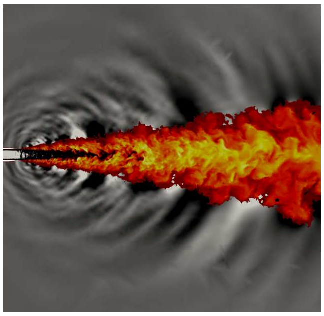

(a) Instantaneous temperature and fluctuation pressure flow fields

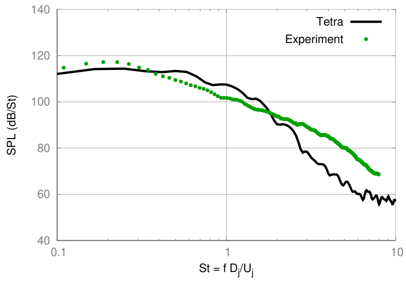

(b) SPL at 30°

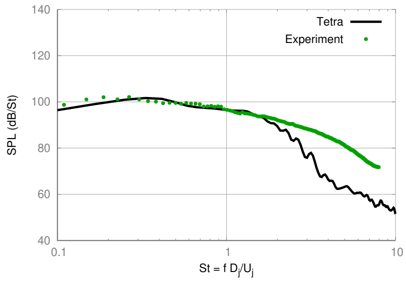

(c) SPL at 90°

Figure 2.14: Unheated single jet at Mach number $M = 0.9$

The temperature and pressure fluctuations fields provided by LES are shown in Fig. 2.14a. Sound pressure level (SPL), in agreement with the experiment, up to the mesh cut-off frequency $St = 2$, are shown in Fig. 2.14b and Fig. 2.14c in decibel per Strouhal obtained at 30° and 90° respectively at a distance of $r/D_j = 50$ from the nozzle exit.

2.3.8 Time-domain impedance boundary condition

In the context of the laminar flow control of subsonic and hypersonic boundary layers, the complex microstructure of acoustic metasurfaces is a bottleneck to accurately capture the flow behavior using Direct Numerical Simulations (DNS). To model the impact of the acoustic metasurfaces on boundary layer disturbances, a time-domain acoustics impedance boundary condition (TDIBC) was implemented in JAGUAR [23, 10]. This impedance boundary condition is derived from a formulation based on the oscillatory diffusive representation (ODR). This formulation recasts an arbitrarily complex impedance law into a finite set of weighted acoustic poles, which must be fine-tuned to provide a broadband-accurate discrete approximation. Recently, the solver has incorporated a novel TDIBC from recent research by Roncen et al. [28], which introduced a parameter-free method capable of accommodating a wide range of impedance operators, as long as the frequency-domain characteristics of the material are available. The impulse response (IR) TDIBC is a technique that relies on a direct convolution to implement the TDIBC using the impulse response of the reflection coefficient. The latter is obtained by inverse Fourier transform. Both TDIBC implementations are evaluated using a benchmark test case that replicates the configuration outlined by Jones et *al.* [16]. This test case simulates the impact of an acoustic liner on a grazing right-running planar wave. The results of this benchmark test serve to validate the appropriateness of employing TDIBCs alongside the Navier-Stokes equations, as illustrated in Figure 2.15.

2.3.9 Turbulent Kinetic Energy Budget

In the context of direct numerical simulations, the computation of high-order turbulent statistics is necessary to confirm data reliability on one hand and to serve as a base for modeling purposes on the other. For this purpose, work has been carried out to enable to recover the high-order turbulent statistics in JAGUAR. Indeed, the Turbulent Kinetic Energy (TKE) balance gives an insight into the quality of the flow and solver properties.

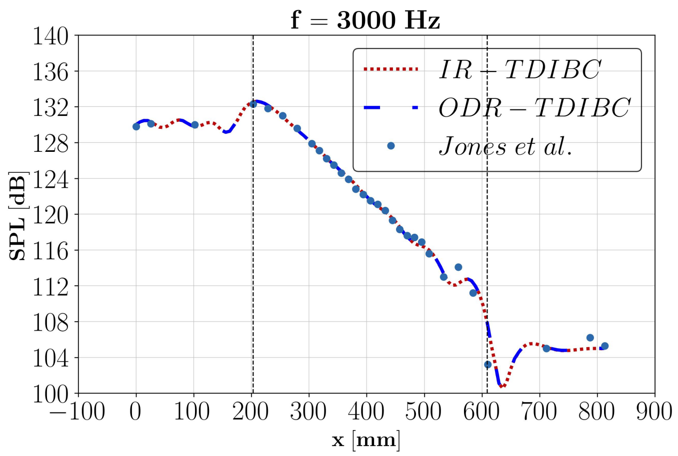

Figure 2.15: Sound pressure levels measured along the top wall for an incident harmonic wave-train at a frequency $f = 3000$Hz. The acoustic liner's boundaries are marked by the black dashed lines.

The post-processing method of 128 terms involved in the Reynolds stress budgets has been applied to the direct numerical simulation of a low Reynolds channel flow ($Re_\tau = 186$) and the output has been confronted to the DNS data of Hoyas & Jimenez [13]. Since the Mach number of the flow is very low, the statistics are directly compared as shown in Figure 2.16. The budget of the main contributor to the turbulent kinetic energy ($< u'u' >$) agrees well with the reference. However, the wall-normal component ($< v'v' >$) exhibits spurious pressure oscillations that highlight numerical instabilities from the flow solver. Nevertheless, these instabilities seem not to affect the mean values of the flow since the average velocity and Reynolds stress perfectly match the reference values.

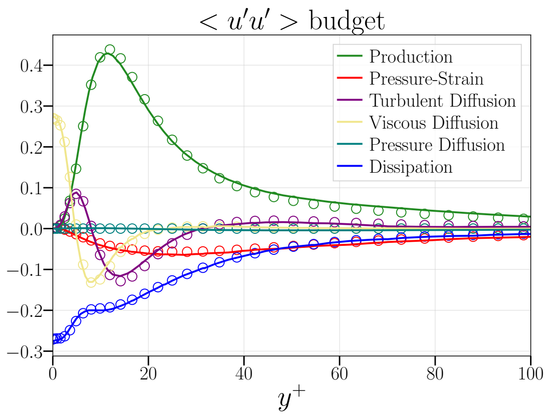

(a) Axial component

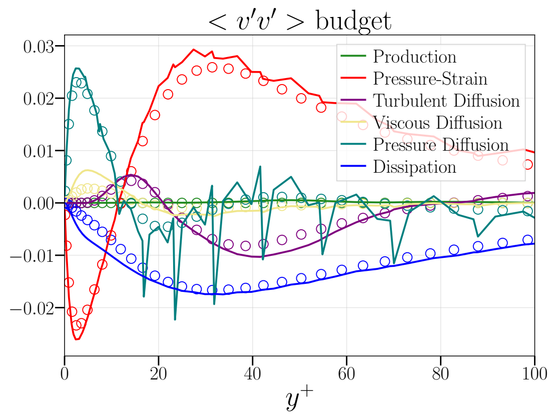

(b) Wall-normal component

Figure 2.16: JAGUAR computation of Reynolds stress budgets based on the $Re_\tau = 186$ turbulent channel flow test case. — : JAGUAR simulation, $\circ$: Hoyas & Jimenez [13] DNS.

2.4 Lattice Boltzmann Method

2.4.1 Stability Analysis of Hybrid Thermal Schemes

Classical LBM approaches are limited to low Mach number and constant temperature flows. These approaches make use of standard lattices (D1Q3, D2Q9, D3Q19, and D3Q27), which allow for a compact and efficient numerical scheme, but produce errors in the momentum viscous stress tensor and fail completely to recover the physics of the energy equation. These problems can be resolved via the hybrid LBM approach, which involves:

- The use of additional corrective terms to eliminate the errors in the viscous stress tensor.
- The addition of an additional transport equation of an energy variable which is resolved via the finite difference or finite volume approach, which is then coupled with the LBM system.

However, many hybrid approaches suffer from a lack of numerical stability. A Linear Stability Analysis (LSA) was performed to examine the origins of the instabilities of HLBM approaches [58]. Different energy variables were examined: $s, e, E, \rho s, \rho e, \rho E$. It was found that the collision parameter σ and the lattice speed of sound parameter T_{ref} could be used as independent levers on the stability of the scheme. Furthermore, explicit resolution of the pressure work terms for the conservation equations of $e, E, \rho e, \rho E$ led to unstable solutions, leaving only entropy-based schemes as viable solutions.

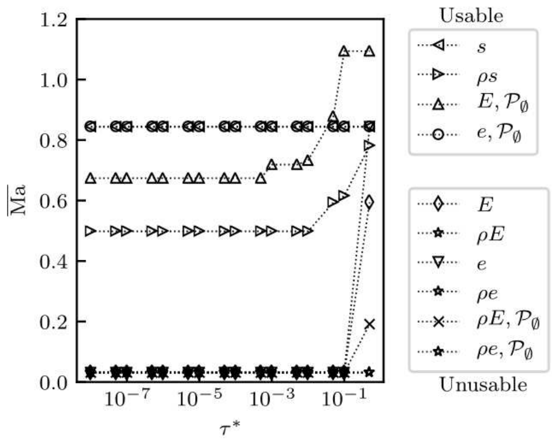

Figure 2.17: Maximum achievable Mach number relative to a given nondimensional relaxation time τ^*. $\mathcal{P}_\varnothing$ corresponds to conservation equations where the pressure work term was set to zero.

2.4.2 Extension of the Compressible Scheme to the D3Q27 Lattice

The developments of the compressible HLBM scheme at CERFACS [57], combined with the aforementioned LSA of hybrid compressible schemes [58], contributed to the development of a more robust model at the M2P2 laboratory [49], here called the ”improved density-based model”, which makes it possible to perform stable simulations without excessive numerical dissipation. However, this model remains based on the D3Q19 lattice, which has shown itself to be prone to isotropy errors [43]. Thus, at CERFACS, the improved density-based approach was extended to the D3Q27 lattice.
Fig. 2.18 compares the results of the two lattices for a circular free jet with a bulk speed of $Ma = 0.9$, where it can be seen that the D3Q27 approach significantly improves the isotropy of the scheme, at the cost

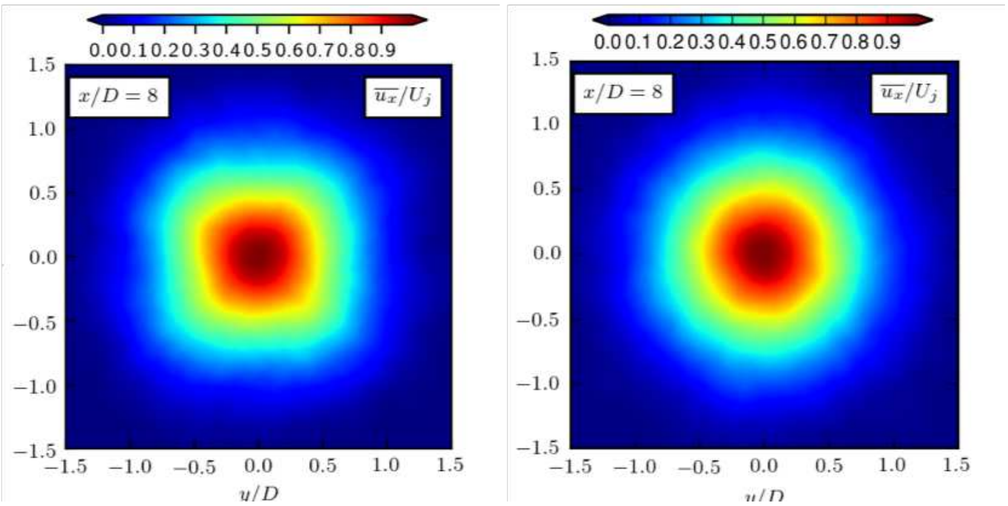

(a) D3Q19 Lattice.

(b) D3Q27 Lattice.

Figure 2.18: Comparison of the mean axial velocity profile of a circular free jet $8D$ downstream of the nozzle for the improved density-based model using the D3Q19 (left) and D3Q27 (right) lattices.

of additional computation time. However, studies on isentropic convected vortex test cases were performed, showing that at $Ma > 0.5$, the D3Q27 lattice enables the use of higher CFL numbers, meaning that the additional cost related to the larger lattice can be compensated by the use of a larger time step.

2.4.3 Boundary condition

To perform turbomachinery simulations, the development of a new inlet boundary condition imposing total pressure, total temperature, azimuthal angle, and radial angle has been performed. The method relies on the use of non-reflective conditions based on a Navier-Stokes Characteristic Boundary Condition (NSCBC) formalism. This approach is based on a treatment of the characteristic waves of the local flow [56]. This limits the level of wave reflection coming from the boundary conditions which can be a major issue when simulating compressible flows. This condition has been validated on several test cases to ensure that a wide range of values usually encountered in turbomachinery applications can be applied with a limited level of reflection. Finally, radial profiles of the different quantities measured experimentally can be set up to perform S-duct simulations as illustrated in Fig. 2.19a.

The NSCBC formalism has also been applied to develop an outlet boundary condition that lets the physical radial pressure gradient establish naturally at the outlet of turbomachinery simulations, where strong flow rotation is found, without additional treatment (see Fig. 2.19b) [50].

While these two boundary conditions are sufficient to simulate the target applications, a valve law condition [48] has been added to the outlet static pressure. The idea is that, in practice, as the total pressure and total temperature are imposed at the inlet, the mass flow obtained in the turbomachine is prescribed by adjusting the outlet static pressure. The challenge lies in the fact that this static pressure is unknown a priori and will depend on the pressure losses generated in the system or the work exchange with the flow. The user must manually find a correct value until the target mass flow is reached. When several operating points are to be simulated, this approach is not practical and too costly. Thus, an approach where the outlet static pressure is dynamically adjusted throughout a given simulation [56] was implemented into the LBM solver. This approach has demonstrated its applicability in a variety of configurations, ranging from a multi-perforated pipe to a closed and open Ultra High By-Pass Ratio simulation.

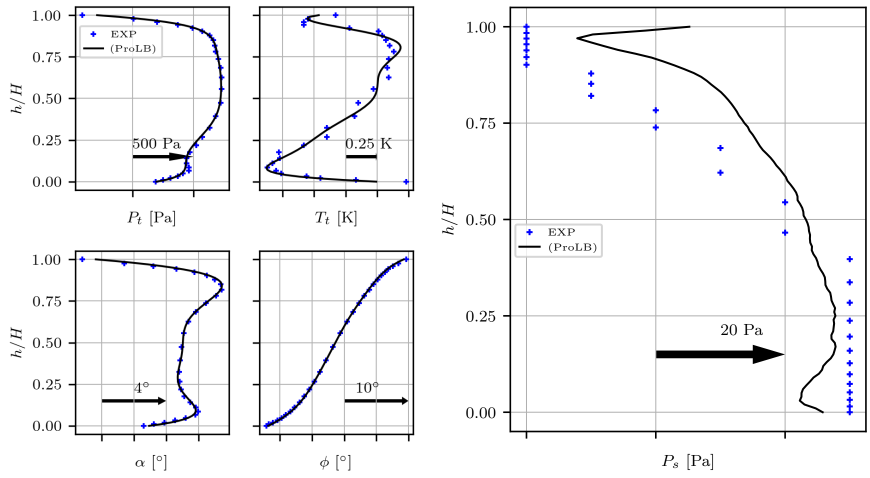

(a) (b)

Figure 2.19: Plot of the inlet radial profiles (left) and check of the Radial Equilibrium Assumption at the outlet.

2.4.4 Turbulence

Wall Treatment

For flows at high Reynolds numbers, Lattice Boltzmann approaches must be coupled with wall modeling to keep computational costs reasonable, particularly since the LBM relies on Cartesian grids. Thus, even approaches where the LBM is coupled with RANS or hybrid-RANS turbulence models must use wall functions to avoid the prohibitive cost of meshes where $y^+ \approx 1$. Furthermore, the cut-cell approach, wherein arbitrarily shaped solids are embedded into the computational domain with the corresponding elimination of the fluid nodes, leads to geometric irregularities, even with smooth surfaces.
Within this context, an improved wall treatment was developed [47]. It removes the grid points that are too close to the wall where wall functions are not viable. It calculates the shear velocity u_τ on numerous fluid nodes and interpolates u_τ onto the target node. Lastly, it constructs the off equilibrium distribution function f_i^{neq} using the shear stress $\frac{\partial u}{\partial n}$ calculated via the wall function, rather than via finite differences.
This enhanced wall treatment was tested on a NACA0012 airfoil (see Fig. 2.20) and was found to significantly enhance both the accuracy and smoothness of the solution.

Turbulence Inflow Methods

In many configurations, the flow entering the domain of interest is already turbulent, making turbulence injection critically important for high-fidelity simulations. Although there are many different approaches to turbulence inflow (see the literature review of Wu [61]), the synthetic random Fourier sum approach was retained due to its low computational cost and user-friendliness. Fluctuations are super-imposed on the imposed velocity profile at the inlet such that:

$$\boldsymbol{u'}(\boldsymbol{x}, t) = 2\sum_{n=1}^{N} u_n^{amp} \cos\left[\boldsymbol{\kappa}_n \cdot (\boldsymbol{x} - t\boldsymbol{u_c}) + \psi_n + \omega_n t\right]\boldsymbol{\sigma}_n, \tag{2.6}$$

where each mode has a length scale l_n. u_n^{amp} is the amplitude, $\boldsymbol{\kappa_n}$ is the wavevector, ϕ_n is the phase, ω_n is the angular frequency, and $\boldsymbol{\sigma_n}$ is the direction of the mode. $\boldsymbol{u_c}$ is the convection velocity of the turbulent

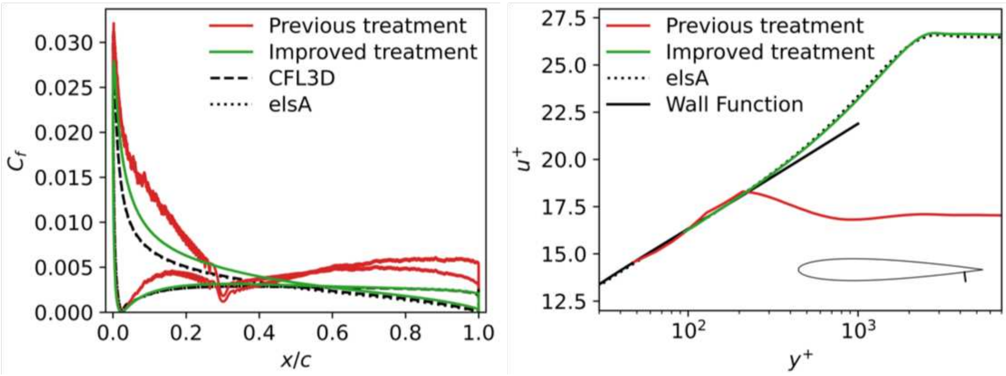

(a) Skin friction coefficient C_f.

(b) Velocity profile on the pressure side.

Figure 2.20: Comparison of the baseline and improved wall treatment for a NACA0012 airfoil test case.

fluctuations. These fluctuations represent homogeneous isotropic turbulence (HIT). They can be scaled by an imposed Reynolds stress tensor to represent non-homogeneous anisotropic turbulence (NHAT).

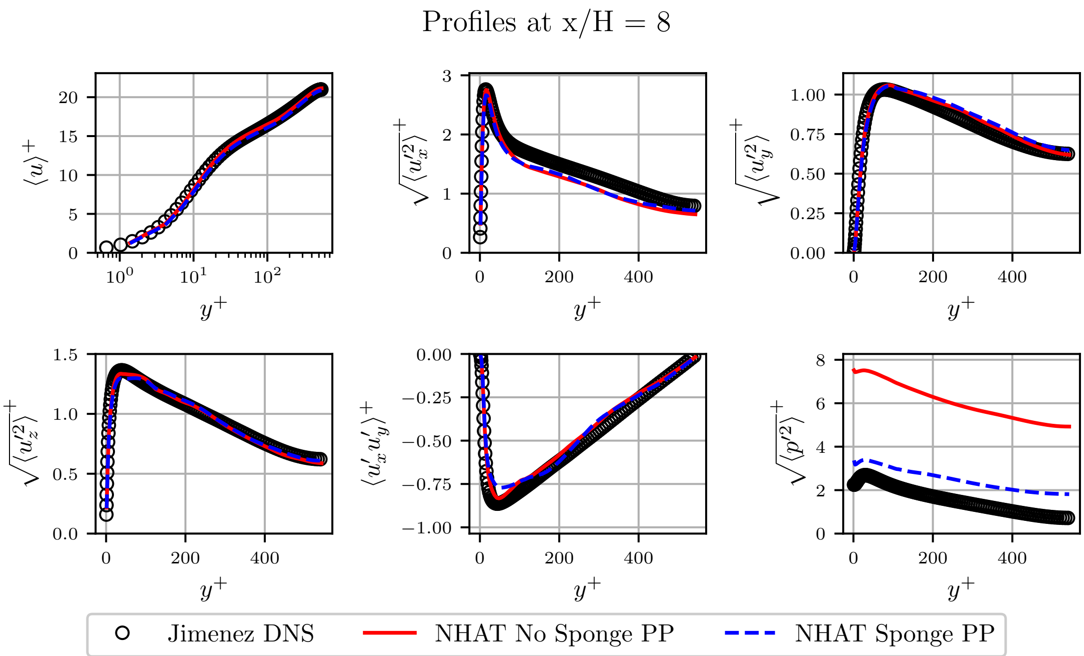

Figure 2.21: Aerodynamic profiles eight channel half-heights downstream of the inflow condition for the turbulence injection with and without sponge conditions.

The effectiveness of the non-homogeneous anisotropic turbulence injection technique was evaluated in the context of a planar turbulent channel flow featuring both inlet and outlet boundaries. The primary objective was to assess whether the imposed boundary conditions could generate realistic turbulent profiles at a location reasonably close to the inlet. While the method successfully achieved the desired profiles, it introduced significant spurious pressure fluctuations. To address this issue, the turbulence injection method was combined with a sponge condition that specifically influenced the mass equation, leaving the momentum equations unaffected, as depicted in Fig. 2.21. Notably, the sponge condition demonstrated compatibility with the turbulence inflow by mitigating pressure fluctuations while preserving the accurate velocity profiles.

2.4.5 Rotating Flow

In modeling rotating flows within the local non-Galilean rotating reference frame, two fictitious forces emerge: the centrifugal and Coriolis forces, which are computed from the velocity vector $\boldsymbol{u}$, a fixed rotational speed vector $\boldsymbol{\Omega}$, and a fixed center $\boldsymbol{x}_0$. By implementing the algorithm proposed by Guo *et al.*[51], these forces are incorporated into the collision step as the source term Φ_i:

$$\boldsymbol{F} = -\rho\left[\boldsymbol{\Omega} \times (\boldsymbol{\Omega} \times \boldsymbol{\delta}_0) + 2\boldsymbol{\Omega} \times \boldsymbol{u}\right], \tag{2.7a}$$

$$\Phi_i = w_i \left[\frac{\boldsymbol{c}_i - \boldsymbol{u}}{c_s^2} + \frac{\boldsymbol{c}_i \cdot \boldsymbol{u}}{c_s^4}\boldsymbol{c}_i\right] \cdot \boldsymbol{F}, \tag{2.7b}$$

where $\boldsymbol{\delta}_0 = \boldsymbol{x} - \boldsymbol{x}_0$ and w_i represent the lattice weights. To obtain the density ρ and the momentum $\rho\boldsymbol{u}$ at each time step, the zeroth and first-order moment reconstruction of f_i are employed. Given that the definition of $\boldsymbol{F}$ depends on $\boldsymbol{u}$ itself, a linear system must be inverted which gives the following moment reconstruction[53]:

$$\rho = \sum_i \tilde{f}_i, \tag{2.8a}$$

$$\rho\boldsymbol{u} = \begin{bmatrix} 1 & -\Omega_z & \Omega_y \\ \Omega_z & 1 & -\Omega_x \\ -\Omega_y & \Omega_x & 1 \end{bmatrix}^{-1} \left(\sum_i \boldsymbol{c}_i \tilde{f}_i - \frac{1}{2}\rho\boldsymbol{\Omega} \times (\boldsymbol{\Omega} \times \boldsymbol{\delta}_0)\right). \tag{2.8b}$$

Thus, the modified collide-and-stream algorithm effectively incorporates the centrifugal and Coriolis forces within the local rotating reference frame, allowing for proper density and momentum recovery. This approach has been validated based on a configuration involving a heated, rotating turbulent channel flow, as referenced by Liu[54] and Kristoffersen[52]. Figure 2.22 illustrates logarithmic and averaged profiles while Figure 2.23 depicts the averaged fluctuation profiles.

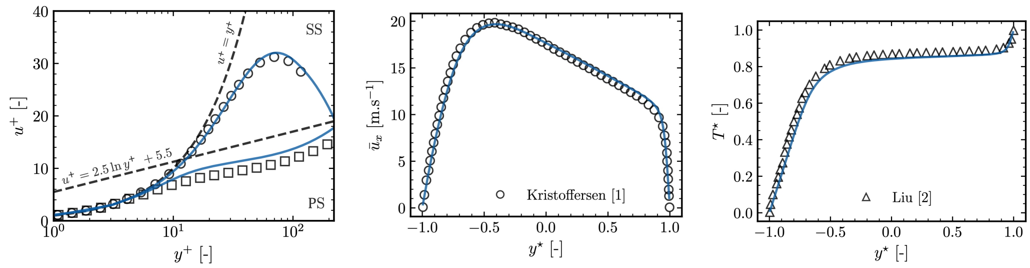

Figure 2.22: Averaged logarithmic and mean profiles

2.4.6 Mesh refinement

Handling spurious noise from numerical artifacts during grid refinement is crucial in LBM simulations. Usually discretized on an octree Cartesian grid, certain distribution populations are missing during the

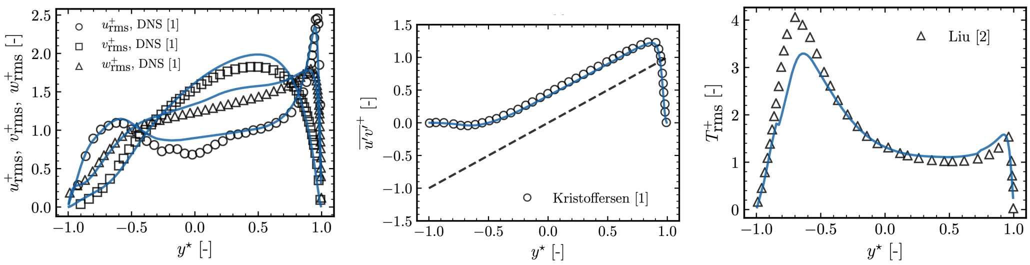

Figure 2.23: Averaged fluctuation profiles

propagation step when the mesh size doubles at the mesh interface, requiring specific algorithms for reconstruction. Existing algorithms lack precision, resulting in unwanted noise as vortices cross interfaces. Previous work at Cerfacs[42] divided these noises into two types: one inherent to the LBM requiring specific collision models, and the other due to the imprecision of grid coupling algorithms. The latter has been addressed by a new algorithm, referred to as Direct-Coupling (DC) by Astoul *et al.*[41], which does not use grid overlap (STD). The missing populations are reconstructed by satisfying the solvability conditions of the collision operator. Using a unique reconstructed equilibrium function, the DC algorithm allows for the reduction of spurious noise compared to the standard algorithm (STD), as evidenced in Fig. 2.24.

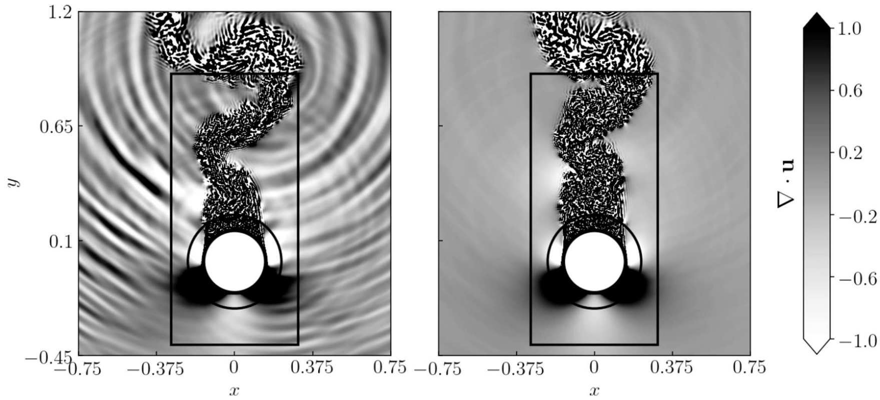

Figure 2.24: Velocity dilatation field of the turbulent cylinder with a mix of layers and box-shaped grid interface. Left: STD, right: DC.

Recently, the DC approach has undergone improvements to integrate force terms. This inclusion necessitates modifications to the solvability conditions within the Lattice-Boltzmann equation.
This helps to prevent any discontinuities and mass loss at grid transitions in the presence of force fields and large temperature gradients, as illustrated in Fig. 2.25.

2.4.7 Porous media

Porous media have broad applications in engineering. In the field of aeronautics, the use of these materials for the attenuation of airframe noise, particularly trailing edge noise, has been a subject of interest since the early 1970's. Given the dimensions of the pores in these materials, it is nearly impossible to resolve them for numerical studies which of practical interest. However, modeling approaches exist that could reproduce the effect of these materials without the need to resolve them. One of the methods is the volume averaging

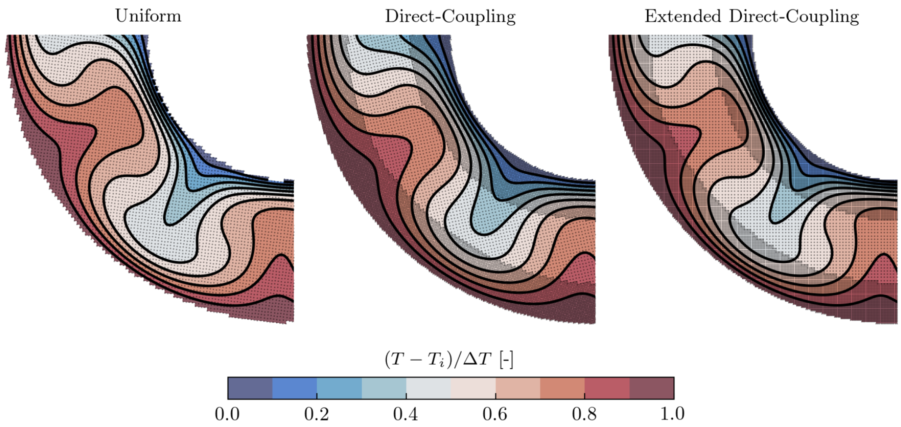

Figure 2.25: Quarter view of the mesh overlaid on the normalized temperature field and isotherms after 300 revolutions. The case is a 2D centrifugal buoyancy-induced annulus where Rayleigh-Bénard convection rolls occur. ΔT exceeds 100 K, and the rotational speed is around 38 rev.s^{-1}. The extended algorithm successfully captures the correct isotherms while the previous approach fails and presents a dissipated temperature field due to significant mass loss.

method [55] which, instead of using the porous material in the computation, replaces this material with an equivalent force term. The effectiveness of this method therefore lies in the accuracy of the model used for the force term.
This approach was tested in the LBM code LEOPARD for purely acoustic applications with the simplest model for the force term, the Darcy Force which is dependent on the porosity($\overline{\phi}$) and permeability(κ) of the material of interest and the fluid viscosity(μ).

$$\rho F^p = -\overline{\phi}\frac{\mu}{\kappa} \cdot \mathbf{u} \tag{2.9}$$

The negative sign indicates that this force term acts as a resistance to the flow. This method was used in correspondence with the compressible HLBM [57] but adapted to two dimensions and was validated against theory and later with the NASA Grazing Impedance Tube Test with no mean flow as an application case. The results for the application case were also compared with those of PowerFlow[60] and elsA[46], which used Time Domain Impedance Boundary Condition (TDIBC).
The attenuation of the acoustic wave over the porous material for different frequencies tested is shown in Fig.2.26. The simplest model used to represent porous material can provide good results for frequencies up to 2 kHz while for higher frequencies, the attenuation trend is obtained albeit the absolute values are different. It must be noted that this model was able to capture well the attenuation of resonant frequency (Fig.2.26a) of the material chosen for the simulation. More sophisticated models to represent the porous materials could improve the results for higher frequencies.

2.4.8 Two phase flow

Efforts have been conducted to propose a lattice-Boltzmann framework for the prediction of a liquid-gas interface, in a compressible context. A two-distribution method has been developed, leading to a so-called Color-Gradient approach. The work conducted during the PhD of T. Lafarge (2019-2022) has allowed a thorough theoretical description of this framework, demonstrating the connection between the recoloration step and the Allen-Cahn equation. Such an equation characterizes a diffuse interface at thermo-mechanical equilibrium. This theoretical work allows us to enforce the desired diffuse interface thickness. Furthermore,

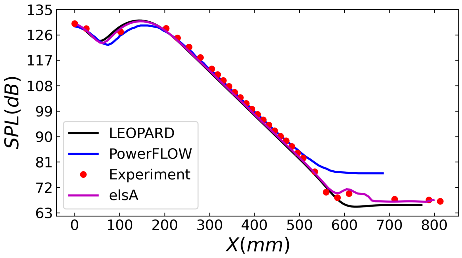

(a) $f_{sim} = 1.0\ kHz$

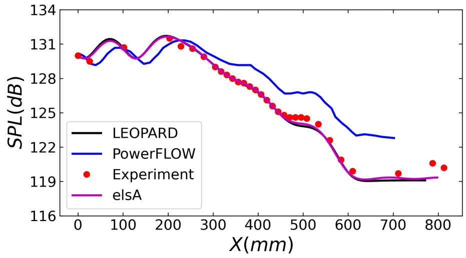

(b) $f_{sim} = 1.5\ kHz$

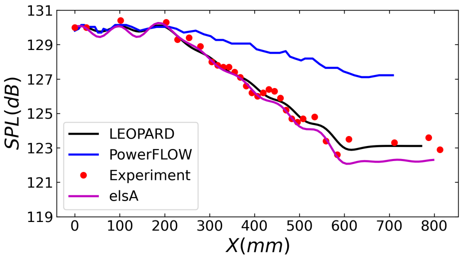

(c) $f_{sim} = 2.0\ kHz$

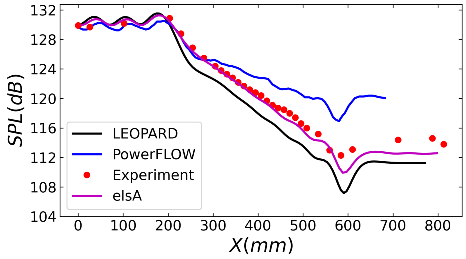

(d) $f_{sim} = 2.5\ kHz$

Figure 2.26: Comparison of simulation results with experimental results and similar numerical studies.

dedicated operators have also been proposed, to accurately impose surface tension while significantly reducing spurious currents, known to be a challenge for such simulations ([CFD162]).

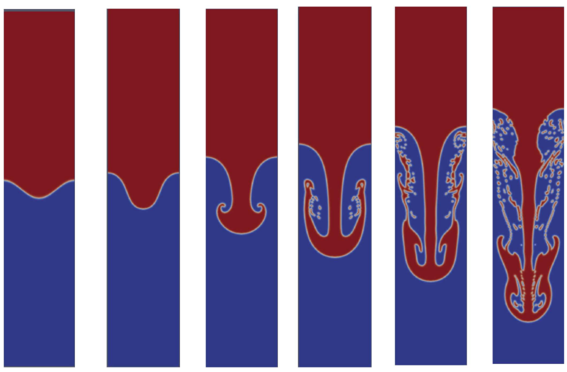

Figure 2.27: Rayleigh-Taylor instability with surface tension

Promising results have been obtained for academic liquid-gas instability configurations (Fig. 2.27). More complex configurations require an extension of boundary conditions for two-phase flows, which constitutes a perspective work.

References

[1] C. Bailly and D. Juve, (1999), A stochastic approach to compute subsonic noise using linearized Euler's equations, In *5th AIAA/CEAS aeroacoustics conference and exhibit*, 1872.

[2] W. Bechara, C. Bailly, P. Lafon, and S. M. Candel, (1994), Stochastic approach to noise modeling for free turbulent flows, *AIAA Journal*, **32**, 455–463.

[3] J. Boudet, J.-F. Monier, and F. Gao, (2015), Implementation of a roughness element to trip transition in large-eddy simulation, *Journal of Thermal Science*, **24**, 30–36.

[4] M. H. Carpenter, T. C. Fisher, E. J. Nielsen, and S. H. Frankel, (2014), Entropy Stable Spectral Collocation Schemes for the Navier–Stokes Equations: Discontinuous Interfaces, *SIAM Journal on Scientific Computing*, **36**, B835–B867.

[5] T. Chen and C.-W. Shu, (2017), Entropy stable high order discontinuous Galerkin methods with suitable quadrature rules for hyperbolic conservation laws, *Journal of Computational Physics*, **345**, 427–461.

[6] G. Christophe and R. Jean-François, (2009), Gmsh: A 3-D finite element mesh generator with built-in pre- and post-processing facilities, *Int. J. Numer. Methods Eng.*, **79**, 1309–1331.

[7] O. Colin, F. Ducros, D. Veynante, and T. Poinsot, (2000), A thickened flame model for large eddy simulations of turbulent premixed combustion, *Physics of Fluids*, **12**, 1843–1863.

[8] J. C. Del Alamo and J. Jiménez, (2003), Spectra of the very large anisotropic scales in turbulent channels, *Physics of Fluids*, **15**, L41–L44.

[9] N. S. Dhamankar, G. A. Blaisdell, and A. S. Lyrintzis, (2018), Overview of turbulent inflow boundary conditions for large-eddy simulations, *AIAA Journal*, **56**, 1317–1334.

[10] R. Fiévet, H. Deniau, and E. Piot, (2020), Strong compact formalism for characteristic boundary conditions with discontinuous spectral methods, *Journal of Computational Physics*, **408**, 109276.

[11] G. J. Gassner, A. R. Winters, and D. A. Kopriva, (2016), Split form nodal discontinuous Galerkin schemes with summation-by-parts property for the compressible Euler equations, *Journal of Computational Physics*, **327**, 39–66.

[12] C. Hank, A. Sean D., A. James, B. Andrew C., B. Janine, W. B. E., B. Peer-Timo, B. Eric, C. Joseph, D. Matthieu, D. Soumya, F. Jean M., F. Thomas, F. Steffen, G. Christoph, G. Berk, G. William F., H. Charles D., H. Cyrus, H. Bernd, I. Joseph, J. Chris R., K. Scott, K. Aaron, K. James, L. Matthew, L. Jay, M. Kwan-Liu, M. Preeti, M. Jeremy, M. Kenneth, N. Paul, O. Patrick, P. Manish, P. Valerio, P. John, P. Tom, P. Steve, P. Norbert, P. David, R. Michel, R. Silvio, R. David H., S. Sudhanshu, S. Franz, S. Robert, S. Han-Wei, U. Will, V. Rhonda, V. Venkatram, W. Ingo, W. Ruonan, W. Gunther H., W. Brad, W. Matthew, Y. Hongfeng, and Z. Sean B., (2020), A terminology for in situ visualization and analysis systems, *The International Journal of High Performance Computing Applications*, **34**, 676–691.

[13] S. Hoyas and J. Jiménez, (2008), Reynolds number effects on the Reynolds-stress budgets in turbulent channels, *Physics of Fluids*, **20**, 101511.

[14] K. Jiaqing, H.-d.-M. Aurelio, J. Saumitra, L. C. Soledad, and F. Esteban, (2022), Eigensolution analysis of immersed boundary method based on volume penalization: Applications to high-order schemes, *Journal of Computational Physics*, **449**.

[15] K. Jiaqing, J. Saumitra, H.-d.-M. Aurelio, P. Kunal, H. Charles, and F. Esteban, (2022), Immersed boundary method for high-order flux reconstruction based on volume penalization, *Journal of Computational Physics*, **448**.

[16] M. Jones, W. Watson, and T. Parrott, (2005), Benchmark data for evaluation of aeroacoustic propagation codes with grazing flow, In *11th AIAA/CEAS Aeroacoustics Conference*, 2853.

[17] R. H. Kraichnan, (1970), Diffusion by a random velocity field, *The Physics of Fluids*, **13**, 22–31.

[18] G. Lodato, (2019), Characteristic modal shock detection for discontinuous finite element methods, *Computers & Fluids*, **179**, 309–333.

[19] T. Marchal, H. Deniau, J.-F. Boussuge, B. Cuenot, and R. Mercier, (2023), Extension of the Spectral Difference method to premixed laminar and turbulent combustion, *Flow, Turbulence and Combustion*, **111**, 141–176.

[20] T. Marchal, (2023), *Extension de la méthode des Différences Spectrales à la combustion*, PhD thesis.

[21] M. Maunoury, (2019), *Méthode de visualisation adaptée aux simulations d'ordre élevé. Application à la compression-reconstruction de champs rayonnés pour des ondes harmoniques*, theses, Université Toulouse 3 Paul Sabatier.

[22] F. Monteghetti, D. Matignon, and E. Piot, (2018), Energy analysis and discretization of nonlinear impedance boundary conditions for the time-domain linearized Euler equations, *Journal of Computational Physics*, **375**, 393–426.

[23] F. Monteghetti, D. Matignon, E. Piot, and L. Pascal, (2016), Design of broadband time-domain impedance boundary conditions using the oscillatory-diffusive representation of acoustical models, *The Journal of the Acoustical Society of America*, **140**, 1663–1674.

[24] T. Passot and A. Pouquet, (1987), Numerical simulation of compressible homogeneous flows in the turbulent regime, *Journal of Fluid Mechanics*, **181**, 441–466.

[25] T. Poinsot and S. K. Lele, (1992), Boundary conditions for direct simulations of compressible viscous flows, *J. Comp. Physics*, **101**, 104–129.

[26] J.-F. Remacle, N. Chevaugeon, É. Marchandise, and C. Geuzaine, (2006), Efficient visualization of high-order finite elements, *Int. J. Numer. Methods Eng.*, **69**, 750–771.

[27] F. Rémi, M. Matthieu, and L. Adrien, (2021), On pixel-exact rendering for high-order mesh and solution, *J. Comput. Phys.*, **424**, 109860.

[28] R. Roncen and J. I. Cardesa, (2023), Generic and broadband non-linear time domain impedance boundary condition, *Journal of Sound and Vibration*, **554**, 117691.

[29] M. L. Shur, P. R. Spalart, M. K. Strelets, and A. K. Travin, (2014), Synthetic turbulence generators for RANS-LES interfaces in zonal simulations of aerodynamic and aeroacoustic problems, *Flow, Turbulence and Combustion*, **93**, 63–92.

[30] A. Sjunnesson, P. Henrikson, and C. Lofstrom, (1992), CARS measurements and visualization of reacting flows in a bluff body stabilized flame, In *28th Joint Propulsion Conference and Exhibit*, 3650.

[31] A. Smirnov, S. Shi, and I. Celik, (2001), Random flow generation technique for large eddy simulations and particle-dynamics modeling, *Journal of Fluids Engineering*, **123**, 359–371.

[32] M. Sweeney, S. Hochgreb, and R. Barlow, (2011), The structure of premixed and stratified low turbulence flames, *Combustion and Flame*, **158**, 935–948.

[33] G. R. Tabor and M. Baba-Ahmadi, (2010), Inlet conditions for large eddy simulation: A review, *Computers & Fluids*, **39**, 553–567.

[34] A. Veilleux, G. Puigt, H. Deniau, and G. Daviller, (2022), A stable Spectral Difference approach for computations with triangular and hybrid grids up to the 6th order of accuracy, *Journal of Computational Physics*, **449**, 110774.

[35] A. Veilleux, G. Puigt, H. Deniau, and G. Daviller, (2022), Stable Spectral Difference approach using Raviart-Thomas elements for 3D computations on tetrahedral grids, *Journal of Scientific Computing*, **91**.

[36] L. Victor J., K. Jiaqing, V. Eusebio, and E. Ferrer, (2023), A modified equation analysis for immersed boundary methods based on volume penalization: Applications to linear advection–diffusion equations and high-order discontinuous Galerkin schemes, *Computers and Fluids*, **257**.

[37] G. Wang, F. Duchaine, D. Papadogiannis, I. Duran, S. Moreau, and L. Y. M. Gicquel, (2014), An overset grid method for large eddy simulation of turbomachinery stages, *Journal of Computational Physics*, **274**, 333–355.

[38] P. Woodward and P. Colella, (1984), The numerical simulation of two-dimensional fluid flow with strong shocks, *Journal of computational Physics*, **54**, 115–173.

[39] X. Wu, (2017), Inflow turbulence generation methods, *Annu. Rev. Fluid Mech*, **49**, 23–49.

[40] X. Zhang and C.-W. Shu, (2010), On positivity-preserving high order discontinuous Galerkin schemes for compressible Euler equations on rectangular meshes, *Journal of Computational Physics*, **229**, 8918–8934.

[41] T. Astoul, G. Wissocq, J.-F. Boussuge, A. Sengissen, and P. Sagaut, (2021), Lattice Boltzmann Method for Computational Aeroacoustics on Non-Uniform Meshes: A Direct Grid Coupling Approach, *Journal of Computational Physics*, **447**, 110667.

[42] T. Astoul, (2020), Analysis and Reduction of Spurious Noise Generated at Grid Refinement Interfaces with the Lattice Boltzmann Method, *Journal of Computational Physics*, 51.

[43] M. Bauer and U. Rüde, (2018), An improved lattice Boltzmann D3Q19 method based on an alternative equilibrium discretization, *arXiv preprint arXiv:1803.04937*.

[44] C. Brown and J. Bridges, (2006), Small hot jet acoustic rig validation, tech. rep.

[45] G. Brès, J. Nichols, S. Lele, and F. Ham, (2012), Towards best practices for jet noise predictions with unstructured large eddy simulations, In *42nd AIAA fluid dynamics conference and exhibit*, 2965.

[46] L. Casadei, H. Deniau, T. Nodé-Langlois, E. Piot, and C. Polacsek, (2022), Acoustic Mode Attenuation in Ducts (Using CFD) with Time-Domain Impedance Boundary Condition, *AIAA Journal*, 1–20.

[47] J. Degrigny, S. G. Cai, J. F. Boussuge, and P. Sagaut, (2021), Improved wall model treatment for aerodynamic flows in LBM, *Computers & Fluids*, **227**, 105041.

[48] F. Duchaine and L. Gicquel, (2019), Inlet and Outlet Characteristics Boudary Conditions For Large Eddy Simulations of Turbomachinery.

[49] G. Farag, T. Coratger, G. Wissocq, S. Zhao, P. Boivin, and P. Sagaut, (2021), A unified hybrid lattice-Boltzmann method for compressible flows: Bridging between pressure-based and density-based methods, *Physics of Fluids*, **33**, 086101.

[50] T. Gianoli, J. F. Boussuge, P. Sagaut, and J. de Laborderie, (2022), Development and validation of Navier-Stokes Characteristic Boundary Conditions applied to turbomachinery simulations using the Lattice Boltzmann Method, 1–32.

[51] Z. Guo, C. Zheng, and B. Shi, (2002), Discrete Lattice Effects on the Forcing Term in the Lattice Boltzmann Method, *Physical Review E*, **65**, 046308.

[52] R. Kristoffersen and H. I. Andersson, (1993), Direct Simulations of Low-Reynolds-number Turbulent Flow in a Rotating Channel, *Journal of Fluid Mechanics*, **256**, 163–197.

[53] T.-M. Liou and C.-S. Wang, (2018), Large Eddy Simulation of Rotating Turbulent Flows and Heat Transfer by the Lattice Boltzmann Method, *Physics of Fluids*, **30**, 015106.

[54] N.-S. Liu and X.-Y. Lu, (2007), Direct numerical simulation of spanwise rotating turbulent channel flow with heat transfer, *International Journal for Numerical Methods in Fluids*, **53**, 1689–1706.

[55] M. Moeßner and R. Radespiel, (2013), Numerical simulations of turbulent flow over porous media, In *21st AIAA Computational Fluid Dynamics Conference*, 2963.

[56] N. Odier, M. Sanjosé, L. Gicquel, T. Poinsot, S. Moreau, and F. Duchaine, (2019), A characteristic inlet boundary condition for compressible, turbulent, multispecies turbomachinery flows, *Computers and Fluids*, **178**, 41–55.

[57] F. Renard, Y. Feng, J. F. Boussuge, and P. Sagaut, (2021), Improved compressible hybrid lattice Boltzmann method on standard lattice for subsonic and supersonic flows, *Computers and Fluids*, **219**, 104867.

[58] F. Renard, G. Wissocq, J. F. Boussuge, and P. Sagaut, (2021), A linear stability analysis of compressible hybrid lattice Boltzmann methods, *Journal of Computational Physics*, **446**, 110649.

[59] A. P. Schneider, A. L. Fiquet, B. Paoeltti, X. Ottavy, and C. Brandstetter, (2023), Experiments on Tuned UHBR Open-Test-Case Fan ECL5/CATANA: Performance and Aerodynamics, In *Turbo Expo: Power for Land, Sea, and Air*, vol. 87080, American Society of Mechanical Engineers, V13AT29A038.

[60] C. Sun, F. Pérot, R. Zhang, P.-T. Lew, A. Mann, V. Gupta, D. M. Freed, I. Staroselsky, and H. Chen, (2015), Lattice Boltzmann formulation for flows with acoustic porous media, *Comptes Rendus Mécanique*, **343**, 533–544.

[61] X. Wu, (2017), Inflow Turbulence Generation Methods, *Annual Review of Fluid Mechanics*, **49**, 23–49.

Modelling

3.1 Introduction

Complementary to Numerical Methods, Code development and High-Performance Computing, Modelling remains at the root of many real CFD applications. It is a necessary component of simulations that makes the difference in terms of design, allowing to reduce the price of computations otherwise impractical while addressing multiple physical phenomena. Being at the root of the CERFACS' CFD expertise, especially when it comes to problems of industrial relevance, multiple aspects of industrial flow physics are hence covered. Among others, near-wall modelling remains a fundamental issue in CFD just like turbulence. Likewise if dealing with turbulent reacting flows, the need for de-carbonation and the emergence of new fuels stress the need to master this modelling process by (a) constructing adequate chemistry schemes, (b) predicting pollutant emissions, and (c) dealing with multi-phase flows. The following presents recent subjects covered by the CFD team within this Modelling framework.

3.2 Near Wall Modelling

Although near-wall flow understanding and modeling have benefited from many years of theoretical developments in the context of fully turbulent, laminar, or transitioning regimes, taking into account weak/favorable/unfavorable mainstream pressure gradients... they remain at the heart of simulations especially if LES or multi-physics applications are targeted. Indeed, the wall flow state is crucial in determining the rate of heat transfer through the solid walls of a combustor. It also determines the performance of wing profiles or turbomachinery blades and it plays a critical role in flame stabilization. Recent studies at CERFACS on these specific issues can be divided into three distinct frameworks that are:

- Near wall flow dynamics and modeling,
- Heat transfer and multi-physics.
- Near wall particle deposition

3.2.1 Near wall flow dynamics and modeling

Accurate aerodynamics or heat transfer predictions require fine resolution of the flow boundary layer, which in LES and more broadly in CFD can be addressed in a wall-resolved or wall-modeled manner. In the former, the grid resolution and associated sub-grid scale modeling need to respect the near-wall scaling laws of the flow. This entails a significant computational effort often accessible for academic like LES but inaccessible for real applications. In the latter, a low grid resolution level is maintained (and thereof at a lower computational cost) while the necessary quantities to advance the simulation are obtained from models thereby putting the effort on modeling.

For wall-resolved LES around profiles, requirements aside from the near wall grid resolution, are to adequately represent the flow state around and prior to the blade to trigger the proper flow mechanisms possibly responsible for the spatial and temporal evolution of the near wall dynamics.

Such requirements are not necessarily easy to master due to uncertainties in measurements or in numerics as well as implementations of boundary conditions in fully unsteady CFD solvers.

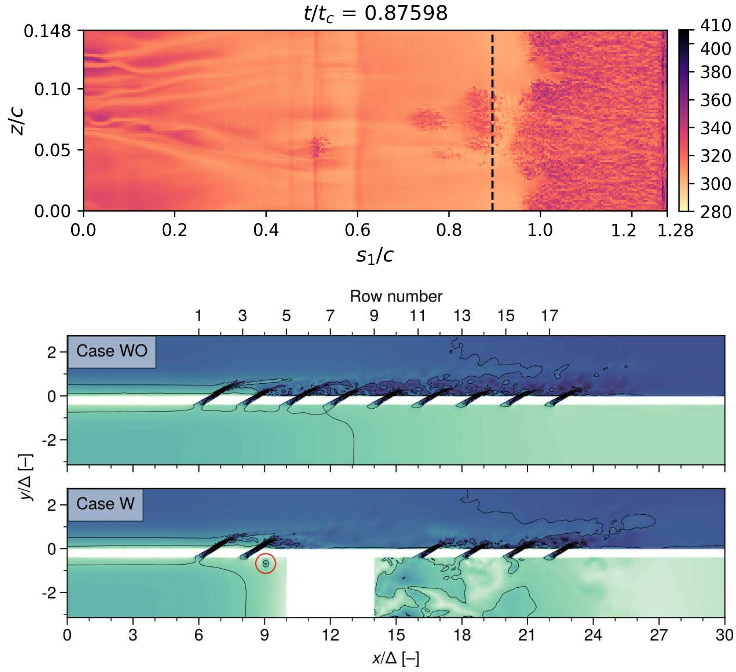

Figure 3.1: Typical wall-resolved LES predictions recently obtained: (a) instantaneous view of the pressure side boundary layer intermittent transition for the LS89 configuration, (b) comparisons of the flow response within a liner subject to the absence (top) or presence (bottom) of a buff body in the suction vein.

For wall-resolved LES, support from the CN2020 SAFRAN project at CERFACS was continued to address numerics, modeling and impact on the flow prediction of the LS89 blade cascade from VKI. Of specific interest, the case of a boundary layer transition submitted to turbulence and intermittency was specifically targeted. A recent study by D. Dupuy (RTRA postdoctorate located at CERFACS) [84] demonstrated that wall-resolved LES can reproduce this transitioning process and that intermittency is one key element that needs now to be quantified properly to recover the heat transfer measurements, Fig. 3.1(a). Following this initial demonstration, several actions have been pursued to understand turbomachinery flows and the impact of blade interactions [CFD13]. In this case, shock boundary layer interactions have been encountered and multi-stage simulations have been obtained for various operating conditions taking advantage of the Turbo-AVBP solution. Due to the intense resolution required for wall-resolved LES of such problems, only reduced span simulations are investigated: *i.e.* $1,5D$ simulations.

In parallel, wall-resolved LES of technological effects such as hole geometries of effusion cooling systems, multiperforated liners... present in combustion chambers and for blade cooling have been produced, Fig. 3.1(b). The objectives of such reference computations are multi-folds: (a) understand the key elements of these flows and their impact on their cooling efficiency; (b) constitute a detailed data basis for modeling purpose and (c) enter in a LES-based optimization loop of such geometries [CFD101, CFD3, CFD100, 73, 74, 75].

For wall-modeled LES, the complexity arises from the law hypothesized and needed to construct models which then provide quantities of interest: *i.e.* wall friction. Such hypotheses usually infer a given boundary layer state and a set of flow properties that are often far from the true industrial problem. These simplifications are however emphasized in LES solvers where numerical or sub-grid scale model interactions and the implementations of these laws can yield different solutions. Investigations are necessary and the subject of new developments while implementing new laws to consider the presence of pressure gradients as encountered in turbomachinery flows for example.

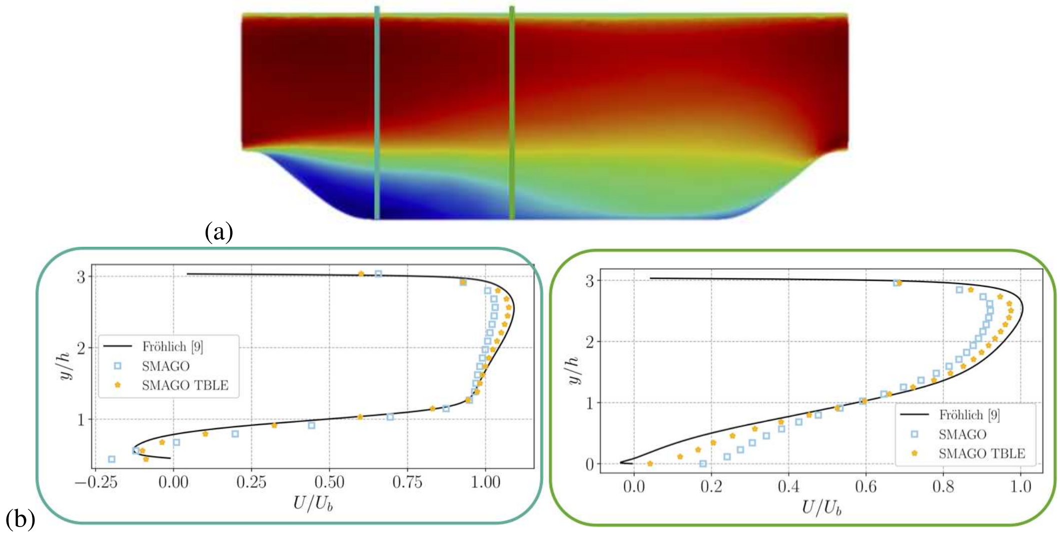

Figure 3.2: Turbulent channel hill wall-modeled LES predictions by use of the standard Smagorinsky and log-law compared to the standard Smagorinsky sub-grid scale model and a TBLE approach considering pressure gradient effects: (a) mean axial view of the flow prediction using TBLE and (b) profile comparisons against a reference wall-resolved simulation.

Current questions addressed in the above context are, for example, the universal behavior and boundary layer predictions of wall-modeled simulations irrespectively from the sub-grid scale model employed [CFD116]. In parallel, extended laws are being probed by typically considering the Turbulent Boundary Layer Equation (TBLE) that is locally solved in $1D$ between the first gird node off the wall and the wall to provide the needed information. Preliminary tests on simple flows evidence the potential of these methods as pursued by the PhD work of M. Costes financed by SAFRAN, Fig. 3.2.

Finally, such a context of derivation is also covered taking into account recent capacities of Machine Learning tools, as shown in Fig. 3.3.

3.2.2 Heat transfer

Multiple effects are at play when it comes to heat transfers in combustion chambers. These are however not only determinant for the design of cooling systems, but they also directly impact the flame shape as well as

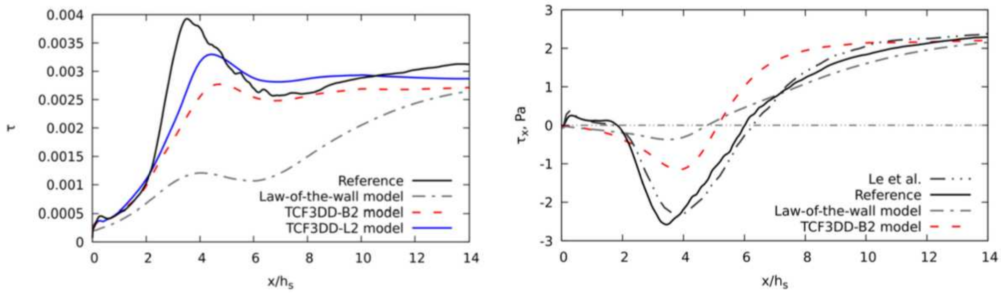

Figure 3.3: Wall-modeled simulation of Backward facing step with AVBP on a Cartesian mesh. Comparison between wall-resolved, classical law-of-the-wall, and Machine-Learned wall model.

its stabilization process and emission of pollutants.

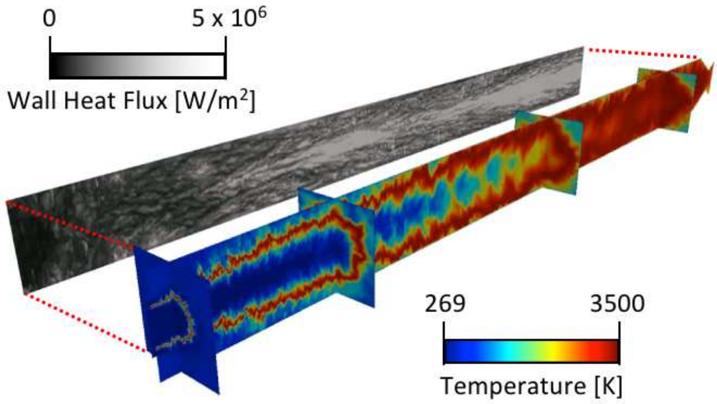

Figure 3.4: LES of the Methane-Oxygen flame of TU Munich at 20 bars

For combustion, heat transfer at walls can be either imposed if measurements are available or modeled through different methods. In the case of high-pressure methane-oxygen combustion, studied experimentally at TU Munich in the context of liquid rocket engines [CFD115, CFD252, 77], heat transfers were measured but its wall distribution was not accessible. One important objective in such cases is to see if adopted models for simulations of the flames are adequate. As an example, the turbulent diffusion flame at 20 bars is illustrated in Fig. 3.4 with an instantaneous view of the numerical solution. By applying the coupled wall-law of AVBP, the correct wall heat flux was recovered [CFD252]. This indicates that the flame although not visible experimentally was predicted with the correct power and length, leading to the correct burnt gas state, a fundamental component of rocket engine design. Likewise, the consideration of coupled LES-based CHT simulations of the PRECCINSTA burner [CFD104, CFD103, CFD247], indicated that such effects can be of critical importance for thermo-acoustic stability of the prediction while operating with multiple H_2/CH_4 mixtures.

For heat transfer without combustion, actions and models obtained are very much linked to section 3.2.1. As said dedicated thermal modelling and analyses have been obtained for multiperforated liners and

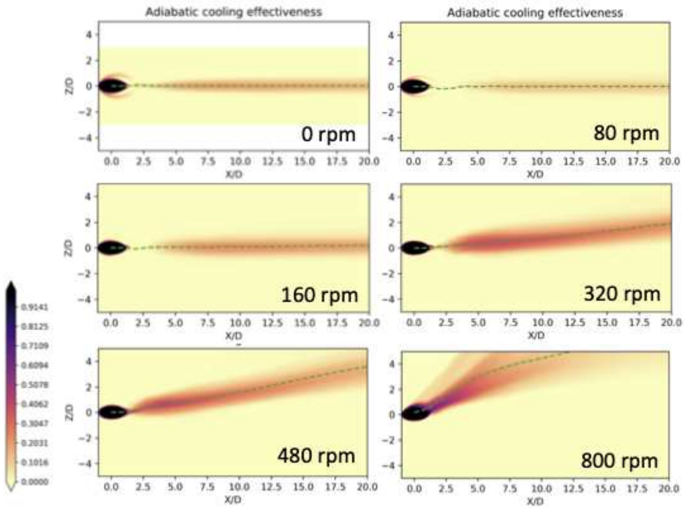

Figure 3.5: Adiabatic cooling effectiveness of a cooling perforation on a plate subject to different speed of rotation.

shaped holes [CFD185, CFD144, 90]. In these specific contexts, the model named the thickened hole model [76] has been specifically developed and extended to take into account the specificities of each problem [CFD144]. For static perforations, sensitivities to inflow specifications, required for the thickened hole approach, showed the need for improvement if thermal mixing is to be properly reproduced in a wall-modeled context. Likewise, the response of such a perforation subject to different rotation rates as encountered for cooled turbine blades has been pursued in the PhD work of A. Perrot financed by SAFRAN, Fig. 3.5.

The current status on the above matters is a strong push towards the industrialization of the proposed solutions for the use of wall-resolved simulations so CERFACS' partners can address specific designs internally. Likewise, models developed for the wall-modeled context are being assessed on real industrial problems.

3.2.3 Particle deposition at walls

The accurate prediction of particle deposition is an important topic, ranging from matter deposition in turbomachinery to the soiling of solar panels. Large Eddy Simulation can accurately predict the bulk flow turbulence that controls particle dynamics and the subsequent particle flux toward the near-wall region. However, the complex near-wall dynamics of boundary layers make the prediction of particle deposition inaccurate in a wall-modeled context, as it does not represent important features such as ejection events in the buffer layer. While there have been efforts to enrich wall-resolved large-eddy simulation with sub-grid scale fluctuation models, literature contributions to near-wall particle dynamics in a wall-model context remain scarce, in particular for particle deposition. The postdoctoral work of T. Appel, funded by TotalEnergies in the context of solar farm soiling, aimed to evaluate the ability of wall-modeled to describe the interaction of particle dynamics with the near-wall turbulence, and to develop a dedicated model to predict deposition rates accurately. In the proposed approach, a stochastic model acts at the first wall cells (Fig. 3.6(a)) to impose a probability of deposition, constructed from theoretical arguments, resulting from a collaborative work with O. Simonin from IMFT. Once implemented in AVBP, the model was validated in a

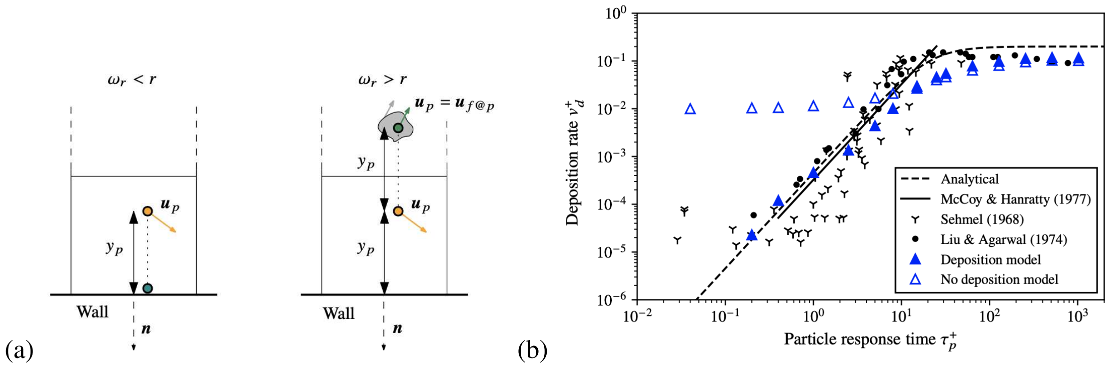

Figure 3.6: (a) Principle of the particle deposition acting at the first wall cells: the particle either deposits or rebounds based on a stochastic model. (b) Particle deposition rate versus particle response time in a turbulent channel flow configuration: comparison between experimental data and wall modeled large eddy simulation with and without deposition model.

turbulent channel flow configuration (Fig. 3.6(b)), where it demonstrated a significant improvement in the prediction of the deposition rate compared to conventional wall-modeled large eddy simulation.

3.3 Hydrogen combustion

Hydrogen combustion has become the main research topic of most combustion laboratories over the last five years. CERFACS, together with IMFT, was already working on this topic in the framework of the ERC advanced grant SCIROCCO (cerfacs.fr/scirocco) since 2019 and had developed dedicated models to cover the many specificities of hydrogen flames: chemical schemes, effects of thermodiffusive instabilities, modified transport. When the hydrogen expansion began in 2021, CERFACS had a head start. Today, activities on hydrogen are very intense in two fields:

- In almost all fields using fossil fuels, decarbonization calls for moving partially or totally to hydrogen: this includes virtually all fields of industry - transportation, power generation, heat generation, furnaces, small burners, etc.

- This amazingly fast development of hydrogen in all fields has implications for safety: hydrogen raises significant issues in this field which will be discussed specifically in the Safety section.

For decarbonization as well as for safety, the main challenge for CERFACS is the same: develop combustion models which can predict hydrogen flames accurately. This is done through a large network of collaborations where CERFACS distributes AVBP to users (in CNRS laboratories such as IMFT) and gathers experimental data for validation (from IMFT again but also from Pprime or INERIS). In addition to these collaborations, an initiative to setup a worldwide workshop on the validation of CFD codes for hydrogen flames has been launched by CERFACS and collaborators: IMFT, Cambridge (Pr Mastorakos), and RWTH (Pr Pitsch), with the support of the European CLEAN AVIATION program. In this program, the experimental results of three configurations are made available to the whole community for CFD validation. More than 15 groups are computing these configurations worldwide, starting with HYLON, and comparisons (including AVBP) will take place in 2024 during an event called the Hydrogen week.

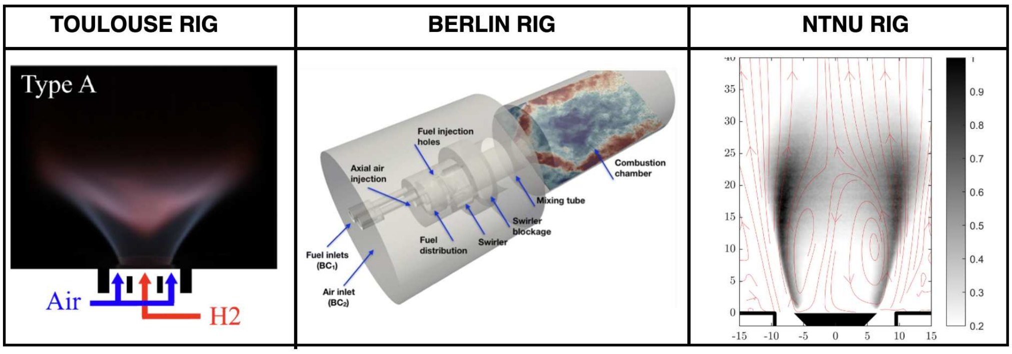

Figure 3.7: The CAW H2 CFD workshop of comparison of CFD codes for hydrogen. Note that the left configuration is the HYLON setup developed during SCIROCCO. This configuration has been used to develop the H2 version of AVBP in the last four years [CFD108, CFD172] and it is today, the most documented configuration in terms of experimental data.

3.3.1 Hydrogen combustion modelling

The first need for any LES solver in the context of H2 combustion including AVBP is to improve the description of molecular transport: until 2021, viscosity was computed using the Sutherland law for air, a model which works for most gases but not for hydrogen. To fix this problem, N. Rouland has coded a multispecies, complex transport model for viscosity and diffusivities of all gases in AVBP. In addition, a simpler formulation based on Wilke's law was also introduced by F. Garnier to avoid paying the price of complex transport models.

The chemistry of hydrogen in AVBP for most computations is the San Diego scheme. This is a well-established procedure in AVBP now and chemistry is not the main issue for hydrogen flames except at walls where low temperature chemistry requires to change the boundary condition and limit the production of H radicals in this specific region (PhD of L. Denardi). The main issue is actually flame-turbulence interaction modeling as discussed in the next sections. For the moment, hydrogen flames are treated using the TFLES model in premixed regions and without any dedicated model in diffusion zones. This works reasonably well for small size domains and low pressures where DNS-type meshes can be used in diffusion regions.

Various improvements among which the first model including the effects of thermodiffusive instabilities on premixed turbulent flames, developed during the Center for Turbulence Summer Research program of 2022, in collaboration with RWTH Aachen: correlations for increased flame speeds due to thermodiffusive effects were extracted from the DNS of Aachen and have been introduced into AVBP.

When it comes to applications and hydrogen combustion, two distinct contexts of validation and development appear. These are detailed following this logic in what follows.

3.3.2 Experimental, reduced power hydrogen flames

Both DNS and LES of hydrogen flames have been computed since 2021 to understand hydrogen combustion. This section presents a few selected examples.

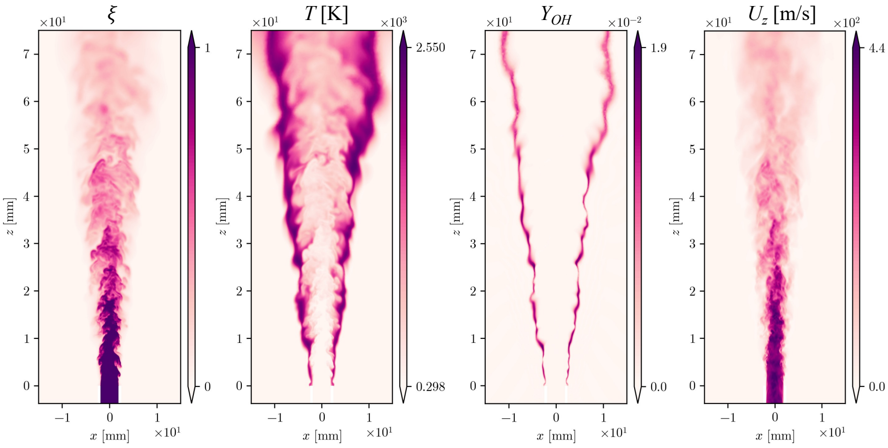

Figure 3.8: AVBP results for a jet flame. Fields of mixture fraction, temperature, OH radical, and axial velocity. TNF workshop flame of ETH Zurich and Sandia.

Jet flames are usually the first academic test case for CFD. Very fine meshes are used, providing DNS-like accuracy. Figure 3.8 displays AVBP results for one of the flames of the TNF workshop (https://tnfworkshop.org) computed during the PhD of F. Garnier.

A second illustrative result of the present power of CFD is the comparison between AVBP and PIV data for the HYLON setup (Fig. 3.9). The agreement is excellent for axial and radial velocities, both for mean and RMS components. This type of agreement is obtained today for most flames at 1 bar in small domains (see Sect. 3.3.3 for a detailed discussion on the generality of this statement). AVBP also predicts the transition between flames that are anchored at the lips of the injector and flames that are lifted. To do this, AVBP is coupled to AVTP, the heat transfer solver of CERFACS which computes the temperature in all solid walls of the chamber.

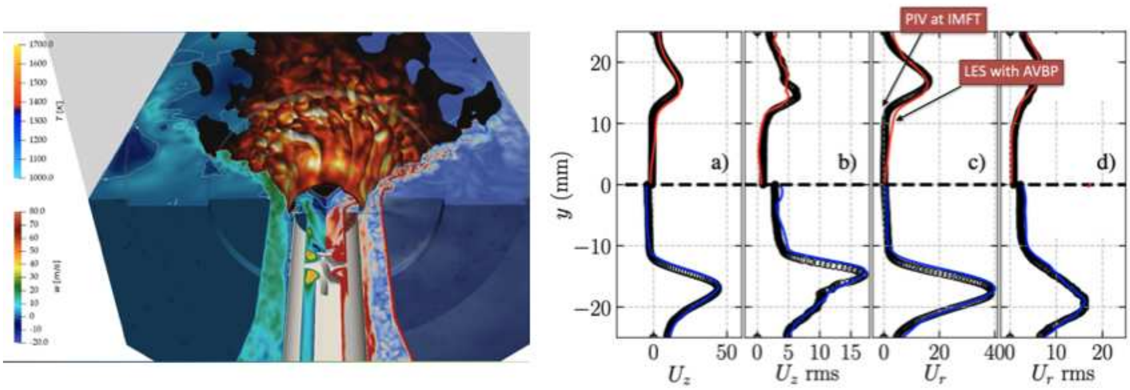

Figure 3.9: AVBP results for the HYLON H2 air swirled flame [CFD108, CFD172]. Left: a snapshot of velocity and isosurface of temperature. Right: axial and radial velocity profiles (mean and RMS). PIV vs time-averaged LES data.

3.3.3 High pressures, large domains hydrogen flames

The present state of the art is that LES computations of AVBP at one bar in domains of reasonable sizes are quite precise as seen in Fig. 3.9. The impact of flame-turbulence modeling is indeed relatively weak in these cases so precision depends only on chemistry models. Unfortunately, real applications differ from small-scale experiments. Pressure is much higher and the domains to compute significantly larger. The main challenge for modeling is therefore to extend the precision reached today at one bar for small chambers, in two directions:

- High pressures as found in the propulsion applications handled by CERFACS for SAFRAN for example. Typically, going to 20 bars is a minimum.
- Large sizes are a second issue, especially for safety applications where domains of the order of tens of meters are common.

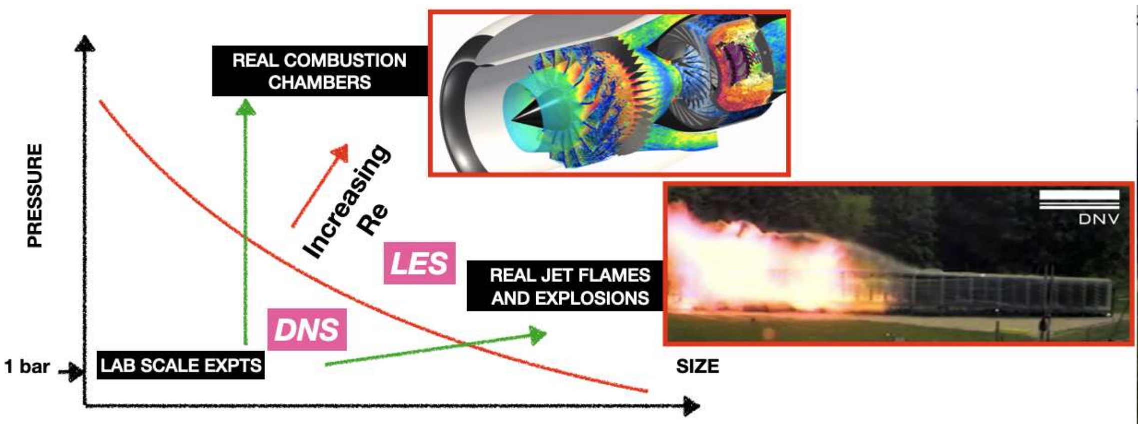

Figure 3.10: The challenges of hydrogen combustion: going to high pressures (for propulsion applications, furnaces, etc) and/or large domain sizes (for explosions).

For both needs (high-pressures and large domains), modeling becomes critical. First, the flame front thicknesses become much thinner, and at 20 bars, for example, this creates a resolution need that can not be reached anymore. Second, the flow structure itself is much more turbulent as measured by the Reynolds number which goes up when pressure goes up (since the kinematic viscosity goes down like $1/P$) and when the domain size increases. Figure 3.10 illustrates this evolution which is now the center of CERFACS activities and requires the development of reliable subgrid models since pure force itself can not be used anymore. An additional difficulty is the lack of reliable data in those high Reynolds flames. For high pressures, CERFACS has been collaborating with ONERA and KAUST in various projects to construct databases sharing the HYLON injector to go at higher pressures (typically 8 to 12 bar) to validate codes in these conditions. The development of new flame turbulence models is the most critical aspect of this work.

3.4 Sustainable Aviation Fuel (SAF) combustion

Drop-in Sustainable Aviation Fuels (SAFs) are thought of as a short-term solution to reduce the emissions of the aviation sector. Numerical investigation is useful to provide information on the differences between the use of SAFs and conventional Jet-A1 fuel in real combustors. In the framework of the H2020 JETSCREEN project and the PhDs of Q. Cazères [CFD254], J. Wirtz [CFD280] and V. Shastry [CFD275], conventional Jet-A1 fuel has been compared to an Alcohol-to-Jet (At-J) and a high aromatic alternative fuels in configurations with increasing complexity, from one-dimensional laminar spray flames to turbulent spray flames. Using the in-house reduction ARCANE co-developed with Cornell University, the fuel effect has been taken into account for these three fuels using a three-component surrogate fuel model and an Analytically Reduced Chemistry (ARC) for computing the gas phase reactions. Additionally in the in-house LES solver AVBP, a discrete multi-component model for spray vapourisation has been implemented and the TFLES turbulent combustion model has been adapted to multi-component fuels. Such a modeling approach has enabled to study the impact of SAFs on various configurations.

In one-dimensional laminar spray flames [CFD201], the preferential evaporation effect, unique to multicomponent fuels causes a variation of fuel vapour composition on both sides of the flame front and this has a direct impact on the spray flame structure and propagation speed. In rich cases, multiple flame structures exist due to the staged release of vapours across the reactive zone. Spray flame speed correlations originally proposed for single-component fuels have been extended to multi-component fuels and may be used in turbulent combustion modeling of multicomponent sprays.

In the Standard Spray Burner experimentally studied at DLR [CFD97, CFD96], LES has been performed for the three fuels, showing a good agreement between the experimental and numerical flows and flames. The multi-component fuel description leads to structural differences in how fuel vapor is spread inside the chamber. Moreover, differences between the fuels in the chamber's thermal behavior have been explained by different levels of preferential- and pre-evaporation, which modifies the location of the combustion process.

Finally, the LOTAR semi-industrial configuration operated at moderate pressure at ONERA Fauga has been studied to predict and understand the potential effects of staged vaporization and consumption of the fuel components, and their impact on the spray flame structures [CFD201, CFD85]. LES has confirmed the capacity of the methodology developed to reproduce the role of preferential evaporation in establishing and stabilizing the reaction zone. JetA-1 evaporation zones extend deep into the rich burnt gasses resulting in a combustion regime with the possibility of droplet clusters burning individually. On the contrary, At-J which is more volatile leads to complete combustion with the majority occurring due to the premixed lean reactions of the smaller pyrolysed components (Fig. 3.11).

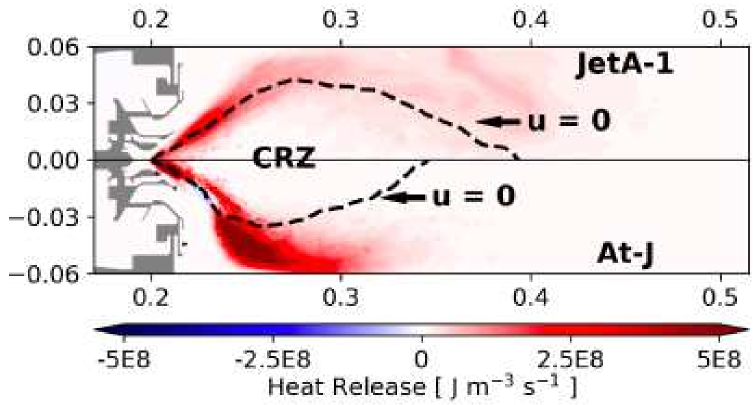

Figure 3.11: Fuel effect in the LOTAR turbulent spray flame configuration from ONERA Fauga: Time-averaged heat release field for conventional Jet-A1 fuel (top) and At-J fuel (bottom).

The methodology and tools developed to study the impact of SAFs are today mature to 1. study the impact of SAFs on aircraft engine operability in terms of flame structure, high-altitude ignition capability, extinction limit, and combustion instabilities, and 2. extend such multicomponent fuel models to any alternative fuel (e.g. marine alternative fuels).

3.5 Soot and NOx pollutant emissions

Soot particles have been proven to play a part in both climate change and public health issues. Consequently, regulations on soot particles emission become more and more stringent, pushing aircraft engine manufacturers towards new solutions for both the combustor technology and the fuel. To support such developments, numerical simulation is an essential tool. However, modeling soot production is complex for four main reasons. First, soot particles inception is triggered by the collision of Polycyclic Aromatic Hydrocarbons (PAH) generated by the combustion process. Having an accurate description of the formation process of PAHs is thus of prior importance. Second, soot particles react at their surface with the gas phase (condensation of PAHs, oxidation by O2) as well as with each other (aggregation of particles). Having an accurate description of the reactions that soot particles undergo during their lifespan is also a major challenge. Then, soot population shows a large range of sizes and shapes depending on their history, which requires to solve their number density function. Finally, if soots are initially spherical, their evolution then results in the formation of large fractal aggregates which should also be modeled. Within the PhD of L. Gallen [CFD152] in the framework of the H2020 SOPRANO project, a methodology based on ARC with accurate PAH chemistry coupled to a semi-deterministic Lagrangian approach for soot particles (Lagrangian Soot Tracking (LST) method) has been proposed. The approach has been evaluated in both canonical laminar configurations and complex turbulent spray Jet-A1 flames, showing both good agreement compared to reference but expensive sectional methods and measurements as well as affordable computational cost.

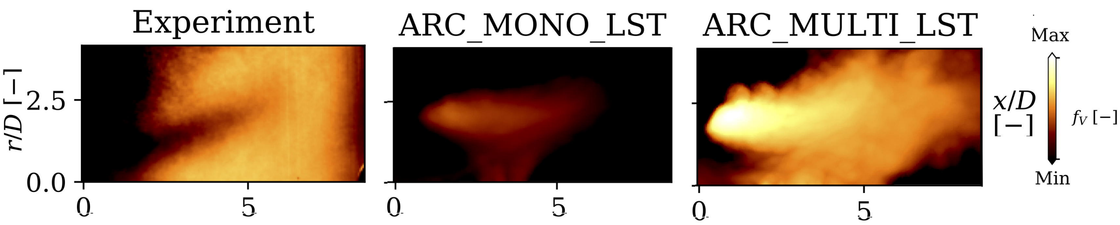

Figure 3.12: HERON RQL: cut fields of average soot volume fraction in the burner rich zone. Comparison of experiment (left), LES with a mono-component fuel model (middle), and LES with a multi-component fuel model (bottom). Results are represented in logarithmic scale.

In the PhD of E. Lameloise (2020-2024) in the framework of the ANR ASTORIA project (2018-2023) led by CERFACS, the objective was to extend this methodology to real fuels, accounting for multi-component fuel composition at a reasonable computational cost. This was achieved in several steps, starting from the selection of the detailed kinetic model for combustion and soot precursors growth, followed by the determination of a multi-component fuel surrogate model describing the complex real fuel blend. Finally, the selected kinetic model was analytically reduced with the reduction code ARCANE while controlling the error on flame properties and soot prediction for the considered fuel surrogate. To perform all evaluation and reduction tests on canonical sooting flames, a Discrete Sectional Model (DSM) for soot was also implemented in the open-source kinetic solver Cantera. The resulting code (Cantera-soot) is now available for the fast calculation of soot production in laminar flames for any fuel. The obtained reduced kinetic scheme was finally validated in the HERON Rich-Quench-Lean (RQL) burner measured at CORIA, in terms of soot prediction capabilities by comparison of LES coupled to the LST model with measurements (Fig. 3.12). Results showed a significant improvement in the soot level prediction when using the reduced chemistry based on a multi-component surrogate fuel model compared to a mono-component surrogate model, which also allowed a more detailed analysis of the soot emission mechanisms.

To improve the numerical predictions of soot in such complex configurations, the next steps consist of both improving the soot oxidation model which lacks reproducing the physical oxidation process whatever the soot model employed and accounting for soot morphology. In parallel, the effect of fuel will be studied by combining the approach developed for complex fuel modeling with the LST approach.

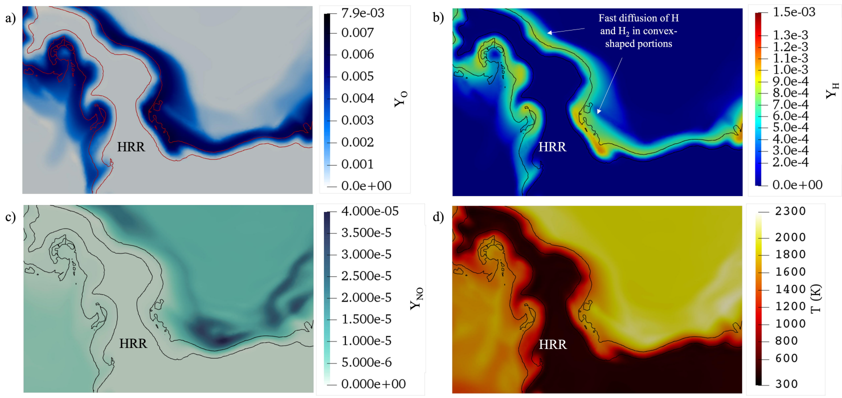

Figure 3.13: TUB Burner: Instantaneous fields of O, H, NO mass fractions and temperature in a vertical cut plane close to the chamber inlet.

For similar severe environmental and human health consequences, stringent regulations have also been put forward on NOx emissions. Consequently, NO prediction is also mandatory in the development of novel combustion devices. Including NOx in LES of turbulent flames is simpler than soot, mainly because it is a gaseous chemical process only. As a first step towards decarbonized and renewable alternative fuels, the capacity to accurately predict NOx in turbulent hydrogen/air flames has been shown in the post-doctoral work of T. Capurso [CFD119]. High-fidelity LES of a 3D partially premixed turbulent flame, whose experiments have been performed at the Berlin Institute of Technology (TUB) accounting for NOx production. To properly capture the right level of NOx, a new skeletal kinetic scheme for H2/air combustion (15 species and 47 reactions) has been reduced on purpose using ARCANE from the detailed CRECK mechanism taking into account all the NOx pathways. With the purpose to accurately solve the combustion process and the NOx production level, the static mesh refinement (SMR) and the conjugate heat transfer (CHT) techniques have been applied and their impact on the numerical solution was discussed. A detailed analysis (Fig. 3.13) of the preferential diffusion and NO formation was presented proving that the numerical model for 3D turbulent flame including complex transport phenomena and the new H2/air reduced chemistry can both accurately reproduce NOx emissions at the burner exit by comparison with measurements and predict the NO dynamic formation accounting for the primary and secondary routes: N2O and NNH.

Future work will focus on NOx for heavier hydrocarbon and drop-in SAFs. However, NOx measurements remain scarce for heavy fuels like n-heptane and heavier hydrocarbons, and recent experimental works tend to show that the most detailed chemical mechanisms used as a reference up to now may lack the accuracy to predict NOx in canonical flames, requiring additional optimisation prior being reduced [CFD69].

3.6 Low-temperature plasma modeling and simulation

Plasma applications and developments within AVBP followed two distinct paths. The first one addresses fundamentals of plasma physics and thrust generation intending to develop dedicated solvers taking advantage of the massively parallel environment of AVBP. The second one addresses more directly issues related to combustion and the potential interest of introducing plasma in this framework.

3.6.1 Hall-effect thrusters

Mega-satellite constellations will be mainly equipped with electric propulsion systems, and in particular Hall-effect thrusters, in which neutrals (typically xenon) are ionized and placed in an electric field to accelerate and produce thrust. The design of such thrusters is however not straightforward as the underlying physics is very complex and not yet fully understood, which leads manufacturers to carry out costly and laborious experimental campaigns. Numerical simulations, either based on Particle-In-Cell (PIC) or fluid methods are therefore very helpful. However, they raise a number of modeling and computational issues, which are the subject of many research works reported in the literature.

To contribute to these challenges, and to assist SAFRAN Spacecraft Propulsion in the design of their electric engines, CERFACS is developing the AVIP code [CFD126] as a predictive tool capable of modeling industrial configurations. To do this, AVIP works with unstructured meshes, which is original in the community. The work reported here was performed in the framework of the thesis of W. Villafana [CFD278].

AVIP offers both PIC and fluid formulations. Because of its innovative character, important efforts

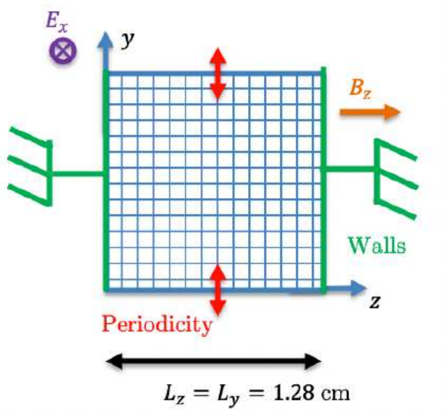

Figure 3.14: 2D radial-azimuthal (z; y) setup.

have been made to systematically validate AVIP. Participation to international benchmarks proved to be very useful. In 2019, AVIP (PIC) was applied to a $2D$ configuration in the axial-azimuthal plane for comparison with many international groups and obtained excellent results [65]. Still in the perspective of code validation, a $2D$ configuration in the radial-azimuthal plane (Fig. 3.14) was then studied in a benchmark work conducted by CERFACS and involving six international groups [CFD209]. In this test case, a radial-azimuthal instability, also called modified two-stream instability and coupled to the electron drift instability, was found (Fig. 3.15).

The validated AVIP (PIC) code was then used to simulate a $3D$ simplified Hall-effect thruster configuration [CFD208]. Such simulation was never performed before and allowed us to identify the $3D$ electron drift

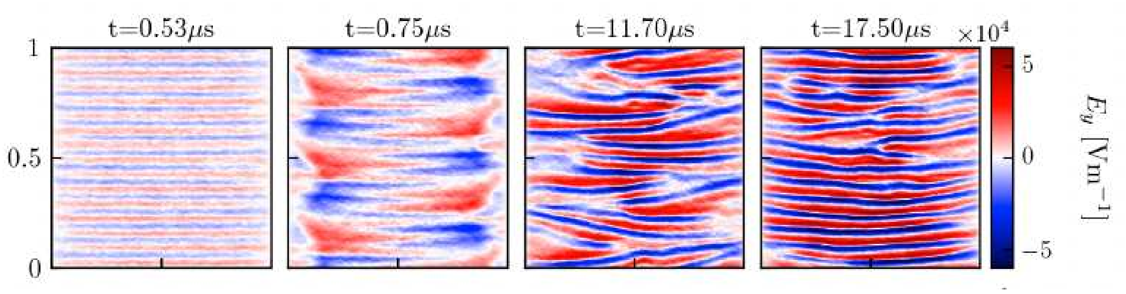

Figure 3.15: Snapshots of azimuthal electric field Ey in the 2D radial-azimuthal setup.

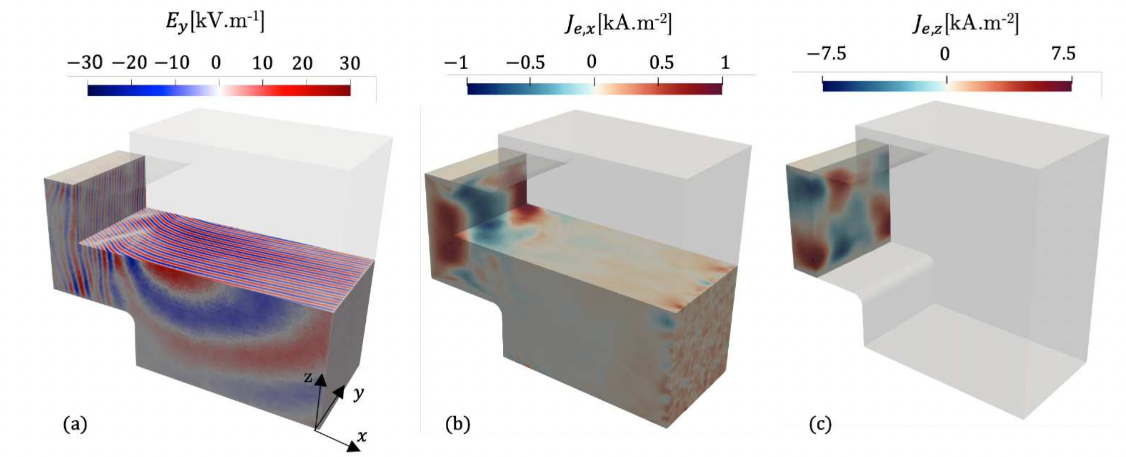

Figure 3.16: 3D clip view of the main reconstructed modes for (a) the azimuthal electric field, (b) the axial electron current density, and (c) the radial electron current density.

instability as well as a possible signature of the radial-azimuthal instability. In comparison with previous $2D$ cases, taking into account the 3 dimensions was found to affect plasma properties and therefore all oscillatory phenomena. Beyond these findings on physics, this simulation demonstrated the capability of AVIP to achieve $3D$ simulations on unstructured grids, which is a crucial step towards numerically-assisted thruster design.

3.6.2 Plasma-assisted combustion

The mitigation of pollutant emissions from both aircraft engines and power plants has risen as a significant concern for gas turbine manufacturers. This issue is a direct consequence of increasingly stringent environmental regulations and growing environmental awareness. One promising approach to minimize the formation of pollutants involves maintaining a relatively low temperature in the primary combustion zone of engines and power plants. This can be achieved by reducing the mixture equivalence ratio. However, the challenge with this approach is that lower flame temperatures can lead to slower chemical reaction rates, which in turn, may result in flame instability and even flame extinction.

An emerging solution to address the challenge of igniting and stabilizing flames under leaner conditions involves the generation of electrical discharges at the base of the flame. Among these various types of discharges, Nanosecond Repetitively Pulsed (NRP) discharges have demonstrated notable efficiency. Despite their proven effectiveness, there remains a significant gap in our understanding of the fundamental mechanisms behind plasma-assisted combustion. In particular, tools relevant to industrial applications have to be developed to bridge the gap between research and industry needs. Several of these issues are being considered individually as detailed hereafter.

Plasma-combustion chemistry

The fundamental principles of plasma-assisted combustion lie in the chemical interactions of discharges with their surrounding environment. Indeed, chemistry plays a central role in driving the majority of observed effects, encompassing rapid radical production, as well as fast and slow gas heating. A CERFACS numerical tool has been developed to address non-equilibrium plasma chemistry, leveraging the Cantera solver and an EEDF solver [68]. This tool facilitates an in-depth exploration of plasma chemistry, including the plasma phase, coupled with conventional combustion chemical mechanisms. Using this tool, an exhaustive plasma mechanism has been meticulously built and subsequently validated for plasma-assisted methane combustion, as detailed in [66]. Furthermore, adaptations within the ARCANE library [64] have been introduced to accommodate the plasma peculiarities. Consequently, comprehensive chemistry analysis and mechanism reduction have been done to perform the simulations outlined in Sections 3.6.2 and 3.6.2.

Fully coupled plasma-assisted ignition simulations

Enhancements to a in-house streamer code have been made to enable its use on an unstructured grid comprising triangles and tetrahedra. Specifically, a vertex-centered version of the Lax-Wendroff scheme with a Sweby limiter [71] has been successfully implemented and tested on the Bagheri [62] benchmark, as illustrated in Fig. 3.17 and documented in [67, CFD256, CFD251].

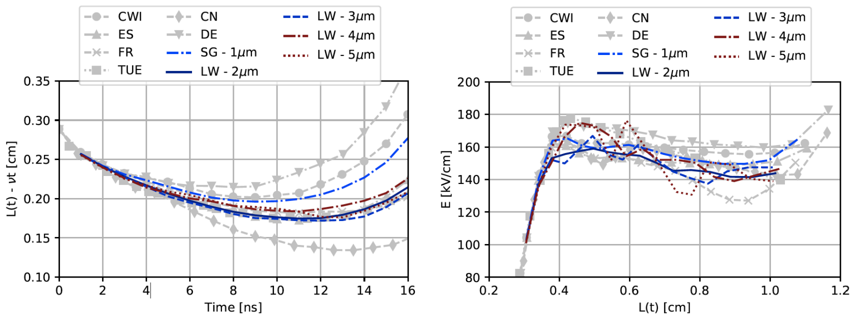

Figure 3.17: Comparison of the steamer code results with those of [62] for case 1 using triangular elements: (left) L(t) - νt versus time (ν = 0.05 cm.ns^{-1}) and (right) maximum electric field versus streamer length.

The streamer code has then been coupled to the reactive compressible Navier-Stokes equations, solved within the framework of AVBP, to investigate the ignition of a lean gaseous methane-air mixture in a pin-pin configuration [CFD113]. For that purpose, a reduced plasma-combustion mechanism, derived using the tools described in previously has been incorporated into the AVBP-PAC code. This integration has been enabled through the inclusion of the EEDF solver, BOLSIG+, within the code. The investigation encompasses both single-pulse and burst-of-pulse scenarios, which have been systematically compared to ignition induced solely by heat deposition as shown in Fig. 3.18. This comprehensive exploration has revealed the essential role of plasma chemistry in accelerating ignition and diminishing the Minimum Ignition Energy (MIE). Notably, the synergistic effects of low-energy deposition at high frequencies have been identified as particularly efficient in the context of ignition.

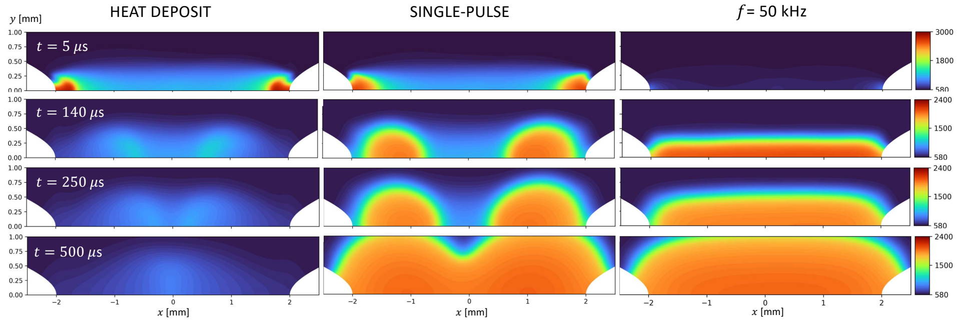

Figure 3.18: Temperature fields in Kelvin at different instants for the Heat Deposition, Single-Pulse and 50 kHz-Burst-of-pulse cases (left to right) with an energy deposition of 500, 500 and 350 μJ respectively.

Phenomenological modeling of plasma-assisted combustion

Fully coupled simulations, such as the one described before , are computationally expensive and are unsuitable for practical applications relevant to industry. To address this limitation, the team developed a reduced-order model for plasma-assisted combustion (referred to as PACMIND [CFD112]) based on the foundation provided by the Castela model [63]. The PACMIND model is based on the utilization of tabulated coefficients, which are systematically computed using the tools and chemistry discussed above , incorporating essential species and processes.

The simplicity and computational efficiency of the PACMIND model allow for its seamless integration into Large-Eddy Simulations (LES) of $3D$ turbulent combustion scenarios, with a minimal computational overhead. To assess its performance, the PACMIND model has been rigorously validated through comparisons with experimental data [69] and multi-dimensional coupled plasma-combustion simulations. The results demonstrate a significant accuracy enhancement, particularly in modeling kinetic effects and rapid gas heating, resulting in improved precision in predicting ignition processes for a wide range of operational conditions as shown in Fig. 3.19. In conclusion, the PACMIND model represents a valuable tool for understanding the impact of NRP on combustion processes, with promising potential for a wide range of applications such as ignition, lean blow-off extension, and instability mitigation.

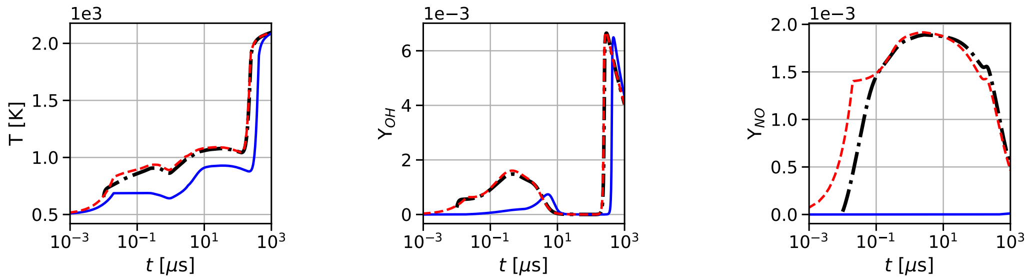

(a) (b) (c)

Figure 3.19: Time evolution of selected quantities in the middle of the 4 mm gap in a pin-pin configuration [CFD112]. Comparison between (black - dash-dotted) Reference AVBP-PAC (blue - solid line) AVBP Castela and (red - dashed) AVBP PACMIND.

Plasma-assisted flame stabilization

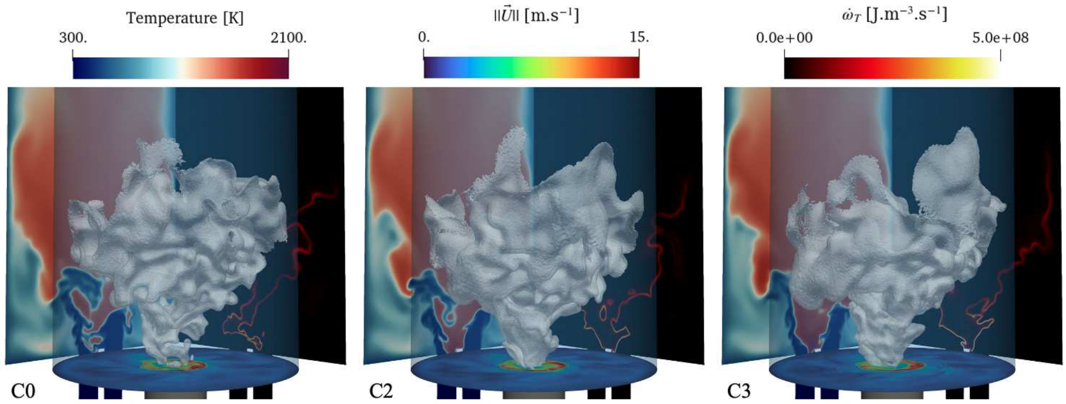

Figure 3.20: Simulation of the PACCI burner with thermal flame power of 4 kW [70]: without plasma (C0-left), 20 kHz - 28.8 W mean plasma power (C2-middle) and 30 kHz - 46.8 W mean plasma power (C3-right).

The PACMIND model described above has been used to numerically investigate the use of Nanosecond Repetitively Pulsed (NRP) discharges to enhance flame stabilization in a swirl burner [CFD114, 70]. First, a simulation of a lean atmospheric pressure scenario ($\phi = 0.67$), without plasma actuation, has been conducted and compared with experimental OH* chemiluminescence images. Both the numerical and experimental results unveil the presence of an unstable turbulent flame with intermittent attachment to the injection exit. Then, two plasma-actuated conditions have been investigated. In both cases, a significant stabilization effect has been observed, showing that NRP discharges can effectively suppress flame lifting (See Fig. 3.20). Good agreements with experimental results have been obtained regarding the upstream shift of the flame centre of gravity. Results also show that a net power gain is obtained by applying NRP discharges to combustion by comparing the thermal flame power to the plasma power. In particular, an increase in plasma actuation efficiency from 4 to 6 has been observed in the cases studied when increasing the plasma power.

3.7 Two Phase Flow

Two-phase flow physics is a key feature of many industrial burners and it is recognized as of first-order importance in many combustion applications. Due to this importance, two-phase flow modeling has been very early at the center of many developments within the AVBP team. Recent efforts have in that respect been focused on improving the code capacity in providing detailed atomization physics description while improving more heuristic Lagrangian-based methods existing today for real applications.

3.7.1 Diffuse interface method

Two numerical methods are investigated at CERFACS for the prediction of liquid atomization under gaseous shear. Note that both approaches intend to predict the large primary droplets resulting from primary atomization. These large subsequent droplet history is then modeled under a Lagrangian dedicated formalism. Only the primary atomization process is here discussed.

Both investigated approaches rely on the diffuse interface method. The first one uses a 3-equation model closed thanks to a cubic equation of state, well-suited for super-critical or trans-critical conditions. This model accounts for surface tension in sub-critical conditions and can predict the sub-critical to super-critical transition. It has allowed the prediction of a liquid core length under realistic pressure conditions, for a non-reactive rocket engine simulation [CFD53].

The second model consists of a 4-equation model, closed thanks to a Noble-Abel Stiffened Gas equation of state. Such equation of state is well suited for subcritical conditions. This methodology has allowed simulations of air-assisted liquid film at rather low pressures. It has also allowed to investigate the effect of the chamber pressure on the interfacial dynamics, with very good agreement when compared to theoretical frequencies predicted by linear stability analysis [CFD189]. Such good agreement opens the door to spray-acoustics interaction simulations. Note that an evaporation solver has also been implemented and validated in this later context and future work will investigate evaporating liquid under reactive conditions.

3.7.2 Lagrangian modelling for industrial applications

When dealing with industrial applications, two strategies are possible.

In the first approach, dedicated modeling capacities and numeric are present in the code to treat the intricate physics of primary atomization. This framework is typical of the previously described actions. In that case and for efficient simulations, a Lagrangian simulation framework is usually adopted to carry on the prediction and consider the subsequent processes of atomization and evaporation. A key feature in such approaches is the transfer between the primary atomization modeling module which is most a Euler-based formalism and its Lagrangian counterpart.

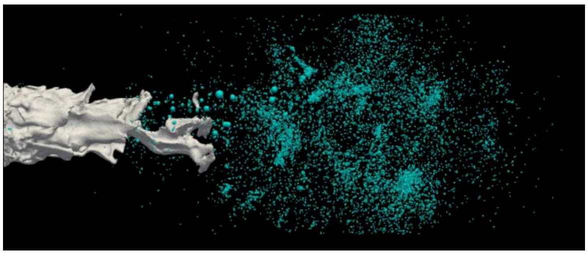

Figure 3.21: Eulerian-Lagrangian transition for spray atomization

To do so a dedicated algorithm has been developed and implemented in AVBP which automatically detects closed liquid structures, evaluates their volume, shape, momentum, temperature, and creates a single, or multiple lagrangian droplets with similar physical characteristics if physical and geometrical criteria are reached (Fig. 3.21). These primary droplets are then submitted to secondary atomization through the already existing stochastic model FAST in AVBP.

In the second approach, a purely Lagrangian framework is adopted to cover the entire physics, and dedicated models have been improved for practical use in realistic industrial configurations. Typically, the PAMELA model, accounting for primary atomization downstream of a lip has been reworked to remove any user input parameters. The joint use of existing lagrangian models in AVBP has proven its accuracy and reliability on several industrial use cases, both reactive and non-reactive ([CFD121, CFD202]) (Fig.3.22).

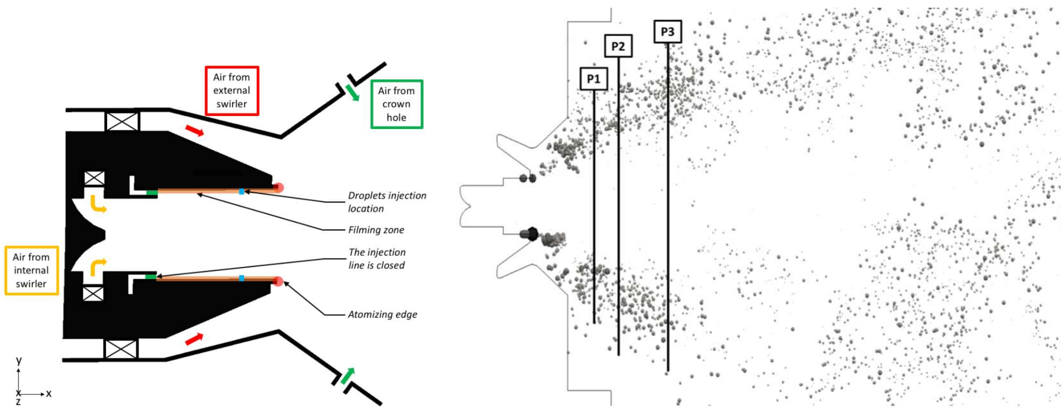

Figure 3.22: Realistic fuel injector and resulting spray generated thanks to lagrangian models.

References

[62] B. Bagheri, J. Teunissen, U. Ebert, M. M. Becker, S. Chen, O. Ducasse, O. Eichwald, D. Loffhagen, A. Luque, D. Mihailova, J. M. Plewa, J. van Dijk, and M. Yousfi, (2018), Comparison of six simulation codes for positive streamers in air, *Plasma Sources Sci. Technol.*, **27**, 095002.

[63] M. Castela, B. Fiorina, A. Coussement, O. Gicquel, N. Darabiha, and C. O. Laux, (2016), Modelling the impact of non-equilibrium discharges on reactive mixtures for simulations of plasma-assisted ignition in turbulent flows, *Combust. Flame*, **166**, 133–147.

[64] Q. Cazères, P. Pepiot, E. Riber, and B. Cuenot, (2021), A fully automatic procedure for the analytical reduction of chemical kinetics mechanisms for Computational Fluid Dynamics applications, *Fuel*, **303**, 121247.

[65] T. Charoy, J.-P. Boeuf, A. Bourdon, J. A. Carlsson, P. Chabert, B. Cuenot, D. Eremin, L. Garrigues, K. Hara, I. D. Kaganovich, et al., (2019), 2D axial-azimuthal particle-in-cell benchmark for low-temperature partially magnetized plasmas, *Plasma Sources Science and Technology*, **28**, 105010.

[66] L. Cheng, N. Barleon, B. Cuenot, O. Vermorel, and A. Bourdon, (2022), Plasma assisted combustion of methane-air mixtures: Validation and reduction, *Combustion and Flame*, **240**, 111990.

[67] L. Cheng, N. Barleon, O. Vermorel, B. Cuenot, and A. Bourdon, (2021), AVIP: a low temperature plasma code, *arXiv preprint arXiv*.

[68] G. J. M. Hagelaar and L. C. Pitchford, (2005), Solving the Boltzmann equation to obtain electron transport coefficients and rate coefficients for fluid models, *Plasma Sources Sci. Technol.*, **14**, 722–733.

[69] D. Rusterholtz, D. Lacoste, G. Stancu, D. Pai, and C. Laux, (2013), Ultrafast heating and oxygen dissociation in atmospheric pressure air by nanosecond repetitively pulsed discharges, *J. Phys. D Appl. Phys.*, **46**, 4010–.

[70] F. D. Sabatino, T. F. Guiberti, J. P. Moeck, W. L. Roberts, and D. A. Lacoste, (2020), Actuation efficiency of nanosecond repetitively pulsed discharges for plasma-assisted swirl flames at pressures up to 3 bar, *J. Phys. D Appl. Phys.*, **54**, 075208.

[71] E. Toro, (2009), *Riemann Solvers and Numerical Methods for Fluid Dynamics: A Practical Introduction*.

[72] G. Wang, F. Duchaine, D. Papadogiannis, I. Duran, S. Moreau, and L. Y. M. Gicquel, (2014), An overset grid method for large eddy simulation of turbomachinery stages, *Journal of Computational Physics*, **274**, 333–355.

Applications

4.1 Introduction

Application is the final objective of CFD. When it comes to CERFACS, it is also the link to CERFACS' industrial partners. It finally allows the demonstration of the team and code capacities to address leading edge problems by the use of the most advanced HPC facilities while producing valuable data on these dedicated flows. The following presents therefore recent progresses on various subjects covered in the past years.

4.2 AVBP-based LES and Application

4.2.1 Full engine simulations

Numerical simulation of multiple components in turbomachinery applications is very CPU-intensive but is still necessary in the majority of cases to achieve correct coupling and reliable flow prediction. During the design phase, however, the cost of simulation is an important criterion that often defines the numerical methods to be used as well as the size of the computational to consider for a given engine component. For such reduced size simulations, the use of realistic boundary conditions capable of accurately reproducing the coupling between components becomes of great if not of crucial interest, and thus justifies the need for simulations of multiple components configurations.

In this context, the last three years saw the advent of several breakthroughs in high-fidelity simulations of multiple component configurations, supported by 60 million CPU-hours through CPU allocations like PRACE, GENCI, or "Grand Challenge" (roughly $1,2$M euros).

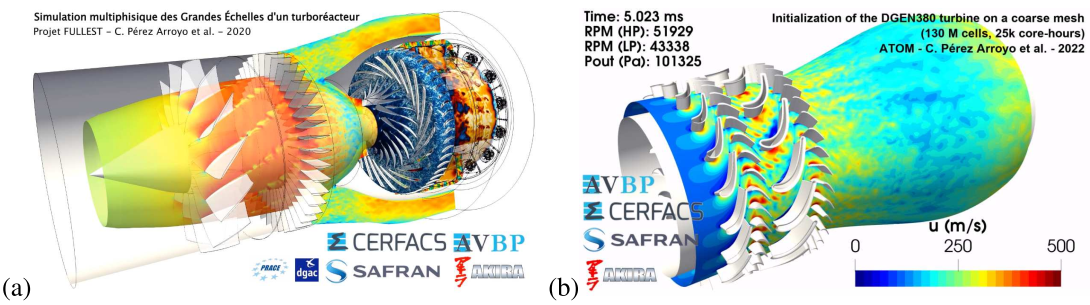

Figure 4.1: (a) DGEN380 engine configuration from inlet to combustion chamber and (b) its full 360 degrees turbine stages.

In 2021, the first 360-degree coupled Large-Scale Simulation of the DGEN380 engine (Fig. 4.1 (a)) was carried out, including inlet, fan, rectifiers, bypass, radial compressor and combustion chamber [89, 91, 92].

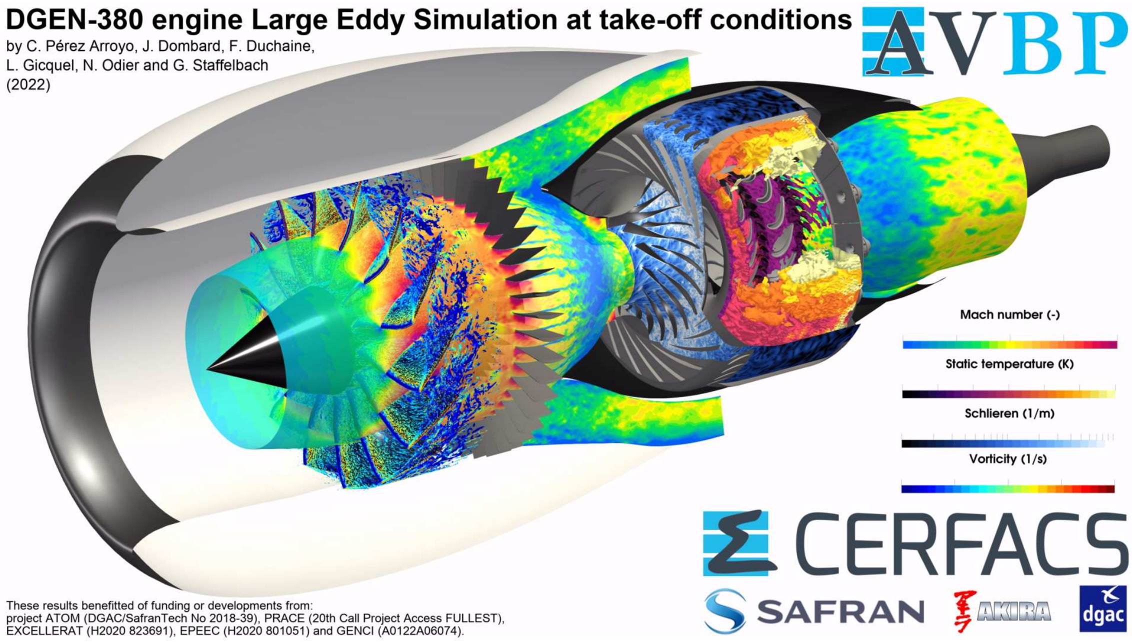

Figure 4.2: DGEN380 motor configuration from Fan inlet to turbine outlet.

This simulation of over $2,000$ million cells was carried out using the PRACE allocation named FULLEST. Although unique in terms of achievement, this first simulation only covered the first aft part of the true engine: *i.e.* with the missing turbine stage for it to be a true full engine simulation. Thanks to the GENCI A12 allocation, an occasion to add the turbine stages was given to the team. This new challenge in which the true full-engine LES could be achieved was covered in two stages: first, the 360-degree isolated turbine stage was considered geometrically and simulated to be then added to the FULLEST original simulation domain.

The isolated turbine was first set up and calculated in 360 degrees (Fig. 4.1(b)). As illustrated, this turbine has two stages (high and low pressure) with prime numbers of blades, making it impossible to periodize or simulate in a reduced size domain unless major hypotheses are enforced on the flow behavior. To reduce computational costs, the simulation was first initialized on a coarse mesh of 130 M cells using inflow information extracted from the FULLEST prediction. This first coarse grid prediction was then interpolated on a fine mesh of 280 M cells to take the last turn of the high-pressure turbine wheel, which rotates at over 50k rpm. The cost of this transient phase was 50k computing hours on the TGCC's Irene Rome machine.

Following these two initial steps, the complete calculation has been performed. One key to this goal was the capacity to handle the mesh generation of such a complex multi-component configuration. To leverage this critical step, the adaptation parallel tool currently under development within CERFACS, TreeAdapt / TreePart [86] appeared valuable. Indeed, this tool made it possible to manipulate and refine an initial mesh composed of 50M cells up to $1,200$M cells in less than 20 minutes on 760 Icelake cores. This tool was also used to partition the mesh. The final mesh size for the full engine ended up not exceeding $2,200$ million cells, as refinement and adaptation were limited to certain parts of the domain to avoid having too heavy of a mesh. The full engine setup was finally run for 8 ms of physical time, consuming around 2M CPU hours,

Fig. 4.2.

This simulation resulted in a demonstration of capacity pictured in Fig. 4.2, the associated video, as well as 20 TB of data. Unfortunately, the cost of such a calculation will not allow to analyze the physics of chamber-turbine coupling, nor to publish scientific papers. For the time being, however, this demonstration remains a very important milestone and showcase as well as a proof-of-concept for CERFACS and its partners.

The problem of combustion/turbine interaction being at the root of many modeling questions in terms of design practices in the industry, a specific collaboration with SAFRAN Tech has been initiated on this issue. To do so, the experimental test bench named BEARCAT (Banc d'Essai Avancé pour la Recherche en Combustion et Aérothermique des Turbomachines) developed by Safran Tech has been considered for such full multi-component simulations. BEARCAT, based on the Makila engine and located at Bordes (Safran Helicopter Engines), is a highly instrumented engine test bench for the hot section of real engines and intends to cover the lack of a representative partial test facility. It aims to fill the gap in measurements for these hot, confined environments and is dedicated to the fine characterization of the flows in the combustion chamber as well as the high-pressure turbine. Preliminary simulation results, shown in Fig. 4.3 proved that the tools and setup developed for the DGEN simulation are functional. Post-treatments are under analysis. To the best of our knowledge, this test rig is the only one of its kind in the world and shows great potential for publication.

Figure 4.3: 360 degrees simulation of the BEARCAT configuration, from the combustion chamber to the two-stage high-pressure turbine.

4.2.2 Liquid rocket engines (LRE)

As the market of space applications, and therefore the demand for space launchers grows, it becomes more and more competitive and the question of profitability is currently reevaluated. Among others, potential leverages such as reusability have emerged as a major one, as illustrated by the success of the Falcon 9 of SpaceX, the demonstrator Callisto (CNES/DLR/JAXA cooperation) or the demonstrator program Themis by ESA and ArianeGroup. In this context, new designs must be developed, for which accurate simulations are of crucial help. CERFACS works on the two major elements of an LRE: the combustion chamber and the nozzle.

Combustion and heat transfer in LRE chamber

Combustion efficiency and heat transfer in various regimes (subcritical and transcritical) with methane-LOx ergols are major elements of chamber design. Indeed, despite its lower performance, methane is more and more considered in place of hydrogen for competitiveness and its practicality in terms of usage and storage. Switching to methane raises however new questions about flame stability and ignition [CFD83]. To answer them, Large Eddy Simulation (LES) is performed with the code AVBP, using realistic reduced finite rate chemistry with about 15 species. To cope with the high stiffness of methane oxy-combustion at high pressure, a new integration method for the chemical source terms was proposed, allowing to save significant computational cost while preserving the result accuracy [CFD115, CFD178]. Another particularity of the combustion in LRE is a purely non-premixed regime, for which a turbulent diffusion flame modeling is required. First steps were made in [CFD131], showing the impact of mesh resolution on diffusion flames. Figures 4.4a and 4.4b illustrate a typical methane-LOx flame obtained by LES in a configuration representative of a LRE combustion chamber. The complex flame structure demonstrates the need to use semi-detailed chemistry for this type of configuration. This is made possible only with the new chemistry integration method which handles the stiffness of the chemical system.

The use of reduced chemistry also allows to predict more precisely the wall heat fluxes. To confirm such observations, periodic turbulent channels are computed to compare the resolved and non-resolved turbulent boundary layer, with or without chemical reactions. Indeed, results obtained in such turbulent channels show that the near-wall reactions may have a real impact on wall heat fluxes and that wall models should take into account this effect in the context of wall-modeled LES [CFD252]. A first attempt was made in [CFD116], based on a stochastic-based approach and applied to two test cases: the supercritical 5-injectors GCH4/GOx from ONERA and the subcritical single-injector GCH4/LOx from TUM. Figure 4.5 shows the good agreement obtained between the heat flux predicted with LES and the measurements. Finally, the use of conjugate heat transfer modeling was found to significantly improve the heat flux prediction [CFD187].

Flow Separation and Side-loads in LRE Nozzle

The design process is a critical issue to improve rocket engine performance. Among other subjects of importance in such a process, the capability of properly balancing the efforts applied on the engine exit nozzle is clearly a must for durability and control of flight. Reliable prediction of these aerodynamic forces and more specifically the off-axis loads, however still remains very challenging even for modern CFD methods. In an attempt to position CERFACS modeling and tools, the flow of an exit Mach number $Md = 3.5$ Truncated Ideal Contour (TIC) nozzle was numerically investigated by means of LES, using the unstructured compressible AVBP solver, shown in Fig. 4.6a. In such a configuration, an over-expanded regime characterized by a Free-Shock Separation (FSS) is addressed. To obtain accurate predictions of the flow while limiting the computational effort, an Adaptive Mesh Refinement (AMR) methodology is used. As a result, predictions show that a wall-modeled LES combined with AMR allows to adequately capture the jet flow dynamics while at the same time reducing the CPU time to exploitation of LES: both the location

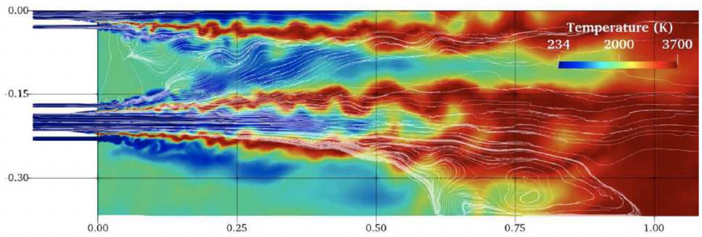

(a) Instantaneous temperature field with superimposed streamlines in a methane-LOx combustion chamber.

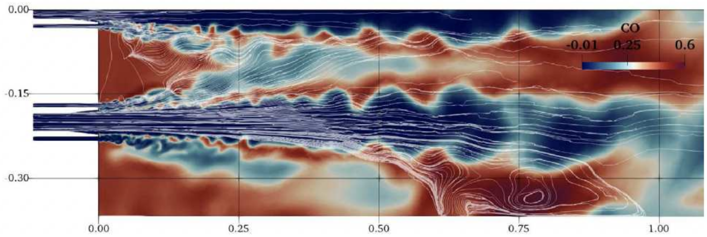

(b) Instantaneous CO mass fraction field with superimposed streamlines in a methane-LOx combustion chamber.

Figure 4.4: LES of Liquid Rocket Engines: combustion and heat transfer effects.

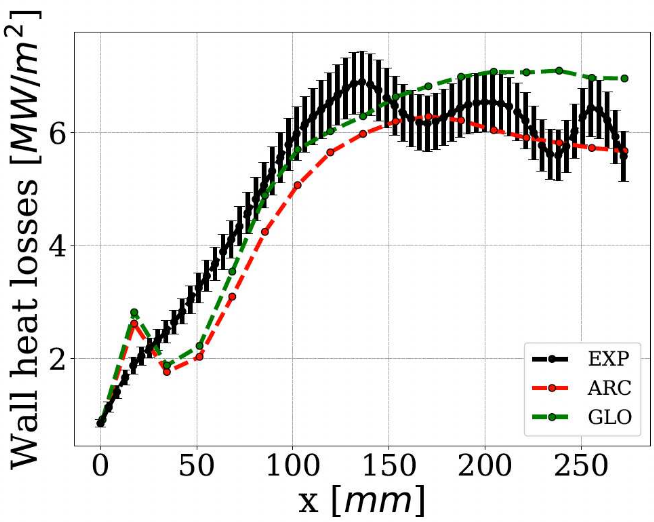

Figure 4.5: Averaged axial profile of wall heat losses obtained in the LES of the TUM configuration with reduced (ARC, w/o improved integration) and global (GLO) chemistry, compared to the experiment.

of the mean separation point and pressure fluctuations inside the nozzle are well captured (see Fig. 4.6b). In particular and from Fig. 4.6c, the two peaks of the pressure Power Spectral Density contributing to the

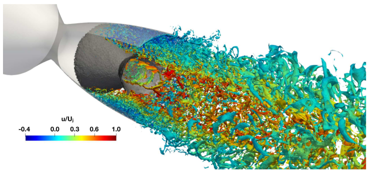

(a) Instantaneous flow field: iso-surface of the Q criteria

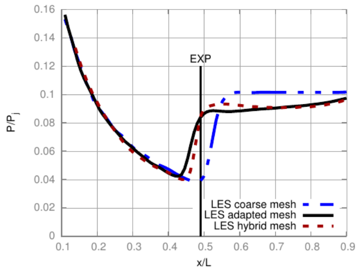

(b) Mean wall pressure

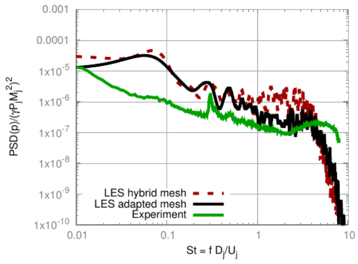

(c) PSD of fluctuating pressure

Figure 4.6: Prediction of flow separation and side-loads in rocket nozzle, from [82].

side-load mechanism are observed to be correctly predicted if compared to the experiment. Results have been published in [82].

4.2.3 Ignition

Under the increasing environmental constraints, the technology of aeronautical combustion chambers is moving towards lean operating conditions and the use of alternative fuels (so-called SAFs: Sustainable aviation Fuels). The subsequent design modifications must therefore be certified and in particular, engine relight at high altitude must be ensured after extinction due to water, ice, sand, or bird ingestion.

Ignition of a gaseous mixture was studied in a lab-scale configuration reproducing conditions of a spinning combustion (SCT) chamber [CFD130] under atmospheric conditions at first. This technology has several advantages, among which improved igniting capability, greater temperature homogeneity at the combustor exit, and reduced mass and cost. Ignition was studied experimentally in the Radius test case of PPRIME Institute. It consists in a constant volume vessel composed of a cylindrical chamber and equipped with a dynamic pressure gauge and optical access allowing pressure evolution measurements and high-frequency visualization. Special care was taken to accurately measure and control the energy deposited at sparking. The corresponding LES was able to reproduce the ignition event, as shown in Fig. 4.7. For this configuration, the parameter β used in the efficiency function of the thickened flame model was however found to significantly impact the results.

High altitude (10 km) conditions correspond to temperature and pressure of respectively $T = -40°\mathrm{C}$ (233K) and $P = 0.3$ bar. Such conditions are much detrimental for ignition, for both lower reactivity and fuel spray quality. These two aspects were studied in the PhD of A. Pestre [CFD271]. It was found that even though low pressure and temperature conditions significantly reduced the reactivity of the mixture, the chemical paths were not modified, so that reduced chemical schemes could be derived over a large validity range of pressure and temperature, allowing the simulation of ignition events. The ignition of a droplet mist proved however to be very complex, and difficult to achieve due to the very dilute spray usually found at the location of the ignition system. In [CFD74], the impact on ignition of the multi-component nature of liquid fuels was studied with Direct Numerical Simulation. Results clearly highlighted preferential evaporation effects, with a dominant role of the most volatile species in the early phases. The ARC scheme allowed to describe the endothermic pyrolysis of the fuel components, which was also found to play a role in the ignition scenario. Figure 4.8 illustrates this effect in a cut-plane of the ignition kernel.

Ignition is however a stochastic phenomenon, and the optimization of an ignition system is ultimately based on ignition probability maps. Building such maps from experiments or numerical simulations means

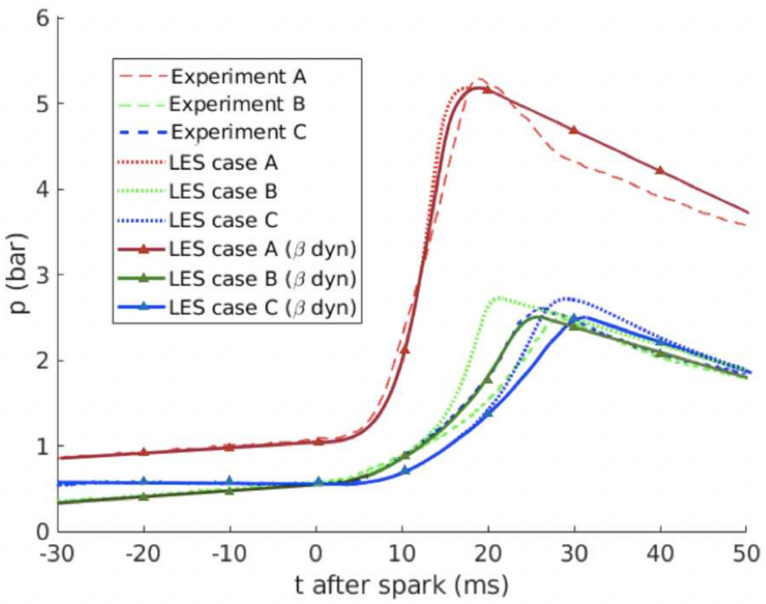

Figure 4.7: Pressure time evolution for the three cases obtained with the static and the dynamic efficiency formulations and compared to experiments.

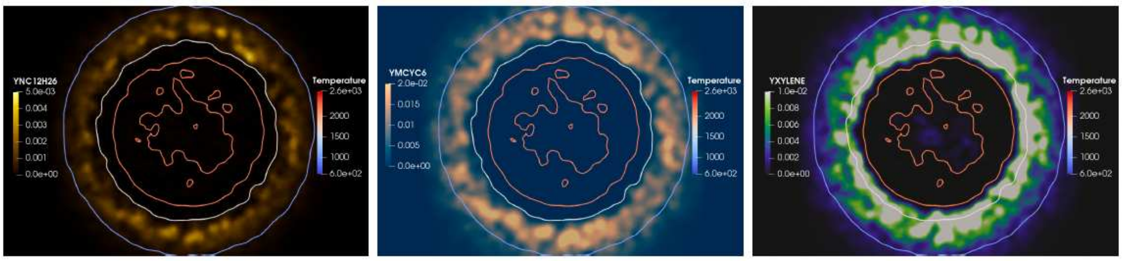

Figure 4.8: NC12 (left), MCYC6 (center) and XYL (right) mass fraction cut-plane fields with temperature iso-contours at T = 1000K; 1600K and 2200K, at t = 100 μs. The visualization window height is 1cm.

running a high number of tests, and is therefore far too costly. An alternative was proposed in [CFD146], where these maps are built from non-reacting flow statistics, i.e., with only one simulation or test. The originality of the approach is to construct statistical flame kernel trajectories and to combine them with local ignition criteria. Figure 4.10 illustrates the application to a swirled burner (Fig. 4.9) operated in premixed, non-premixed, and spray combustion modes, demonstrating the ability of the model to recover the experimental ignition map with good accuracy.

4.2.4 Safety

The topic of CFD for safety has grown rapidly in the last three years, leading to the creation of a dedicated research unit in the CFD team. Safety computations in the team include many scenarios linked to combustion but also to other fields. While many scenarios investigated at CERFACS involve a leak of

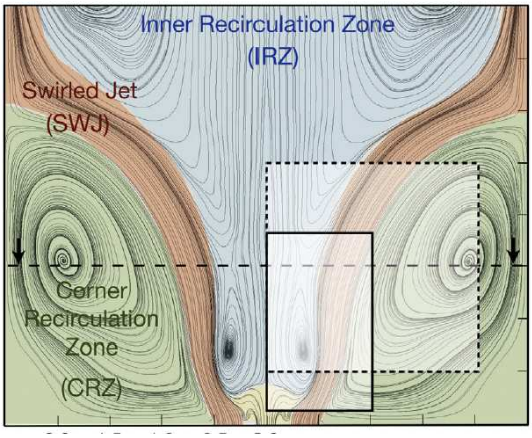

Figure 4.9: Ignition test case, non-reacting flow. Time-averaged pseudo-streamlines in a central x-normal plane. Swirled Jet (SWJ, red), Inner Recirculation Zone (IRZ, blue), and Corner Recirculation Zone (CRZ, green). Boxes respectively indicate the experimental ignition maps for premixed (P), non-premixed (NP) (plain), and Spay (SP)(dashed) cases.

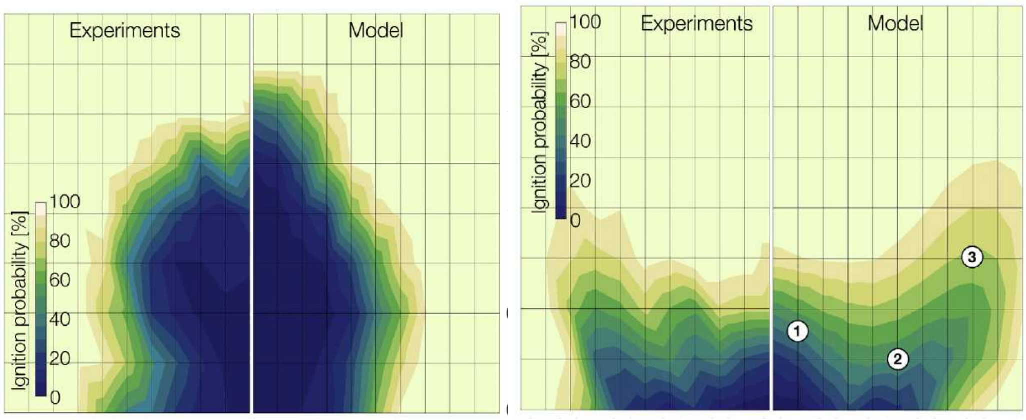

Figure 4.10: P (left) and NP (right) cases. Comparison between experimental (left) and MIST (right) ignition probability maps in the solid line box of Fig. 4.9.

combustible gas into the air, many other safety scenarios are also of interest. For example, the dispersion of viruses for example (Sect. 4.2.4) is a field where AVBP can be used directly. The safety of batteries is another problem where thermal runaway can lead to a sequence of events for which simulation is needed.

In the classical field of combustion, safety issues have become a key to many fields where decarbonization is ongoing. Many energy vectors indeed lead to situations where important quantities of pressurized gases have to be handled. For hydrogen, the corresponding lines and tanks can be at very high pressures (900 bar). Any leak can lead to various events of growing danger. With this new field of application for the team, CERFACS works with various industrial partners to evaluate scenarios and analyze them. These correspond to one of the main unsolved problems in the combustion community: how a flame accelerates when it travels between obstacles and if it stabilizes around the leak, what are the risks.

Explosions and transition to detonation

When a leak of gas does not ignite right away, the combustible gas can mix with air and ignite at a later time. When such a flame starts in a volume where gas and air have been more or less mixed, it is usually very difficult to stop. The public calls these events 'explosions' abusively. In practice, these flames can remain slow and weak or transition to detonation with dramatic effects. Preventing flames from accelerating and going to detonation is the key issue for all safety scientists and regulators.

Detonations and fast flames in general, create pressure waves that destroy buildings, engines, and whatever is found in their paths. Understanding how a flame accelerates and sometimes goes to detonation has been a key research topic in the combustion world for decades. The numerical prediction of these phenomena has now become a key question at CERFACS and for many companies interested in safety.

Numerically, these simulations are very complex since they start from a laminar quiescent state, with small flames, near the ignition point (moving at 40 cm/s) and can end up as detonations (moving at 2 km/s). The LES solver must transition from laminar to turbulent flows, from incompressible flows to highly compressible regimes with shock waves. AVBP has been adapted to perform these tasks. Since the pioneer LES of the Sydney so-called MASRI experiment [93], the main difficulty has been and remains in most cases, to increase the size of the domains, an effort tackled with multiple partners: Air Liquide, Totalenergies, Airbus, GRTgaz, Alstom. Modeling of flame-turbulence interactions (Sect. 3.3.3) is another key problem in this field and CERFACS explores multiple paths to cover these difficulties.

A sample of present state-of-the-art LES of explosions is given in Fig. 4.12 where the GRAVENT experiment of TU Munich (Fig. 4.11) is computed (PhD of F. Meziat).

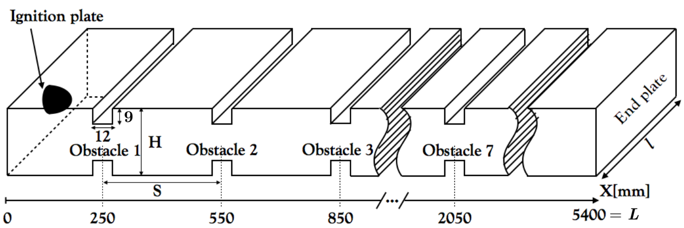

Figure 4.11: The GRAVENT experiment of TU Munich: a prototype of confined vessels to study explosions

This experiment is a proper prototype of flame acceleration scenarios: the flame starts in a confined vessel with obstacles, which here are regularly spaced but can take any shape in real accidents.
The LES captures all phases of this highly complicated flame which begins as a laminar kernel and finally ends up as a detonation. For all these cases, subgrid-scale modeling for flame turbulence interaction remains a key issue (Sect. 3.3.3).

Flames stabilized on gas leaks

In opposition to the previous case, when a leak of gas occurs, its ignition can be instantaneous, leading to a flame anchored on the lips of the hole generating the leak and extending into the domain. This is of course a serious hazard for the whole installation. The most well-known flame of this type is the Concorde kerosene flame attached to the wings of the plane. Today, safety issues focus more on gaseous cases and especially on hydrogen leaks.

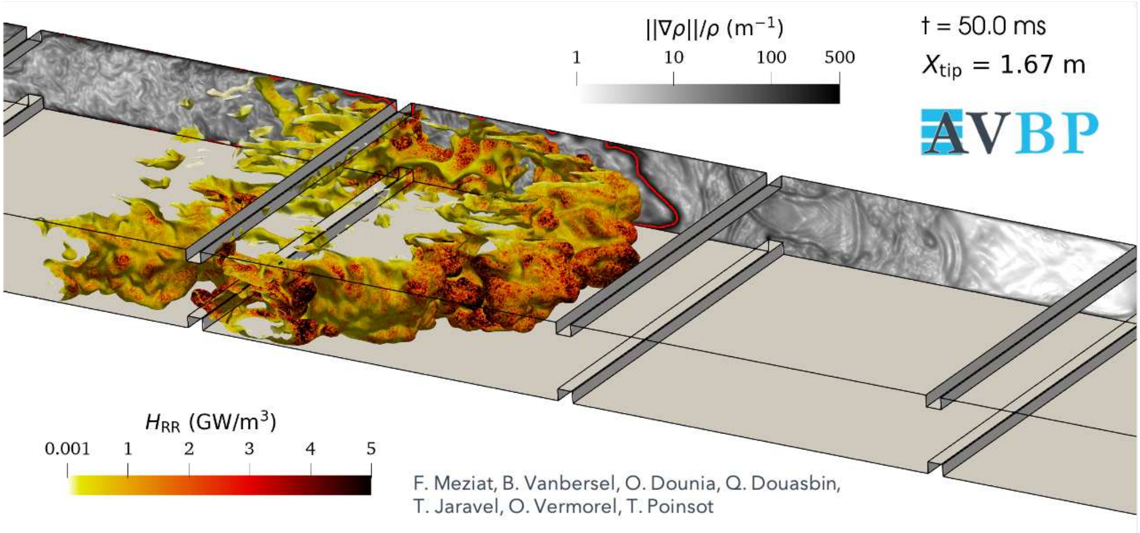

Figure 4.12: LES of flame acceleration in the GRAVENT experiment. The fuel is hydrogen.

To address such problems, CERFACS is performing simulations of jet flames at low speeds (Fig. 3.8 but, with the development of hydrogen, a new type of leak-stabilized flames has come forward in CERFACS research: the case where the pressure of the hydrogen tank which leaks, is higher than 2 bar (and can reach 900 bar in certain applications as for refueling of cars). In this case, the hydrogen jet is supersonic, exhibits shocks, and can even auto-ignite in the absence of any spark through shock-boundary layer interaction in the tube. CERFACS is simulating supersonic jet flames stabilized on small holes since these are a basic configuration for many CERFACS partners: Fig. 4.13 displays a hydrogen jet flame issuing from a high-pressure tank. The jet exhibits a network of shocks followed by a lifted flame.

Note that the ignition of supersonic gaseous jets is also an important mechanism in safety scenarios for batteries where CERFACS has been working with Pprime, SAFT, and TOTALENERGIES to quantify the combustion of gases leaking from a battery (Ph.D. of A. Cellier) during thermal runaway, a mechanism of critical importance today, considering the exponential growth of the batteries number. For those scenarios, the fuel is not pure hydrogen but a mixture of multiple hydrocarbons and hydrogen.

Flame - wall interaction

Flames created by fuel leaks can propagate in free space (like for the Concorde accident) or be confined if they take place in a finite size vessel. In this case, one main issue is to determine the heat fluxes on the vessel walls. Flames, especially hydrogen flames, can indeed lead to heat fluxes of the order of 1 MW/m2 destroying walls in a short time. CERFACS has started computing such flames for AIRBUS and SAFRAN but also within the framework of a new ERC advanced grant with IMFT called SELECT-H (PI: Pr T. Schuller) where experiments will be performed at IMFT and simulations run with AVBP at CERFACS (Phd of F. Gaipl).

Dispersion of virus and mitigation strategies

Airborne viruses such as COVID-19 and influenza can infect an individual through direct or indirect transmissions. SARS-CoV-2 victims generate virus-laden droplets in their respiratory tract and can exhale

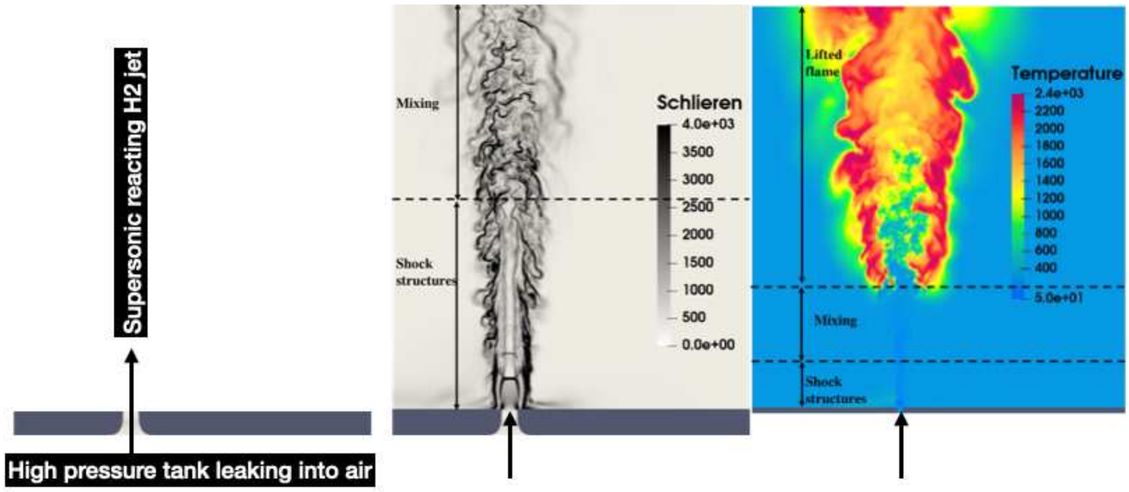

Figure 4.13: Supersonic hydrogen jet flame in air. Left: setup. Center: Schlieren view showing the shock structure at the lip of the 1200 m/s hydrogen jet. Right: temperature field (post-doc of S. Sengupta).

them during any activity like regular breathing, sneezing, coughing, etc. Statistical reports around the world during the pandemic reveal that droplet nuclei containing virus can survive more than one hour and travel distances more than 2 m. Research suggests that the survivability and propagation of these virus-laden droplets are heavily dependent on numerous factors such as humidity, temperature, turbulence dispersion, wind speed, and orientation. Computational studies on airborne virus propagation reveal an infection rate that is higher in a closed environment like restaurants, classrooms, buses, etc compared to outdoor. The use of masks, optimizing the ventilation systems, and application of air filters are some of the mitigation solutions suggested to implement in closed environments.

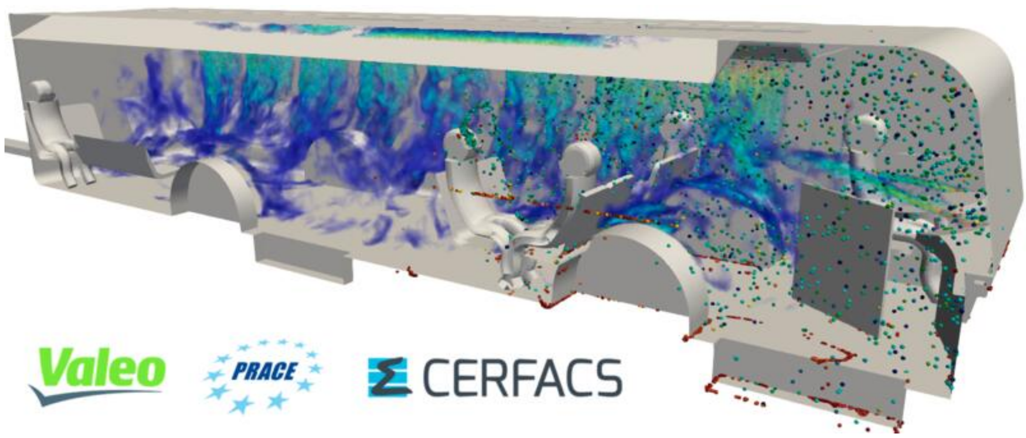

Figure 4.14: Turbulent dispersion of respiratory droplets in a city bus [CFD141].

Virology studies show that UV-C radiation also known as germicidal UV radiation can inactivate SARS-CoV-2 virus and the idea of UV air purifiers as a mitigation solution came into existence. The efficiency mitigation solution in stopping the propagation of airborne viruses inside closed areas needs to be tested. Several important phenomena like virus-laden droplet dispersion, evaporation, UV radiation accumulation, inactivation, etc should be modeled and coupled to perform a simulation on UV air purifier (UVP).

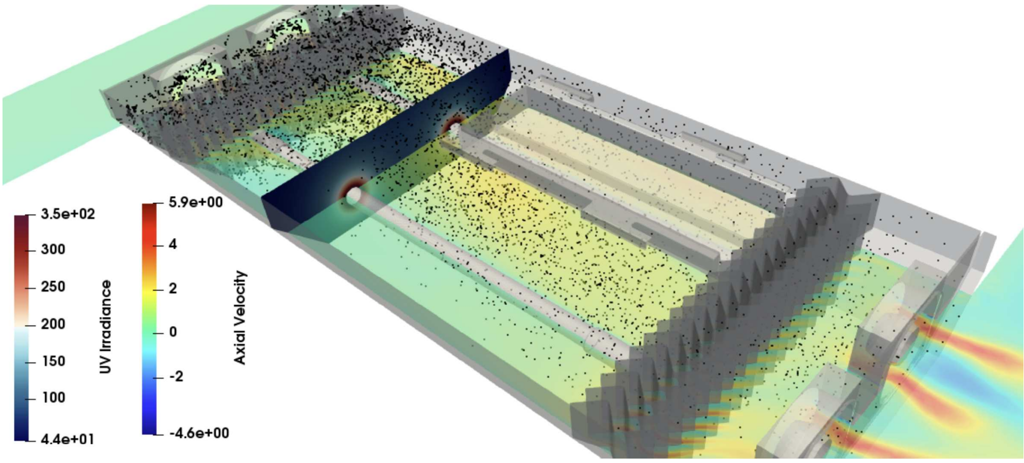

Figure 4.15: Time averaged axial velocity and UV irradiance contours in a UVP with virus-laden droplets.

Since the beginning of the SARS-CoV-2 pandemic, CERFACS worked with VALEO on the turbulent dispersion of droplets in a city bus (Fig. 4.14 [CFD141]) as well as on the characterization of a UVP designed by VALEO. In the context of the Phd thesis of Shriram Sankurantripati, the efficiency of a specific purifier is qualitatively and quantitatively studied with high-fidelity simulation strategies including Large Eddy Simulations coupled with a Lagrangian tracking of droplets and UV-radiation disinfection solver (Fig. 4.15). This model is tested and validated with available literature. Note that this model can be used for other UV air purifiers and other airborne viruses. Simulations showed that 99 % of the SARS-CoV-2 virus injected into the purifier are inactivated. In the third year of the thesis, this purifier will be installed in a bus and the complete environment will be simulated using the coupled model and a complete simulation of this environment will determine the efficiency of this solution.

4.3 Lattice Boltzmann Method and Applications

4.3.1 LBM Aerodynamic Applications

Compressor Simulations

Aerodynamic characteristics of an inter-compressor S-duct have been investigated through numerical simulations performed with a compressible hybrid thermal lattice Boltzmann method (LBM) approach. Comparative analyses were conducted between LES-LBM results, Reynolds Averaged Navier-Stokes (RANS) computations, and experimental data from a representative S-duct sourced from the AIDA project. The simulations considered progressively complex scenarios, incorporating additional rows surrounding the duct. The impact of each row on flow field development and loss levels was examined. The effectiveness of LES-LBM in capturing the aerodynamic behavior and the evolution of total pressure loss within the duct was demonstrated. The results indicated that LES-LBM accurately represented the flow evolution within the S-duct, aligning with experimental observations and prior RANS findings. Notably, integrating the upstream stator row or the Low-Pressure Compressor (LPC) stage led to an increase in total pressure loss,

consistent with existing literature. This configuration also exhibited a more intricate flow field with complex features contributing to loss generation. An entropy-based approach was introduced to further analyze the loss mechanism, emphasizing that most losses originated near the hub wall due to the migration of upstream stator wakes.
Utilizing the knowledge obtained from the CAM1 configuration (Fig. 4.16), the investigation were extended to assess an industrial case operating at Mach 0.6. Numerical simulations of an S-duct featuring a prominently curved upstream stator row produced results that closely mirrored experimental data. Despite experiencing slightly larger wakes caused by early flow separation from the stator blades, the simulations provided meaningful insights.

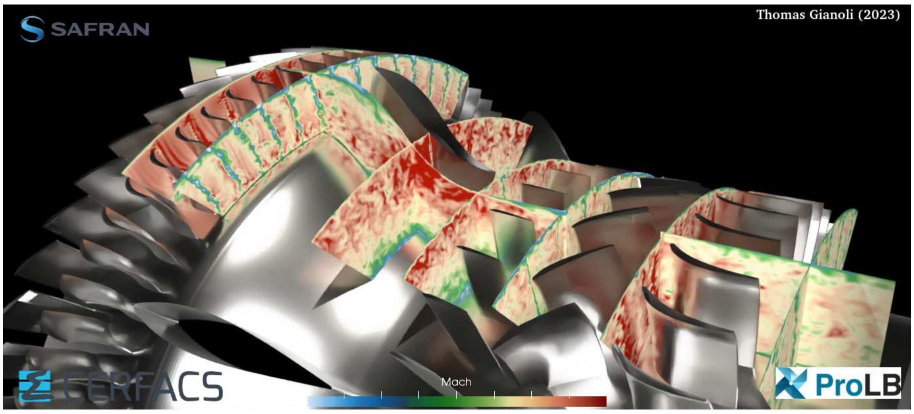

Figure 4.16: Simulation of the full CAM1 machine.

Fan-OGV Simulations

The Lattice Boltzmann Method is gaining popularity for high-fidelity simulations in turbomachinery, particularly for Fan-OGV configurations as highlighted in [80]. Recent progress in compressible LBM simulations has extended the capability to model fan configurations at elevated Mach numbers. Recent activities at CERFACS focused on the ECL5 UHBR Fan-OGV configuration, employing the compressible lattice Boltzmann method, and examined two operational points: 55% and 80%.

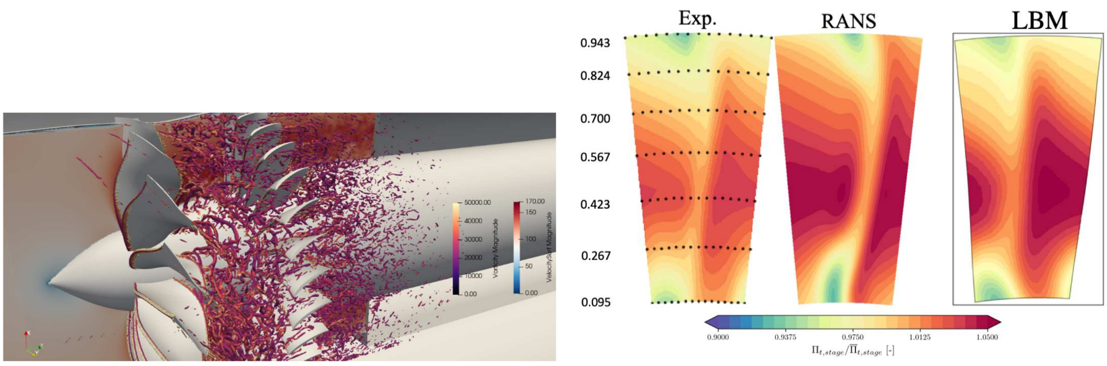

(a) 3D view of the ECL5 module
(b) Azimuthally-averaged pressure ratio profiles [59]

Figure 4.17: Simulation of the ECL5 Fan-OGV module

Figure 4.17 shows the simulated configuration along with the aerodynamic results at the stage exit plane (downstream of the stators). It can be seen that the LBM simulation produced good agreement with the reference experiment.

4.3.2 LBM Aerothermal Applications

Bore Cooling

The efficiency and reliability of turbofan engines are strongly influenced by the blade tip clearances in the high-pressure compressor counterpart. Consequently, precise prediction of the compressor rotor's thermal expansion becomes crucial, as it is dictated by the temperature distribution of their disks, which is, in turn, regulated by the heat transfer on their surfaces. Turbofan compressor cooling circuits exhibit inherent unsteadiness within their cavities due to the interplay of forced and natural convection phenomena. Recent developments at CERFACS, including an extension of the compressible hybrid LBM in the rotating frame, a new mass-conserving boundary treatment, and an adapted direct grid-refinement strategy, allow for the modeling of sealed and open rotating compressor cavity rigs [78, 79], spanning a large range of Rayleigh numbers (from 10^6 to 10^9). The proposed algorithm accurately replicates heat transfer on both upstream and downstream disks as depicted in Fig. 4.18. Particularly, it precisely predicts the heat transfer at the jet impact on the downstream disk, a maxima that tends to be overestimated by other solvers.

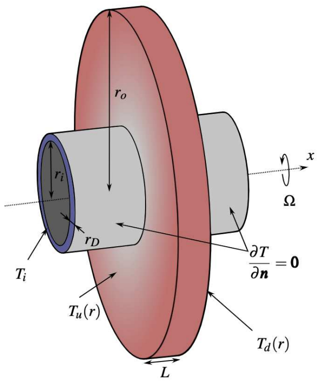

(a)

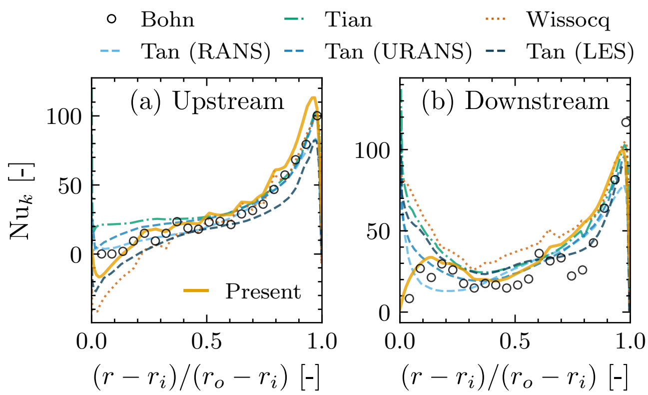

(b)

Figure 4.18: (a) Sketch of the rotating rig from Bohn [79]. An axial cooling flow is passing through a cavity formed by two disks. Disks are heated non-uniformly while the cylinder surfaces of the annular gap are made adiabatic. (b) Azimuthally and time-averaged local Nusselt numbers for each disk. Comparison among the experimental data and numerical studies from the literature.

Impinging Jet

Impinging jet flows are widely used in industry as a means of cooling or heating, as they can produce high rates of convective heat transfer. They can be found in such configurations as turbine blade cooling systems, active clearance control systems, or wing anti-icing systems. The accurate prediction of impinging jet heat transfer presents an enormous challenge for RANS approaches [95], and there is thus a major interest in performing such simulations using higher-fidelity approaches, such as the Lattice Boltzmann Method.

The successive developments at CERFACS, including turbulence injection and mesh refinement, have made possible the first LBM simulation of a fully turbulent thermal impinging jet [87]. This simulation of a single axisymmetric impinging jet with a spacing $H/D = 2$ and $Re = 23\ 000$ produced results with very good agreement with the experimental literature, including the secondary peak in the Nusselt number.

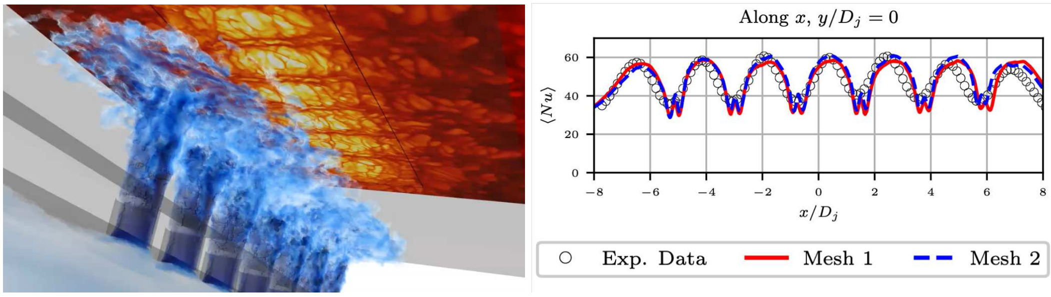

(a) (b)

Figure 4.19: (a) 3D volume rendering of the multi-impinging jet test case.(b) Nusselt number along the row of jets.

The single jet simulation was followed by a multi-impinging jet simulation, with upstream crossflow, representative of a simplified Low-Pressure Turbine Active Clearance Control (LPTACC) system. Good agreement with the experimental data was retrieved. A further investigation was performed on the effect of the Mach number on the Nusselt number, finding a moderate positive correlation between the two near stagnation points.

4.3.3 LBM Aeroacoustic Applications

Jet Noise

The development of increasingly stringent noise regulations has rendered paramount the reduction in aircraft noise. One major source of noise is the jet exhaust from the engines. This presents a specific challenge to the Lattice Boltzmann Method, due to the high speeds involved as well as the large variations in temperature. To this end, the LBM solver is tested on the single stream jet configuration (SMC000). This test case involves a jet that reaches a Mach number of $Ma \approx 0.9$, and requires non-reflecting boundary conditions and a $P_t - T_t$ inflow condition.

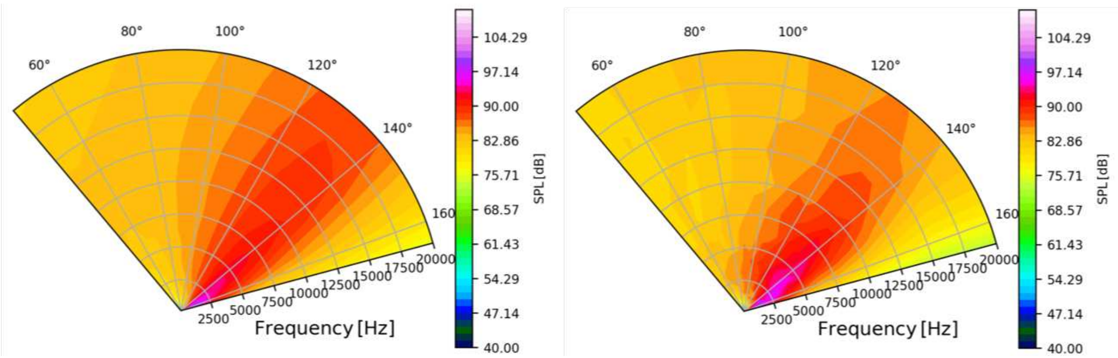

(a) Directivity of the noise source for the experimental data (b) Directivity of the noise source for the LBM simulations [44]

Figure 4.20: Results for the jet noise simulations

The simulations are able to capture the directivity of the jet noise fairly well (see Fig. 4.20). Higher frequency sound pressure levels are somewhat underestimated, particularly between $120°$ and $140°$. However, between $90°$ and $120°$ degrees, the overall sound pressure level is in good agreement with the experimental data.

Linear Blade Cascade

Another major source of noise is the interaction between the wakes of the aircraft fan and the outlet guide vanes (OGVs). The development of new stator designs, including innovative designs like slits or wavy forms, is one way of reducing this noise. The relative performance of these stators can first be evaluated via a simpler blade cascade configuration.

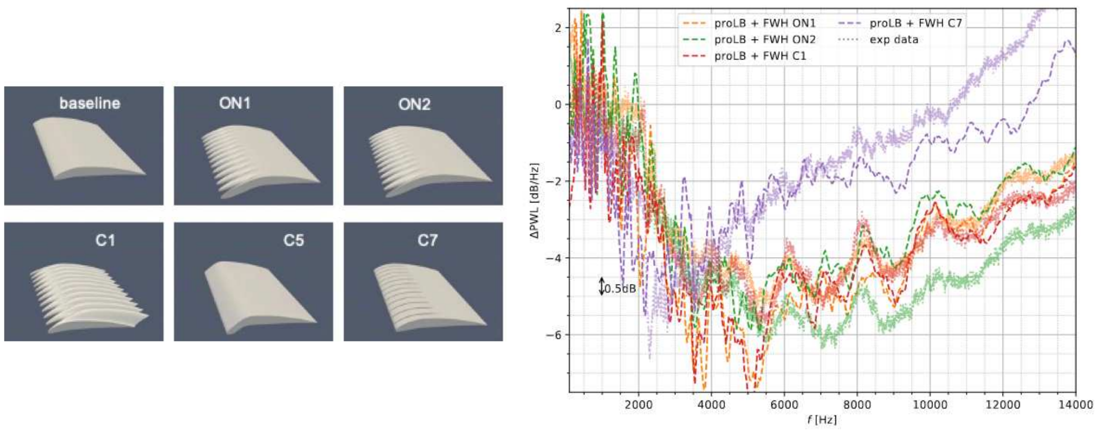

(a) Different concepts for the different stator geometries

(b) Relative performance of the geometries compared to the baseline

Figure 4.21: Different stator concepts along with their relative performance

The higher speeds involved with this configuration (up to $Ma \approx 0.53$ for freestream velocity) require a fully compressible scheme, and the compressible LBM is thus a good candidate for evaluating the performance of these concepts. Thus, many LBM simulations using different stator concepts were performed (see Fig. 4.21), and it was shown that the slit concept produced the greatest noise reduction, in good agreement with the corresponding experiments.

References

[73] S. Agarwal, L. Gicquel, F. Duchaine, N. Odier, and J. Dombard, (2020), Analysis of the unsteady flow field inside a fan-shaped cooling Hole predicted by Large-Eddy Simulation, In *Proceedings of ASME Turbo Expo 2020 - September 21-25, 2020*, Virtual conference, GT2020–14201.

[74] S. Agarwal, L. Gicquel, F. Duchaine, N. Odier, and J. Dombard, (2020), Effect of the in-hole vortical structures on the cylindrical-hole Film-cooling effectivenessEffect of the in-hole vortical structures on the cylindrical-hole Film-cooling effectiveness, In *Proceedings of ASME Turbo Expo 2020*, Virtual conference, GT2020–14258.

[75] S. Agarwal, (2018), Rapport de Stage - CERFACS SAFT, working note, Cerfacs, Toulouse, France.

[76] R. Bizzari, D. Lahbib, A. Dauptain, F. Duchaine, S. Richard, and F. Nicoud, (2018), Low order modeling method for assessing the temperature of multi-perforated plates, *International Journal of Heat and Mass Transfer*, **127**, 727–742.

[77] S. Blanchard and B. Cuenot, (2019), Large Eddy Simulation of a single-injector LOx/GCH4 combustion chamber using Analytically Reduced Chemistry, In *DFG-TRR-40 Summer Program 2019*, no. 1, 69–86.

[78] D. Bohn, E. Deuker, R. Emunds, and V. Gorzelitz, (1995), Experimental and Theoretical Investigations of Heat Transfer in Closed Gas-Filled Rotating Annuli, *Journal of Turbomachinery*, **117**, 175–183.

[79] D. E. Bohn, G. N. Deutsch, B. Simon, and C. Burkhardt, (2000), Flow Visualisation in a Rotating Cavity With Axial Throughflow, In *Volume 3: Heat Transfer; Electric Power; Industrial and Cogeneration*, Munich, Germany, American Society of Mechanical Engineers, V003T01A084.

[80] M. Daroukh, T. L. Garrec, and C. Polacsek, (2022), Low-Speed Turbofan Aerodynamic and Acoustic Prediction with an Isothermal Lattice Boltzmann Method, *AIAA Journal*, **60**, 1152–1170.

[81] G. Daviller, M. Brebion, P. Xavier, G. Staffelbach, J.-D. Mueller, and T. Poinsot, (2017), A mesh adaptation strategy to predict pressure losses in LES of swirled flows, *Flow Turbulence and Combustion*, **99**, 93–118.

[82] G. Daviller, J. Dombard, G. Staffelbach, J. Herpe, and D. Saucereau, (2020), Prediction of Flow Separation and Side-loads in Rocket Nozzle Using Large-eddy Simulation, *International Journal of Computational Fluid Dynamics*, **34**, 622–632.

[83] G. Daviller, G. Oztarlik, and T. Poinsot, (2019), A generalized non-reflecting inlet boundary condition for steady and forced compressible flows with injection of vortical and acoustic waves, *Computers and Fluids*, **190**, 503–513.

[84] D. Dupuy, L. Gicquel, N. Odier, F. Duchaine, and T. Arts, (2020), Analysis of the effect of intermittency in a high-pressure turbine blade, *Physics of Fluids*, **32**, 095101.

[85] D. Maestro, B. Cuenot, and L. Selle, (2019), Large Eddy Simulation of combustion and heat transfer in a single element GCH4/GOx rocket combustor, *Flow Turbulence and Combustion*, **103**, 699–730.

[86] P. Mohanamuraly and G. Staffelbach, (2020), Hardware locality-aware partitioning and dynamic load-balancing of unstructured meshes for large-scale scientific applications, In *Proceedings of the Platform for Advanced Scientific Computing Conference*, 1–10.

[87] M. Nguyen, J. F. Boussuge, P. Sagaut, and J. C. Larroya-Huguet, (2022), Large eddy simulation of a thermal impinging jet using the lattice Boltzmann method, *Physics of Fluids*, **34**, 055115.

[88] N. Odier, M. Sanjosé, L. Gicquel, T. Poinsot, S. Moreau, and F. Duchaine, (2018), A characteristic inlet boundary condition for compressible, turbulent, multispecies turbomachinery flows, *Computers and Fluids*, **178**, 41–55.

[89] C. Pérez Arroyo, J. Dombard, F. Duchaine, L. Gicquel, and N. Odier, (2021), Numerical Investigation of the Interaction Between Gas-Turbine Engine Components With Dynamic Mode Tracking, In *Turbo Expo: Power for Land, Sea, and Air*, vol. 84928, American Society of Mechanical Engineers, V02CT34A041.

[90] A. Perrot, F. Duchaine, L. Gicquel, T. Grosnickel, N. Odier, and J. Dombard, (2020), Unsteady analysis of heat transfer coefficient distribution in a static ribbed channel for an established flow, In *Proceedings of ASME Turbo Expo 2020*, virtual conference, GT2020–14493.

[91] C. Pérez Arroyo, J. Dombard, F. Duchaine, L. Gicquel, B. Martin, N. Odier, and G. Staffelbach, (2021), Towards the Large-Eddy Simulation of a full engine: Integration of a 360 azimuthal degrees fan, compressor and combustion chamber. Part I: Methodology and initialisation, *Global Power and Propulsion Society*.

[92] C. Pérez Arroyo, J. Dombard, F. Duchaine, L. Gicquel, B. Martin, N. Odier, and G. Staffelbach, (2021), Towards the Large-Eddy Simulation of a full engine: Integration of a 360 azimuthal degrees fan, compressor and combustion chamber. Part II: Comparison against stand-alone simulations, *Global Power and Propulsion Society*.

[93] O. Vermorel, P. Quillatre, and T. Poinsot, (2017), LES of explosions in venting chamber: a test case for premixed turbulent combustion models, *Combustion and Flame*, **183**, 207–223.

[94] G. Wang, F. Duchaine, D. Papadogiannis, I. Duran, S. Moreau, and L. Y. M. Gicquel, (2014), An overset grid method for large eddy simulation of turbomachinery stages, *Journal of Computational Physics*, **274**, 333–355.

[95] N. Zuckerman and N. Lior, (2006), Jet Impingement Heat Transfer: Physics, Correlations, and Numerical Modeling, *Advances in Heat Transfer*, **39**, 565–631.

Publications

5.1 Books

[CFD1] A. Balan, F. Bassi, J.-F. Boussuge, A. de Brauer, J.-S. Cagnone, A. Colombo, V. Couaillier, O. Coulaud, A. Crivellini, M. Franciolini, A. Ghidoni, K. Hillewaert, M. de la Llave Plata, G. Manzinali, F. Naddei, g. Noventa, G. Puigt, B. Vermeire, and P. Vincent, (2021), *Space Adaptative Methods/Meshing*, vol. 148, Springer International Publishing, editors: hirsch, c., hillewaert, k., hartmann, r., couaillier, v., boussuge, j.-f., chalot, f., bosniakov, s., haase, w. ed.

[CFD2] J.-F. Boussuge, R. Biolchini, M. Lorteau, M. de la Llave Plata, N. Lupoglazoff, F. Vuillot, and V. Couaillier, (2021), *Large Eddy Simulation of Single Stream Jet Using High-Order Methods*, vol. 148, Springer International Publishing, editors: hirsch, c., hillewaert, k., hartmann, r., couaillier, v., boussuge, j.-f., chalot, f., bosniakov, s., haase, w. ed.

5.2 Conferences Proceedings

[CFD3] S. Agarwal, L. Gicquel, F. Duchaine, N. Odier, J. Dombard, and D. Bonneau, (2022), Large Eddy Simulation Based Optimization of a Fan-Shaped Cooling Hole Geometry to Enhance Cooling Performance - GT2022-79923, In *ASME Turbo Expo 2022: Turbomachinery Technical Conference and Exposition, Volume 6A, Heat Transfer Combustors, Film Cooling, Rotterdam, Netherlands*.

[CFD4] P. Agostinelli, Y. Kwah, S. Richard, G. Exilard, J. Dawson, L. Gicquel, and T. Poinsot, (2021), Design through LES of a spinning flame combustor, Impact of operating conditions on flame stabilization and thermal load, In *Colloque INCA 2021 (Initiative en Combustion Avancée) – Visioconférence*.

[CFD5] E. Ajuria-Illarramendi, M. Bauerheim, and B. Cuenot, (2021), Analysis of downscaled branches and Receptive field on a CNN-based incompressible solver - Invited conference, In *74th Annual Meeting of the APS Division of Fluid Dynamics - 21 - 23 Nov, Phoenix, Arizona*.

[CFD6] E. Ajuria-Illarramendi, M. Bauerheim, N. Ashton, C. Lapeyre, and B. Cuenot, (2023), Performance Study of Convolutional Neural Network Architectures for 3D Incompressible Flow Simulations, In *PASC '23: Proceedings of the Platform for Advanced Scientific Computing Conference, Davos, Switzerland, 26- 28 June*, vol. 17, 1–11.

[CFD7] E. Ajuria-Illarramendi, B. Cuenot, and M. Bauerheim, (2021), Embedding temporal error propagation on CNN for unsteady flow simulations - Online event, In *Machine Learning and the Physical Sciences Workshop at the 35th Conference on Neural Information Processing Systems (NeurIPS) - 13 Dec*.

[CFD8] A. Badhe, D. Laera, and L. Gicquel, (2021), High-fidelity Large Eddy Simulations of the Flame Transfer Function of a turbulent swirling spray flame, In *10th European Combustion Meeting*, Virtual conference, Combustion Institute.

[CFD9] A. Badhe, C. Laurent, C. Lapeyre, and F. Nicoud, (2021), Low-Order Thermoacoustic Analysis of Real Engines, In *Colloque INCA 2021 (Initiative en Combustion Avancée) – Visioconférence*.

[CFD10] A. Badhe, C. Laurent, C. Lapeyre, and F. Nicoud, (2021), Low-Order Thermoacoustic Analysis of Real Engines - Paper No 8496 - Virtual Conference, In *Symposium on Thermoacoustics in Combustion (SoTiC): Industry meets Academia, 6-10 Sept - Munich*.

[CFD11] G. Bogopolsky, B. Laurent, O. Vermorel, and B. Cuenot, (2022), Atelier propulsion électrique – CERFACS - invited conference, In *Atelier propulsion électrique, Paris, France*.

[CFD12] G. Bogopolsky, O. Vermorel, and B. Cuenot, (2022), Dielectric boundary condition for an unstructured 2D radial-axial fluid simulation of a Hall thruster, In *Gaseous Electronics Conference, Sendei, Japan*.

[CFD13] A. Boudin, J. Dombard, F. Duchaine, L. Gicquel, N. Odier, S. Lavagnoli, L. Simonassi, and C. Uribe, (2023), Analysis of wakes interactions in a high-speed low-pressure turbine cascade using large-eddy simulations, In *15th European Conference on Turbomachinery Fluid dynamics and Thermodynamics ETC15, Budapest, Hungary, April 24-28*.

[CFD14] M. Buszyk, L. Vienne, T. Le Garrec, J.-F. Boussuge, C. Polacsek, and R. Barrier, (2022), Lattice Boltzmann Method for Broadband Noise Predictions on a Turbulence-Cascade Test Rig Including Serrated Vanes, In *33 RD Congress of the International Council of the Aeronautical Sciences (ICAS), Stockholm, Sweden*.

[CFD15] T. Capurso, D. Laera, E. Riber, and B. Cuenot, (2022), Large Eddy Simulation of swirling technically-premixed H2/air flame with accurate NOx prediction, In *2nd Low Carbon Combustion meeting, Cambridge, UK*.

[CFD16] Q. Cazères, T. Ogier, T. Lesaffre, E. Riber, and B. Cuenot, (2022), Automatic reduction of HEFA bio-jet fuel. From detailed composition to CFD compatible reduced kinetics, In *2nd Low Carbon Combustion meeting, Cambridge, UK*.

[CFD17] Q. Cazères, E. Riber, and B. Cuenot, (2021), Numerical study of a confined hydrogen-enriched premixed methane/air swirling flame using detailed chemistry, In *Colloque INCA 2021 (Initiative en Combustion Avancée) – Visioconférence*.

[CFD18] A. Cellier, F. Duchaine, T. Poinsot, M. Leyko, G. Okyay, and M. Pallud, (2022), Large Eddy Simulation of Lithium-ion battery fires for the diagnostic of Thermal Runaway, In *MATHIAS days 2022, Magny-le-Hongre, France, October 03-06*.

[CFD19] A. Cellier, F. Duchaine, T. Poinsot, G. Okyay, M. Leyko, and M. Pallud, (2023), Large Eddy Simulation of lithium-ion vent gas explosions: effect of wall heat loss on tulip flame formation and propagation, In *11th European Combustion Meeting, Rouen, 26-28 April*.

[CFD20] A. Cellier, F. Duchaine, O. Vermorel, T. Poinsot, M. Leyko, G. Okyay, and M. Pallud, (2021), Large Eddy Simulation of Lithium-ion battery fires for the diagnostic of Thermal Runaway, In *MATHIAS days 2021, Serris, France, October 03-07*.

[CFD21] A. Cellier, C. Lapeyre, G. Oztarlik, T. Poinsot, T. Schuller, and L. Selle, (2021), Detection of precursors of Thermoacoustic Instability using Deep Learning Techniques, In *Colloque INCA 2021 (Initiative en Combustion Avancée) – Visioconférence*.

[CFD22] A. Costes, C. Lac, M. Rochoux, and V. Masson, (2021), Validité de l'hypothèse anélastique pour la simulation du comportement d'un incendie de forêt dans un modèle couple feu/atmosphère, In *29èmes journées du Groupement de Recherche CNRS Feux, online event, 1-2 July*.

[CFD23] A. Coudray, E. Riber, and B. Cuenot, (2023), Hybrid approach for modelling Polycyclic Aromatic Hydrocarbons (PAHs) in Large Eddy Simulation of turbulent flames, In *11th European Combustion Meeting, Rouen, 26-28 April*.

[CFD24] J. Crespo-Anadon, B. Cuenot, E. Riber, S. Richard, M. Bellenoue, and J. Sotton, (2021), Comparison of LES and experiments of methane-air ignition in a closed chamber under various turbulent conditions, In *Colloque INCA 2021 - visioconférence*.

[CFD25] B. Cuenot, O. Vermorel, N. Barleon, and L. Cheng, (2022), Plasma-assisted combustion: modeling and simulation - invited conference, In *RECENT DEVELOPMENTS IN COMBUSTION RESEARCH Webinars 11-14 of the Dutch Section of the Combustion Institute, TU Eindhoven*.

[CFD26] B. Cuenot, (2021), 1st Plenary session at the HPCCOMB2021 - invited conference, In *3rd HPC Spanish Combustion Workshop*, online.

[CFD27] B. Cuenot, (2021), Modelling and simulation of soot formation and evolution in turbulent flames - invited conference, In *UK Consortium on Turbulent Reacting Flow Annual Meeting*, online, UKCTRF.

[CFD28] B. Cuenot, (2021), Numerical prediction of pollutants and soot emissions in turbulent flames - invited conference, In *The Combustion Webinar*, online, Georgia Tech Reacting Flow and Diagnostic Group.

[CFD29] B. Cuenot, (2022), Chemical kinetics in flames: general description and how to handle it in computations - Turbulent combustion modeling in LES: methods and applications - invited conference, In *CoEC Combustion Autumn School, Sofia, Bulgaria*.

[CFD30] B. Cuenot, (2022), Fundamentals of combustion: laminar flames - invited conference, In *PRACE advanced training centres - INTRODUCTION TO HIGH-FIDELITY COMBUSTION SIMULATIONS USING HPC, online*.

[CFD31] B. Cuenot, (2022), Modeling and Simulation of Turbulent Spray Flames - invited conference, In *JMBC-ERCOFTAC combustion course, TU Eindhoven, Jan 31 - Feb 4*.

[CFD32] B. Cuenot, (2022), modelling fuel effects in combustion chambers - invited seminar, In *Sustainable Aviation Fuels (SAF) - Imperial College UK*.

[CFD33] B. Cuenot, (2022), Theory and fundamentals of H2 combustion II - invited conference, In *Understanding and PredictingHydrogen Combustion, 30 November- 02 December, Barcelona, Spain*.

[CFD34] B. Cuenot, (2023), Interactions of burning particles with a turbulent flow: problems and methodology, In *EIRES Lunch seminars, January 20, online*.

[CFD35] B. Cuenot, (2023), Invited course on combustion, In *Valencia University, October*.

[CFD36] B. Cuenot, (2023), Numerical simulation as a support for energy decarbonation: methods and applications - invited seminar, In *Melbourne University, July*.

[CFD37] B. Cuenot, (2024), DNS and LES of turbulent reacting gas flows with detailed kinetics and liquid or solid particles, In *invited seminar, Magdeburg University, September*.

[CFD38] J. Dabas, L. Gicquel, N. Odier, and F. Duchaine, (2022), Large Eddy Simulations of Wind Turbine Flows - GT2022-82096, In *Proceedings of ASME Turbo Expo and Turbomachinery Technical Conference and Exposition GT2022*.

[CFD39] J. Degrigny, G. Pont, J.-F. Boussuge, and P. Sagaut, (2021), Simulation of High-Lift Flows through IDDES in LBM, In *Comparison of Turbulence Modeling Approaches on a High-Lift Airfoil in LBM - 55th 3AF International Conference on Applied Aerodynamics 23 — 25 March 2020, Poitiers – France - Virtual edition*.

[CFD40] N. Detomaso, D. Laera, P. Pouech, F. Duchaine, and T. Poinsot, (2022), Large Eddy Simulation of a pistonless constant volume combustor: a new concept of pressure gain combustion - paper n° GT 2022-81366, In *ASME Turbo Expo, Rotterdam, Netherlands*.

[CFD41] M. Di Renzo and B. Cuenot, (2021), Direct numerical simulation of a turbulent diffusion flame impinged by an external electric field, In *74th Annual Meeting of the APS Division of Fluid Dynamics Sunday–Tuesday, November 21–23, 2021; Phoenix Convention Center, Phoenix, Arizona*.

[CFD42] M. Di Renzo, A. Ceci, A. Palumbo, J. Larsson, and S. Pirozzoli, (2022), Wall-pressure spectra in shock wave/turbulent boundary layer interactions with a crossflow, In *ParCFD2022 - 33rd International Conference on Parallel Computational Fluid Dynamics, Alba, Italy*.

[CFD43] F. Duchaine, (2021), High-Performance Computational Fluid Dynamics for Virus Propagation in Closed Domains - invited conference, In *HPC User Forum, Hyperion Research - May 2021*, online.

[CFD44] F. Duchaine, (2021), High-Performance Computational Fluid Dynamics for Virus Propagation in Closed Domains - invited conference, In *SIAME CSE21 - MS12 Highlights of HPC Response to the COVID19 Pandemic - March 2021*, Virtual Conference.

[CFD45] F. Duchaine, (2021), Presentation of the PRACE project CFD for COVID - invited conference, In *EURO HPC SUMMIT WEEK - COVID-19 Day PRACE days21 - Scientific Parallel Track COVID-19*, online.

[CFD46] J. Gaucherand, T. Poinsot, D. Laera, and C. Schulze-Netzer, (2023), Intrinsic instabilities of hydrogen and hydrogen/ammonia premixed flames: influence of equivalence ratio, and fuel composition, In *2nd Symposium on Ammonia Energy, Orléans, July 11-13*.

[CFD47] J. Gaucherand, (2023), Direct numerical simulation of premixed turbulent ammonia/hydrogen-air flames, In *11th European Combustion Meeting, Rouen, 26-28 April*.

[CFD48] Y. Gentil, G. Daviller, S. Moreau, and T. Poinsot, (2023), Combustion composition noise mechanism analysis, Paper AIAA 2023-3940, In *AIAA Aviation Forum, San Diego, USA, June 12-16*.

[CFD49] T. Gianoli, J.-F. Boussuge, J. de Laborderie, and P. Sagaut, (2022), S-Duct Turbomachinery Simulations using the Lattice Boltzmann Method, In *56th 3AF International Conference on Applied Aerodynamics, Toulouse, France*.

[CFD50] T. Gianoli, J.-F. Boussuge, P. Sagaut, and J. de Laborderie, (2023), Inter-compressor annulars-duct simulation using the lattice Boltzmann method., In *15th European conference on turbomachinery fluid dynamics and Thermodynamics ETC2023, Budapest, Hungary, April 24-28*.

[CFD51] L. Gicquel, N. Sekularac, G. Daviller, G. Staffelbach, A. Dauptain, O. Vermorel, and T. Poinsot, (2023), Combustion noise and engine noise: current computational capabilities and fuel expected issues, In *Resonance conference, JISFA section, July 10-13*.

[CFD52] L. Gicquel, (2021), Large Eddy Simulations to address gas turbine issues and design issues - invited conference, In *ANIMATE project*, online lectures, Czstochowa Univerity of Technology (Poland).

[CFD53] T. Gioud, N. Odier, B. Cuenot, T. Schmitt, D. Saucereau, and M. Martin-Benito, (2022), Injection modelling in LOX/GCH4 rocket engines with a diffuse interface method, In *8th International Conference on Space Propulsion, Estoril, Portugal*.

[CFD54] C. Gout, D. Papadogiannis, J. Dombard, F. Duchaine, L. Gicquel, and N. Odier, (2021), Assessment of profile transformation for turbomachinery Large Eddy Simulations - from academic to industrial applications, In *Proceedings of ASME Turbo Expo, June 7-11*, vol. V02CT34A020, GT2021–59293.

[CFD55] J.-J. Hok, O. Vermorel, T. Jaravel, and Q. Douasbin, (2022), Effect of Flame Front Thermo-Diffusive Instability on Flame Acceleration in a Tube, In *28th International Colloquium on the Dynamics of Explosions and Reactive Systems, Napoli, Italy*.

[CFD56] C. Irimiea, A. Vincent Randonnier, J. Dufitumukiza, S. Puggelli, J. May Carle, N. Treleaven, T. Lesaffre, A. Coudray, E. Lameloise, B. Cuenot, E. Riber, N. Fdida, P. Cherubini, and X. Mercier, (2022), ALTERNATE: Experimental and modeling study of soot formation in high-pressure kerosene and SAF combustion, In *TSAS2022 - 15th Towards Sustainable Aviation - Toulouse, France*.

[CFD57] J. Kim, M. Nabavi, and M. Di Renzo, (2021), On the roles of clustered inertial particles in inter-phase, cross-scale momentum transfer, In *74th Annual Meeting of the APS Division of Fluid Dynamics Sunday–Tuesday, November 21–23, 2021; Phoenix Convention Center, Phoenix, Arizona*.

[CFD58] E. Lameloise, A. Coudray, Q. Cazères, E. Riber, and B. Cuenot, (2022), Reduced chemical kinetics with pathway lumping of Polycyclic Aromatic Hydrocarbons., In *18th International Conference on Numerical Combustion - La Jolla, California*.

[CFD59] D. Lamidel, G. Daviller, M. Roger, and H. Posson, (2021), Numerical investigation of the tip leakage vortex of an isolated plate/airfoil T-junction with gap, In *European Conference on Turbomachinery Fluid dynamics & Thermodynamics*, Gdansk, Poland.

[CFD60] E. Laroche, D. Dupuy, F. Duchaine, and L. Gicquel, (2023), Towards an Improved Description of Film-Cooling Heat Transfer Through Anisotropic RANS Modeling: A Combined LES/RANS Contribution; Paper GT2023-101447, In *ASME Turbo Expo 2023: Turbomachinery Technical Conference and Exposition, Boston, Massachusetts, June 26-30*, V07AT12A005.

[CFD61] T. Laroche, N. Odier, T. Schmitt, M. Pelletier, and B. Cuenot, (2021), A diffuse interface method with real-gas thermodynamic equilibrium closure applied to capillary problems, In *ICLASS 2021, 15th Triennial International Conference on Liquid Atomization and Spray Systems, Edinburgh, UK, 29 Aug. - 2 Sept*, vol. 1.

[CFD62] J. Larsson, V. Kumar, N. Oberoi, M. Di Renzo, and S. Pirozzoli, (2021), The effect of crossflow on a canonical shock/boundary-layer interaction, In *74th Annual Meeting of the APS Division of Fluid Dynamics Sunday–Tuesday, November 21–23, 2021; Phoenix Convention Center, Phoenix, Arizona*.

[CFD63] T. Lesaffre, J. Wirtz, E. Riber, and B. Cuenot, (2023), Impact of wall heat flux on the LBO prediction, In *11th European Combustion Meeting, Rouen, 26-28 April*.

[CFD64] K. Maeda, M. Di Renzo, T. Teixeira, J. Wang, J. Hokanson, C. Melone, S. Jones, J. Urzay, and G. Iaccarino, (2021), A task-based parallel framework for ensemble simulations of rocket ignition, In *74th Annual Meeting of the APS Division of Fluid Dynamics Sunday–Tuesday, November 21–23, 2021; Phoenix Convention Center, Phoenix, Arizona*.

[CFD65] T. Marchal, A. de Brauer, H. Deniau, J.-F. Boussuge, B. Cuenot, and R. Mercier, (2022), Efficiency of the high-order Spectral Difference method in combustion, In *39th International Symposium on Combustion, Vancouver, Canada*.

[CFD66] B. Martin, F. Duchaine, L. Gicquel, N. Odier, and J. Dombard, (2021), Accurate Inlet Boundary Conditions to Capture Combustion Chamber and Turbine Coupling With Large-Eddy Simulation, In *ASME Turbo Expo 2021, Gas Turbine Technical Congress & Exposition*, vol. 2D, Virtual conference, GT2021–58854.

[CFD67] A. Mouze-Mornettas, A. Bertolino, A. Parente, M. Martin Benito, G. Dayma, F. Halter, and B. Cuenot, (2022), Optimization of a mechanism for methane-oxygen rocket engine applications, In *18th International Conference on Numerical Combustion, San Diego, USA*.

[CFD68] A. Mouze-Mornettas, G. Dayma, F. Halter, B. Cuenot, and M. Martin Benito, (2022), Modelling and reduction of LOx-Methane chemical kinetics for rocket engine application, In *9th European Conference for Aeronautics and Space Sciences (EUCASS), Lille, France*.

[CFD69] T. Naess, B. Cuenot, and E. Riber, (2023), Numerical prediction of nitric oxide formation in a turbulent n-heptane spray flame using Large Eddy Simulation, In *11th European Combustion Meeting, Rouen, 26-28 April*.

[CFD70] M. Nguyen, J.-F. Boussuge, P. Sagaut, and J. Larroya-Huguet, (2022), Aerothermal jet simulations using the lattice Boltzmann method - Invited Conference, In *56th 3AF International Conference on Applied Aerodynamics, Toulouse, France*.

[CFD71] M. Noun, L. Gicquel, and G. Staffelbach, (2021), Global Stability Analysis of an Academic Rotor/Stator Cavity Subject to Simple and Periodic Wall Oscillations - Invited Conference, In *Proceedings of the ASME 2021 Turbo Expo: Turbomachinery Technical Conference & Exposition Turbomachines for Clean Power and Propulsion Systems GT2021 - Pittsburgh, USA*, vol. V09AT23A012.

[CFD72] A. Pestre, B. Cuenot, and E. Riber, (2021), Evaluation of numerical methods for explicit chemistry integration and application on DNS of turbulent kerosene ignition at high altitude conditions, In *10th European Combustion Meeting - Virtual edition*.

[CFD73] A. Pestre, T. Lesaffre, Q. Cazères, E. Riber, and B. Cuenot, (2023), Euler-Lagrange numerical simulation of a kerosene droplet mist ignition in air using analytically reduced chemistry, In *Mediterranean Combustion Symposium 12, Louxor, Egypt, 23-26 January*.

[CFD74] A. Pestre, E. Riber, and B. Cuenot, (2023), Numerical simulation of two-phase ignition at high altitude conditions, In *11th European Combustion Meeting, Rouen, 26-28 April*.

[CFD75] T. Poinsot, (2021), Les jumeaux numériques des turbines à gaz - invited conference, In *Séminaire de l´Académie des technologies - 24 Mars*.

[CFD76] T. Poinsot, (2021), Les sciences mécaniques et la simulation: des turbines aux virus - invited conference, In *Académie des Sciences. Janvier*.

[CFD77] T. Poinsot, (2021), Simulation haute performance en mécanique - Invited conference, In *Haut Comité Mécanique, Centrale Supelec, Février*.

[CFD78] T. Poinsot, (2021), Thermoacoustics of hydrogen enriched flames and effects of thermal boundary conditions. Plenary Thursday session - invited conference, In *SOTIC Meeting Munich, 6-10 Sept*, online TU Munich.

[CFD79] T. Poinsot, (2021), Using hydrogen combustion to store renewable energies - invited conférence, In *Séminaire du Laboratoire de Mécanique des Fluides de Lille. 11 février*.

[CFD80] T. Poinsot, (2022), Can we simulate safety scenarios linked to combustion ? invited conference, In *Conférence annuelle de l'EPSC (European Process Safety Center), Anvers, Belgium, 12-14 septembre*.

[CFD81] T. Poinsot, (2023), Hydrogen as an energy vector for transportation ? - Invited conference, In *International Conference on Clean Energy for Carbon Neutrality. Hong Kong Institute for Clean Energy. 7-10 mars*.

[CFD82] R. Roncen, J. Cardesa Duenas, and T. Marchal, (2023), Developments of the time-domain impedance boundary condition for combustion problems, In *Symposium on Thermoacoustics in Combustion: Industry meets Academia (SoTiC 2023) - Zurich, Switzerland, Sept 11-14*.

[CFD83] T. Schmitt, D. Marchal, S. Ducruix, and B. Cuenot, (2022), REST HF-10 test case: Large-Eddy Simulations using the AVBP solver, In *9th European Conference for Aeronautics and Space Sciences (EUCASS), Lille, France*.

[CFD84] V. Shastry, E. Riber, B. Cuenot, L. Gicquel, and L. Voivenel, (2021), Numerical study of swirled multicomponent spray flames in gas turbine combustors, In *Colloque INCA 2021 (Initiative en Combustion Avancée) – Visioconférence*.

[CFD85] V. Shastry, E. Riber, L. Gicquel, B. Cuenot, and V. Bodoc, (2022), Large Eddy Simulations of complex multicomponent swirling spray flames in a realistic gas turbine combustor, In *39th International Symposium on Combustion, Vancouver, Canada*.

[CFD86] J. Tillou, J. Leparoux, J. Dombard, E. Riber, and B. Cuenot, (2021), Evaluation and Validation of Two-Phase Flow Numerical Simulations Applied to an Aeronautical Injector Using a Lagrangian Approach, In *ASME Turbo Expo 2020: Turbomachinery Technical Conference and Exposition - September 21 -25*, vol. V04BT04A018, Virtual conference, GT2020–15612.

[CFD87] B. Vanbersel, F. Meziat-Ramirez, O. Dounia, Q. Douasbin, T. Jaravel, and O. Vermorel, (2023), Large Eddy Simulations of a hydrogen-air deflagration in an obstacle-laden channel using Adaptive Mesh Refinement, In *11th European Combustion Meeting, Rouen, 26-28 April*.

[CFD88] B. Vanbersel, F. Meziat-Ramirez, O. Vermorel, T. Jaravel, Q. Douasbin, and O. Dounia, (2023), Large Eddy Simulations of a Hydrogen-Air Explosion in an Obstructed Chamber Using Adaptive Mesh Refinement, In *International Conference on Hydrogen Safety ICHS 2023, Quebec, September 19-21*.

[CFD89] B. Vanbersel, F. Meziat-Ramirez, O. Vermorel, T. Jaravel, Q. Douasbin, and O. Dounia, (2023), LES of Explosions and Adaptive Mesh Refinement, In *Journée de la combustion turbulente, Paris, 30 March*.

[CFD90] W. Villafana, G. Fubiani, L. Garrigues, G. Vigot, B. Cuenot, and O. Vermorel, (2022), 3D Particle-In-Cell modeling of anomalous electron transport driven by the Electron Drift Instability in Hall thrusters, In *37th International Electric Propulsion Conference Massachusetts Institute of Technology, Cambridge, MA, USA*.

[CFD91] B. Vincze, S. Agarwal, N. Odier, L. Gicquel, and F. Duchaine, (2023), Optimization of a Fan-Shaped Film-Cooling Jet and Its Implementation in a High-Pressure Turbine Vane With Large-Eddy Simulations ; Paper GT2023-101923, In *ASME Turbo Expo 2023: Turbomachinery Technical Conference and Exposition, Boston, Massachusetts, June 26-30*, V07AT12A008.

[CFD92] A. Voci, M. Di Renzo, K. Maeda, T. Teixeira, and G. Iaccarino, (2021), A multiblock compressible Navier-Stokes solver in the Legion environment, In *74th Annual Meeting of the APS Division of Fluid Dynamics Sunday–Tuesday, November 21–23, 2021; Phoenix Convention Center, Phoenix, Arizona*.

[CFD93] J. Wang, M. Di Renzo, H. Wang, and J. Urzay, (2021), Laser-induced ignition of a methane-oxygen turbulent shear layer, In *74th Annual Meeting of the APS Division of Fluid Dynamics Sunday–Tuesday, November 21–23, 2021; Phoenix Convention Center, Phoenix, Arizona*.

[CFD94] C. Williams, M. Di Renzo, J. Urzay, and P. Moin, (2021), Effect of dissociation/vibrational-relaxation coupling on laminar hypersonic boundary layers, In *74th Annual Meeting of the APS Division of Fluid Dynamics Sunday–Tuesday, November 21–23, 2021; Phoenix Convention Center, Phoenix, Arizona*.

[CFD95] C. Wingel, N. Binder, Y. Bousquet, J.-F. Boussuge, N. Buffaz, and S. Le Guyader, (2022), Influence of RANS Turbulent Inlet Set-Up on the Swirled Hot Streak Redistribution in a Simplified Nozzle Guide Vane Passage: Comparisons With Large-Eddy Simulations - Paper n° GT2022-78239, In *ASME Turbo Expo 2022: Turbomachinery Technical Conference and Exposition, Volume 10B, Turbomachinery, Axial Flow Turbine Aerodynamics, Deposition, Erosion, Fouling, and Icing, Radial Turbomachinery Aerodynamics, Rotterdam, Netherlands*.

[CFD96] J. Wirtz, B. Cuenot, and E. Riber, (2023), Fuel effect in a swirl-stabilized spray burner, In *11th European Combustion Meeting , Rouen, 26-28 April*.

[CFD97] J. Wirtz, E. Riber, and B. Cuenot, (2021), Numerical Dual Swirl Spray Stabilized Burner: Comparison of conventional and alternative fuels, In *Colloque INCA 2021 (Initiative en Combustion Avancée) – Visioconférence*.

[CFD98] J. Wirtz, (2023), LES modelling for the combustion of SAF, In *EM2C, Gif-sur-Yvette, 30 March*.

5.3 HDR

[CFD99] G. Daviller, (2023), *Computational Fluid Dynamics Applied to Aeroacoustics: From Numerical Methods to Flow Physics Analysis*, hdr, Cerfacs.

5.4 Journal Publications

[CFD100] S. Agarwal, L. Gicquel, F. Duchaine, N. Odier, and J. Dombard, (2021), Analysis of the Unsteady Flow Field Inside a Fan-Shaped Cooling Hole Predicted by Large Eddy Simulation - Paper n° TURBO-20-1235, *Journal of Turbomachinery*, **143**, 031011.

[CFD101] S. Agarwal, N. Odier, F. Duchaine, L. Gicquel, D. Bonneau, and M. Slusarz, (2023), Efficient Global Optimization of a laidback fan-shaped cooling hole using Large-Eddy Simulation, *Applied Thermal Engineering*, **in press**, Article number 121453.

[CFD102] P. Agostinelli, D. Laera, I. Boxx, L. Gicquel, and T. Poinsot, (2021), Impact of wall heat transfer in Large Eddy Simulation of flame dynamics in a swirled combustion chamber, *Combustion and Flame*, **234**, 111728.

[CFD103] P. Agostinelli, D. Laera, I. Chterev, I. Boxx, L. Gicquel, and T. Poinsot, (2022), On the impact of H2-enrichment on flame structure and combustion dynamics of a lean partially-premixed turbulent swirling flame, *Combustion and Flame*, **241**, 112120.

[CFD104] P. Agostinelli, D. Laera, I. Chterev, I. Boxx, L. Gicquel, and T. Poinsot, (2023), Large eddy simulations of mean pressure and H2 addition effects on the stabilization and dynamics of a partially-premixed swirled-stabilized methane flame, *Combustion and Flame*, **249**, Article number 112592.

[CFD105] P. Agostinelli, B. Rochette, D. Laera, J. Dombard, B. Cuenot, and L. Gicquel, (2021), Static mesh adaptation for reliable large eddy simulation of turbulent reacting flows, *Physics of Fluids*, **33**, 035141.

[CFD106] E. Ajuria-Illarramendi, M. Bauerheim, and B. Cuenot, (2021), Performance and accuracy assessments of an incompressible fluid solver coupled with a deep convolutional neural network, arXiv e–print 2109.09363.

[CFD107] E. Ajuria-Illarramendi, M. Bauerheim, and B. Cuenot, (2022), Performance and accuracy assessments of an incompressible fluid solver coupled with a deep convolutional neural network, *Data-Centric Engineering*, **3**, e2.

[CFD108] A. Aniello, D. Laera, S. Marragou, H. Magnes, L. Selle, T. Schuller, and T. Poinsot, (2023), Experimental and numerical investigation of two flame stabilization regimes observed in a dual swirl H2-air coaxial injector, *Combustion and Flame*, **249**, Article number 112595.

[CFD109] A. Aniello, D. Laera, S. Marragou, T. Poinsot, T. Schuller, and L. Selle, (2023), Influence of pilot H2 injection on methane-air swirled flame stabilization and acoustic response, *Combustion and Flame*, **253**, Article number 112749.

[CFD110] A. Aniello, D. Schuster, P. Werner, J.-F. Boussuge, M. Gatti, C. Mirat, L. Selle, T. Schuller, T. Poinsot, and U. Ruede, (2022), Comparison of a finite volume and two Lattice Boltzmann solvers for swirled confined flows, *Computers and Fluids*, **241**, 105463.

[CFD111] T. Astoul, G. Wissocq, J.-F. Boussuge, A. Sengissen, and P. Sagaut, (2021), Lattice Boltzmann method for computational aeroacoustics on non-uniform meshes: A direct grid coupling approach, *Journal of Computational Physics*, **447**, 110667.

[CFD112] N. Barleon, L. Cheng, B. Cuenot, and O. Vermorel, (2023), A phenomenological model for plasma-assisted combustion with NRP discharges in methane-air mixtures: PACMIND, *Combustion and Flame*, **253**, Article number 112794.

[CFD113] N. Barleon, L. Cheng, B. Cuenot, O. Vermorel, and A. Bourdon, (2023), Investigation of the impact of NRP discharge frequency on the ignition of a lean methane-air mixture using fully coupled plasma-combustion numerical simulations, *Proceedings of the Combustion Institute*, **39**, 5521–5530.

[CFD114] N. Barleon, B. Cuenot, and O. Vermorel, (2023), Large-Eddy Simulation of swirled flame stabilisation using NRP discharges at atmospheric pressure, *Applications in Energy and Combustion Science*, **15**, Article number 100163.

[CFD115] S. Blanchard, Q. Cazères, and B. Cuenot, (2022), Chemical modeling for methane oxy-combustion in Liquid Rocket Engines, *Acta Astronautica*, **190**, 98–111.

[CFD116] S. Blanchard, N. Odier, L. Gicquel, B. Cuenot, and F. Nicoud, (2021), Stochastic forcing for sub-grid scale models in wall-modeled large-eddy simulation, *Physics of Fluids*, **33**, 095123.

[CFD117] D. Brouzet, M. Talei, M. Brear, and B. Cuenot, (2021), The impact of chemical modelling on turbulent premixed flame acoustics, *Journal of Fluid Mechanics*, **915**, A3.

[CFD118] S.-G. Cai, J. Degrigny, J.-F. Boussuge, and P. Sagaut, (2021), Coupling of turbulence wall models and immersed boundaries on Cartesian grids, *Journal of Computational Physics*, **429**, 109995.

[CFD119] T. Capurso, D. Laera, E. Riber, and B. Cuenot, (2023), NOx pathways in lean technically premixed swirling H2-air turbulent flame, *Combustion and Flame*, **248**, Article number 112581.

[CFD120] J. Carmona, N. Odier, O. Desjardins, B. Cuenot, A. Misdariis, and A. Cayre, (2021), A Comparative Study of Direct Numerical Simulation and Experimental Results on a Prefilming Airblast Atomization Configuration, *Atomization and Sprays*, **31**, 9–32.

[CFD121] J. Carmona, N. Treleaven, N. Odier, and B. Cuenot, (2023), Lagrangian Simulation Methodology for Large-Eddy Simulations of Prefilming Air-Blast Injectors, *Journal of Propulsion and Power*, Article in Advance.

[CFD122] Q. Cazères, P. Pepiot, E. Riber, and B. Cuenot, (2021), A fully automatic procedure for the analytical reduction of chemical kinetics mechanisms for Computational Fluid Dynamics applications, *Fuel*, **303**, 121247.

[CFD123] A. Cellier, F. Duchaine, T. Poinsot, G. Okyay, M. Leyko, and M. Pallud, (2023), An analytically reduced chemistry scheme for large eddy simulation of lithium-ion battery fires, *Combustion and Flame*, **250**, Article number 112648.

[CFD124] A. Cellier, C. Lapeyre, G. Oztarlik, T. Poinsot, T. Schuller, and L. Selle, (2021), Detection of precursors of combustion instability using convolutional recurrent neural networks, *Combustion and Flame*, **233**, 111558.

[CFD125] L. Cheng, N. Barleon, B. Cuenot, O. Vermorel, and A. Bourdon, (2022), Plasma assisted combustion of methane-air mixtures: Validation and reduction, *Combustion and Flame*, **240**.

[CFD126] L. Cheng, N. Barleon, O. Vermorel, B. Cuenot, and A. Bourdon, (2022), AVIP: a low temperature plasma code, arXiv e–print 2201.01291.

[CFD127] F. Collin-Bastiani, E. Riber, and B. Cuenot, (2021), Study of inter-sector spray flame propagation in a linear arrangement of swirled burners, *Proceedings of the Combustion Institute*, **38**, 6299–6308.

[CFD128] A. Colombié, E. Laroche, F. Chedevergne, R. Manceau, F. Duchaine, and L. Gicquel, (2021), Large-Eddy-Simulation-based analysis of Reynolds-stress budgets for a round impinging jet, *Physics of Fluids*, **33**, 115109.

[CFD129] V. Coulon, J. Gaucherand, V. Xing, D. Laera, C. Lapeyre, and T. Poinsot, (2023), Direct numerical simulations of methane, ammonia-hydrogen and hydrogen turbulent premixed flames, *Combustion and Flame*, **256**, Article number 112933.

[CFD130] J. Crespo-Anadon, C. Benito-Parejo, S. Richard, E. Riber, B. Cuenot, C. Strozzi, J. Sotton, and M. Bellenoue, (2022), Experimental and LES investigation of ignition of a spinning combustion technology combustor under relevant operating conditions, *Combustion and Flame*, **242**, 112204.

[CFD131] B. Cuenot, F. Shum Kivan, and S. Blanchard, (2022), The thickened flame approach for non-premixed combustion: Principles and implications for turbulent combustion modeling, *Combustion and Flame*, **239**, 111702.

[CFD132] J. Degrigny, S.-G. Cai, J.-F. Boussuge, and P. Sagaut, (2021), Improved wall model treatment for aerodynamic flows in LBM, *Computers and Fluids*, **227**, 105041.

[CFD133] N. Detomaso, J.-J. Hok, O. Dounia, D. Laera, and T. Poinsot, (2023), A generalization of the Thickened Flame model for stretched flames, *Combustion and Flame*, **258**, article number 113080.

[CFD134] N. Detomaso, D. Laera, P. Pouech, F. Duchaine, and T. Poinsot, (2022), Large Eddy Simulation of a Pistonless Constant Volume Combustor: a New Concept of Pressure Gain Combustion - Paper n° GTP-22-1524, *Journal of Engineering for Gas Turbines and Power-Transactions of the ASME*, **145**, 021025.

[CFD135] M. Di Renzo and B. Cuenot, (2022), A reduced chemical mechanism for the simulation of electrified methane/air flames, *Combustion and Flame*, **244**, 112246.

[CFD136] M. Di Renzo and B. Cuenot, (2023), Direct numerical simulation of a turbulent methane/air flame impinged by a sub-breakdown electric field, *Combustion and Flame*, **253**, Article number 112823.

[CFD137] M. Di Renzo, (2022), HTR-1.3 solver: Predicting electrified combustion using the hypersonic task-based research solver, *Computer Physics Communications*, **272**, 108247.

[CFD138] O. Dounia, T. Jaravel, and O. Vermorel, (2022), On the controlling parameters of the thermal decomposition of inhibiting particles: A theoretical and numerical study, *Combustion and Flame*, **240**, 111991.

[CFD139] O. Dounia, O. Vermorel, T. Jaravel, and T. Poinsot, (2021), Time scale analysis of the homogeneous inhibition/suppression of premixed flames by alkali metals, *Proceedings of the Combustion Institute*, **38**, 2371–2378.

[CFD140] L. Drozda, P. Mohanamuraly, L. Cheng, C. Lapeyre, G. Daviller, Y. Realpe, A. Adler, G. Staffelbach, and T. Poinsot, (2023), Learning an optimised stable Taylor-Galerkin convection scheme based on a local spectral model for the numerical error dynamics, *Journal of Computational Physics*, **493**, Article number 112430.

[CFD141] F. Duchaine, M. Cizeron, N. Odier, J. Dombard, S. Marchall, N. Francois, and T. Poinsot, (2022), High-performance CFD for Respiratory Droplet Turbulent Dispersion in a Ventilated City Bus, *International Journal of Computational Fluid Dynamics*, **35**, 758–777.

[CFD142] F. Dupuy, O. Mestre, M. Serrurier, V. Kivachuk Burdá, N. Cabrera-Gutiérrez, M. Chafik Bakkay, M. Mader, G. Oller, and J.-C. Jouhaud, (2021), ARPEGE Cloud Cover Forecast Post-Processing with Convolutional Neural Network, *Weather and Forecasting*, **36**, 567–586.

[CFD143] D. Dupuy, N. Odier, C. Lapeyre, and D. Papadogiannis, (2023), Modeling the wall shear stress in large-eddy simulation using graph neural networks, *Data-Centric Engineering*, **4**, e7.

[CFD144] D. Dupuy, A. Perrot, N. Odier, L. Gicquel, and F. Duchaine, (2021), Boundary-condition models of film-cooling holes for large-eddy simulation of turbine vanes, *International Journal of Heat and Mass Transfer*, **166**, 120763.

[CFD145] P. Duquesne, J. Chanéac, G. Mondin, and J. Dombard, (2022), Topology Rule-Based Methodology for Flow Separation Analysis in Turbomachinery, *International Journal of Turbomachinery, Propulsion and Power*, **7**, Article number 21.

[CFD146] L. Esclapez, F. Collin-Bastiani, E. Riber, and B. Cuenot, (2021), A statistical model to predict ignition probability, *Combustion and Flame*, **225**, 180–195.

[CFD147] S. Esnault, F. Duchaine, L. Gicquel, and S. Moreau, (2023), Analysis of Upstream Turbulence Impact on Wall Heat Transfer in an Acoustic Liner with Large-Eddy Simulations, *Applied Sciences*, **13**, Article number 3145.

[CFD148] M. Fiore, M. Daroukh, and M. Montagnac, (2021), Broadband noise prediction of a counter rotating open rotor based on LES simulation with phase-lagged assumption, *Journal of Sound and Vibration*, **514**, 116420.

[CFD149] M. Fiore, M. Daroukh, and M. Montagnac, (2021), Loss assessment of a counter rotating open rotor using URANS/LES with phase-lagged assumption, *Computers and Fluids*, **228**, 105025.

[CFD150] M. Fiore, M. Daroukh, and M. Montagnac, (2022), Loss assessment of the NASA SDT configuration using LES with phase-lagged assumption, *Computers and Fluids*, **234**, 105256.

[CFD151] M. Fiore, M. Daroukh, and M. Montagnac, (2022), Loss Assessment of the NASA Source Diagnostic Test Configuration using URANS with Phase-Lagged Assumption, *Journal of Turbomachinery*, **144**, 051006.

[CFD152] L. Gallen, E. Riber, and B. Cuenot, (2023), Investigation of soot formation in turbulent spray flame burning real fuel, *Combustion and Flame*, **258**, Article number 112621.

[CFD153] J. Gaucherand, D. Laera, C. Schulze-Netzer, and T. Poinsot, (2023), DNS of Turbulent Premixed Ammonia/Hydrogen Flames: The Impact of Thermo-Diffusive Effects, *Flow Turbulence and Combustion*.

[CFD154] J. Gaucherand, D. Laera, C. Schulze-Netzer, and T. Poinsot, (2023), Intrinsic instabilities of hydrogen and hydrogen/ammonia premixed flames: Influence of equivalence ratio, fuel composition and pressure, *Combustion and Flame*, **256**, Article number 112986.

[CFD155] T. Gianoli, J.-F. Boussuge, P. Sagaut, and J. de Laborderie, (2023), Development and validation of Navier–Stokes characteristic boundary conditions applied to turbomachinery simulations using the lattice Boltzmann method, *International Journal for Numerical Methods in Fluids*, **95**, 528–556.

[CFD156] S. Grimonprez, J. Wu, A. Faccinetto, S. Gosselin, E. Riber, B. Cuenot, M. Cazaunau, E. Pangui, P. Formenti, J.-F. Doussin, D. Petitprez, and P. Desgroux, (2021), Hydrophilic properties of soot particles exposed to OH radical: a possible new mechanism involved in the contrail formation, *Proceedings of the Combustion Institute*, **38**, 6441–6450.

[CFD157] T. Jaravel, O. Dounia, Q. Malé, and O. Vermorel, (2021), Deflagration to detonation transition in fast flames and tracking with chemical explosive mode analysis, *Proceedings of the Combustion Institute*, **38**, 3529–3536.

[CFD158] B. Jiang, D. Brouzet, M. Talei, R. Gordon, Q. Cazères, and B. Cuenot, (2021), Turbulent flame-wall interactions for flames diluted by hot combustion products, *Combustion and Flame*, **230**, 111432.

[CFD159] B. Joshi, A. Sengupta, and P. Sundaram, (2023), Exploring role of aspect ratio for compressible flow in a rectangular lid-driven cavity with a vertical temperature gradient, *Physics of Fluids*, **35**, Article number 066135.

[CFD160] Y. Kwah, P. Agostinelli, S. Richard, G. Exilard, S. Pascaud, L. Gicquel, and J. Dawson, (2022), Effect of Strong Azimuthal Swirl on Ignition and Light-Around in an Annular Combustor, *Journal of Engineering for Gas Turbines and Power-Transactions of the ASME*, **144**, 111010.

[CFD161] D. Laera, P. Agostinelli, L. Selle, Q. Cazères, G. Oztarlik, T. Schuller, L. Gicquel, and T. Poinsot, (2021), Stabilization mechanisms of CH4 premixed swirled flame enriched with a non-premixed hydrogen injection, *Proceedings of the Combustion Institute*, **38**, 6355–6363.

[CFD162] T. Lafarge, P. Boivin, N. Odier, and B. Cuenot, (2021), Improved color-gradient method for lattice Boltzmann modeling of two-phase flows, *Physics of Fluids*, **33**, 082110.

[CFD163] S. Lai, S. Tang, C. Xu, N. Sekularac, and X. Fang, (2023), Computational diagnostics for flame acceleration and transition to detonation in a hydrogen/air mixture, *Combustion and Flame*, **258**, Article number 113054.

[CFD164] D. Lamidel, G. Daviller, M. Roger, and H. Posson, (2021), Numerical Prediction of the Aerodynamics and Acoustics of aTip Leakage Flow Using Large-Eddy Simulation, *International Journal of Turbomachinery, Propulsion and Power*, **6**, article number 27.

[CFD165] J. Larsson, V. Kumar, N. Oberoi, M. Di Renzo, and S. Pirozzoli, (2022), Large-Eddy Simulations of Idealized Shock/Boundary-Layer Interactions with Crossflow, *AIAA Journal*, **60**, 1–13.

[CFD166] C. Laurent, A. Badhe, and F. Nicoud, (2021), Representing the geometrical complexity of liners and boundaries in low-order modeling for thermoacoustic instabilities, *Journal of Computational Physics*, **428**, 110077.

[CFD167] C. Laurent, G. Staffelbach, F. Nicoud, and T. Poinsot, (2021), Heat-release dynamics in a doubly-transcritical LO2/LCH4 cryogenic coaxial jet flame subjected to fuel inflow acoustic modulation, *Proceedings of the Combustion Institute*, **38**, 6375–6383.

[CFD168] T. Lesaffre, A. Pestre, E. Riber, and B. Cuenot, (2023), Correction Methods for Exchange Source Terms in Unstructured Euler-Lagrange Solvers with Point-Source Approximation, *Flow Turbulence and Combustion*, **111**.

[CFD169] E. Lo Schiavo, D. Laera, E. Riber, L. Gicquel, and T. Poinsot, (2021), On the impact of fuel injection angle in Euler-Lagrange Large Eddy Simulations of swirling spray flames exhibiting thermoacoustic instabilities, *Combustion and Flame*, **227**, 359–370.

[CFD170] Q. Malé, O. Vermorel, F. Ravet, and T. Poinsot, (2021), Jet Ignition Prediction in a Zero-Dimensional Pre-Chamber Engine Model, *International Journal of Engine Research*, 14680874211015002.

[CFD171] T. Marchal, H. Deniau, J.-F. Boussuge, B. Cuenot, and R. Mercier, (2023), Extension of the Spectral Difference Method to Premixed Laminar and Turbulent Combustion, *Flow Turbulence and Combustion*, **111**, 141–176.

[CFD172] S. Marragou, H. Magnes, A. Aniello, L. Selle, T. Poinsot, and T. Schuller, (2022), Experimental analysis and theoretical lift-off criterion for H2/air flames stabilized on a dual swirl injector, *Proceedings of the Combustion Institute*.

[CFD173] B. Martin, F. Duchaine, O. Gicquel, and N. Odier, (2021), Generation of Realistic Boundary Conditions at the Combustion Chamber/Turbine Interface Using Large-Eddy Simulation, *Energies*, **14**, article number 8206.

[CFD174] B. Martin, F. Duchaine, L. Gicquel, N. Odier, and J. Dombard, (2022), Accurate Inlet Boundary Conditions to Capture Combustion Chamber and Turbine Coupling With Large-Eddy Simulation - Paper n° GTP-21-1355, *Journal of Engineering for Gas Turbines and Power-Transactions of the ASME*, **144**, 021007.

[CFD175] P.-A. Masset, F. Duchaine, A. Pestre, and L. Selle, (2023), Modelling challenges of volume-averaged combustion in inert porous media, *Combustion and Flame*, **251**, Article number 112678.

[CFD176] C. Mocquard, D. Laera, J. Dombard, and T. Poinsot, (2023), A two-step chemical scheme for auto-igniting and propagating kerosene flames at reheat conditions, *Combustion and Flame*, **248**, Article number 112558.

[CFD177] J. Moran, A. Poux, F. Cepeda, F. Escudero, A. Fuentes, L. Gallen, E. Riber, B. Cuenot, and J. Yon, (2023), Multi-scale soot formation simulation providing detailed particle morphology in a laminar coflow diffusion flame, *Combustion and Flame*, **256**, Article number 112987.

[CFD178] A. Mouze-Mornettas, M. Martin Benito, G. Dayma, C. Chauveau, B. Cuenot, and F. Halter, (2023), Laminar flame speed evaluation for CH4 /O2 mixtures at high pressure and temperature for rocket engine applications, *Proceedings of the Combustion Institute*, **39**, 1833–1840.

[CFD179] L. Muscat, G. Puigt, M. Montagnac, and P. Brenner, (2021), Mathematical analysis of the spatial coupling of an explicit temporal adaptive integration scheme with an implicit time integration scheme, *International Journal for Numerical Methods in Fluids*, **93**, 774–815.

[CFD180] M. Nabavi, M. Di Renzo, and J. Kim, (2022), Modulation of inter-phase, cross-scale momentum transfer by preferentially-concentrated inertial particles, *Physical Review Fluids*, **7**, 044305.

[CFD181] S. Nadakkal-Appukuttan, E. Riber, and B. Cuenot, (2022), Analysis and design of a local time stepping scheme for LES acceleration in reactive and non-reactive flow simulations, *Journal of Computational Physics*, **470**, 111580.

[CFD182] M. Nguyen, J.-F. Boussuge, P. Sagaut, and J. Larroya-Huguet, (2022), Large Eddy Simulation of a Thermal Impinging Jet using the Lattice Boltzmann Method, *Physics of Fluids*, **34**, 0055115.

[CFD183] M. Nguyen, J.-F. Boussuge, P. Sagaut, and J. Larroya-Huguet, (2023), Large eddy simulation of a row of impinging jets with upstream crossflow using the lattice Boltzmann method, *International Journal of Heat and Mass Transfer*, **212**, Article number 124256.

[CFD184] N. Odier, A. Thacker, M. Harnieh, G. Staffelbach, L. Gicquel, F. Duchaine, N. Garcia-Rosa, and J.-D. Mueller, (2021), A mesh adaptation strategy for complex wall-modeled turbomachinery LES, *Computers and Fluids*, **214**, 104766.

[CFD185] A. Perrot, L. Gicquel, F. Duchaine, N. Odier, J. Dombard, and T. Grosnickel, (2021), Unsteady Analysis of Heat Transfer Coefficient Distribution in a Static Ribbed Channel for An Established Flow - paper n° TURBO-20-1259, *Journal of Turbomachinery*, **143**, 121004.

[CFD186] A. Pestre, T. Lesaffre, Q. Cazères, E. Riber, and B. Cuenot, (2023), Euler-Lagrange numerical simulation of a kerosene droplet mist ignition in air using analytically reduced chemistry, *International Journal of Spray and Combustion Dynamics*, **15**, 207–217.

[CFD187] L. Potier, F. Duchaine, B. Cuenot, D. Saucereau, and J. Pichillou, (2022), Prediction of Wall Heat Fluxes in a Rocket Engine with Conjugate Heat Transfer Based on Large-Eddy Simulation, *Entropy*, **24**, Article number 26.

[CFD188] P. Pouech, F. Duchaine, and T. Poinsot, (2021), Premixed flame ignition in high-speed flows over a backward facing step, *Combustion and Flame*, **229**.

[CFD189] B. Péden, J. Carmona, P. Boivin, T. Schmitt, B. Cuenot, and N. Odier, (2023), Numerical assessment of Diffuse-Interface method for air-assisted liquid sheet simulation, *Computers and Fluids*, **266**, Article number 106022.

[CFD190] C. Pérez-Arroyo, J. Dombard, F. Duchaine, L. Gicquel, B. Martin, N. Odier, and G. Staffelbach, (2021), Towards the Large-Eddy Simulation of a full engine: Integration of a 360 azimuthal degrees fan, compressor and combustion chamber. Part I: Methodology and initialisation, *Journal of the Global Power and Propulsion Society*, **Special Issue: Data-driven modelling and high-fidelity simulations**, 1–16.

[CFD191] C. Pérez-Arroyo, J. Dombard, F. Duchaine, L. Gicquel, B. Martin, N. Odier, and G. Staffelbach, (2021), Towards the Large-Eddy Simulation of a full engine: Integration of a 360 azimuthal degrees fan, compressor and combustion chamber. Part II: Comparison against stand-alone simulations, *Journal of the Global Power and Propulsion Society*, **Special Issue: Data-driven modelling and high-fidelity simulations**, 1–16.

[CFD192] F. Renard, Y. Feng, J.-F. Boussuge, and P. Sagaut, (2021), Improved compressible hybrid lattice Boltzmann method on standard lattice for subsonic and supersonic flows, *Computers and Fluids*, **219**, 104867.

[CFD193] F. Renard, G. Wissocq, J.-F. Boussuge, and P. Sagaut, (2021), A linear stability analysis of compressible hybrid lattice Boltzmann methods, *Journal of Computational Physics*, **446**, 110649.

[CFD194] P. Sagaut, V. Suman, P. Sundaram, M. Rajpoot, Y. Bhumkar, S. Sengupta, A. Sengupta, and T. Sengupta, (2023), Global spectral analysis: Review of numerical methods, *Computers and Fluids*, **261**, Article number 105915.

[CFD195] N. Sekularac, K. Bushe, and X. Fang, (2023), An a priori analysis on principal component analysis based conditional source-term estimation model for Sandia jet flames, *Combustion and Flame*, **260**, Article number 113274.

[CFD196] N. Sekularac, X. Fang, K. Bushe, and M. Davy, (2023), Conditional space evaluation of progress variable definitions for Cambridge/Sandia swirl flames, *Combustion Theory and Modelling*, 1–32.

[CFD197] A. Sengupta and P. Sundaram, (2023), Compressibility effects on the flow past a T106A low-pressure turbine cascade, *Physics of Fluids*, **35**, Article number 106110.

[CFD198] S. Sengupta, S. Nadakkal-Appukuttan, P. Mohanamuraly, G. Staffelbach, and L. Gicquel, (2022), Global spectral analysis of the Lax–Wendroff-central difference scheme applied to Convection–Diffusion equation, *Computers and Fluids*, **242**, 105508.

[CFD199] T. Sengupta, V. Suman, S. Sengupta, and P. Sundaram, (2023), Quantifying parameter ranges for high fidelity simulations for prescribed accuracy by Lax–Wendroff method, *Computers and Fluids*, **254**, Article number 105794.

[CFD200] V. Shastry, Q. Cazères, B. Rochette, E. Riber, and B. Cuenot, (2021), Numerical study of multicomponent spray flame propagation, *Proceedings of the Combustion Institute*, **38**, 3201–3211.

[CFD201] V. Shastry, E. Riber, L. Gicquel, B. Cuenot, and V. Bodoc, (2023), Large Eddy Simulations of complex multicomponent swirling spray flames in a realistic gas turbine combustor, *Proceedings of the Combustion Institute*, **39**, 2693–2702.

[CFD202] N. Treleaven, D. Laera, J. Carmona, N. Odier, Y. Gentil, J. Dombard, G. Daviller, L. Gicquel, and T. Poinsot, (2022), Coupling of Combustion Simulation with Atomisation and Filming Models for LES in Swirled Spray Flames, *Flow Turbulence and Combustion*, **109**, 759–789.

[CFD203] K. Töpperwien, F. Collin-Bastiani, E. Riber, B. Cuenot, G. Vignat, K. Prieur, D. Durox, S. Candel, and R. Vicquelin, (2021), Large-Eddy Simulation of Flame Dynamics During the Ignition of a Swirling Injector Unit and Comparison With Experiments, *Journal of Engineering for Gas Turbines and Power-Transactions of the ASME*, **143**, 021015.

[CFD204] J. Urzay and M. Di Renzo, (2021), Engineering aspects of hypersonic turbulent flows at suborbital enthalpies, *Annual Research Briefs*, 7–32.

[CFD205] A. Veilleux, G. Puigt, H. Deniau, and G. Daviller, (2022), A stable Spectral Difference approach for computations with triangular and hybrid grids up to the 6th order of accuracy, *Journal of Computational Physics*, **449**, 110774.

[CFD206] A. Veilleux, G. Puigt, H. Deniau, and G. Daviller, (2022), Stable Spectral Difference Approach Using Raviart-Thomas Elements for 3D Computations on Tetrahedral Grids, *Journal of Scientific Computing*, **91**, article number 7.

[CFD207] G. Vignat, E. Lo Schiavo, D. Laera, A. Renaud, L. Gicquel, D. Durox, and S. Candel, (2021), Dynamics of spray and swirling flame under acoustic oscillations : A joint experimental and LES investigation, *Proceedings of the Combustion Institute*, **38**, 6015–6024.

[CFD208] W. Villafana, B. Cuenot, and O. Vermorel, (2023), 3D particle-in-cell study of the electron drift instability in a Hall Thruster using unstructured grids, *Physics of Plasmas*, **30**, Article number 033503.

[CFD209] W. Villafana, F. Petronio, A. Denig, J. Jimenez, D. Eremin, L. Garrigues, F. Taccogna, A. Alvarez Laguna, J. Boeuf, A. Bourdon, P. Chabert, T. Charoy, B. Cuenot, K. Hara, F. Pechereau, A. Smolyakov, D. Sydorenko, A. Tavant, and O. Vermorel, (2021), 2D radial-azimuthal particle-in-cell benchmark for E x B discharges, *Plasma Sources Science and Technology*, **30**, 075002.

[CFD210] J. Wirtz, B. Cuenot, and E. Riber, (2021), Numerical Study of a Polydisperse Spray Counterflow Diffusion Flame, *Proceedings of the Combustion Institute*, **38**, 3175–3182.

[CFD211] J. Zapata Usandivaras, A. Urbano, M. Bauerheim, and B. Cuenot, (2022), Data Driven Models for the Design of Rocket Injector Elements, *Aerospace*, **9**, Article number 594.

5.5 Technical Reports

[CFD212] P.-A. Baranger, (2022), Modélisation LES d´une chambre de combustion de micro-turbine avec écoulement diphasique, working note, Cerfacs.

[CFD213] A. Berthelot, (2022), Simulation de la combustion turbulente appliquée à la configuration Volvo à l'aide du solveur JAGUAR, working note, Cerfacs - Sorbonne Université.

[CFD214] A. Boudin, (2021), Turbulence injection methods for Large-Eddy Simulations, working note, Cerfacs - ISAE SUPAERO.

[CFD215] M. Cances, (2021), Modèles réduits pour l´étude et le contrôle des instabilités thermo-acoustiques dans les turbines à gaz aéronautiques et foyers de réchauffe, working note, Cerfacs - Université Paris-Saclay.

[CFD216] E. Charles, G. Daviller, and J.-F. Boussuge, (2023), Deliverable D2.3-24a: "High-order simulation on baseline configuration, technical report, Cerfacs - Toulouse, France.

[CFD217] E. Costes, (2023), Rapport de Stage : Cycle à zéro émission : développement de la chimie réduite de méthanol et/ou d'hydrogène en conditions supercritiques, working note, Cerfacs.

[CFD218] A. Coudray, (2021), Numerical study of NH3-H2/Air flames and pollutants emissions, working note, POLYTECH ORLEANS - CERFACS.

[CFD219] J. Dabas, (2022), Simulation aux grandes échelles d´écoulements éoliens, working note, Cerfacs - Ecole Normale Supérieure Paris-Saclay.

[CFD220] L. de Nardi, (2022), Scénarios et simulations de fuites d'hydrogène pour l'aviation du futur, working note, INSA - Cerfacs.

[CFD221] H. Divel, (2021), Test de fiabilité de la version 7.8 du code de simulation aux grandes echelles AVBP sur des écoulements variés, working note.

[CFD222] Y. Djebien, (2022), Simulation haute fidélité de la postcombustion dans les futurs avions de combat, working note, Université Toulouse III Paul Sabatier - Cerfacs.

[CFD223] A. Dutka, (2021), Development and study of a performance portable Spectral Differences CFD code, working note, ISAE SUPAERO - CERFACS.

[CFD224] F. Garnier, (2021), Simulation numérique de flammes jets d'hydrogène pour l'aéronautique, working note, INPT ENSEEIHT ET CERFACS, TOULOUSE.

[CFD225] R. Gaujard, (2021), Simulations de flammes canoniques dans des configurations de flammes de prémélange et de diffusion avec les logiciels opensource Cantera et Ember, working note, IPSA Toulouse.

[CFD226] L. Gopalakrishnan, (2022), Development and Validation of Porous Media Modelling for Acoustic Applications using the Lattice Boltzmann Method, working note, ISAE SUPAERO - CERFACS.

[CFD227] S. Hoflack, (2023), End-of-study internship report: Cerfacs Zero-carbon energy production: ammonia as a fuel, working note, Cerfacs - Toulouse, France.

[CFD228] K. Kaeda, J. Wang, and M. Di Renzo, (2021), Assessment of a high-order curvilinear finite-difference method for compressible reacting flows, technical report, Center for Turbulence Research Annual Research Briefs, pp. 197-204.

[CFD229] E. Matas Mur, (2022), Physical analysis of Heat Exchange in Dimpled Tubes by Large Scale Simulation, working note, INP ENSEEIHT - Cerfacs - Toulouse.

[CFD230] F. Meziat-Ramirez, (2021), Hydrogen Flame Acceleration in a Smooth Tube, working note, ISAE-SUPAERO.

[CFD231] M. Montecchia, E. Charles, G. Daviller, and J.-F. Boussuge, (2023), Deliverable D2.3-36a: "High-order simulation on installed configuration, technical report, Cerfacs - Toulouse, France.

[CFD232] S. Mrini, (2023), Exploration of the potential of self-supervised learning for numerical fluid dynamics substitution modeling, working note, ISAE SUPAERO - CERFACS.

[CFD233] D. Perkins, (2023), Large Eddy Simulations of a High Speed Low Pressure Turbine Cascade with Purge Flow, working note, ISAE SUPAERO - CERFACS.

[CFD234] J. Petit, (2021), Interaction turbulence - ondes de choc Implémentation d'une méthode à capture de choc dans un code de Différences Spectrales, working note, Mines Saint Etienne - Cerfacs.

[CFD235] B. Péden, (2021), Impact de la prédiction de l´atomisation primaire par méthode d´interface diffuse, working note, Cerfacs - ISAE ENSMA.

[CFD236] S. Recio Balmaseda, (2021), H2 Flame - Wall Interaction, working note, ISAE SUPAERO - CERFACS.

[CFD237] I. Rocchi, (2022), Simulation numérique du brûleur industriel Volvo par la méthode Lattice Boltzmann, working note, INSA Toulouse - Cerfacs.

[CFD238] F. Roqué, (2021), Modélisation et simulation d´un moteur à effet Hall, working note, Université Paris-Saclay , Cerfacs Toulouse.

[CFD239] S. SUBRAMANYA, (2021), Distributed Propulsion with Propellers, working note, ISAE SUPAERO - CERFACS.

[CFD240] J. Urzay and M. Di Renzo, (2021), Engineering aspects of hypersonic turbulent flows at suborbital enthalpies, technical report, Center for Turbulence Research Annual Research Briefs, pp. 7-32.

[CFD241] N. Villenave, (2021), Étude numérique des espèces radicales OH* et CH* dans des flammes laminaires CH4-H2/Air et comparaison avec des mesures de chimiluminescence, working note, CERFACS.

[CFD242] B. Vincze, (2022), Large Eddy Simulation of an optimized cooling system of a turbine vane, working note, ISAE SUPAERO - CERFACS.

[CFD243] J. Wang, M. Di Renzo, C. Williams, J. Urzay, and G. Iaccarino, (2021), Progress on laser ignition simulations of a CH4/O2 subscale rocket combustor using a multi-GPU task-based solver, technical report, Center for Turbulence Research Annual Research Briefs, pp. 129-142.

[CFD244] C. Williams, M. Di Renzo, and J. Urzay, (2021), Two-temperature extension of the HTR solver for hypersonic turbulent flows in thermochemical nonequilibrium, technical report, Center for Turbulence Research Annual Research Briefs, pp. 95-107.

[CFD245] C. Williams, M. Di Renzo, P. Moin, and J. Urzay, (2021), Locally self-similar formulation for hypersonic laminar boundary layers in thermochemical nonequilibrium, technical report, Center for Turbulence Research Annual Research Briefs, pp. 119-128.

5.6 Thesis

[CFD246] S. Agarwal, (2022), *Development of a predictive methodology for film cooling on blades*, phd thesis, Ecole doctorale MEGeP - CERFACS.

[CFD247] P. Agostinelli, (2022), *Assessment of Large Eddy Simulation in the Conjugate Heat Transfer context for engine operability: application to Hydrogen enrichment and Spinning Combustion Technology*, phd thesis, Ecole doctorale MEGeP - CERFACS.

[CFD248] E. Ajuria-Illarramendi, (2022), *Utilisation de réseaux de neurones pour l´accélération des codes de calculs*, phd thesis, MEGeP: Mécanique, Energétique, Génie civil, Procédés.

[CFD249] T. Astoul, (2021), *Towards improved Lattice Boltzmann aeroacoustic simulations with non-uniform grids: application to landing gears noise prediction*, phd thesis, Université de Toulouse III - INP Toulouse - MEGeP.

[CFD250] A. Badhe, (2022), *Low-order Thermoacoustic Network Modeling and Simulation of Spray Flame Transfer Function*, phd thesis, Ecole doctorale MEGeP - CERFACS.

[CFD251] N. Barleon, (2022), *Detailed modeling and simulations of Nanosecond Repetitively Pulsed Discharges for Plasma-Assisted Combustion (PAC)*, phd thesis, Ecole doctorale MEGeP - CERFACS.

[CFD252] S. Blanchard, (2021), *Multi-physics large-eddy simulation of methane oxy-combustion in liquid rocket engines*, phd thesis, Ecole doctorale MEGeP - Dynamique des fluides - CERFACS.

[CFD253] J. Carmona, (2021), *Modélisation des phénomènes diphasiques dans des injecteurs aéronautiques de type Airblast*, phd thesis, Ecole doctorale MEGeP - Mécanique, Energétique, Génie civil, Procédés - CERFACS.

[CFD254] Q. Cazères, (2021), *Analysis and reduction of chemical kinetics for combustion applications*, phd thesis, Université de Toulouse III -INP Toulouse : MEGeP.

[CFD255] A. Cellier, (2023), *Large Eddy Simulation of lithium-ion battery fires for the diagnostic of thermal runaway*, phd thesis, Ecole doctorale MEGeP - CERFACS.

[CFD256] L. Cheng, (2022), *Detailed Numerical Simulation of Multi-Dimensional Plasma Assisted Combustion*, phd thesis, Ecole doctorale MEGeP - CERFACS.

[CFD257] J. Crespo-Anadon, (2023), *Large Eddy Simulation of Aircraft Engine Ignition under Relevant Operating Conditions and Application to the Spinning Combustion Technology*, phd thesis, Ecole doctorale MEGeP - CERFACS.

[CFD258] J. Degrigny, (2021), *Towards the Computational Prediction of Low-Speed Buffet: Improved Wall Modeling for the Lattice-Boltzmann Method*, phd thesis.

[CFD259] L. Drozda, (2023), *On the development of data-driven numerical schemes in Computational Fluid Dynamics*, phd thesis, Ecole doctorale MEGeP - CERFACS.

[CFD260] S. Esnault, (2021), *Large Eddy Simulations of Heat Transfer within Aircraft Engine Acoustic Treatments*, phd thesis, Université Toulouse III - INP Toulouse MEGeP.

[CFD261] C. Garcia Guillamon, (2022), *Modeling of Multipoint Fuel Injector for the Large Eddy Simulation of Aeronautical Combustion Chambers*, phd thesis, Ecole doctorale: MEGeP, Mécanique, Energétique, Génie civil, Procédés.

[CFD262] J. Gaucherand, (2023), *Direct Numerical Simulation of premixed ammonia/hydrogen flames: the effects of thermo-diffusive instabilities*, phd thesis, Cerfacs.

[CFD263] C. Gout, (2022), *Mono-channel methods and modeling for LES of turbomachinery stage*, phd thesis, Ecole doctorale MEGeP - CERFACS.

[CFD264] T. Lafarge, (2022), *Investigation of Lattice Boltzmann methods applied to multiphase flows*, phd thesis, Ecole doctorale MEGeP - CERFACS.

[CFD265] D. Lamidel, (2022), *Aerodynamic noise sources of the tip flow in the fan stage of turbofan engines*, phd thesis, Ecole doctorale MEGeP - CERFACS.

[CFD266] T. Marchal, (2023), *Extension of the Spectral Difference method to combustion*, phd thesis, Ecole doctorale MEGeP - CERFACS.

[CFD267] B. Martin, (2021), *Méthodes numériques et conditions limites pour la simulation aux grandes échelles du couplage entre plusieurs composants d´une turbomachine*, phd thesis, Ecole doctorale MEGeP - CERFACS.

[CFD268] A. Mouze-Mornettas, (2023), *Modelling and reduction of the LOx-Methane chemical kinetics for rocket engine applications*, phd thesis, Energie, Matériaux, Sciences de la Terre et de l´univers - EMSTU.

[CFD269] S. Nadakkal-Appukuttan, (2022), *Large Eddy Simulation of the steam cracking process in refinery furnaces*, phd thesis, Ecole doctorale MEGeP - CERFACS.

[CFD270] M. Nguyen, (2023), *Investigation of the Lattice Boltzmann Method for the Simulation of Turbine Active Clearance Control Systems*, phd thesis, Aix-Marseille.

[CFD271] A. Pestre, (2023), *Numerical simulations of aeronautical engine ignitions under realistic high altitude conditions*, phd thesis, Ecole doctorale MEGeP - CERFACS.

[CFD272] F. Renard, (2021), *Hybrid Lattice Boltzmann method for compressible flows*, phd thesis, Aix Marseille Université - Science pour l´ingénieur : Mécanique, physique, micro et nanoélectronique.

[CFD273] D. Schuster, (2021), *Large scale simulations of swirling and particle-laden flows using the Lattice-Boltzmann Method*, phd thesis, Université de Toulouse III -INP Toulouse : MEGeP.

[CFD274] S. Sengupta, (2022), *Advanced methods for meshes in High Performance Computing of explosion simulation*, phd thesis, Ecole doctorale MEGeP - CERFACS.

[CFD275] V. Shastry, (2022), *Simulation of multicomponent spray combustion in gas turbine engines*, phd thesis, Ecole doctorale MEGeP - CERFACS.

[CFD276] M. Thomas, (2021), *combustor – turbine interactions: hot spot migration and thermal environment prediction for a better understanding and design of helicopter engines*, phd thesis, Université de Toulouse III - MEGeP.

[CFD277] A. Veilleux, (2021), *Extension of the spectral difference method to simplex cells and hybrid grids*, phd thesis, Université Toulouse III - INP Toulouse MEGeP.

[CFD278] W. Villafana, (2021), *Numerical Particle-In-Cell studies of Hall thrusters using unstructured grids*, phd thesis, Ecole doctorale MEGeP - Energétique et transferts - CERFACS.

[CFD279] C. Wingel, (2023), *Investigation of the RANS approach for the prediction of cooled turbine stage flows submitted to swirled hot streaks*, phd thesis, Ecole doctorale MEGeP - CERFACS.

[CFD280] J. Wirtz, (2022), *Modelling the impact of fuel in aeronautical gas turbines*, phd thesis, Ecole doctorale MEGeP - CERFACS.